CHAPTER 7.

HEAT TRANSFER.

CHAPTER 7.

HEAT TRANSFER.

7.1. INTRODUCTION.

Along with dissociation effects, heat losses from the charge in a spark ignition engine considerably reduce the maximum temperatures attained in combustion processes. As a consequence; the power output and thermal efficiency are much diminished. It has been well established that the heat transferred is lost predominantly by a combination of the three following processes:

a) Forced Convection - which is the process of heat transfer between a fluid and a solid surface in relative motion when the motion is caused by forces other than gravity. This accounts for the greater part of the heat loss in an engine.

b) Radiation - heat transferred by radiation accounts for a much smaller fraction of the total heat losses. It is the process of heat transfer through space and takes place not only in vacua but also through solids and liquids which are transparent to wavelengths in the visible and infra-red range.

c) Conduction - the mechanism of this mode of heat transfer is molecular motion and it represents the heat transfer process through solids and liquids at rest. It is, therefore, the method by which heat flows through deposits and the engine structure.

In digital computer simulations of engine combustion, it is most important to be able to predict accurately the

heat exchange between the working fluid and its surroundings under the many variable engine operating conditions. In this context, the surroundings are considered to comprise the cylinder head, the piston, the cylinder walls, the valves, the deposits and the lubricating oil. For reasons of simplicity, it is here assumed that the combustion chamber is free of deposits, that the valve surfaces are part of the cylinder head surface and that no heat is lost to the lubricating oil.

A further source of heat generation and loss is that caused by piston friction. Strange [18], in his highly idealized analysis of spark-ignition engine combustion, included a simplified expression to allow for these friction losses. Again, such effects are ignored in this study.

Many quantitative estimates have been made over the years of the overall heat losses during the various phases of the spark ignition engine cycle. These are found to vary from worker to worker, however, which is only to be expected when many different engine designs and operating conditions have been used in the determinations. The importance of accurate estimates of such losses to this analytical study is that they give an indication of the magnitudes of the heat losses during the separate phases of the engine cycle to which the computed quantities can be related. Thus, wildly inaccurate predictions of heat flows can be avoided. A condensed literature review of some overall heat loss estimates during compression, combustion and expansion now follows.

During compression, the heat exchange between the working fluid and the surroundings is normally quite small.

Indeed, Lichty[30] has estimated it to be of the order of 0.5% of the heat of combustion. This is not very surprising in view of the comparatively low gas temperatures in the engine at this time. During the initial stages of compression, it is possible for the heat flow to be from the hotter surroundings and to the cooler working fluid. As the compression process proceeds, however, the gas temperatures increase to become higher than the surrounding surface temperatures and the heat flow is once more from the gas to the walls.

During combustion and expansion, the gas temperatures are always much higher than the wall temperatures and the heat flow is invariably from the gases and to the walls. Lanchester[184] has estimated them to be about 4% of the heat of combustion during combustion and about 6% during expansion. Janeway[185] performed a heat balance on an 8-cylinder, L-head engine and concluded that the losses are very dependent on engine speed. During both combustion and expansion, he reported that they varied from 16-25% of the heat of combustion of which approximately a fourth or a fifth is lost during combustion alone. Ricardo[101] suggested figures of 6% during combustion and 7% during expansion. Pye[186] proposed losses of 5% of the heat of combustion during combustion and 10% during expansion. David and Leah[187] suggest that the heat loss, expressed as a percentage of the heat of combustion, is $\frac{15000}{n}$ and $\frac{75000}{n}$ during combustion and expansion respectively where 'n' is the engine speed in revolutions per minute. Finally, Lichty[30] obtained values of 7% and 9% of the heat of combustion during combustion and expansion respectively.

The influence that these losses have on the power output and thermal efficiency of an engine depends of course on the crankangle at which they are lost. Energy lost during combustion can be completely forgotten in so far as any useful work production is concerned. Excessive losses during this phase are very detrimental to engine performance therefore. Energy lost during expansion, on the other hand, has a very much smaller influence on the thermal efficiency and power output. Its principle effects during this phase of the cycle are:

i) to reduce the temperatures and pressures.

ii) as a consequence of this, to retard the recombination reactions which occur at this time. As explained in Chapter 6, these reactions can produce a supplementary work output.

7.2. FACTORS WHICH INFLUENCE HEAT TRANSFER IN S.I. ENGINES.

In analytical determinations of the heat transfer during each phase of the spark ignition engine cycle, the problem is made considerably more difficult by the great confusion of variables which prevail. Each factor known to influence the heat exchange is subject to continual change. Among such factors are:

a) mixture motion.

b) charge temperatures.

c) combustion chamber surface temperatures.

d) combustion chamber surface areas.

e) wall conductivity.

f) charge pressures.

g) charge viscosity.

h) charge thermal conductivity.

i) charge heat capacity.

Additionally, many other parameters and operating conditions can influence the magnitude of the heat losses. These include:

i) engine (and piston) speed.

ii) engine size.

iii) compression ratio.

iv) spark timing.

v) manifold temperature and pressure.

vi) air/fuel ratio.

vii) exhaust pressure.

viii) coolant temperature, flow and composition.

ix) fuel used.

x) combustion chamber shape.

xi) metals comprising the engine structure.

xii) lubricating oil quantity.

xiii) deposits.

Thus, the derivation of a general expression to accurately predict the magnitude of the heat losses at any particular stage in a cycle and which is applicable to any engine configuration is seen to be virtually impossible. All that can be done is to try and obtain an expression which predicts as accurately as possible the variation in heat transfer rate with change of the more important measurable parameters such as are listed in a) to i) above. Many such expressions appear in the literature most of which attempt to account for both radiative and convective heat transfer.

7.3. HEAT TRANSFER BY RADIATION.

The theory of radiant heat transfer starts from the concept of a 'black body' i.e. one which has a surface which emits or absorbs equally well radiations of all wavelengths, and which reflects none of any radiation falling upon it. It, thus, has an emissivity of unity. The rate of heat transfer from one 'black body' at temperature T_1 °K to another at temperature T_2 °K across a space containing no absorptive material, is given by

$$q_{RAD} = \sigma . A . (T_1^4 - T_2^4) \text{ cal/sec} \quad \ldots\ldots\ldots 7-1$$

where σ is the Stefan-Boltzmann constant $(1.36 \times 10^{-12} \text{ cal/cm}^2 \text{ sec } °K^4)$. and A is the area (cm^2).

In reality, surfaces are not 'black' but reflect radiation to an extent which depends upon the wavelength. To allow for this deviation from true 'black body' behaviour, an emissivity factor, γ, is incorporated. Equation 7-1 thus becomes

$$q_{RAD} = \sigma . A . \gamma . (T_1^4 - T_2^4) \quad \ldots\ldots\ldots 7-2$$

Such factors are normally expressed as percentages of the 'black body' emissivity.

Additionally, a 'geometric' factor, Fg, is applied to account for the variation of the intensity and the angle of incidence of the radiation over the surface of the body on which it falls. The final expression for heat transfer by radiation is therefore:

$$q_{RAD} = \sigma . A . \gamma . F_g . (T_1^4 - T_2^4) \quad \ldots\ldots\ldots 7-3$$

In the spark ignition engine, the charge temperatures, T_g, are continuously varying and radiation is emitted to

the walls of the combustion chamber according to the expression:

$$q_{RAD} = \sigma . A . \delta . F_g . (T_g^4 - T_w^4) \quad \ldots\ldots\ldots\ldots\ldots 7-4$$

where T_w is the temperature of the combustion chamber walls.

During the compression phase of the cycle, it is clear that the radiation is negligibly small since the charge temperatures are quite low. The combustion process, on the other hand, results in conditions in which the gas temperatures are high and variable and the composition of the combustion products is in a continuous state of change. This situation persists throughout the expansion stroke also and, thus, quite a large amount of heat transfer occurs by radiation during these phases. The gases in the engine at this time are very far from black as they emit and absorb radiation within certain wavelength bands.

Radiation from flames originates predominantly from the following two sources:

i) Radiation from non-luminous flames - these flames are characterized by a faint blue colour and radiate heat as infra-red energy. Only CO_2 and H_2O of the combustion products in such flames emit any appreciable amount. This is usually of low intensity except at very high temperatures when it can become significant. The effective emissivity in such flames is a function of the partial pressures, p, of the radiating constituents and of the thickness, l_e, of the flame. In Ref. 108, curves are given of the effective emissivities of CO_2 and H_2O at various values of temperature and $p.l_e$ functions.

ii) Radiation from luminous flames - these flames are

normally yellow in colour and are rich in suspended solid particles e.g. the solid incandescent carbon particles which appear as intermediate products in the rich combustion of hydrocarbons. Such particles radiate as solid bodies and provide a major contribution to radiant heat transfer.

It is clearly unreasonable to expect to be able to calculate accurately the radiant heat transfer during the combustion and expansion phases of the spark ignition engine cycle. Indeed, Annand[23] was reduced to determining only an average empirical factor which remains invariant during these phases.

Although the radiative component of heat transfer is small in comparison with the convective component, it is still an important contributory factor to the overall heat loss. Baker and Lacerson[189] have reported it to be as high as 10% of the total heat loss whereas Nusselt[190] has estimated it to be 5% from constant volume bomb experiments.

7.4. HEAT TRANSFER BY TURBULENT FORCED CONVECTION.

7.4.1. GENERAL.

Since turbulent forced convection accounts for the major part of the heat losses from the working fluid in an engine, it is considered here in some detail. In basic, theoretical studies of this process, it is usual to consider the analogy in tubes or over flat plates. A dimension analysis is made involving all the parameters which are considered to be of importance. These include:

L - a characteristic linear dimension.

h - the heat transfer coefficient i.e. the heat flow per unit time per unit area divided by the mean temperature difference between the fluid and the wall. i.e.

$$h = \frac{q_{con}}{A.(T-T_w)}$$

λ - the thermal conductivity of the fluid.

V_f - the velocity of the fluid.

ρ - the density of the fluid.

μ - the viscosity of the fluid.

C_p - the specific heat at constant pressure of the fluid.

On solution, this analysis yields the following equation:

$$\frac{hL}{\lambda} = c_1.\left(\frac{\rho V_f L}{\mu}\right)^{c_2}.\left(\frac{\mu.C_p}{\lambda}\right)^{c_3} \quad \ldots\ldots\ldots\ldots 7\text{-}5$$

where

$\frac{hL}{\lambda}$ = Nusselt Number.

$\frac{\rho V_f L}{\mu}$ = Reynolds Number.

$\frac{\mu C_p}{\lambda}$ = Prandtl Number.

and C_1, C_2 and C_3 are dimensionless constants which depend on the geometry of the flow system and on the régime of the flow. They are determined experimentally and are usually constant for a particular shape of flow system. Finkel[191] has developed a method for determining the average heat transfer coefficient in an internal combustion engine which is based upon this forced convection theory.

Generally, however, because of the considerable difficulty involved in constructing a complete formulation of the heat transfer problem and of solving for the three constants

in Equation 7-5, it is usually decided that, for any given location in an engine, the Reynolds Number exerts a considerably greater influence on the forced convection than does the Prandtl Number. On this basis, Equation 7-5 is reduced to:

$$Nu = c_1 . Re^{c_2} \quad \ldots\ldots\ldots\ldots\ldots\ldots 7\text{-}6$$

This modified approach has been used successfully in many studies aimed at predicting average heat transfer coefficients. Taylor and Toong [192], for example, utilized this basic method in deriving the following expression

$$\frac{h_{AV}.b}{\lambda} = 10.4\,(Re)^{0.75} \quad \ldots\ldots\ldots\ldots\ldots\ldots 7\text{-}7$$

in which h_{AV} is the average heat transfer coefficient over the entire engine cycle and b is the engine bore diameter.

Although results such as this shed light on the overall heat transfer rates in engines, no information about the instantaneous rates or how the convective heat transfer coefficient depends on the state of the working fluid is apparent. Strictly speaking, the use of the heat transfer coefficient, h, and, consequently, also of the expression

$$q_{conv} = A.h.(T - T_w) \quad \ldots\ldots\ldots\ldots\ldots\ldots 7\text{-}8$$

is only valid when the heat transfer occurs under steady conditions. As will be realized, conditions in engine cylinders are most unsteady since they vary cyclically. The applicability of heat transfer estimates, based on Equation 7-8, in engine cylinders is, therefore, debateable and is discussed more fully later in this chapter.

7.4.2. <u>ANALYSIS OF UNSTEADY HEAT TRANSFER.</u>

To understand and analyse the instantaneous heat transfer to and from the gases in an internal combustion engine, the

heat flow can conveniently be divided into steady and unsteady components. Steady heat transfer is defined as that which does not vary with time. It can be easily obtained from a heat balance on an engine. The unsteady component is, however, time dependent and is, thus, much more difficult to obtain.

Overbye et al[193] attempted some unsteady heat transfer measurements on a small, four-stroke, spark ignition engine. Their approach was to record simultaneously the temperature fluctuations in the charge and in the combustion chamber surface over a range of engine operating conditions. The analysis of their results is based on the general method to be described in the next section.

7.4.3. A SIMPLIFIED APPROACH TO THE THEORY OF UNSTEADY HEAT TRANSFER IN I.C. ENGINES.

Dahl[194] has shown that a one-dimensional flat plate analysis is valid for the heat transfer from a fluid to the walls of a cylinder which is either thin-walled or has little curvature. Since these requirements are frequently satisfied in the cylinders of I.C. engines, it is possible to conceive of a simplified model, such as that shown in Fig. 7-1[15], which is based on the flat plate analysis.

If it is now assumed that

i) the heat flow is in one-dimension only.

ii) conduction is the only mode of energy transport.

iii) the wall thermal conductivity is constant.

iv) the wall specific heat at constant pressure is constant

then the familiar one-dimensional Fourier equation for un-

steady heat transfer in a solid can be applied to this model

i.e. $$\frac{\partial T}{\partial t} = \alpha \frac{\partial^2 T}{\partial x^2} \quad \ldots\ldots\ldots 7\text{-}9$$

where $$\alpha = \frac{\lambda_w}{\rho_w C_{p_w}}$$

The gas temperature, T_g, at any instant in the engine cycle can be considered, for analysis purposes, to vary continuously according to the expression

$$T_g = T_{gm} + T_v . \cos(\omega t) \quad \ldots\ldots\ldots 7\text{-}10$$

in which

T_{gm} = the time-averaged value of the gas temperature over a complete engine cycle.

T_v = the maximum deviation of T_g from T_{gm} in the cycle.

ω = the angular frequency.

The solution of this problem has been considered in some detail by Jakob [195], Overbye [196] and Patterson [15] and the reader is referred to these works for an enlarged treatise on the subject. Briefly, however, the problem is conveniently solved by consideration of a steady state condition and a periodic condition at the cylinder wall (see Fig. 7-1).

i.e. $$T(x,t) = T_s(x) + T_p(x,t) \quad \ldots\ldots\ldots 7\text{-}11$$

where x is the distance into the cylinder wall.

On satisfaction of the following boundary conditions for the steady state and periodic considerations,

i) $T(d,t) = T_c$ = constant at $x = d$ (see Fig. 7-1).

ii) $$-\lambda_w . \frac{dT(0,t)}{dx} = h . \left[T_{gm} + T_v . \cos(\omega t) - T_s(0) - T_p(0,t) \right]$$

iii) $T_s(d) = T_c$

iv) $$-\lambda_w . \frac{dT_s(0)}{dx} = h . \left[T_{gm} - T_s(0) \right]$$

the complete solution of equation 7-9 has been found to be [197]

$$T(x,t) = T_c + \left[T_{gm} - T_c \right] . b_h . \frac{(d-x)}{(b_h d + 1)} + T_v . \gamma . e^{-r_\omega x} \cos(\omega t - r_\omega x - \epsilon_t) \quad \ldots\ldots\ldots 7\text{-}12$$

where

T_c = coolant temperature

$$r_\omega = \sqrt{\frac{\omega}{2\alpha}}$$

$$\eta = \sqrt{\frac{1}{1 + \frac{2r_\omega}{b_h} + \frac{2r_\omega^2}{b_h^2}}}$$

$$\epsilon_t = \tan^{-1}\left(\frac{1}{1+\frac{b_h}{\omega}}\right)$$

and $$b_h = \frac{h}{r_\omega}$$

Jakob[195] has tabulated some values of η and ϵ_t at various $\frac{b_h}{r_\omega}$ ratios. A few of these are reproduced below:

$\frac{b_h}{r_\omega}$	η	$\frac{360\epsilon_t}{2\pi}$
0	0	45°
.1	.0673	42°- 16'
1	.447	26°- 34'
10	.905	5°- 12'
100	.990	0°- 34'

By differentiating Equation 7-12 with respect to x and then multiplying by λ_w, an expression is obtained for the instantaneous heat transfer to the wall ($x=0$) per unit area. Thus,

$$\frac{q_{con}}{A} = -\lambda_w \cdot \frac{dT(0,t)}{dx}$$

$$= -\lambda_w\left[T_{gm}-T_c\right]\frac{b_h}{(b_h d+1)} + \sqrt{2}\,\lambda_w r_\omega T_v \eta \cos\left(\omega t - \epsilon_t + \frac{\pi}{4}\right) \quad \ldots\ldots 7\text{-}13$$

which is also seen to be composed of a steady state part and a periodic part.

Computations based on Equations 7-12 and 7-13 using typical values in engines show certain trends in the temperature distribution throughout the wall and in the heat

flux density. For example:

i) the amplitude of the gas temperature is greatly damped at the gas-wall surface ($x=0$) interface.

ii) there is a phase lag of ϵ_t (just less than 45°) between the temperature fluctuations in the gas and the wall ($x=0$). These observations are shown more clearly in Fig. 7-2.

Oguri[198] has shown that this 45° phase lag is approximately double that which actually exist in an engine.

iii) If ϵ_t is exactly equal to 45°, the heat transfer through the surface is exactly in phase with the temperature variation of the main body of gas. For the cosinusoidal gas temperature variation assumed, however, the gas temperature fluctuations lag the surface heat transfer fluctuations by the small amount $\left(\frac{\pi}{4}-\epsilon_t\right)$. This is shown diagrammatically in Fig. 7-2. However, it is known that this phase relationship is not correct since, in actual engines, the gas temperature fluctuations lead the heat transfer fluctuations by a few degrees.

Although this type of analysis gives a better understanding of the unsteady heat transfer in i.c. engines, it is very far removed from reality. Hence, the results are not directly applicable. The principle sources of error are:

a) the assumption that the gas temperature varies cosinusoidally. This completely over-simplifies the problem. A more complete solution may be obtained if the gas temperature is expressed in a Fourier series of the form

$$T_g = T_{gm} + \sum_{n=0}^{\infty} \left[K_n . \sin(n\omega t) + G_n . \cos(n\omega t) \right] \quad \ldots\ldots 7\text{-}14$$

where K_n and G_n are Fourier coefficients and n is the harmonic number.

b) variations in the heat transfer coefficient with change in such parameters as mixture motion, pressure, temperature etc. were not considered.

c) the boundary condition $T_s(d) = T_c$ is only an approximation to reality since Overbye et al[193] found that the wall temperatures at this point in the cylinder always exceed the coolant temperature by a few degrees.

d) boundary layer effects are ignored.

From the foregoing, it is seen that the objections to the use of Equation 7-3 in calculating the instantaneous heat transfer rates in engine cylinders (see Section 7.4.1) can now be reinforced by the phenomenon of the phase lag between the heat transfer and the gas temperature fluctuations. In spite of this, however, it still appears reasonable to regard conditions as at least quasi-steady. This would enable instantaneous values of the heat transfer coefficient, based on the state of the charge at any particular instant, to be used in Equation 7-8. The following reasons are considered to justify this approach:

i) the actual quantity of heat transferred during a period of crankangle rotation when the instantaneous heat transfer coefficient varies widely is only a small fraction of the total heat transferred during a cycle. Thus, errors will tend to be quite small.

ii) Oguri[198] has shown the phase lag between the heat

transfer fluctuations and the gas temperature fluctuations to be quite small. Thus, the instantaneous heat flows are not appreciably influenced by this effect.

In this work, therefore, Equation 7-8 is used to obtain the instantaneous rates of heat transfer when instantaneous values of T_g, T_w and A are used and also when appropriate values of 'h' are correspondingly employed.

Many attempts have been made over the years to accurately predict values of the heat transfer coefficient, h, from expressions which utilize the prevailing conditions of the working fluid at any particular point in the cycle. This has proved most difficult because of the dependence of h on such variable quantities as pressure, temperature, density, mixture motion and heat capacity of the charge. Further complications are that it tends to vary not only from engine to engine but also from point to point in the same engine. This situation led Annand[23] to propound that one must resort to quite unrealistic simplifications in the derivation of such an expression, the final form of which must inevitably be most elementary.

Nevertheless, many investigators have proposed many such expressions, most of which are reviewed in the following section.

7.5. [illegible]

The first concrete expression for the calculation of instantaneous heat transfer rates was put forward in 1923 by Nusselt[190]. He proposed a formula based on measurements of heat losses from the combustion of air/fuel mixtures in

cylindrical bombs. Both convective and radiative heat transfer were considered. His expression is

$$\frac{q}{A} = 0.99\left(P^2 T_g\right)^{1/3}\left(1+1.24V_p\right)\left(T_g - T_w\right) + 0.362\left[\left(\frac{T_g}{100}\right)^4 - \left(\frac{T_w}{100}\right)^4\right] \text{ kcal/m}^2\text{-hr} \quad \ldots\ldots 7\text{-}15$$

in which

A is the surface area exposed to heat transfer (metres^2).

and V_p is the mean piston speed (metres/second).

Orlin[199] adjusted Equation 7-15 to coincide with his own data on overall heat losses. The alteration is confined entirely to the bracketed piston speed term in which the Nusselt quantity $(1 + 1.24V_p)$ is replaced by $(3.5 + 0.184V_p)$.

These two formulae are unacceptable because:

i) the combustion of quiescent mixtures in bombs is in no way comparable to the highly turbulent burnings in spark ignition engines.

ii) the use of the mean piston speed to characterise the gas movement inside the engine cylinder is very approximate.

iii) Nusselt's basic approach can only determine the heat transfer by free convection since his heat loss measurements were made only after combustion had been completed.

Eichelberg[17] was the first to attempt direct measurements of instantaneous heat transfer rates in a firing engine. Because of the historical importance of his formula and its continuing world wide appeal, it is discussed in some detail. Eichelberg's method was to record simultan-

ously the instantaneous metal surface temperatures at a point both inside the combustion chamber and at the corresponding point on the wall-coolant interface. These were then analysed using harmonic techniques to obtain the heat transfer rate at any instant. Eichelberg's formula is

$$\frac{q}{A} = 2.1 \left(V_p\right)^{1/3} . \left(P.T_g\right)^{1/2} . \left(T_g - T_w\right) \text{ kcal/m}^2\text{-hr} \quad \ldots\ldots 7\text{-}16$$

Despite its great simplicity, many criticisms have been levelled against it. These include:

i) it may not be applicable to modern fast running engines since it was derived from measurements on a) a large 600 mm bore x 1000 mm stroke, 2-stroke engine running at 100 rev/min and b) a 4-stroke, 280 mm bore x 420 mm stroke engine running at 211 rev/min.

ii) the separate influences of the radiative and convective components cannot be attained.

iii) radiative heat transfer is allowed for in a most unsatisfactory manner viz. by increasing the power of Tg and decreasing the power of P by empirical means.

iv) the temperature measuring thermocouples employed were very crude and were inserted 0.25 mm below the surface. At such a location, the temperatures are greatly damped (see section 7.4.3.) and, although correction factors were incorporated to allow for this damping, these must be regarded as inaccurate.

v) the representation of the mixture motion in the engine cylinder by the mean piston speed is not realistic.

vi) Annand[23] has shown the expression to be dimensionally inaccurate.

In 1951, Pflaum[200] attempted to overcome some of these objections and did some tests on a 15 cm bore x 19 cm stroke precombustion chamber engine. He amended the speed dependent term in Eichelberg's formula and applied correction factors to account for variations in the intake manifold pressure and in the heat flow to different parts of the combustion chamber. His formula is:

$$\frac{q}{A} = f(K_L).f(P_i).f.(V_p).(P.T_g)^{1/2}.(T_g - T_w)\ chu/ft^2 sec \quad \ldots\ldots 7\text{-}17$$

in which

V_p is the mean piston speed (ft/sec).

A is the surface area exposed to heat losses (ft^2)

$f(K_L)$ is a term intended to cover heat flow variations to different parts of the combustion chamber.

$f(P_i)$ is an empirical factor to represent the effects of induction manifold pressure.

and

$$f(V_p) = 3.0 \pm 2.57\left[1 - exp \pm (1.5 - 0.127\,V_p)\right]$$

where the positive signs are for V_p greater than 11.8 ft/sec and the negative signs are for V_p less than 11.8 ft/sec.

Alcer[201] extended the basic Eichelberg approach in evaluations of the instantaneous heat transfer in 2-stroke and 4-stroke diesel engines with much more refined instrumentation. Using dimensional analysis, the following relationship was obtained:

$$Nu = 6.5.\left(1 + \frac{\Delta s}{2.C_p}\right).\left(Re.Pr.\right)^{1/2} \quad \ldots\ldots 7\text{-}18$$

where Δs is the increase in entropy per unit mass from the

start of compression. This expression provides good agreement when applied to two-stroke engines but poor agreement for four-stroke engines.

Chirkov and Stefanovski[202] in 1958 proposed a rather theoretical relationship based on a dimensional analysis of the convective part only of the heat transfer. This has the form

$$Nu = \text{CONSTANT} \times b^{5/12} (Re)^{0.25} \quad \ldots\ldots 7\text{-}19$$

Annand[23] has criticised this formula on the grounds of its dimensional incorrectness.

In 1960, Oguri[198] experimented with true surface thermocouples on a small, four stroke, spark ignition engine. In the analysis of his results, he adopted the dimensional approach as developed by Elser and finally arrived at the following formula:

$$Nu = 1.75\left(1 + \frac{\Delta s}{c_p}\right) \cdot \left(Re \cdot P_r\right)^{1/2} \cdot \left[2 + \cos\left(\theta - 20^\circ\right)\right] \quad \ldots\ldots 7\text{-}20$$

where Δs has the same significance as in Equation 7-18 and θ is the crankangle from T.D.C. The bracketed term $\left[2 + \cos(\theta - 20^\circ)\right]$ is an attempt to represent the variation in piston speed with crankangle.

In 1960, Overbye et al[193] reported on some detailed tests they performed on the problem of unsteady heat transfer. These were conducted on a small, four-stroke, spark ignition engine and a most refined Bendersky thermocouple was used for the surface temperature measurements. Motored as well as fired engine cycles were analyzed using Eichelberg's basic approach at a variety of intake manifold pressures. The availability of an electronic computer greatly increased the scope of the experiments since it enabled more detailed harmonic analyses of the test measurements to be made. Because of the wide fluctuations in heat trans-

fer coefficients throughout the engine cycle and the phase lag, Overbye et al were discouraged from expressing their measurements in instantaneous heat transfer coefficient terms. They did, however, propose an empirical formula for motored engine instantaneous heat transfer. This is

$$\frac{qS}{3600 A \lambda_i T_{gi}} = \frac{(S V_p \rho_i C_{p_i})}{\lambda_i} \cdot \left(\frac{0.26 P}{CR. P_i} - .035 \right) \times 10^{-4} + \frac{0.1 P}{CR. P_i} - 0.02 \quad chu/ft^2 sec. \qquad \ldots\ldots\ldots 7\text{-}21$$

where

S is the stroke of the engine (ft)

A is the surface area (ft^2)

λ is the thermal conductivity (c.h.u./ft.sec°C).

V_p is the mean piston speed (ft/sec).

ρ is the density of the charge (lb/ft^3).

C_p is the specific heat of the fluid at constant pressure (c.h.u./lb.°C).

and the subscript 'i' refers to conditions at the intake manifold.

This expression has been criticised because the wall temperature, T_w, does not appear. Overbye and his co-workers suggested that estimations of heat transfer rates in fired engines be obtained by multiplying 'q' in Equation 7-21 by the ratio of the difference between the gas and wall temperatures for the fired and motored cases.

Chronologically, the next important heat transfer expression to be published was that of Annand[23]. However, since this is the one which is used in this study to obtain the instantaneous heat flows in the Renault engine, its derivation and description is left until the end of this review.

In 1965, Eichni [203] published the results of his work on heat transfer from constant volume bombs. He did, in fact, repeat Nusselt's [190] technique but with much improved instrumentation. Whereas, however, Nusselt estimated the heat loss using the 1st Law of Thermodynamics in differential form.

i.e. $$\frac{dQ_v}{dt} = \frac{dE}{dt} - \frac{dQ}{dt}$$

where

Q_v is the heat of combustion.

E is the internal energy.

and Q is the heat transfer.

Eichni utilized Michelberg's technique of measuring the variation with time of the wall surface temperatures and using them to solve the Fourier differential equation stated in Equation 7-9.

Using the basic Nusselt-Reynolds Number expression in Equation 7-6, he derived the following relationship

$$h = c_1 L^{(c_2-1)} \cdot P^{c_2} \cdot U^{c_2} \cdot T_g^{(0.75-1.62c_2)} \quad kcal/m^2 hr\,^\circ C. \qquad \ldots\ldots 7\text{-}22$$

where L is a characteristic unit of length (metres) and U is the local average gas velocity in the cylinder (metres/sec).

To an approximation, the velocity is expressed as

$$U = b_1 V_p$$

during the scavenging period where b_1 depends on the fluid flow conditions. At this stage of the engine cycle, Eichni suggests that the instantaneous heat loss can be estimated from

$$\frac{q}{A(T_g - T_w)} = 110\left[L^{-0.2} P^{0.8} (b_1 V_p)^{0.8} T_g^{-0.53}\right] kcal/m^2 hr\,^\circ C. \qquad \ldots\ldots 7\text{-}23$$

and

$b_1 = 6.18.$

during combustion and expansion, b_1 was found to be 2.28 reflecting the decrease in fluid motion during these phases. However, Woschni considered that the mixture motion, U, at this time is supplemented by some flame generated turbulence, U_c. Thus,

$$U = b_1 V_p + U_c .$$

The variation in U_c is obtained from an approximation to the heat release curve since this source of turbulence increases rapidly from zero at the beginning of combustion, reaches a maximum and then decays appreciably during expansion as does the heat release. Its magnitude is estimated from

$$U_c = \frac{b_2 V T_{g1}}{P_1 V_1} \cdot (P - P_o)$$

where

b_2 is a constant.

V is the instantaneous cylinder volume.

P_1 and T_{g1} are the known states of the charge at the reference volume V_1 (e.g. at inlet valve closure).

and P_o is the gas pressure in the cylinder of the corresponding motored engine.

Thus, during combustion and expansion,

$$\frac{q}{A(T_g - T_w)} = 110 . L^{-0.2} . P^{0.8} . T_g^{-0.53} \left[b_1 V_p + \frac{b_2 V T_{g1} (P - P_o)}{P_1 V_1} \right]^{0.8} + \gamma \sigma \left[\frac{(.01 T_g)^4 - (.01 T_w)^4}{(T_g - T_w)} \right] \text{ kcal/m}^2\text{hr}^\circ\text{C} \quad \ldots\ldots\ldots 7\text{-}24$$

and $b_2 = 3.24 \times 10^{-3}$ m/sec.$^\circ$C

and $\gamma = 0.6$ (determined only for steady diesel flames).

Woschni's work appears to be subject to several criticisms. For example:

1) His final heat loss expressions only appear to be

directly applicable to combustion chamber geometries of similar form to that on which his work was conducted.

ii) no information on the compatibility of his formulae to spark ignition engine combustion is given.

Hassan[204] recognized the importance in heat transfer work of actual measurements of the gas velocities in the combustion chamber. Using a hot-wire anemometer, he was able to obtain such quantities in a specially designed pre-combustion chamber engine under motoring conditions. Instantaneous gas temperatures, pressures and wall temperatures were also measured. The computed local Nusselt and Reynolds Numbers were correlated on the basis of flat plate heat flux relationships. The experimental results fitted a relationship of the form

$$Nu = c_1 . Re^{0.8} \quad \ldots\ldots\ldots\ldots\ldots\ldots 7-25$$

where c_1 varies between .0184 and .0276. As with Eichni's expression, however, Hassan's only seems to be applicable to engine combustion chambers of the same form as was used in his work.

As stated previously, the heat transfer expression of Annand[23] is used to estimate the instantaneous heat flows from the working fluid in the Renault engine during the compression, combustion and expansion phases. Annand set out to derive his own heat transfer expression after reviewing the previous work in this field and concluding that no formula satisfied all the requirements. The formulae of Nusselt, Michelberg, Brilling and Chirkov and Stefanovski

be considered to be unreliable because of dimensional incorrectness. Thus, they cannot be extrapolated to predict heat transfer rates under conditions far removed from those of the experiments on which they were based. He faults the formulae of Elser and Eguri because of the inclusion of incorrect terms whilst Overbye's is criticised because the wall temperature variation is not allowed for.

Recognizing the limitations in attempting to include all the parameters which can influence heat transfer, he considered the following requirements to be of prime importance.

i) the convective and radiative components should be clearly distinguished since both are expected to vary not only from engine to engine but also in different parts of the same engine.

ii) in convective heat flow, the influence of the Prandtl Number in equation 7-5 is completely swamped by that of the Reynolds Number. Thus, equation 7-5 is reduced to the form of equation 7-6.

iii) that radiant heat losses should be accounted for by the familiar expression

$$q_{RAD} = e_c . A . (T_g^4 - T_w^4)$$

where $e_c = \sigma \times \delta \times F_g$ (see equation 7-4). Such values of e_c should be appropriate to the different types of surface and mode of combustion which exist.

Thus, from these considerations, Annand proposed that the total heat flux could be represented by an equation of the form

$$\frac{q}{A} = c_1 . \frac{\lambda}{b} . (Re)^{c_2} . (T_g - T_w) + e_c (T_g^4 - T_w^4) \quad \ldots\ldots 7\text{-}26$$

To obtain the constants c_1 and c_2 in this expression,

the measurements of Elser were subjected to re-examination. Comparisons were also made with the measurements of Overbye and Bichelberg, with some local heat flux measurements in spark ignition and compression ignition engines and with mean overall heat transfer data. These appraisals led Annand to suggest the following values of the constants in equation 7-26:

$c_2 = 0.7$

$c_1 = 0.35$ to 0.8 for normal combustion. c_1 increases with increases in the intensity of charge motion.

$e_c = 0$ during compression.

$e_c = 1.03 \times 10^{-13}$ cal/cm^2 sec$^\circ$K^4 for spark ignition engines.

$e_c = 0.777 \times 10^{-12}$ cal/cm^2 sec$^\circ$K^4 for compression ignition engines.

This Annand formula is used to predict the instantaneous heat flow rates in this work because it satisfies more of the basic theoretical requirements more completely than do most of the other expressions. It is also dimensionally correct and can be applied to any combustion space geometrical design. Since, however, the Reynolds Number has to be estimated from

$$Re = \frac{\rho V_p b}{\mu} \qquad \ldots\ldots\ldots\ldots\ldots 7\text{-}27$$

it suffers from the same weakness of characterizing the mixture motion by the mean piston speed as do most other formulae.

Quantitatively, the use of the mean piston speed in this content may not be too inaccurate since Kolchanov[109] has shown that, in engines with no large scale swirl motion, the gas velocities immediately after inlet valve closure approximate closely the mean piston speed.

Some investigators have suggested the use of the instan-

taneous piston speed to represent the mixture motion. This is not considered to be a useful criterion, however, since at or near top dead centre when the heat losses are greatest, this speed is either zero or very low. The reverse situation applies at mid-stroke.

It is apparent from the foregoing that there is a great need for fundamental measurements of gas motion in the engine combustion space from the viewpoint of heat transfer predictions.

7.5.1. APPLICATION OF THE HEAT TRANSFER EXPRESSION OF ANNAND [illegible] SIMULATED COMBUSTION MODEL.

Annand's expression is given in Equation 7-26. In this,

A is the instantaneous surface area across which the heat flow occurs (cm^2)

T_g is the instantaneous charge temperature (^oK)

and T_w is the mean wall temperature in the engine at an instant of time (^oK).

The value of c_1 was chosen to be 0.4 because the total heat losses, expressed as a percentage of the heat of combustion, with this value were found to coincide closely during combustion with those observed by several workers in the literature. i.e. about 6-7% (see Section 7.4.1). It also indicates quite a low degree of mixture motion as might be expected in the Renault hemispherical combustion chamber. The mean piston speed term, used to represent flow velocities in the Reynolds Number grouping (see Equation 7-27) is obtained from

$$V_p = 2S.n/60 \ cm/sec$$

where S is the engine stroke in centimetres.

In all heat transfer calculations, the combustion chamber wall temperatures are basic factors. In practice, these vary not only from point to point in the combustion chamber but also from one instant to another. Allowance for all these individual effects makes heat loss calculations unnecessarily confusing. In this work, therefore, the combustion chamber surface is subdivided into three main zones each having its own characteristic and constant temperature as follows:

i) the area of cylinder head surface involved in the heat flow at an instant of time, A_H, at a temperature, T_H, of 420°K.

ii) the area of piston surface involved in the heat flow at an instant of time, A_p, at a temperature, T_p, of 520°K.

iii) the area of cylinder wall surface involved in the heat flow at an instant of time, A_c, at a temperature, T_c of 395°K.

These temperatures T_H, T_P and T_c were considered by Johnson[42] to be typical of those existing in spark ignition engines. Even if these are in error by ± 25° C however, the inaccuracies in heat loss estimations are only of the order of ± 2%[185]. This is due to the high charge temperatures prevailing during most of the engine cycle.

In Annand's formula, T_w can be calculated from

$$T_w = \frac{A_c T_c + A_p T_p + A_H T_H}{A} \qquad \text{-------- 7-28}$$

where

$$A = A_c + A_p + A_H$$

During compression and expansion, these areas are given by

$A_p = \pi b^2/4$ (cm^2)

$A_c = \pi D.y_c$ (cm^2)

and $A_H = 65.0\ cm^2$

where y_c is the distance (in centimetres) from the instantaneous piston position to the top of the cylinder block.

During the combustion period, however, a flame is propagating across the combustion chamber and the quantities A_c, A_H and A_p, in contact both with the burnt and the unburnt fractions of the charge, are continuously changing. These areas are functions of two parameters:

i) the distance of the flame front from the sparking plug. (see Fig. 5-4).

ii) the piston position. (see Fig. 5-4).

The method used to calculate these surface areas is based on the same technique as was used to obtain the burnt volumes of the charge at the various flame front and piston positions (see Chapter 5). The surface areas were, in fact, determined at the same time as the burnt volume estimations. Thus, results were obtained of the surface areas of the piston, cylinder wall and cylinder head in contact with the 'burnt' volumes of charge at all ten flame front positions and at all eleven piston positions (see Fig. 5-4).

Plots were then constructed of:

i) A_c against flame front position at all eleven piston positions.

ii) A_p against flame front position at all eleven piston positions.

iii) A_H against flame front position - only one plot was needed here since A_H does not vary with piston position.

Polynomial equations were fitted to each of these plots thereby allowing estimations, by interpolation, of A_H, A_p and A_c at intermediate flame front and piston positions between those for which actual measurements were made. A listing of these derived polynomials is given in SUBROUTINE AREA in the complete computer program listing in Appendix 8.

The gas properties involved in the heat loss calculations are evaluated at the prevailing instantaneous temperatures and pressures of the charge. All thermodynamic data and gas properties required are given in Appendix 7.

An additional point to note is that no heat exchange is allowed between the unburnt fraction of the charge and the surroundings during the combustion process. This is considered a good approximation to reality because Livengood et al[205] suggest that any heat loss from the unburnt charge at this time is offset by an equal heat transfer across the flame front from the burnt gases. Consequently, the unburnt gas is assumed to undergo isentropic changes of state. This may not in fact be strictly true since it is difficult to visualize how heat can be transferred from the burnt combustion products across the flame front to the mass of unburnt charge away from the close vicinity of the flame front.

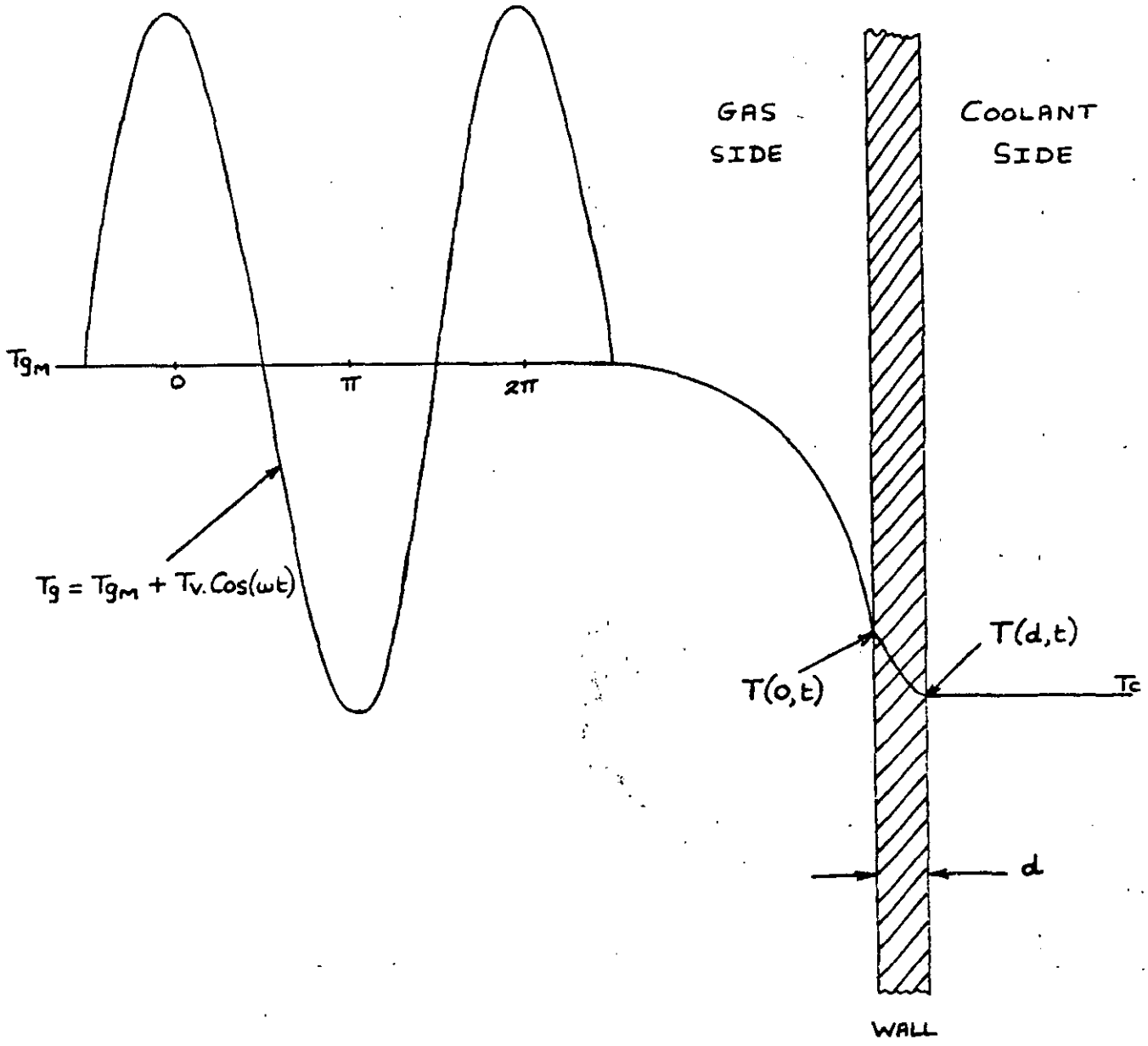

FIG. 7-1 —— HEAT TRANSFER MODEL FOR INTERNAL COMBUSTION ENGINE.

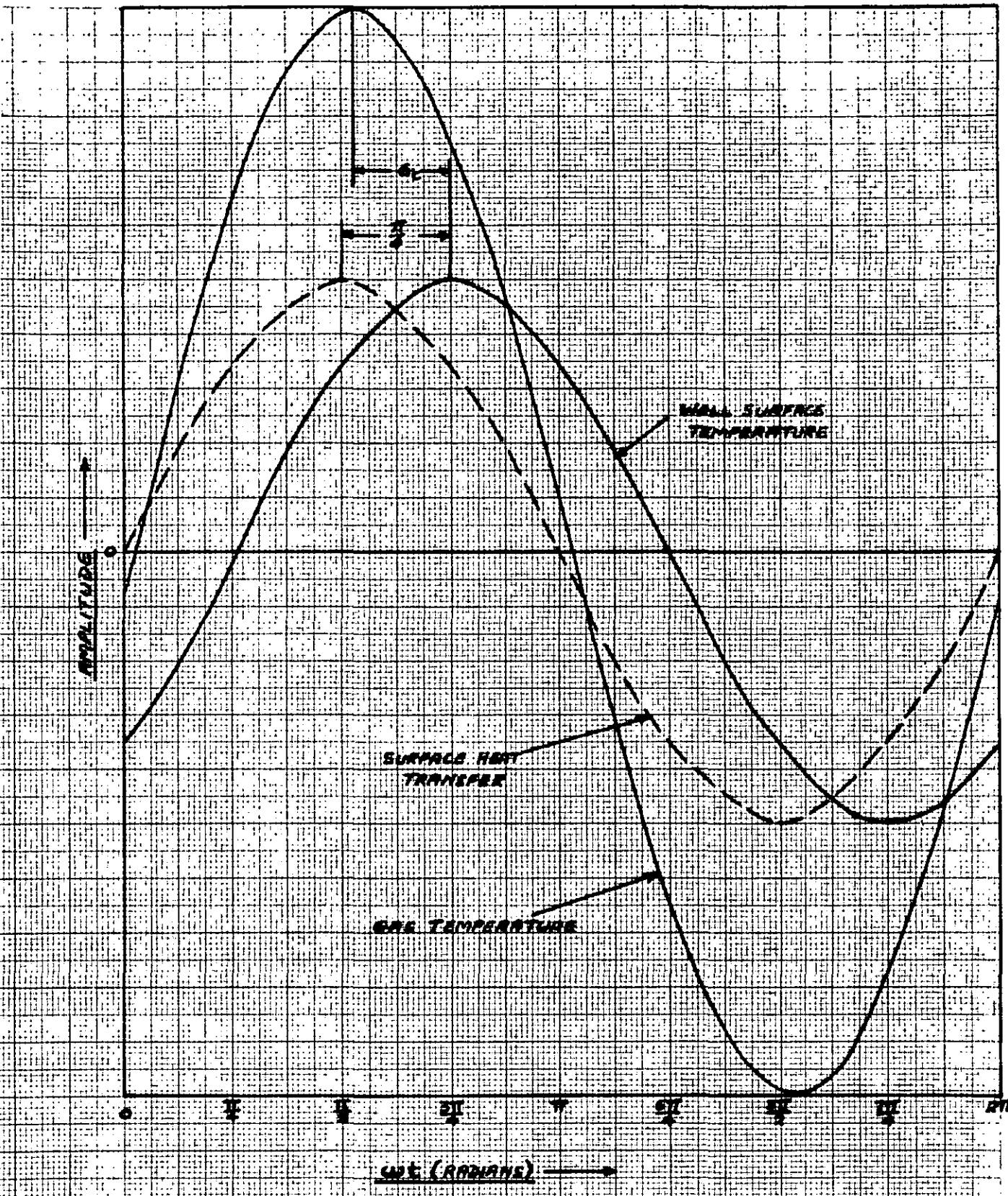

FIG. 7-2 — PHASE RELATIONSHIPS BETWEEN GAS TEMPERATURE, WALL TEMPERATURE AND SURFACE HEAT TRANSFER WHEN GAS TEMPERATURE IS ASSUMED TO VARY COSINUSOIDALLY

CHAPTER 8

ANALYSIS OF RESULTS AND DISCUSSION

CHAPTER 8

ANALYSIS OF RESULTS AND DISCUSSION

In an actual, firing spark ignition engine, whenever one particular variable is altered to observe its effect on, for example, cylinder pressure, flame travel time or σ emissions, the direct influence of this variable is completely obscured by variation in a great many other factors. Thus, if spark timing is retarded, one would expect the engine to react not only to this but also to the secondary effects such action generates, e.g. an increased mass fraction of exhaust residuals in the fresh charge, a higher charge temperature at inlet valve closure, a slight decrease in engine speed, etc.

The computer program which has been derived in this work, however, enables a parametric study of the effects of certain variables to be made without variation in other quantities. Although this tends to detract from the realism of actual engine combustion, it does nevertheless give an indication of the trends involved.

Thus, the computed results in this work refer to an investigation of varying each parameter in turn keeping all the others at specified values. The following parameters were altered during a series of runs:

i) equivalence ratio

ii) charge temperature at inlet valve closure

iii) ignition timing

iv) engine speed

v) charge pressure at inlet valve closure

vi) compression ratio

vii) mass fraction of exhaust residuals in unburnt mixture

viii) mass fraction of injected water in unburnt mixture

ix) fuel type, i.e. propane, iso-octane or benzene

The specified, reference values are:

a) equivalence ratio - 1.2

b) charge temperature at inlet valve closure - 373°K

c) ignition timing - 30°B.T.D.C.

d) engine speed - 2000rev/min.

e) charge pressure at inlet valve closure - 1ATM

f) compression ratio - 9

g) mass fraction of exhaust residuals in unburnt mixture - 0.06

h) mass fraction of injected water in unburnt mixture - zero

i) fuel type - iso-octane

Any deviations from these reference values are stated where they occur.

Details of the Renault engine which was used for the combustion simulation are given in Appendix 9. All flame travel time (F.T.T.) values refer to the number of crankangle degrees it takes the flame to propagate from the sparking plug to the position of ionization probe 2 in Fig. 4-41 (i.e. a distance of 6.85cm).

Before any computed results are given however, it is considered desirable to test the accuracy of the

computer model so that, if any large scale discrepancies occur between computed and experimental results, these are well noted and the limitations of the model fully realised. Such accuracy determinations are considered desirable in regard to three evaluations:

i) comparison of F.T.T. values to the position of ionization probe 2 in Fig. 4-41.

ii) comparisons of computed and experimental pressure-crankangle diagrams under identical engine operating conditions.

iii) comparison of the emission of certain exhaust gases, in particular CO and NO.

COMPARISON OF COMPUTED AND EXPERIMENTAL RESULTS

1) Variation in Flame Travel time with equivalence ratio

Fig. 8-1 shows the results obtained when iso-octane and benzene were the fuels. The techniques involved in experimental flame travel time measurements have been referred to in Chapter 4. It is noted that the agreement is fairly good for benzene up to an equivalence ratio of about 1.35 whereas, for iso-octane, the agreement only appears to be acceptable up to an equivalence ratio of approximately 1.2. After these points, an increasing divergence between computed and experimental results is apparent.

For both fuels, however, the equivalence ratios for minimum F.T.T. (computed results) are in marked disagreement with those for the experimental results which do not appear to have reached their minimum values

over the equivalence ratio range tested. This failure to indicate a minimum value was unexpected since Harrow and Orman[31] and Sale and Vichnievsky[209] observed a pronounced minimum value in their tests at equivalence ratios of approximately 1.34 and 1.25 respectively. Of course, the possible repeatability and accuracy of all these experimental results must be treated with a certain amount of suspicion owing to the difficulties in obtaining average values of the flame travel times due to the presence of cyclic dispersion and the probable variations in residual exhaust gases from one equivalence ratio to another. Nevertheless, they do give an indication of the equivalence ratio at which the F.TT. is a minimum with which the computed results can be compared.

The most probable reason for this discrepancy between computed and experimental results is that a surface model of turbulent flame propagation was used to determine burning velocities in the computer simulation. This means that the laminar burning velocity is the basic, determining factor which is then multiplied by a term proportional to the degree of mixture motion in the combustion chamber. As explained in great detail in Chapter 4 (Section 4.2.5) however, turbulent flame propagation must not be associated with laminar flame propagation. Laminar flame theories tend to predict the maximum burning velocities at the maximum burnt gas temperature which occurs slightly on the rich side of stoichiometric. Thus, the discrepancy in Fig. 8-1 between

equivalence ratios for maximum flame speed was not entirely unexpected. It is proposed that if a Volume turbulent flame propagation theory could be developed (see Section 4.2.4), the agreement between computed and experimental results would be much closer.

Reference should also be made, in this context, to the maintainance of constant conditions of the charge at inlet valve closure over the entire equivalence ratio range for the computed results. In practice, it is safe to hypothesize that this is quite an assumption since fuel evaporation effects, exhaust residual variations, etc., are bound to exist from one air/fuel ratio to another.

A further possible reason for the discrepancy between the computed and experimental results in Fig. 8-1 is the assumption that equilibrium conditions are maintained at all times in the burnt combustion products. The influence of non-equilibrium effects are, however, most difficult to gauge.

In the computed results, a certain amount of scatter is apparent in the curve plots. This is especially noted within the equivalence ratio range 0.9 to 1.2 (see Fig. 8-11 for a clearer indication of the scatter). Unfortunately, this is the range within which the equivalence ratio for minimum P.T.T. occurs and, as a result, it is most difficult to detail accurately where, in fact, this point is.

The cause of the scatter is associated with the make-up of the Semenov laminar burning velocity expression which is given in Equation 4-47. It has been noted that, when using such an expression to obtain the changes in burning velocity with equivalence ratio, certain approximations made in the

derivation of the expression are not consistent for the region near stoichiometric. Such inconsistency is shown graphically in Fig. 8-2 (from Dugger and Simon[147]) for the two fuels pentane and ethylene and it apparently results from assuming that the concentration of the fuel, $C_{f,\,eff}$, is much greater than that of the oxygen, $CO_{2,eff}$, or vice versa in the derivation (see Section 3.1).

To facilitate reasonable results in the region of stoichiometric, therefore, it was necessary to make certain adjustments to the Semenov expression. Dugger and Simon suggest averaging the burning velocities between equivalence ratios of 0.95 and 1.05. This is not considered a very good criterion, however, since the equivalence ratios at which the inconsistencies arise appear to be a function of fuel type (see Fig. 8-2). In this work, therefore, it appeared more reasonable and accurate to assume a linear increase (or decrease) in burning velocity between the equivalence ratios at 0.9 and 1.1. These adjustments are made in SUBROUTINE BURNVEL in the computer program listing (see Appendix 8).

The computed results (Fig. 8-11) indicate, as scatter, the errors which still persist in the modified expression. However, although the equivalence ratio for minimum flame travel time is not very well defined for each of the three fuels used (see Fig. 8-11), it is clear that it is considerably in error compared with the experimental results (see Fig. 8-1) and that it occurs within the range 1.0 to 1.15, i.e. in the region where the burnt gas temperatures are highest, as expected.

A certain amount of the scatter in Fig. 8-11 might also arise from very slight errors in the execution of the computer program especially with regard to the accuracy to which the iterations are taken (see Chapter 3).

ii) Comparison of computed and experimental pressure-crankangle diagrams

Such comparisons were made for both iso-octane and benzene over an equivalence ratio range from approximately stoichiometric up to very rich mixtures. The resulting plots are shown in Figs. 8-3 to 8-8.

All the experimental results were obtained with a Farnboro' Indicator so that a certain amount of scatter was apparent on all diagrams. In each case, a mean pressure-crankangle plot was constructed.

Once more, with regard to the computed results, difficulties were encountered in the inability to accurately set the initial conditions of the charge at inlet valve closure. This was especially so for the charge temperature, pressure and mass fraction of residual exhaust gases. These values were in fact held constant at 373^{o}K, 1.12 atmospheres and 0.06 respectively.

Fig. 8-3 shows the plots obtained at an equivalence ratio of 1.05 for iso-octane combustion. Quite large deviations are apparent in the comparison early on in the combustion which can be attributed to errors in the setting of the charge pressure at inlet valve closure and in the probable inaccuracy of the Farnboro Indicator when operating at low cylinder pressures with high pressure calibration springs fitted. The comparison otherwise seems to be

very reasonable since the rate of pressure rise and peak pressure value agree closely.

At an equivalence ratio of 125 (see Fig. 8-4) with iso-octane as fuel, there is observed to be much better agreement between the charge pressure at ignition and also quite good agreement during the remainder of the combustion and expansion phases.

However, at very rich mixture combustion (see Fig. 8-5 where the equivalence ratio is 1.42), there is seen to be a complete breakdown in the ability to predict, with reasonable accuracy, pressure-crankangle diagrams from the computer model. This is a direct result of the divergence between the computed and experimental flame travel times at very rich mixtures for iso-octane combustion as noted in Fig. 8-1. From this latter figure, it is apparent that the reasonable agreement between F.T.T. computed and experimental results at equivalence ratios of 1.05 and 1.25 is manifested in quite accurate pressure-crankangle diagrams at these ratios (see Figs. 8-3 and 8-4). Moreover, Fig. 8-5 corroborates the results in Fig. 8-1 for rich mixture, iso-octane combustion.

Turning next to some corresponding diagrams obtained for benzene combustion (Figs. 8-6, 8-7 and 8-8), much better agreement is obtained between computed and experimental results over the entire equivalence ratio range tested. This is a manifestation of the comparison shown in Fig. 8-1 between the computed and experimental F.T.T.'s

for benzene. However, in Fig. 8-8 when the equivalence ratio is 1.44, there is a distinct indication of lower computed cylinder pressures throughout combustion and expansion. This observation is in keeping with the divergence of the P.T.T.'s for benzene at rich mixtures (Fig. 8-1),

It should be well noted that such comparisons between computed and experimental pressure-crankangle diagrams cannot be considered entirely reliable since the computed results depend so much on the ability to correctly express the conditions in the unburnt charge at inlet valve closure. Nevertheless, they do appear to be indicative of the trends involved.

iii) Comparison of CO and NO exhaust gas emissions

Carbon Monoxide, CO

The variation in computed CO concentration with equivalence ratio is given in Fig. 8-9 under three sets of conditions:

a) at peak cycle temperature.

b) at the end of flame propagation.

c) at the end of expansion, i.e. at exhaust valve opening.

Additionally, since CO is primarily a function of air/fuel ratio and varies very little with other conditions of engine operation, some experimental results from the work of Huls et al[57] were used for comparison (see Fig. 8-9). These values are observed to lie between the computed CO concentrations at the end of combustion and at the end of expansion tending, at equivalence ratios greater than 1.1, to be closer to the values at the end of combustion.

It thus appears that continuous equilibrium is maintained at such mixture strengths for CO to at least part way down the expansion stroke which observation agrees with the kinetic results of Newhall[86]. The errors in assuming that equilibrium exists in the burnt combustion products at all phases of the engine cycle are clearly in evidence.

In the ensuing results for CO given later in this Chapter, the concentrations are given at all thethree points in the engine cycle noted above.

Nitric Oxide, NO

Unlike CO, NO is greatly affected by virtually every engine operating parameter (see Chapter 2). Thus, the possibility of quoting some experimental concentrations from the literature over the equivalence ratio range is fraught with danger. No measuring equipment was available for use on the Renault engine. Nevertheless, it is considered desirable to at least indicate, with full realisation of the inaccuracies involved, a typical NO concentration variation with equivalence ratio. For thispurpose, the work of Huls et al[57] was again utilized. These workers ran a CFR engine at 8:1 compression ratio on iso-octane, at 1000rev/min and at 30° B.T.D.C. spark timing. Their results are indicated on Fig. 8-10 together with the corresponding computer results at peak temperature, at the end of flame propagation and at exhaust valve opening.

From the comparison, it would appear that the frequently quoted prediction that exhaust gas NO concentrations correspond closely to peak cycle temperature calculations under equilibrium conditions is certainly approximately valid at equivalence ratios richer than 1.05. However, at mixtures

leaner than this point, no such correlation exists any more and it appears that equilibrium is a useless criterion on which to base results and conclusions (see Fig. 8-10). Once more, it must be emphasized that all the computed results refer to constant conditions in the unburnt charge at inlet valve closure.

iv) Concluding Remarks

It is evident from the foregoing that the computer simulated combustion model needs much more development with regard to non-equilibrium, kinetic considerations before a reliable tool for the prediction of obnoxious exhaust emissions can be obtained. What it can do, however, in its present form is to predict trends in CO and NO formation.

With regard to F.T.T., and pressure-crankangle diagram predictions, the model appears to be reasonably accurate over the equivalence ratio range from weak mixtures up to about 1.25. Thereafter, errors creep in which, it is considered, are the direct result of basing turbulent flame propagation on a laminar flame propagation theory. Non-equilibrium effects may also be important.

Operation of the 'digital engine' at an equivalence ratio of 1.2 is considered to be possibly the most accurate point in so far as flame travel time, pressure-crankangle diagrams and CO and NO emissions predictions are concerned. This is the reason why it has been chosen as the specimen reference value for the ensuing computer runs.

EFFECT OF VARYING ENGINE PARAMETERS ON THE COMPUTER RESULTS

Equivalence Ratio

Fig. 8-11 is a plot of the computed flame travel times against equivalence ratio for propane, iso-octane and benzene. It is apparent that benzene is a much faster burning fuel than propane which is, in turn, faster than iso-octane. No experimental tests were conducted in this work for propane combustion but a literature search appears to confirm that the order in which the computed flame travel times occur for the three fuels is correct (see Fig. 8-11). Fig. 8-1 certainly shows this to be so for iso-octane and benzene.

In Fig. 8-11 also, an interesting observation is that the benzene curve does not follow the marked "falls offs" in F.T.T., at very rich and very lean mixtures as exist in the iso-octane and propane curves. Phillipps and Orman[19], in their computer simulation of combustion have likewise noted this effect to a very small extent and their experimental results certainly show this sort of trend. The explanation for it appears to be that the burnt gas temperature does not decrease so greatly at very rich mixtures for benzene as for propane and iso-octane. For example, at an equivalence ratio of 1.5, the burnt gas temperatures at ignition for iso-octane, propane and benzene are 2115^{o}K, 2125^{o}K and 2284^{o}K respectively.

Figs. 8-12 and 8-13 show the trends in the computer predictions of the CO and NO emissions at peak cycle temperature with equivalence ratio variation. The influence of stoichiometry is very apparent.

Initially, it was most surprising that the CO concentrations for iso-octane were slightly higher than for propane. However, close scrutiny in consideration of the stoichiometry of the three fuels revealed the explanation. This is that the stoichiometric air/fuel ratios are 15.6:1, 15.05:1 and 13.2:1 respectively for propane, iso-octane and benzene. This means that:

for propane

1 part of fuel combines with 15.6 parts of air by weight.

for iso-octane

1 part of fuel combines with 15.05 parts of air by weight.

for benzene

1 part of fuel combines with 13.2 parts of air by weight.

Thus, in terms of equivalence ratio plots, a slightly 'leaner' type of combustion is obtained for propane than for iso-octane which, in turn, is leaner than benzene and this gives rise to the plots shown in Fig. 8-12. This is a good illustration that the influence of air/fuel ratio on CO formation is much greater than that of temperature.

The NO emissions at peak cycle temperature (see Fig. 8-13) with equivalence ratio variation for the three fuels used are, on the other hand, seen to follow the burnt gas temperature variation. It should be noted that all these computer runs were conducted at constant ignition timing so that, at a given point during flame propagation, the mass burnt, and thus pressure rise, is greatest in the order benzene, propane, and iso-octane. The influence of pressure on equilibrium NO concentrations is clearly seen in Figs. 6-9, 6-24 and 6-39. The higher pressure

levels for propane combustion at rich mixtures might, therefore, be the reason for the convergence of the iso-octane and propane curves which effect probably predominates over the temperature effect. Conversely, one might argue that the temperature effect is the stronger for benzene (see Fig. 8-13).

Charge Temperature at Inlet Valve Closure

Fig. 8-14 shows the large reduction in flame travel time (F.T.T.) with increase in charge temperature. The same sort of trend was obtained by Phillipps and Orman[19] and is the direct result of the increase in burning velocity arising from the gains in the burnt and unburnt gas temperatures.

Such increases in burning velocity are manifested in very high rates of pressure rise as shown on the accompanying pressure-crankangle diagrams - see Fig. 8-15. From these, it is apparent that a knocking condition probably exists at the higher charge temperatures. The increases in initial charge temperatures result in corresponding decreases in the masses of charge in the cylinder at the inlet valve closure when pressure remains constant at this point. This is reflected in the constancy in the peak cylinder pressures at the higher temperatures.

The effect of increasing this parameter on CO concentrations at various points in the cycle is shown in Fig. 8-16. The expected increase is obtained due to there being more dissociated CO at the higher burnt gas temperatures. Also evident is the tendency for the peak temperatures and end of combustion concentrations to merge at

high initial charge temperatures. This is due to the burning velocity being so high at this time. The concentrations at the end of expansion are constant owing to the assumption that the combustion products are frozen below 1600°K.

The expected variation in NO concentrations at peak cycle temperature with initial charge temperature variation was obtained - see Fig. 8-17.

Ignition Timing

Fig. 8-18 illustrates the computed effect of ignition timing on flame travel time. It is noted that a pronounced minimum occurs at an ignition timing of about 33°B.T.D.C. under the stated engine running conditions. Advances in timing beyond this point tend to result in lower flame speed values. This is possibly due to there being quite low unburnt charge temperatures at ignition with consequent lower burning velocities during the initial stages of combustion. The effect of a retarded spark is also clearly seen.

The corresponding effects on the pressure-crankangle diagrams of ignition timing variations are shown in Fig. 8-19. As expected, the rates of pressure rise and peak cylinder pressure levels increase markedly with spark advance. The plots for the higher spark advance on expansion cross those for the lower spark advance because, at the point of cross-over, the lower spark advance diagrams show combustion still taking place.

Figs. 8-20 and 8-21 plot the effects of ignition timing on CO and NO emissions. The increase in dissociated CO at high burnt gas temperatures (i.e. at high spark advance) is

evident. Also apparent is the divergence between the points of peak temperature and end of combustion at retarded sparks.

The pronounced effect of retarded ignition on peak cycle NO concentrations is clear from Fig. 8-21. This is again primarily a temperature effect.

An additional observation of note is the increase in burnt gas temperature at exhaust valve opening when the spark is retarded. This effect assumes significance as a possible means of reduction of unburnt HC and CO in the exhaust manifold and pipe (see Chapter 2) - Fig. 8-22.

Engine Speed

The graphs of flame travel time - v - engine speed and cylinder pressure v - crankangle at various engine speeds are shown in Figs. 8-23 and 8-24. There is observed to be an increase in F.T.T. with increasing engine speed which is a computer manifestation of the fact that the degree of turbulence in the Renault does not increase proportionately with engine speed. Hence, the necessity to advance the spark. Additionally, it was found that, at a given crankangle in the cycle over the engine speed range tested, the mass burnt (and hence pressure rise and burnt gas temperature) was higher at the lower engine speeds. This resulted in higher burning velocities at such speeds which effect was offset slightly by higher heat losses. Phillipps and Orman[19] presented computed results showing not such a great dependence of F.T.T. on engine speed as was obtained in this work.

The increasing rate of burn is reflected in the pressure-crankangle diagrams (Fig. 8-24) where maximum

pressure rise rates and pressure levels are greater for the lower engine speeds. The plots for the higher engine speeds on expansion cross those for the lower engine speeds because, at the point of cross-over, the high engine speeds diagrams show combustion still taking place. The expansion part of the diagrams is higher for higher engine speeds because combustion is completed later in the engine cycle and because there is less time for heat losses to occur.

Fig. 8-25 shows the computed variations in flame speed with engine speed at various crankangle positions throughout combustion. The large jumps in flame speed just after ignition are the result of the transfer of the burning régime from laminar to turbulent due to the "boundary layer" effect close to the combustion chamber walls (see Chapter 2). Another contributory effect is the flame propagation pattern developing from a spherical form just after ignition to that shown in Fig. 5-4. The very uneven propagation rates during combustion are the direct consequences of certain inaccuracies in the technique of determining burnt gas volumes by the plaster-of-paris method (see Chapter 5). These should not detract from the accuracy of the results, however, since they remain present for all operating conditions. Additionally, they might be considered as giving an unexpected degree of reality to this computer model since it is most probable that combustion does, in fact, develop in this manner, due to inhomogeneous turbulence considerations.

The general appearance of the flame speed over the combustion phase seems to reflect the experimentally

observed trends, i.e. of a 'delay period', followed by very fast burning and culminating in a flame speed 'fall-off' due to the expansion of the newly burnt gases taking place mainly in the direction of the already burnt charge (see Chapter 2).

Fig. 8-26 is the variation in CO concentration with engine speed. The very slight decrease at high speeds is considered attributable to lower peak cycle temperatures. In actual engines, such variations with engine speed are completely obscured by changes in other parameters.

According to this equilibrium combustion model, the NO concentrations at peak cycle temperature decrease with increasing engine speed. This trend (see Fig. 8-27) agrees with some noted experimental observations and a discussion on why this should be is given in Chapter 2 (Section 2.2).

Charge Pressure at Inlet Valve Closure

The Semenov laminar burning velocity expression (Equation 4-47) stipulates that pressure has no effect on burning velocities. Thus, in these computed results, any possible influence which pressure has on the F.T.T. in the engine must arise through its influence on other variables in the charge.

In this context, Fig. 8-28 shows the computed F.T.T. plot obtained with initial charge pressure variation. To obtain an explanation for this, it is expedient to bear in mind that three main factors (besides turbulence levels) determine the rate of flame propagation in the equilibrium computer simulation:

a) burnt gas temperatures which are affected by pressure

levels and heat losses.

b) unburnt gas temperatures.

c) the extent of the expansion of the newly burnt volumes of charge ahead and behind the flame front (see Section 2.1).

The unburnt charge temperatures were found to be constant at ignition and generally unaffected by varying initial pressures throughout combustion for all the computer runs in Fig. 8-28. Thus, this influence can be eliminated as a possible cause of the F.T.T. trend noted.

The burnt gas temperature effect, on the other hand, is much more relevant since it was observed that the following peak cycle temperature values, and some other corresponding values at the peak cycle temperature point, were obtained.

Initial Charge Press. (ATM)	Heat Loss Rate(cal/°CA)	Cylinder Pressure(psi)	Peak cycles Temp.(°K)
0.5	0.181	212.7	2545.3
1.0	0.288	439.7	2570.5
1.25	0.300	508.5	2565.6
1.5	0.341	615.7	2569.1

From this table, it is clear that the burnt gas temperatures do not increase in the same proportion as the pressure. To explain this, it is necessary to consider the effects of pressure on dissociation. The graphs in Figs. 6-3 to 6-47 predict the trend of less dissociation at high pressures and vice versa. Less dissociation correspondingly means higher burnt gas temperatures.

Applying these arguments to the plot obtained in Fig. 8-28 and to the table listed above, it is apparent that, at the low initial pressure of 0.5ATM, dissociation

is relatively high which effect reduces the burnt gas temperatures. This explanation is in agreement with the peak temperature value in the table above. The heat loss rate at this time is comparatively small.

When the charge pressure at inlet valve closure is raised to 1ATM, the cylinder pressures throughout combustion are more than doubled, (see Fig. 8-29). This very large rise in pressure restricts the dissociation phenomenon in comparison with the previous case discussed above and, as a consequence, the burnt gas temperatures are much higher even though the heat loss rates are increased (see the table listed above).

Further increase in charge pressure at inlet valve closure to 1.25ATM gives higher cylinder pressure levels throughout combustion as exppcted (see Fig. 8-29) although the increases above those at 1ATM initial condition are very much less than the increases from 0.5 to 1ATM. As a result, dissociation is slightly less than at the 1ATM condition. This effect, combined with the slightly higher heat losses, produce the noted trend of marginally lower burnt gas temperatures than for the previous case and a longer F.T.T. (see the table listed above and Fig. 8-28). The greater restriction to the expansion of the newly burnt gases at very high pressure levels (see Section 2-1) might also be making a contribution at this time.

At an inlet charge pressure of 1.5ATM, the higher pressure levels apparent throughout combustion further inhibit the extent of the dissociation reactions occurring in the burnt gases so that one might expect a corresponding gain in the burnt gas temperatures. However,

the corresponding increases in heat losses with increase in pressure, as dictated by the Annand expression (Eqn. 7-26), once more restricts the burnt gas temperature levels obtained (see the table above). Additionally, the extent of expansion effect of the newly burnt gases is most probably again significant at such high cylinder pressures (see Fig. 8-29).

Thus, from the foregoing discussion, it appears that all the factors influencing burnt gas temperatures (noted previously) are non-linear. The manner in which they have interacted to produce the computed results presented in Fig. 8-28 is certainly complex.

Fig. 8-29 shows plots of the corresponding cylinder pressure - crankangle diagrams.

Fig. 8-30 illustrates the very small decrease in CO concentrations at peak cycle temperature with increasing charge pressure at inlet valve closure. This appears to be an effect due entirely to the mightier cylinder pressures (see Fig. 8-29) since peak cycle temperatures are very similar. At the end of combustion, on the other hand, the lower pressure levels and temperatures result in an almost constant CO concentration throughout.

Since it has already been noted that the degree of dissociation of the burnt combustion products decreases with increasing pressure, it comes as no surprise to find the NO concentrations, under equilibrium conditions, to be similarly affected. Fig. 8-31 shows this trend.

Compression Ratio

The graph of computed F.T.T. against compression ratio is shown in Fig. 8-32. Such a plot obviously requires some explanation. The same considerations can be applied here, however, as were used in the plot of F.T.T. against inlet charge pressure (Fig. 8-28). Thus, the flame speed determining factors, viz.

a) burnt gas temperature (and the manner in which this is affected by pressure levels through extent of dissociation effects, unburnt gas temperatures and heat losses).

b) unburnt gas temperatures.

c) the extent to which the newly burnt gases can freely expand (influenced by the pressure levels in the cylinder).

are again at work and it is the interplay of all these non-linear effects which has resulted in the plot shown in Fig. 8-32. The following table shows the peak cycle temperatures obtained in the computer calculations over the compression ratio range tested.

Compression Ratio	Peak cycle temperature (^{o}K)
5	2534
7	2560
9	2570
11	2609
14.2	2615

The temperatures certainly bear out the trends noted in Fig. 8-32.

At compression ratios around 5:1, it would appear that the relatively low unburnt gas temperatures and the

extra

relatively high degrees of dissociation are the main factors involved in establishing a fairly long F.T.T. When the compression ratio is increased to about 7:1, the unburnt gas temperatures become higher and there is less dissociation taking place at the higher pressures. From Fig. 8-31 and the table above, it appears that these effects have a greater influence on the burnt gas temperatures and flame travel times than have the increasing heat loss rates and restrictions to the expansion of the newly burnt gases. At around 9:1 compression ratio, the slight increase in the peak cycle temperature over that at 7:1 (see Table above) must result from the higher unburnt gas temperatures and the still lesser degree of dissociation. These effects seem to slightly counteract the greater heat loss rates once more.

Further increases in compression ratio beyond 9:1 give the entirely unexpected trend shown in Fig. 8-32. In terms of the above considerations, this is most difficult to explain unless non-linearities have a much more pronounced effect at this time and the much higher cylinder pressures (Fig. 8-34) reduce dissociation effects considerably. A further possible cause could be that the ignition timing, which has remained constant throughout, is ideal for this particular compression ratio (see Fig. 8-18).

With another increase in compression ratio to 14.2 (the highest to which this computer model could be taken), it seems that even though all the above effects which influence burnt gas temperature are apparent, the restriction to expansion effect of the newly burnt gases is the most significant.

This conclusion is drawn because thecomputed results show the burnt and unburnt gas temperatures to be highest at this compression ratio from which one might reasonably expect the shortest F.T.T. The only factor which could prevent this occurring is the very high cylinder pressures restricting the newly burnt gas expansion.

Fig. 7-33 is a plot (taken from the experimental work of Ellison, Harrow and Hayward[164]) of mean flame travel time against compression ratio in a C.F.R. engine under the conditions stated. It will be observed that the same trend of a marked decrease in F.T.T. with increase in compression ratio at the lower compression ratios is apparent in both the experimental results (Fig. 8-33) and in the computed results (Fig. 8-32). The similarity persists at the higher compression ratios since a further large decrease is apparent in F.T.T. This is considered to be purely fortuitous, however, since knock was induced at this time in the C.F.R. engine experimental results whereas the computer program contained no knock criterion. In the actual engine plot also, the 'late burning' phenomenon (i.e. the increase in F.T.T. at very high compression ratios in the computed results (Fig. 8-32)) does not exist since knock always precludes this condition.

Thus, it seems that, even if progress in fuel technology could advance to produce a fuel which does not knock at very high compression ratios so that progressive flame propagation exists at all times, engine power output would still be restricted, at the very high cylinder pressures generated, by the 'late burn' phenomenon due to the newly burnt gas expansion being inhibited (see Section 2-1

and Fig. 2-2).

Referring back to the plot of F.T.T. against charge pressure at inlet valve closure (Fig. 8-28), it appears from this that the critical cylinder pressure at which the restrictive burnt gas expansion effect becomes really significant is about 42ATM (see Fig. 8-29 where the inlet charge pressure is 1.25ATM). However, with compression ratio variation, this pressure appears to be raised to approximately 53ATM (see Figs. 8-32 and 8-34). The discrepancy between the two values can be attributed to the higher burning velocity values with compression ratio increase (due to higher burnt and unburnt gas temperatures) than for initial pressure increase where the gains in burnt gas temperature were very much smaller and those in unburnt gas temperature were virtually nil.

Fig. 8-34 is a plot of the corresponding cylinder pressure against crankangle diagrams at the various compression ratios. The progressive retardation of the crankangle at which peak pressure is attained with decrease in compression ratio is clearly evident.

The computed CO concentrations with compression ratio variation is given in Fig. 8-35. The inverse sort of plot is achieved to that in Fig. 8-32 which reflects the influences of burnt gas temperature and pressure. Experimentally, the variation in CO with compression ratio change is obscured by exhaust gas residual changes, etc.

The same type of curve is obtained for the NO concentration variation (Fig. 8-36) for the same reasons as were given above for CO.

Fig. 8-37 is a plot of the burnt gas temperature at the exhaust valve opening point with change in compression ratio. The trend is in agreement with that noted experimentally, e.g. Davis[70].

MEA NS OF REDUCTION OF CO AND NO EMISSIONS

Exhaust Gas Recirculation

The allowance for the presence of varying quantities of exhaust gas residuals in the unburnt charge can be considered tantamount to recirculating a controlled flow of exhaust gases back into the induction manifold. This has been proposed as an effective means of keeping down NO and, to a certain extent, CO emissions (see Chapter 2). Newhall has shown that the temperature of the recirculated exhaust has very little influence on the effectiveness of the decrease. Thus, the mass fraction of exhaust residuals in the unburnt charge was allowed to vary from 0 to 0.2 while the remaining conditions at the point of inlet valve closure were kept constant. The following observations were noted:

a) the flame travel time decreased appreciably with increase in exhaust residuals as shown in Fig. 8-38. This is due to decreases in the burnt gas temperatures (see Fig. 8-39) as a result of the exhaust gases in effect absorbing a portion of the chemical energy released during combustion.

b) increases in exhaust gas residuals result in very large decreases in peak cycle pressures and consequently in i.m.e.p. values (Fig. 8-40).

c) the computed variations in CO concentrations with change in exhaust gas residual fractions areshown in Fig. 8-41. As expected, the reductions in burnt gas temperatures (Fig. 8-39) reduce the CO formation tendency.

d) at peak cycle temperature, the NO concentrations, at the particular operating conditions stated, are reduced in the manner shown in Fig. 8-42 with an increasing presence of exhaust residuals. Again, the decrease in cycle temperatures is cited as being primarily responsible.

e) on a percentage basis (Fig. 8-43), it is noted that the presence of only 6% of residuals accounts for a 56% reduction in NO emissions at peak cycle temperature conditions. A decrease of 10% in i.m.e.p. accompanies this. Such a large decrease in NO is explained by the fact that its formation from nitrogen and oxygen is an exponential function of temperature.

Water Injection

As the NO emission problem has become more acute, the suggestion of injecting water to mix with the unburnt charge has been frequently proposed. Some computed results have been obtained to test the validity of this proposal.

Fig. 8-44 shows the decrease in P.T.T. with increase in mass fraction of injected water. This decrease is once more attributable to the diluent water absorbing a certain amount of the chemical energy released during combustion and, in so doing, reducing combustion temperatures (see.Fig. 8-45).

Fig. 8-46 shows the pressure-crankangle diagrams corresponding to the presence of various quantities of injected water in the unburnt mixture.

The CO decrease is given in Fig. 8-47 and is entirely as expected because of the decrease in burnt gas temperatures.

The NO reduction is plotted in Fig. 8-48 at peak cycle temperatures. Two possible mechanisms for this trend were considered:

i) reduction in burnt gas temperatures due to the presence of the water as a diluent.

ii) reduction in the unburnt charge temperature at inlet valve closure (and hence in the burnt gas temperature) due to water evaporation effects.

This latter mechanism was, however, found to be completely overwhelmed by the former mechanism. Results from the computer runs, for example, showed that with 10% of injected water, the evaporation effect resulted in a drop of only 2.87°K in the unburnt gas temperature whereas the diluent effect represented a drop of 480°K in the burnt gas temperature.

Fig. 8-49 illustrates the percentage reduction in NO concentrations at peak cycle temperature and in i.m.e.p. with variation in mass fraction of injected water. For given reductions in NO, the drops in i.m.e.p., seem to be the same for both exhaust gas recirculation and water injection under the operating conditions used here.

Concluding Remarks

From the limited computer runs, it appears that only a very small amount of exhaust gas recirculation or water

injection is required to obtain sbbstantial reductions in NO. Higher amounts, although having the desired effect of reducing CO and NO evenfurther, indicate that the effect on engine power output is unacceptable.

MISCELLANEOUS RESULTS FROM THE COMPUTER PROGRAM

Fig. 8-50 shows plots of the typical development of burnt gas temperature, NO and CO concentrations throughout combustion at the stated running conditions when equilibrium is maintained throughout. It is observed that the peak NO concentration does not occur at peak combustion temperature in this particular case - the effect of the lower cylinder pressure shortly before the peak cycle temperature point is the determining factor. The discrepancy, however, is very small. A similar conclusion can be drawn from close scrutiny of the CO curve.

In Fig. 8-51, the variation in turbulent burning velocity, U_T, and turbulent flame speed, V_T, throughout one particular engine cycle, at the conditions stated, is demonstrated. The turbulent burning velocity increases continually as combustion proceeds up until just before the completion of combustion when it falls off due to the decreasing burnt and unburnt gas temperatures. The flame speed plot has been explained previously - it is higher than the U_T curve because it includes the expansion effect of the newly burnt gases on the unburnt charge.

A typical variation in heat losses throughout the flame propagation period is given in Fig. 8-52. The build-up of losses with crankangle is clearly evident as the burnt gases attain higher temperatures and pressures and

cover greater areas of the combustion chamber surfac es. The tailing-off effect at the end of flame propagation is attributed to the decreasing temperature and pressure. The rate of heat loss (cal/^{o}crankangle) appears virtually constant (corresponding to the linear portion of the plot) over a considerable portion of the propagation.

The computed variations in overall heat losses (expressed as a percentage of the heat of combustion) with engine speed during the combustion and expansion phases of the engine cycle are given in Fig. 8-53 under certain specified conditions. The values pertaining during combustion are in the region of those predicted by various workers experimentally (see Chapter 7) and show the expected variation with engine speed as was noted by Janeway[185] and David and Leah[187]. The reasons for the losses being higher at the lower engine speeds are clearly that the burnt gas temperatures are higher and because there is more time available for heat losses to occur. These factors have a greater influence than the counteracting trend of reduced flame travel times (see Fig. 8-23). During expansion, on the other hand, although the overall heat losses again show the expected variation with engine speed (see Fig. 8-53), their absolute values are well in excess of those predicted experimentally. The most probable explanation for this is the assumption in the Annand formula (Equation 7-26) that the degree of mixture motion (represented by symbol constant c_1) remains unchanged during both combustion and expansion whereas Semenov's

turbulence measurements (see Chapter 4) have shown it to die down as the expansion phase is approached.

Fig. 8-54 is a typical entropy-cylinder volume diagram pertaining to the compression, combustion and expansion phases. Although some heat transfer was included during compression, this is seen to have a negligible influence on the entropy at this time. The combustion process, on the other hand, is observed to be highly irreversible. A large increase in entropy is apparent during this phase, even though heat transfer was allowed for, which tends to decrease entropy. The heat transfer during expansion introduces a further decrease in entropy.

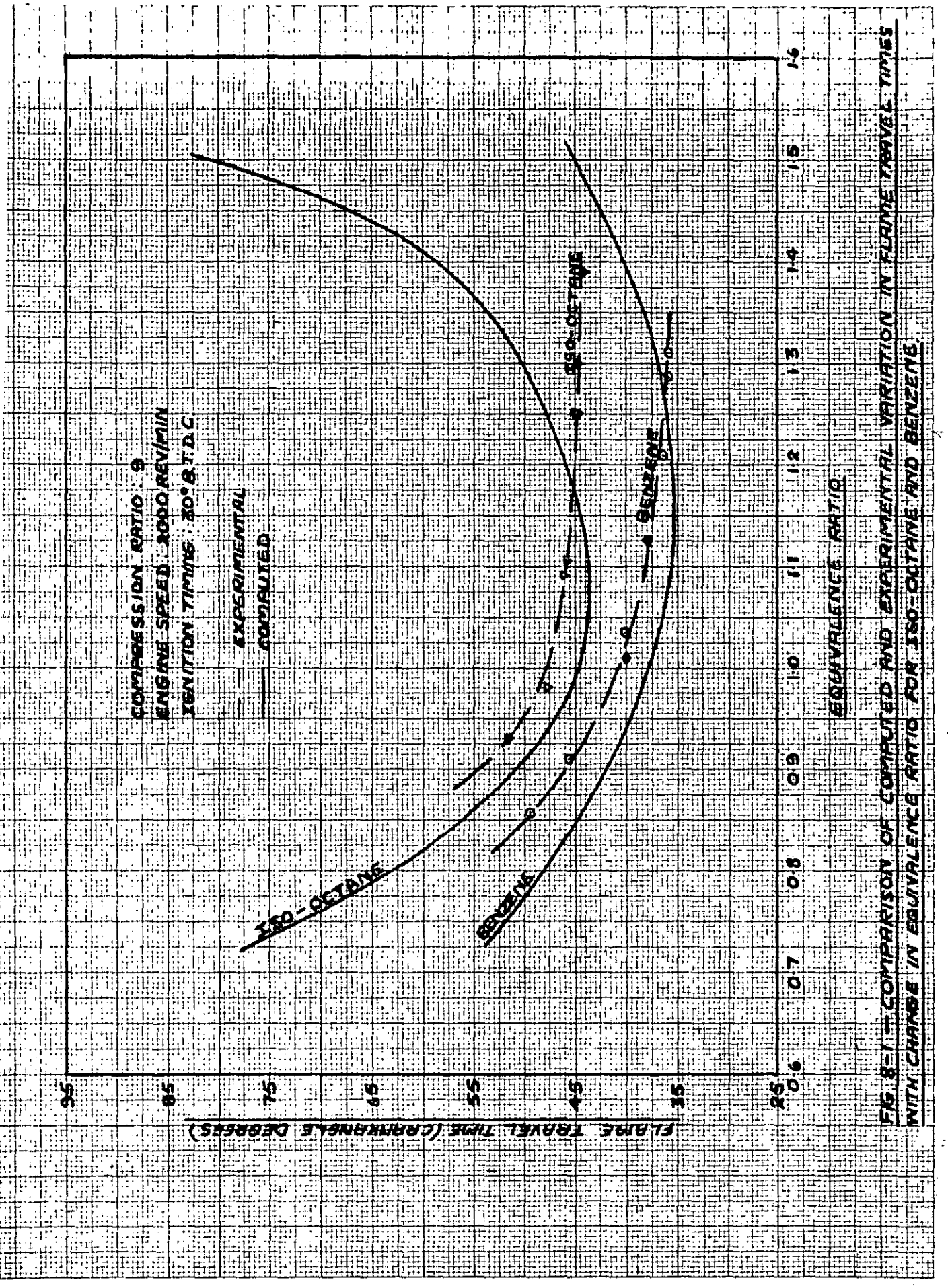

FIG. 8 :— COMPARISON OF COMPUTED AND EXPERIMENTAL VARIATION IN FLAME TRAVEL TIMES WITH CHANGE IN EQUIVALENCE RATIO FOR ISO-OCTANE AND BENZENE.

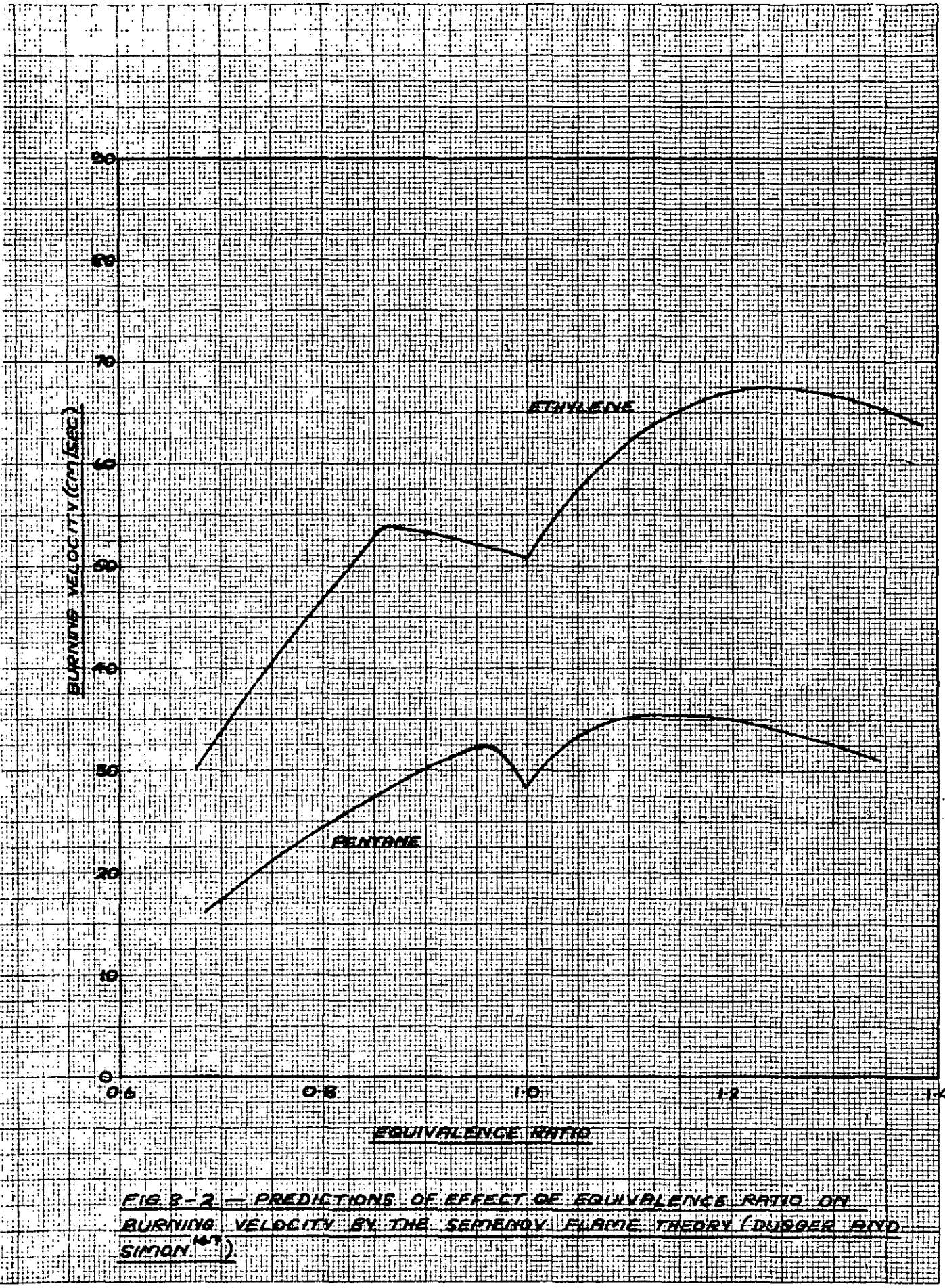

FIG. 8-2 — PREDICTIONS OF EFFECT OF EQUIVALENCE RATIO ON BURNING VELOCITY BY THE SEMENOV FLAME THEORY (DUBBER AND SIMON[147]).

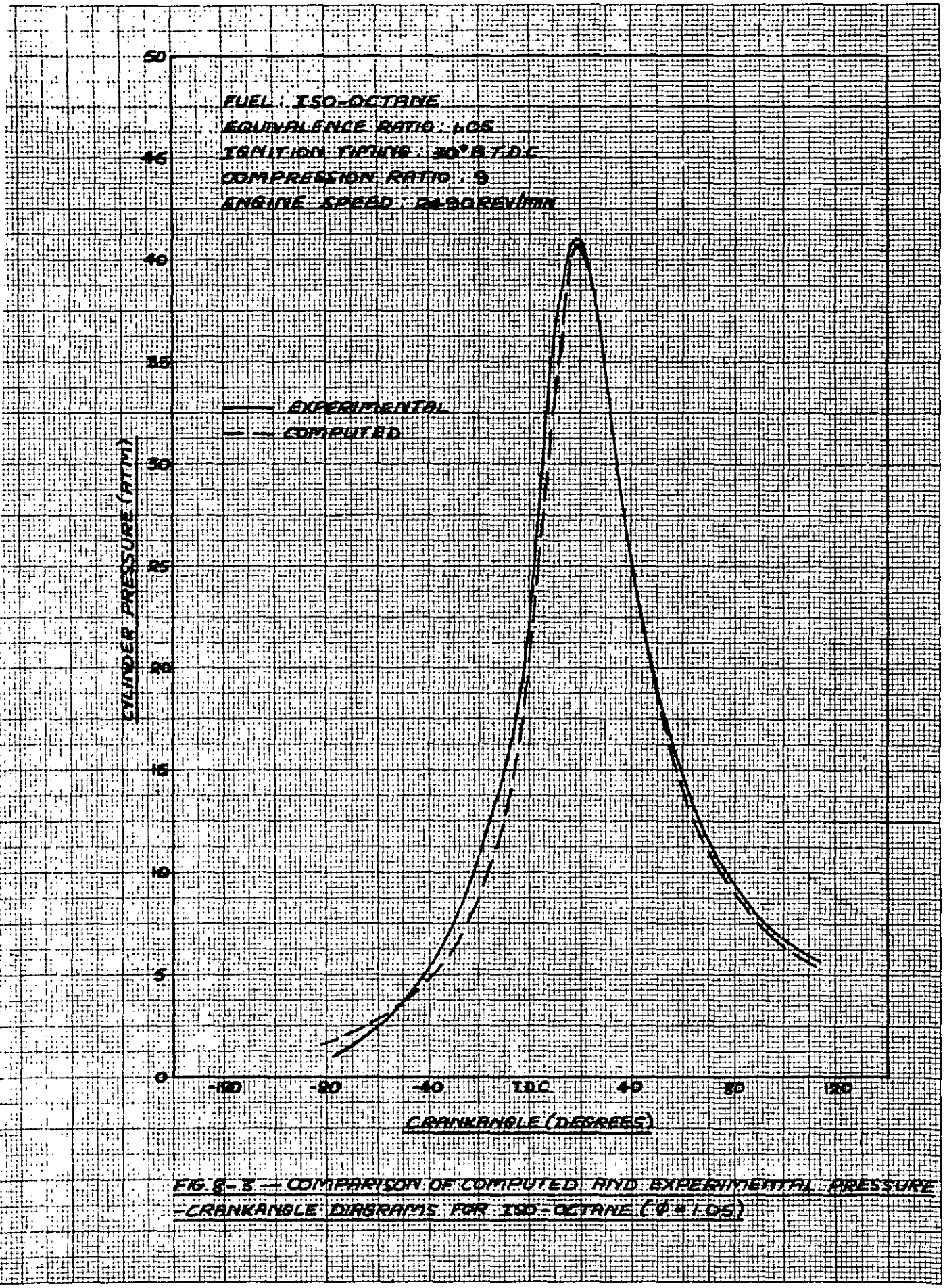

FIG. 8-3 — COMPARISON OF COMPUTED AND EXPERIMENTAL PRESSURE-CRANKANGLE DIAGRAMS FOR ISO-OCTANE ($\phi = 1.05$)

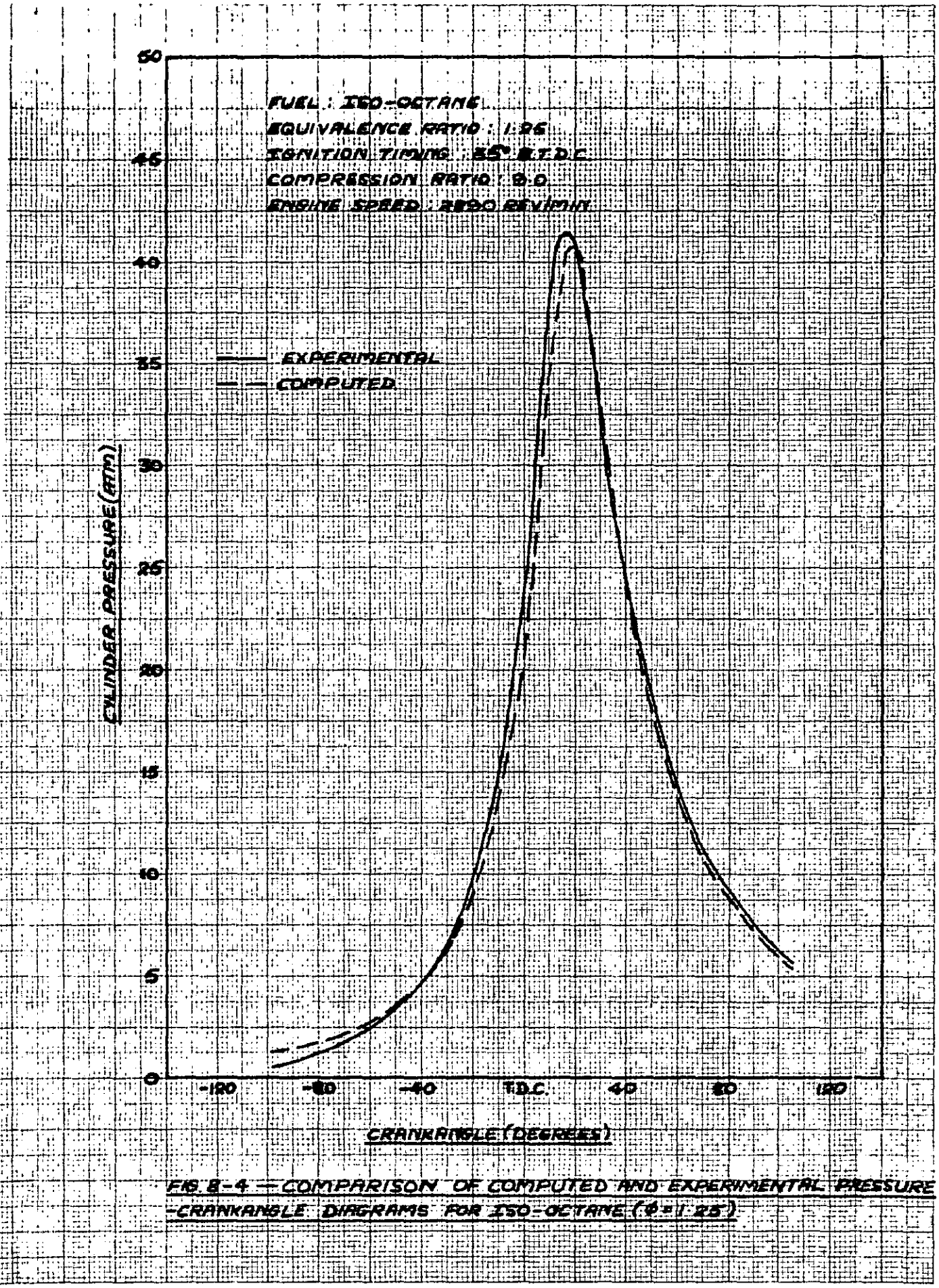

FIG. 8-4 — COMPARISON OF COMPUTED AND EXPERIMENTAL PRESSURE -CRANKANGLE DIAGRAMS FOR ISO-OCTANE ($\phi = 1.25$)

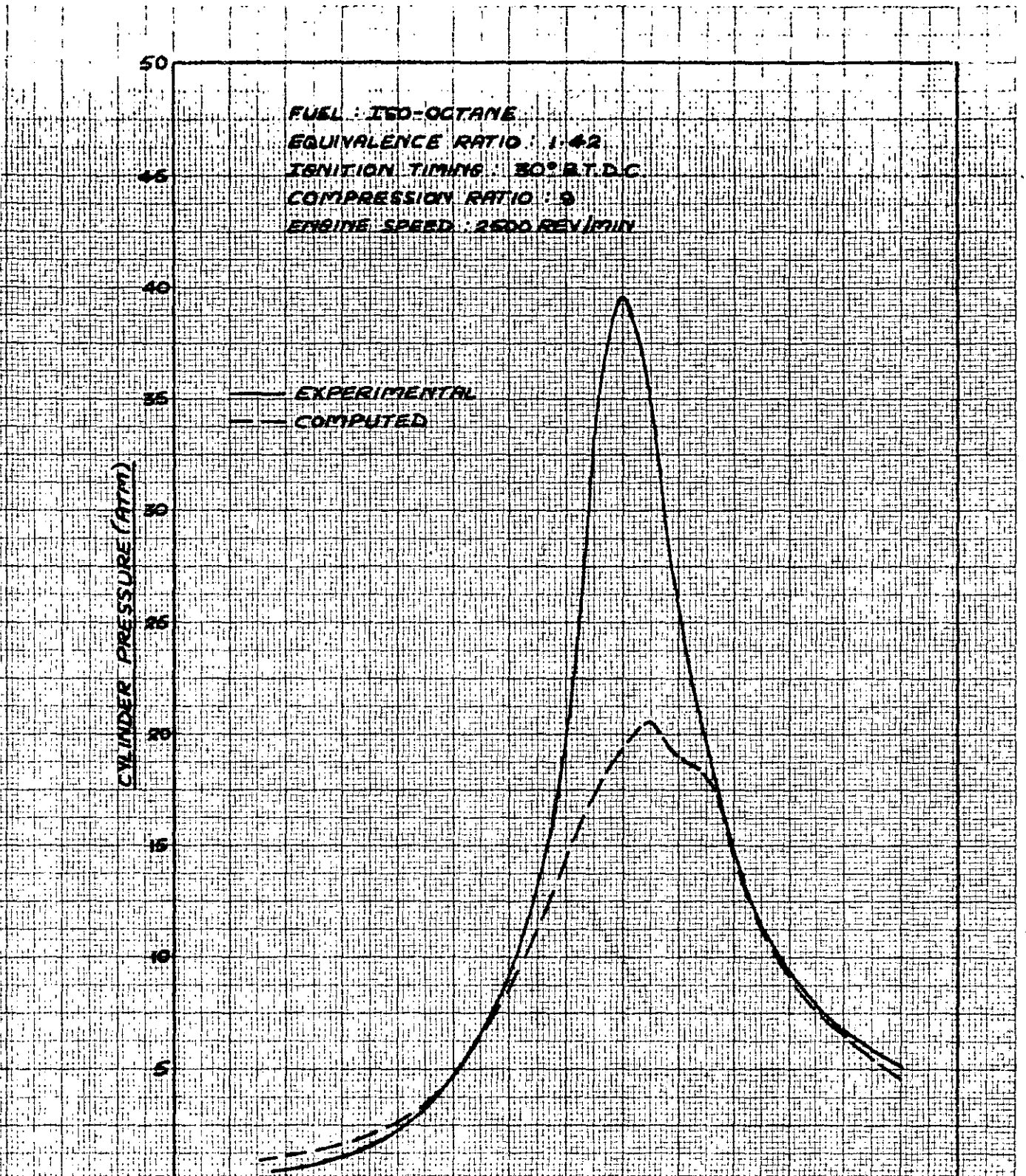

FIG 8-8 — COMPARISON OF COMPUTED AND EXPERIMENTAL PRESSURE — CRANKANGLE DIAGRAMS FOR ISO-OCTANE (ϕ=1·42)

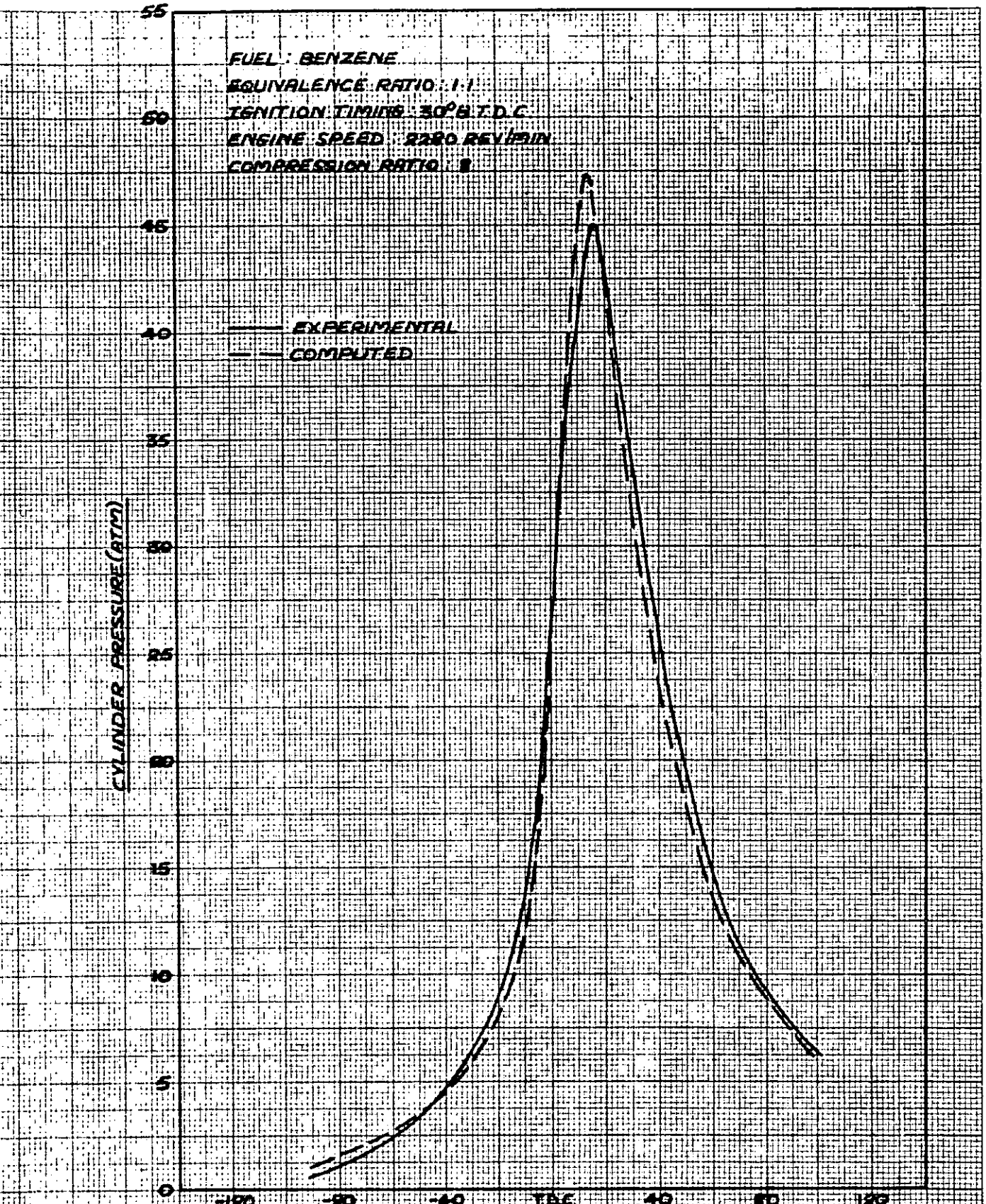

FIG. 8-6 — COMPARISON OF COMPUTED AND EXPERIMENTAL PRESSURE-CRANKANGLE DIAGRAMS FOR BENZENE ($\phi = 1{\cdot}1$)

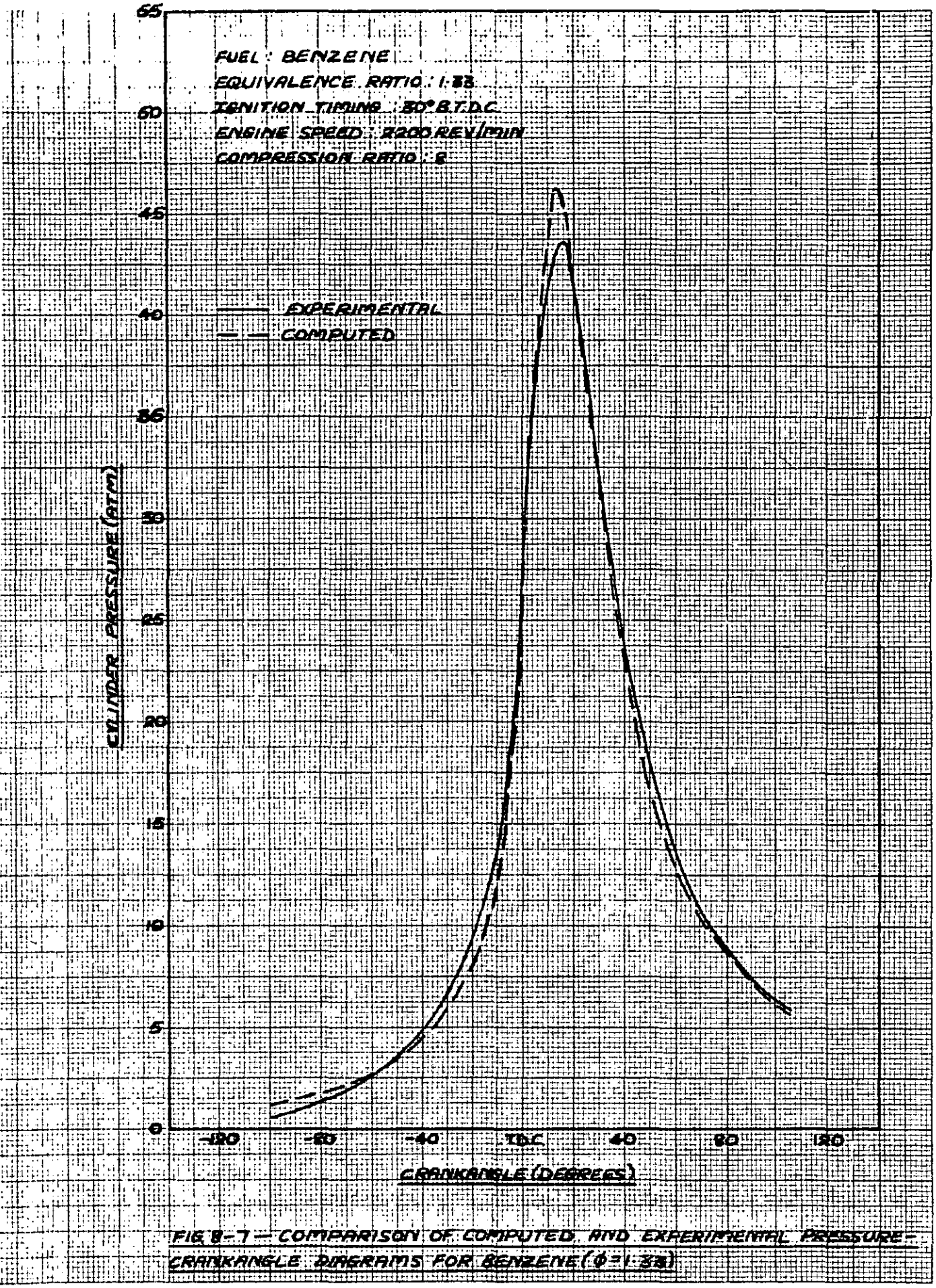

FIG 8-7 — COMPARISON OF COMPUTED AND EXPERIMENTAL PRESSURE-CRANKANGLE DIAGRAMS FOR BENZENE ($\phi = 1 \cdot 33$)

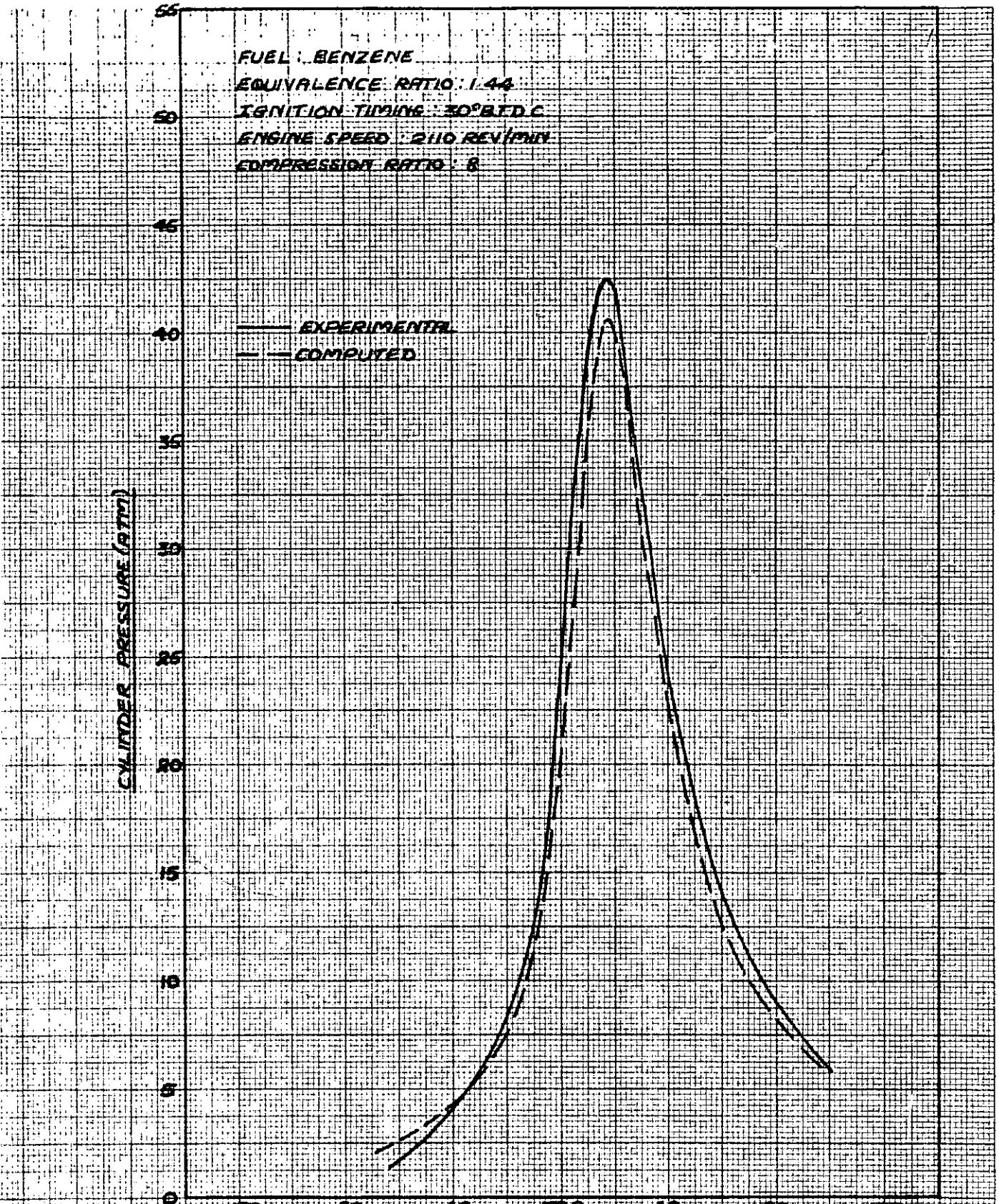

FIG. 8-8 — COMPARISON OF COMPUTED AND EXPERIMENTAL PRESSURE-CRANKANGLE DIAGRAMS FOR BENZENE (ϕ = 1.44)

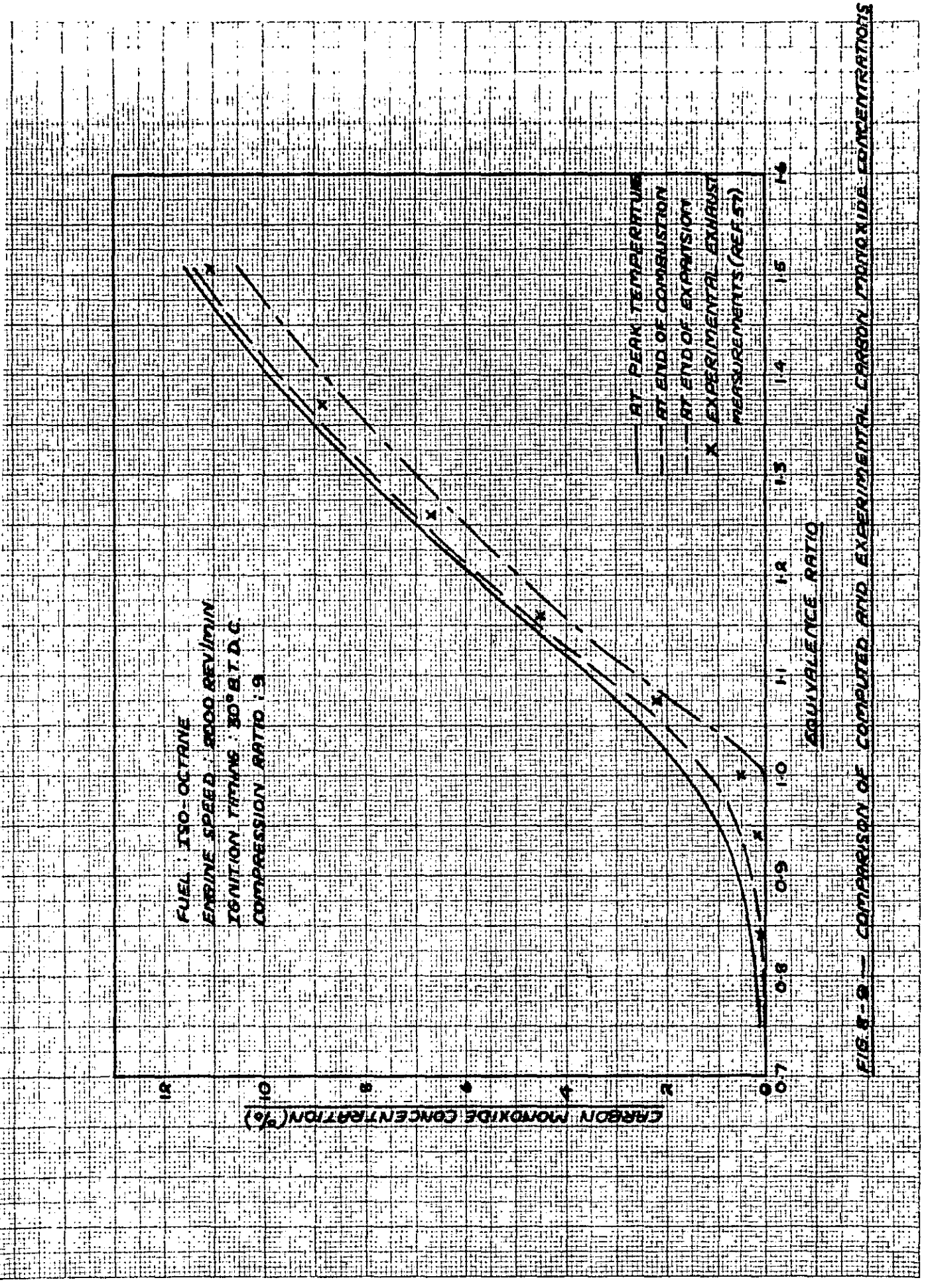

FIG. 8·2 — COMPARISON OF COMPUTED AND EXPERIMENTAL CARBON MONOXIDE CONCENTRATIONS

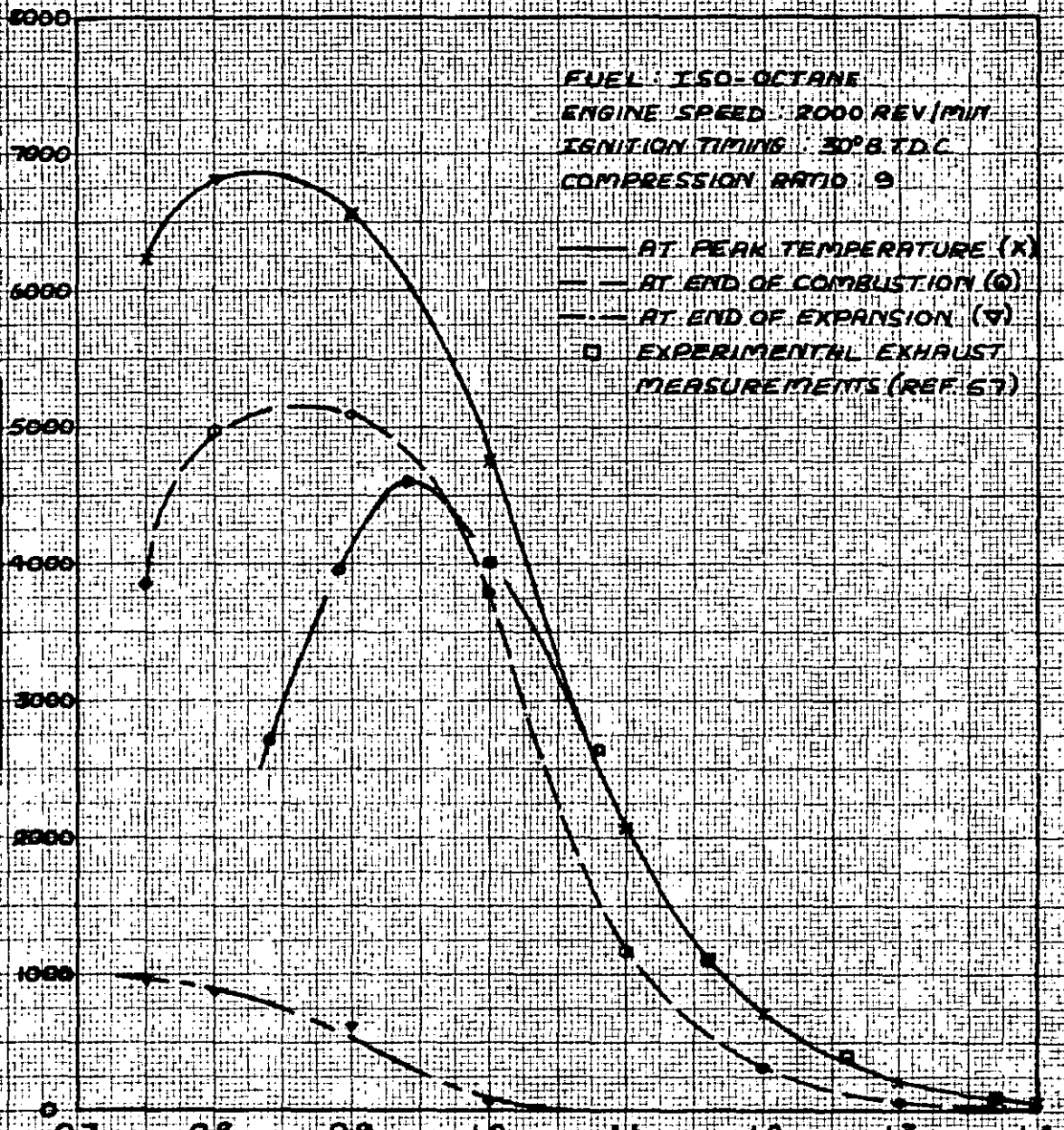

FIG. 2-10 — COMPARISON OF COMPUTED AND EXPERIMENTAL NITRIC OXIDE CONCENTRATIONS

FIG 8-11 — VARIATION IN FLAME TRAVEL TIMES FOR ISO-OCTANE, PROPANE AND BENZENE WITH EQUIVALENCE RATIO.

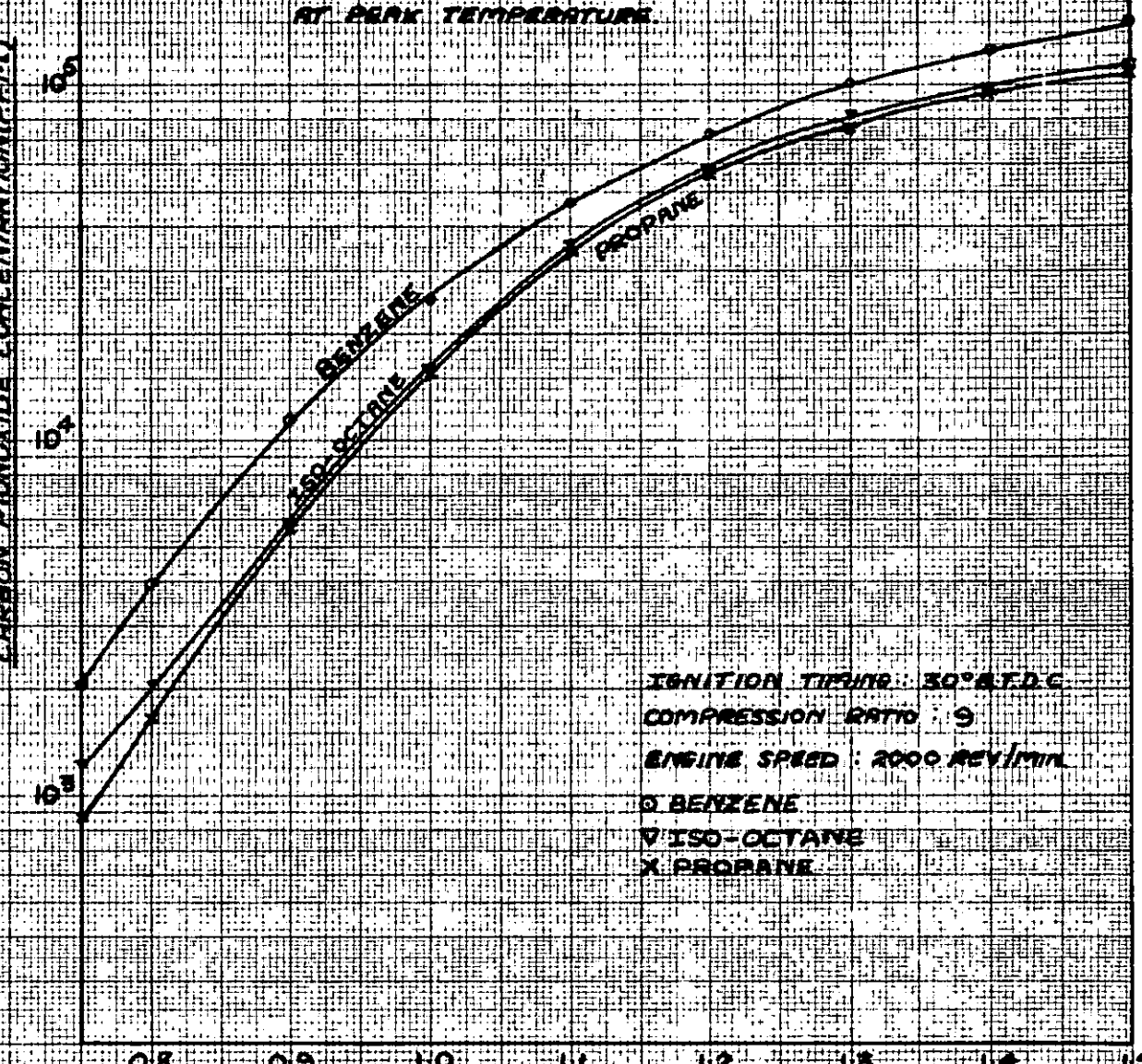

FIG 8-12 — VARIATION IN CARBON MONOXIDE CONCENTRATIONS WITH EQUIVALENCE RATIO FOR ISO-OCTANE, PROPANE AND BENZENE

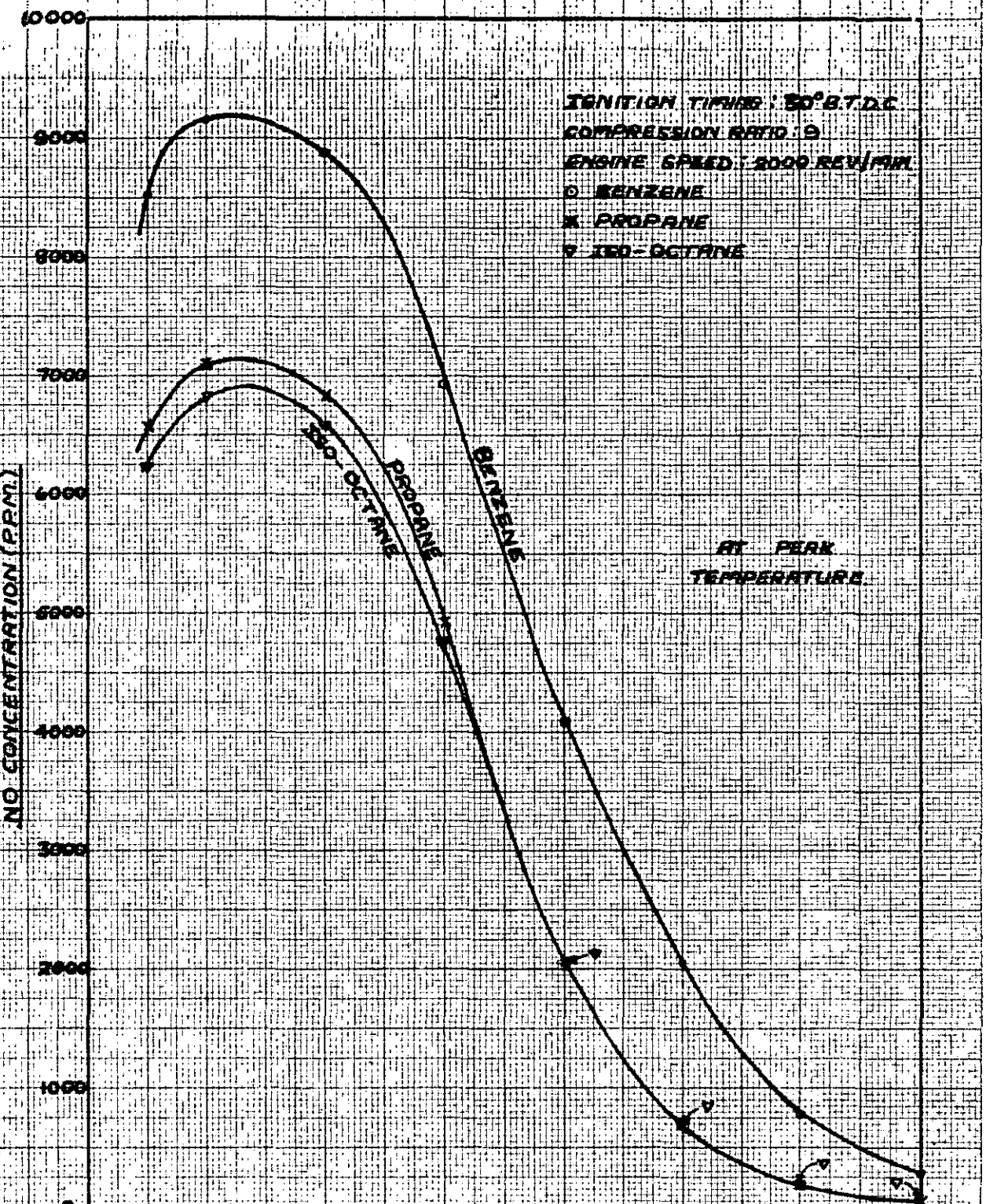

FIG 8-13— VARIATION IN NITRIC OXIDE CONCENTRATIONS WITH EQUIVALENCE RATIO FOR ISO-OCTANE, PROPANE AND BENZENE

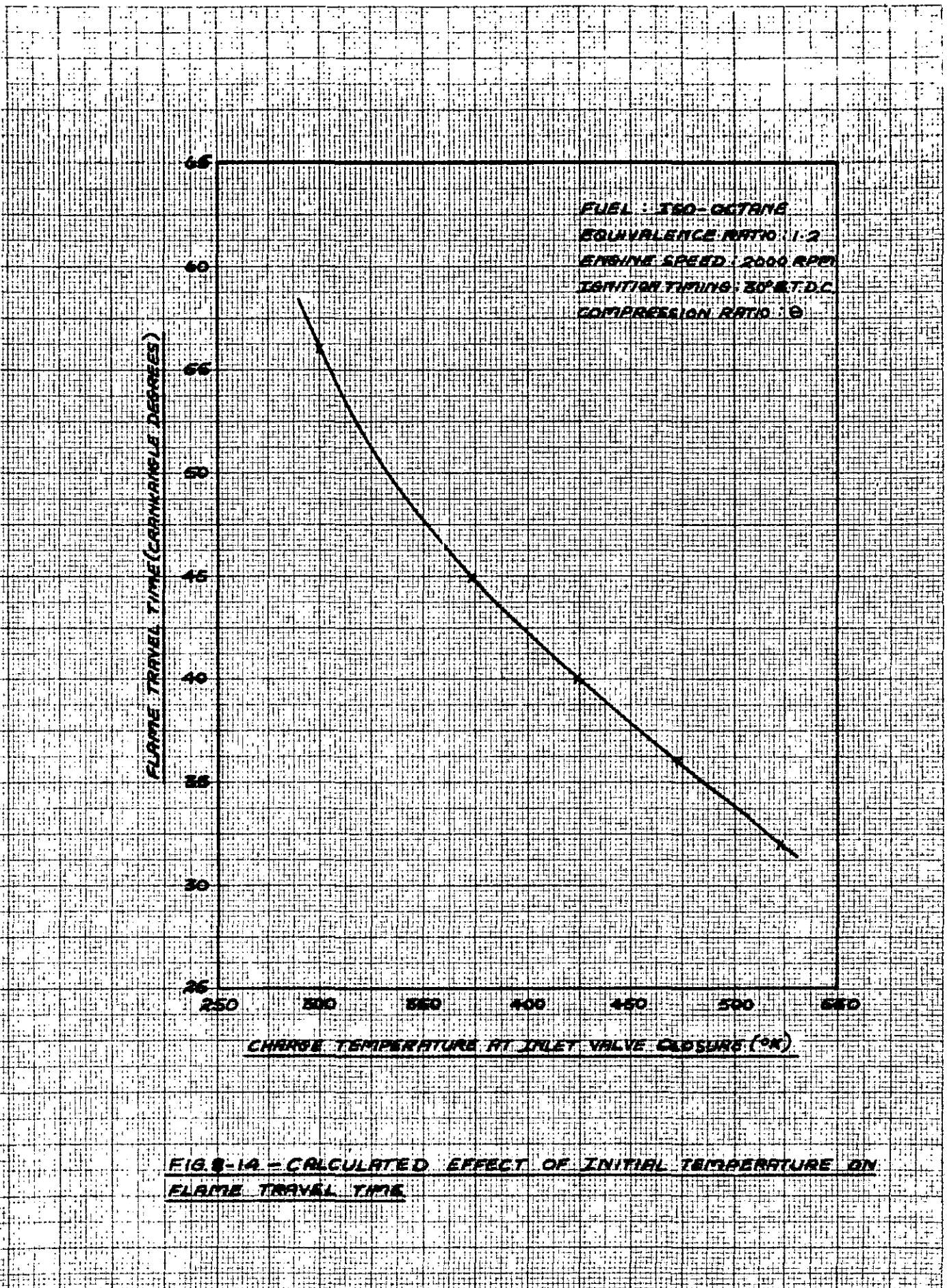

FIG. 8-14 – CALCULATED EFFECT OF INITIAL TEMPERATURE ON FLAME TRAVEL TIME

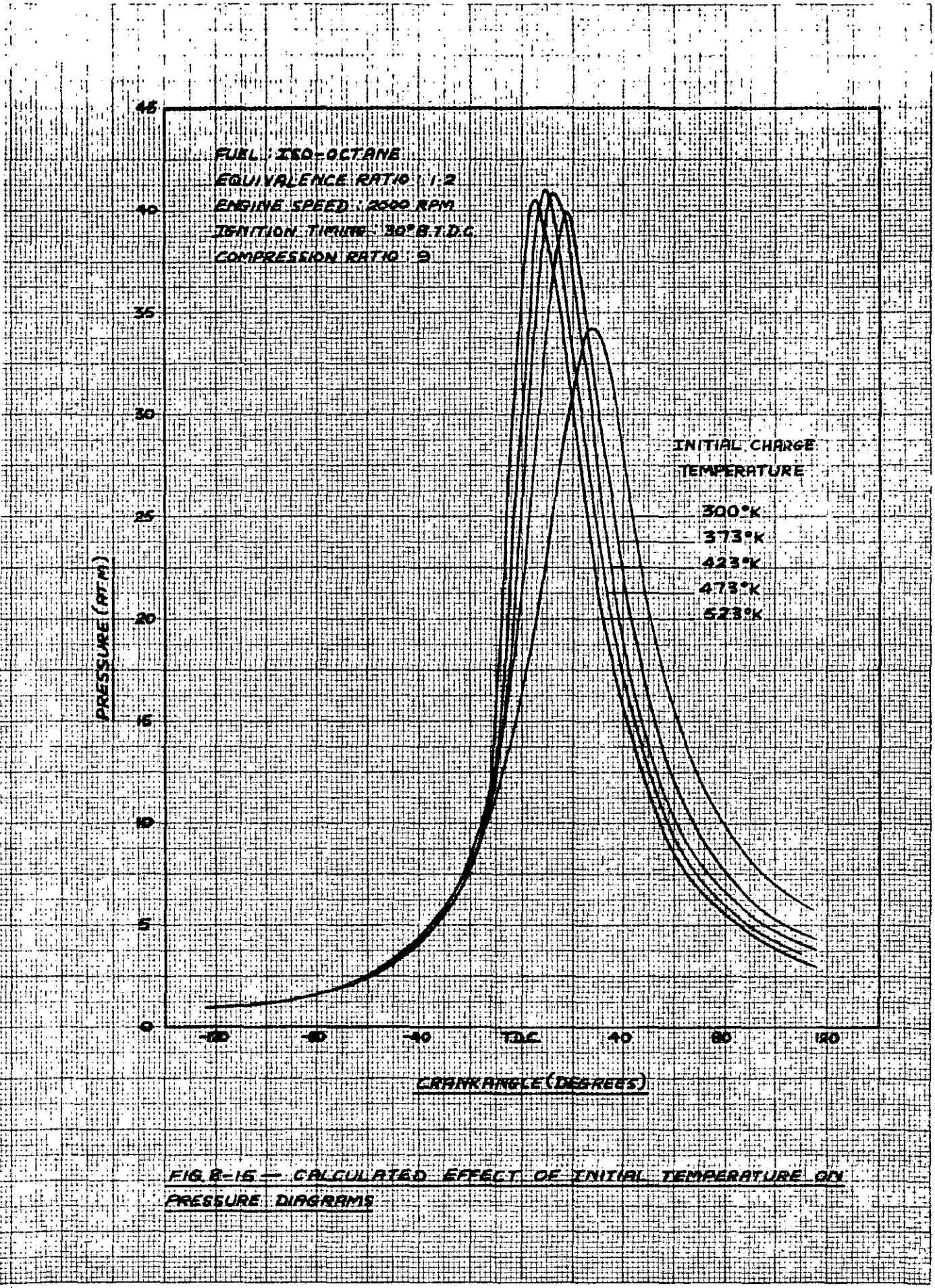

FIG. 8-15 — CALCULATED EFFECT OF INITIAL TEMPERATURE ON PRESSURE DIAGRAMS

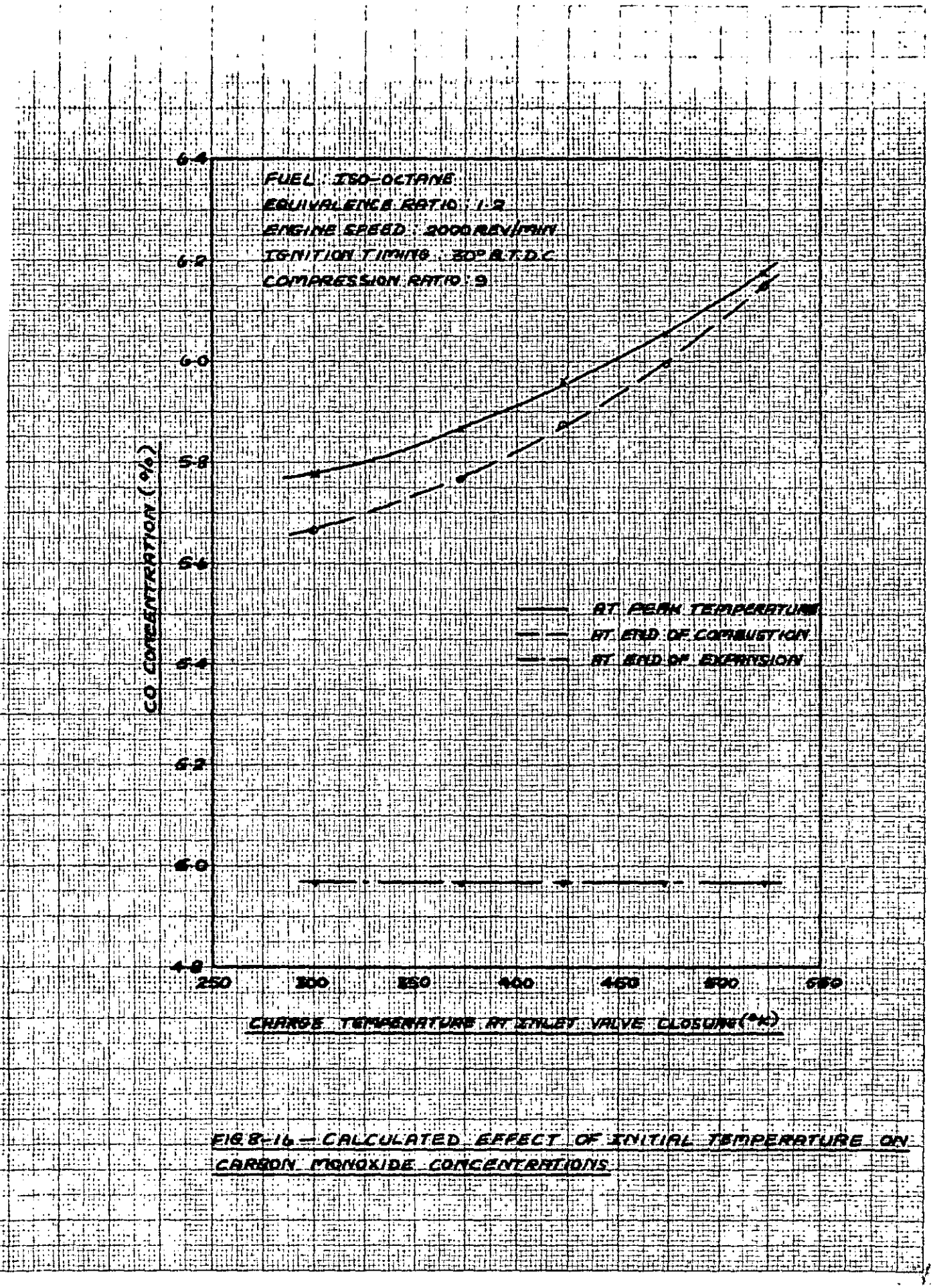

FIG 8-16 — CALCULATED EFFECT OF INITIAL TEMPERATURE ON CARBON MONOXIDE CONCENTRATIONS

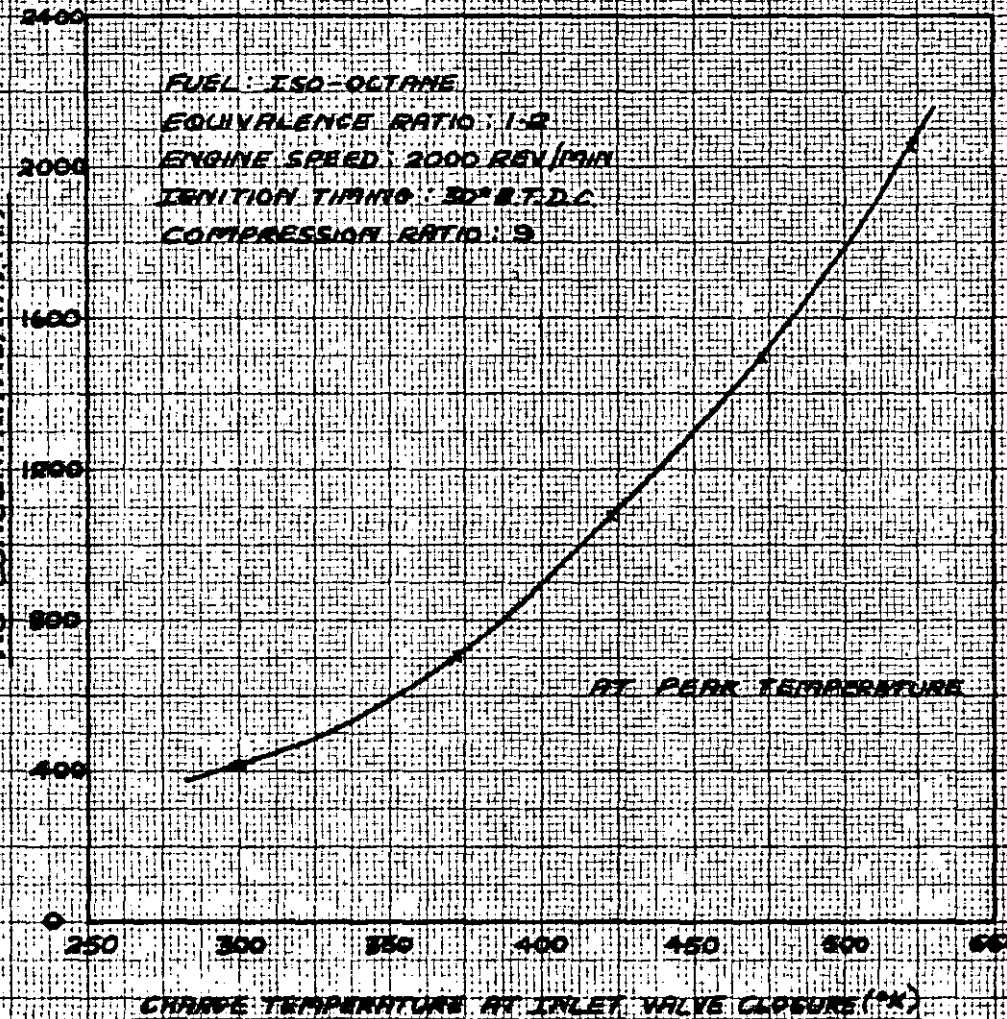

FIG 8-17 — CALCULATED EFFECT OF INITIAL TEMPERATURE ON NITRIC OXIDE CONCENTRATIONS

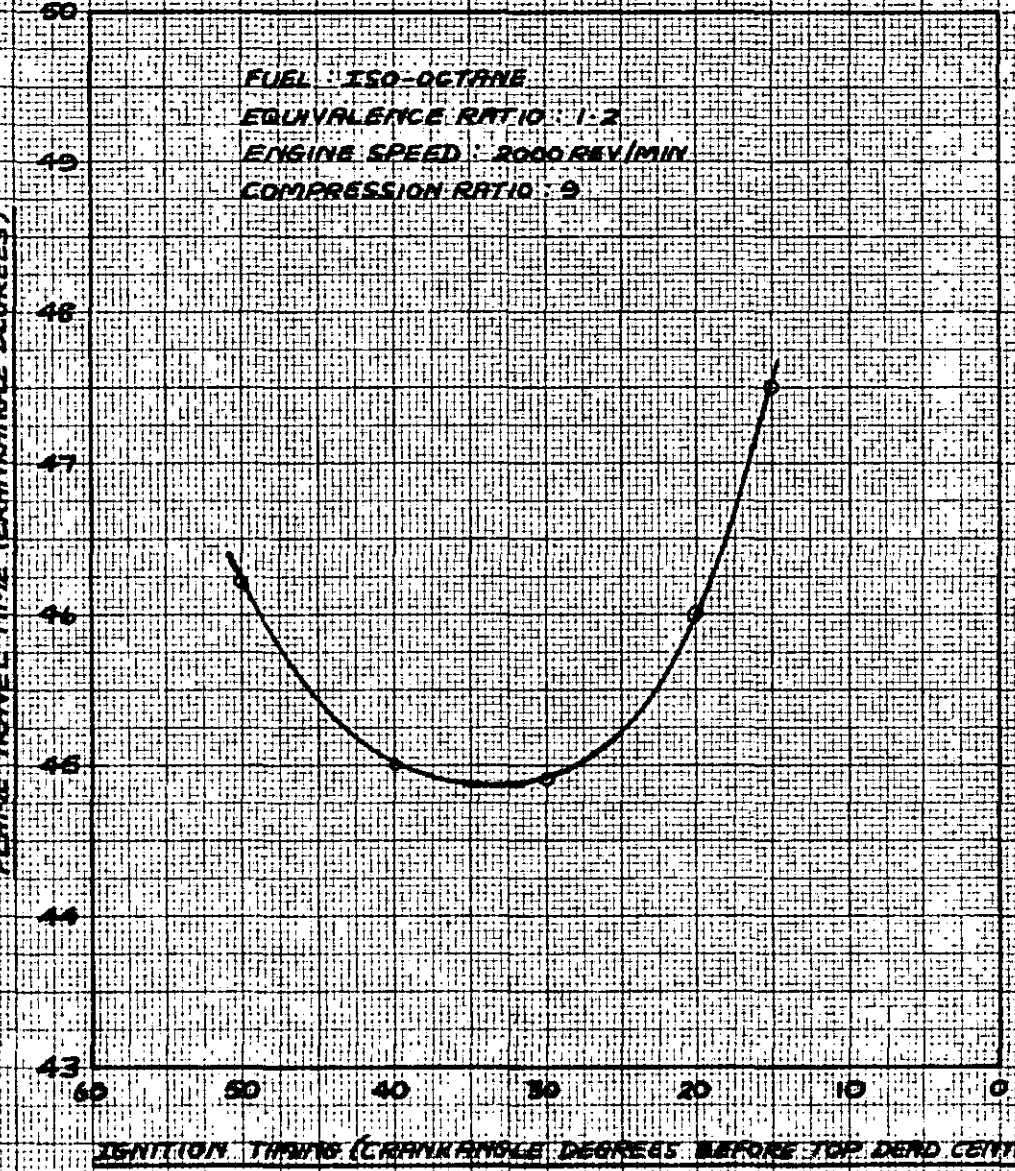

FIG 8-12 — CALCULATED EFFECT OF IGNITION TIMING ON FLAME TRAVEL TIME

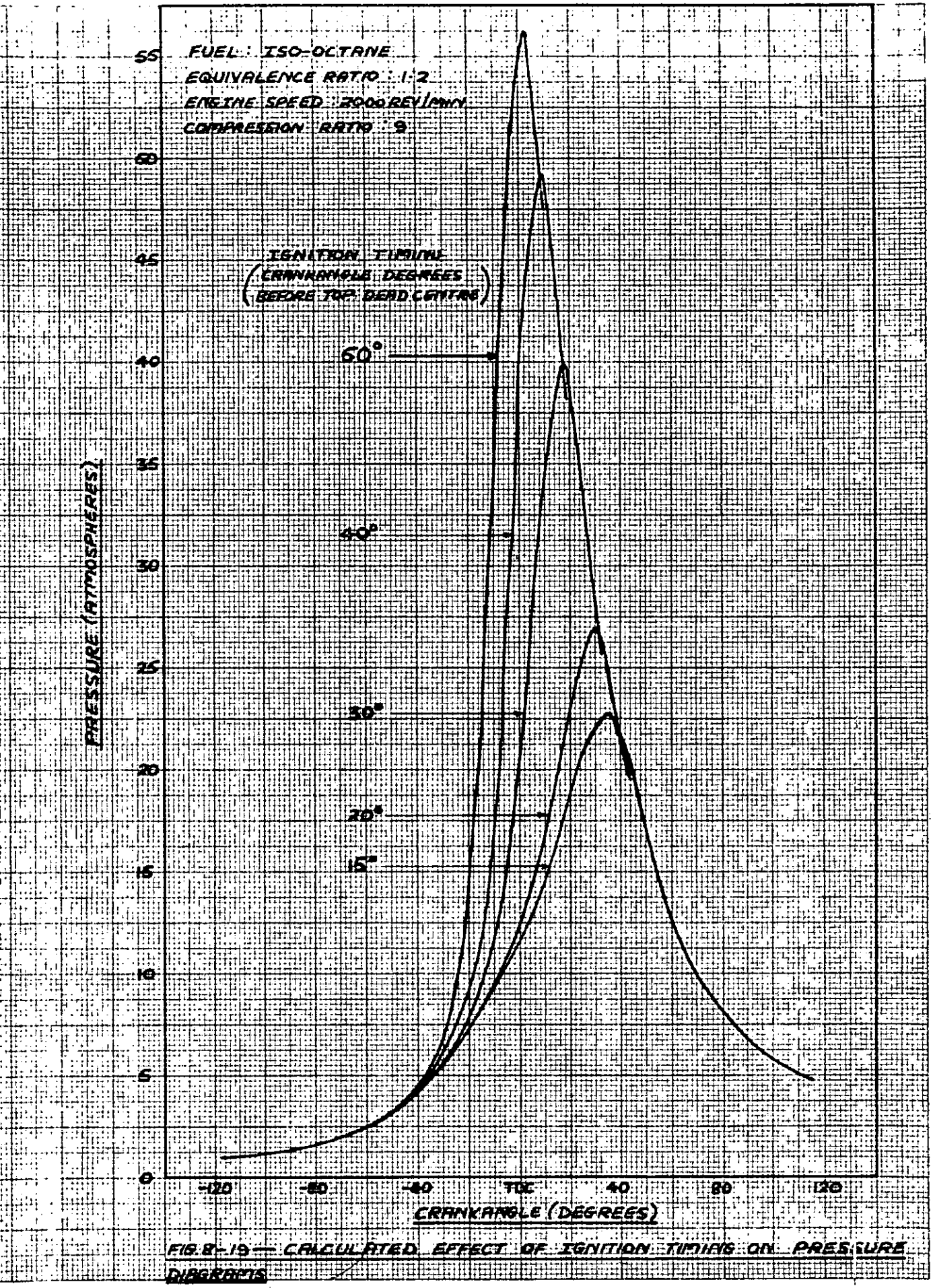

FIG. 8-19 — CALCULATED EFFECT OF IGNITION TIMING ON PRESSURE DIAGRAMS

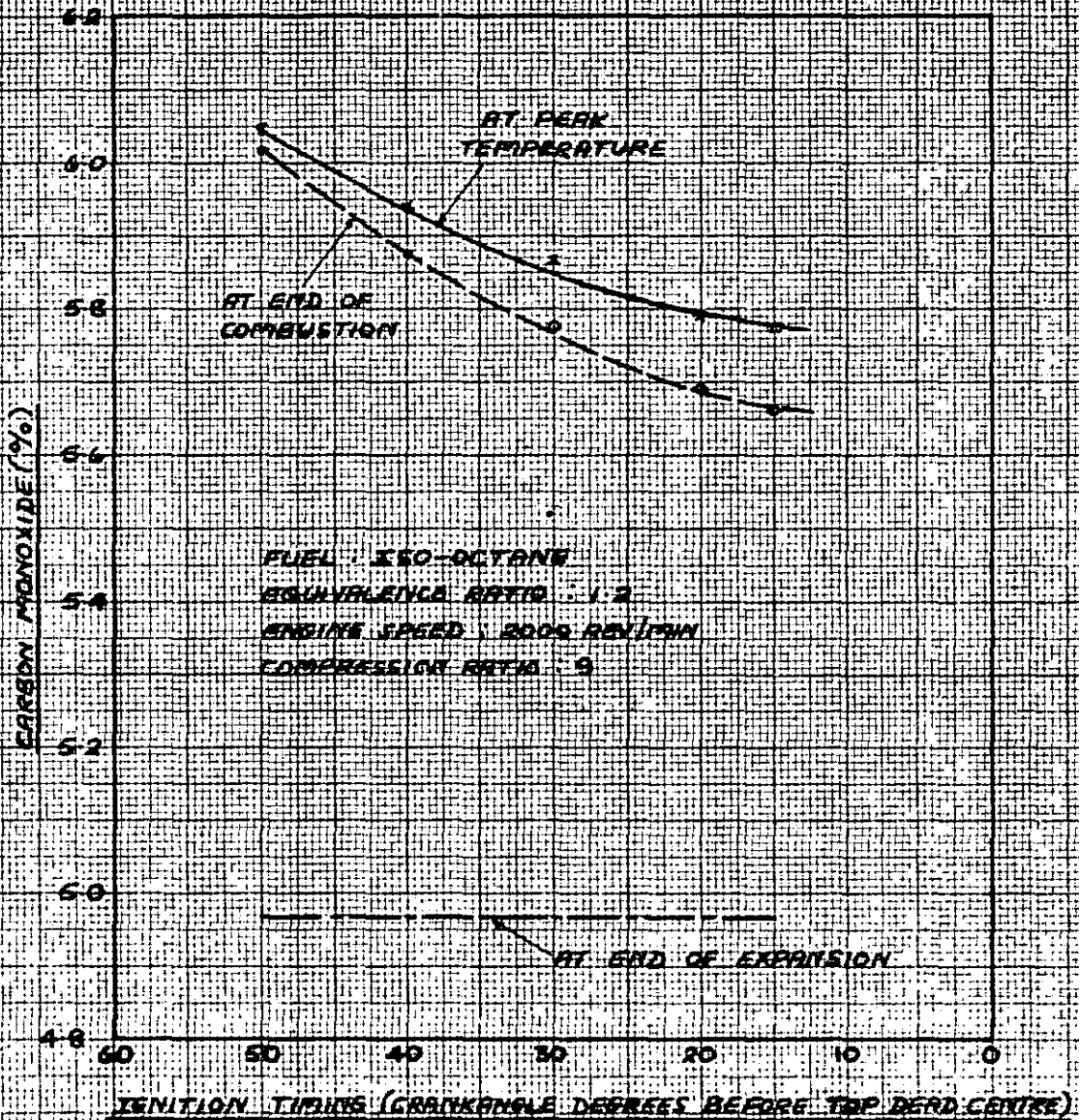

FIG. 8–20 — CALCULATED EFFECT OF IGNITION TIMING ON CARBON MONOXIDE CONCENTRATIONS

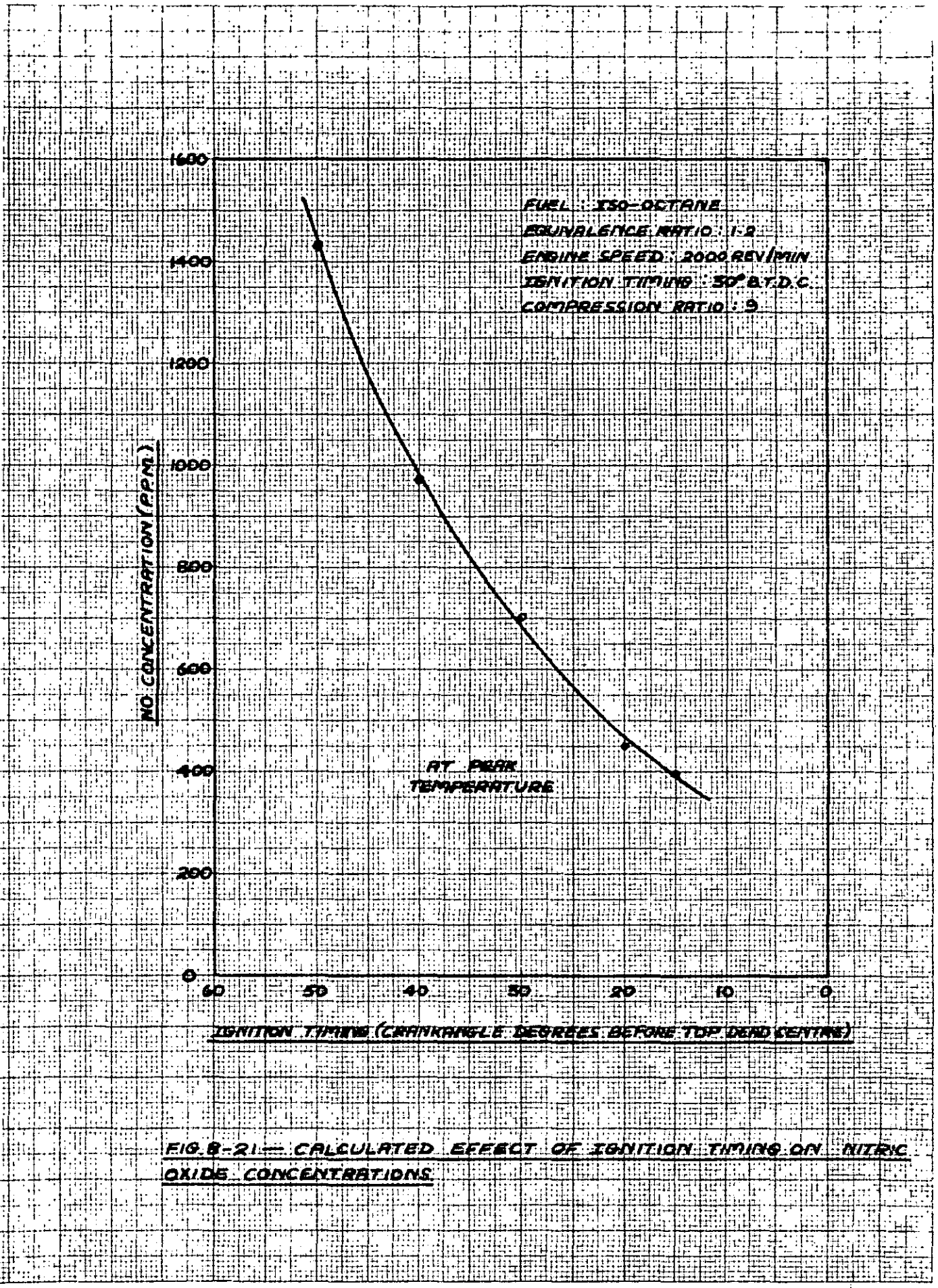

FIG. 8-21 — CALCULATED EFFECT OF IGNITION TIMING ON NITRIC OXIDE CONCENTRATIONS.

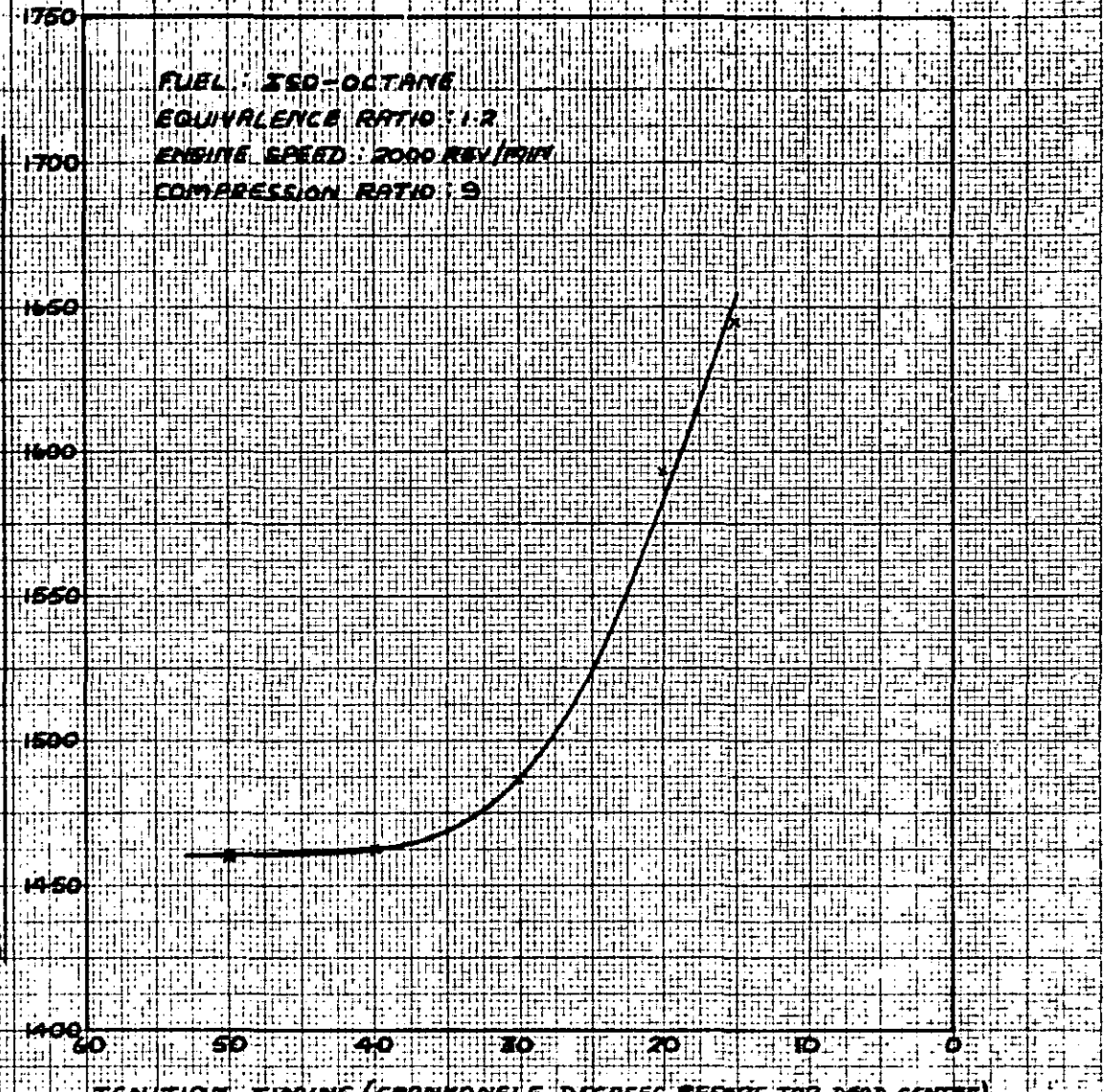

FIG. 8-22 — CALCULATED EFFECT OF IGNITION TIMING ON BURNT GAS TEMPERATURES AT EXHAUST VALVE OPENING

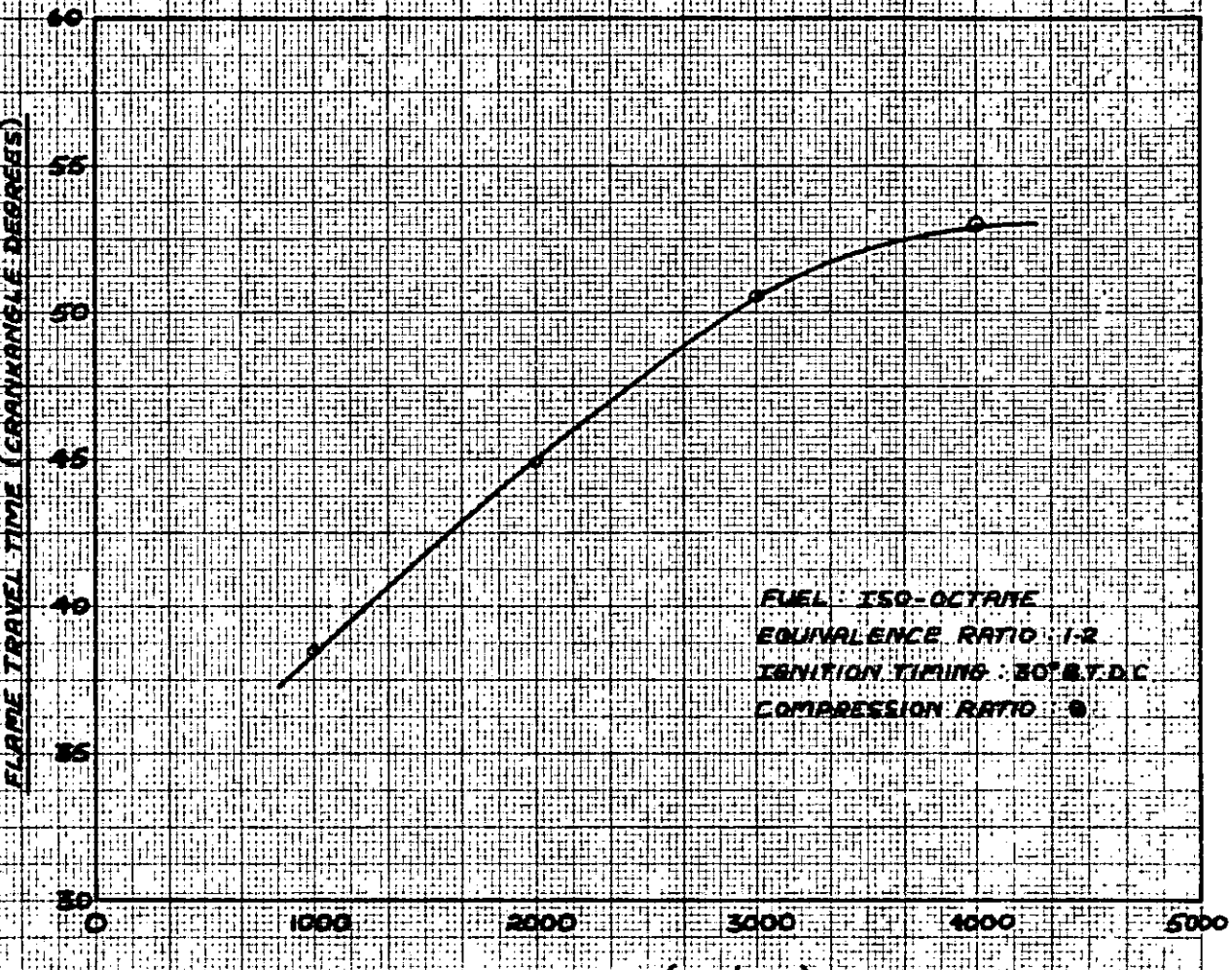

FIG 8-28 — CALCULATED EFFECT OF ENGINE SPEED ON FLAME TRAVEL TIME.

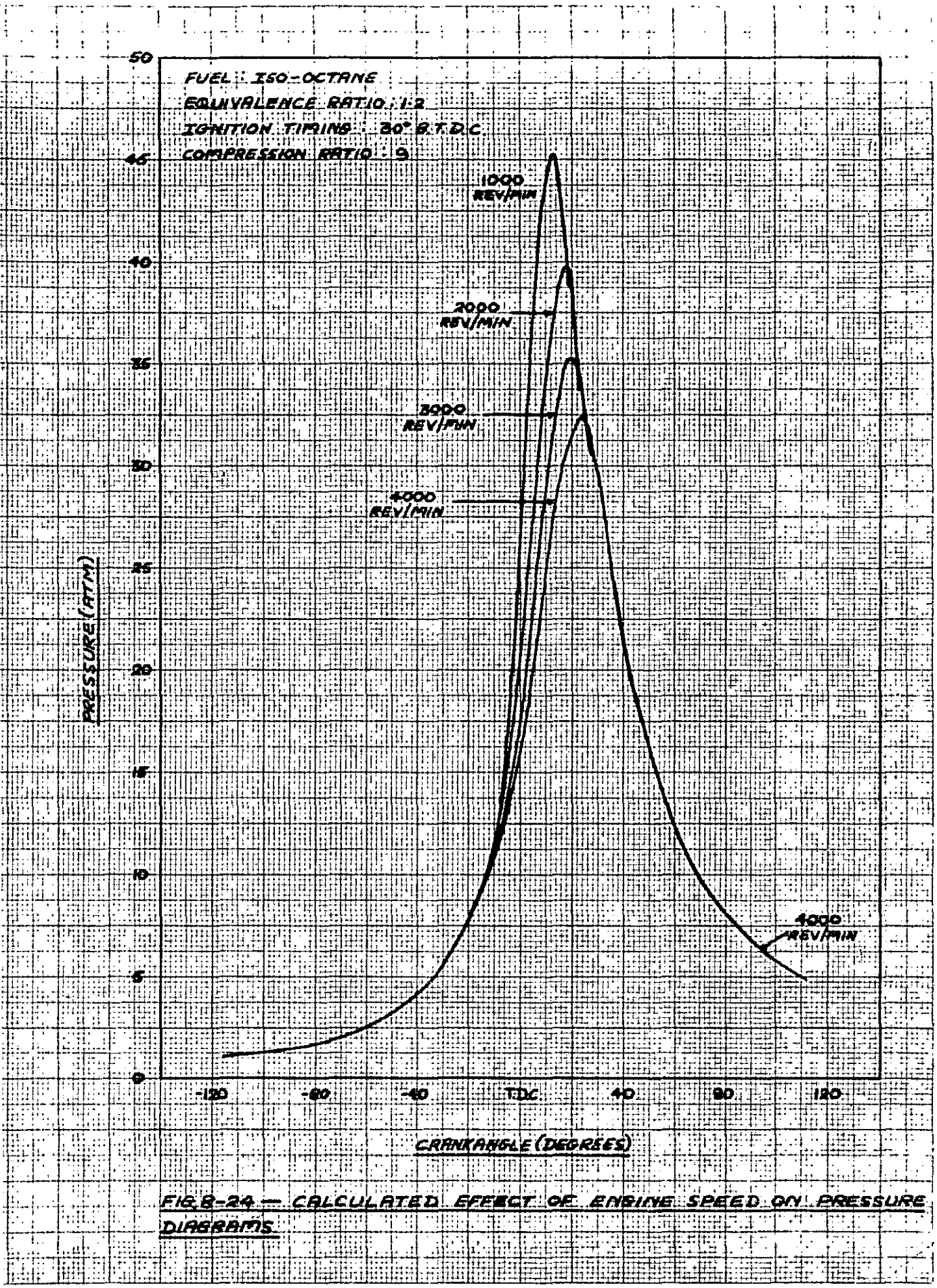

FIG. 8-24 — CALCULATED EFFECT OF ENGINE SPEED ON PRESSURE DIAGRAMS

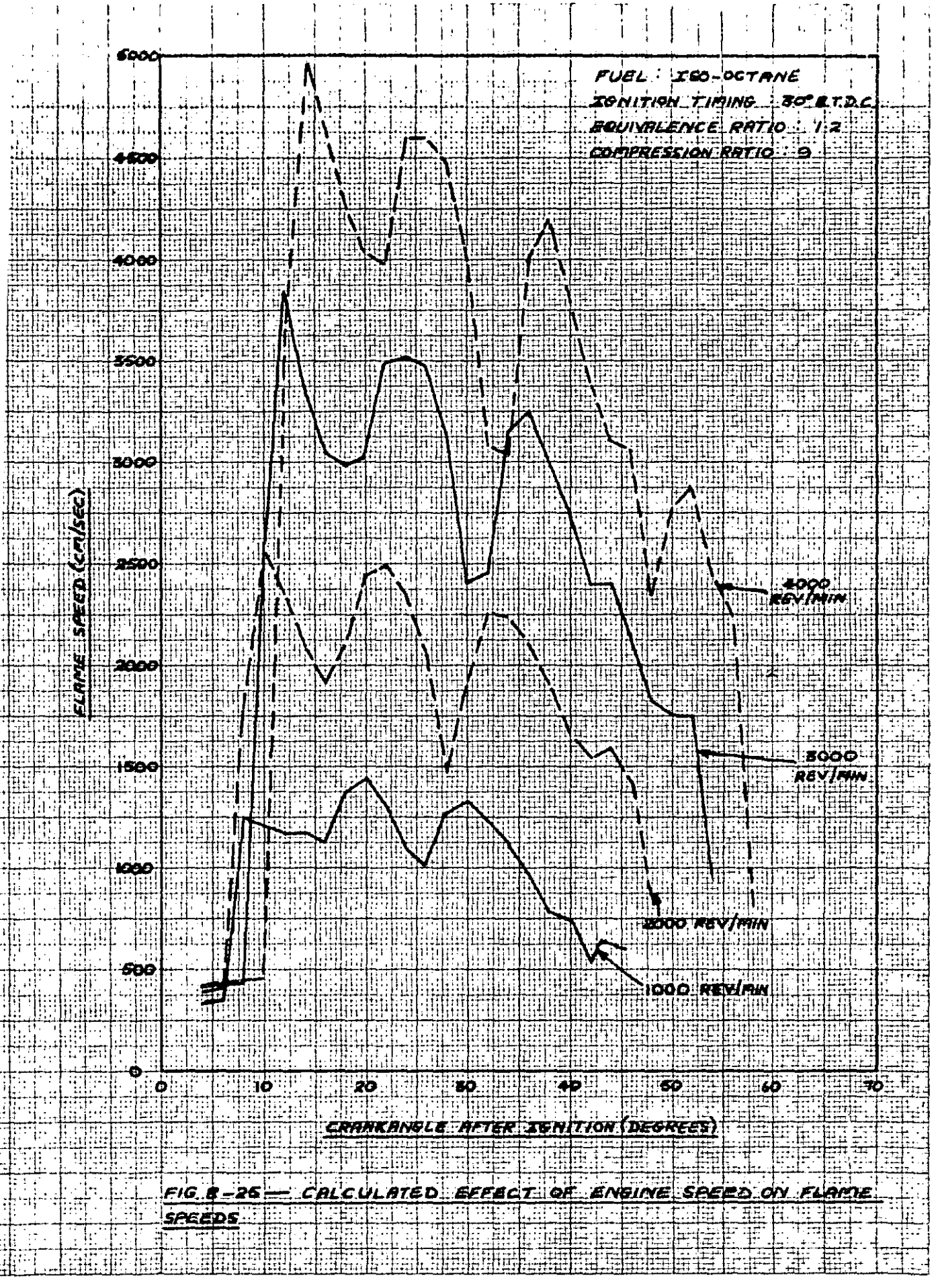

FIG. 8-26— CALCULATED EFFECT OF ENGINE SPEED ON FLAME SPEEDS

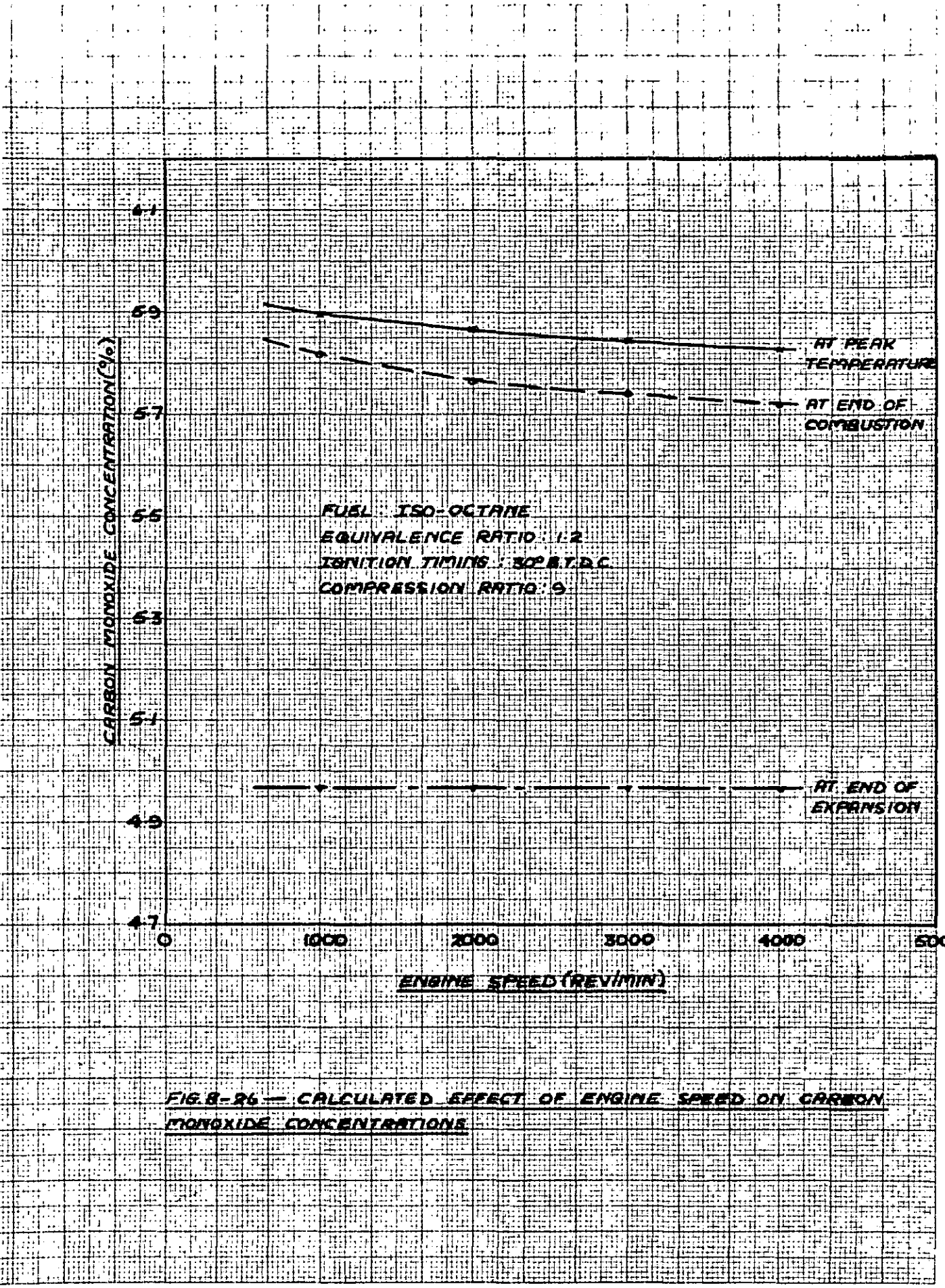

FIG 8-26 — CALCULATED EFFECT OF ENGINE SPEED ON CARBON MONOXIDE CONCENTRATIONS

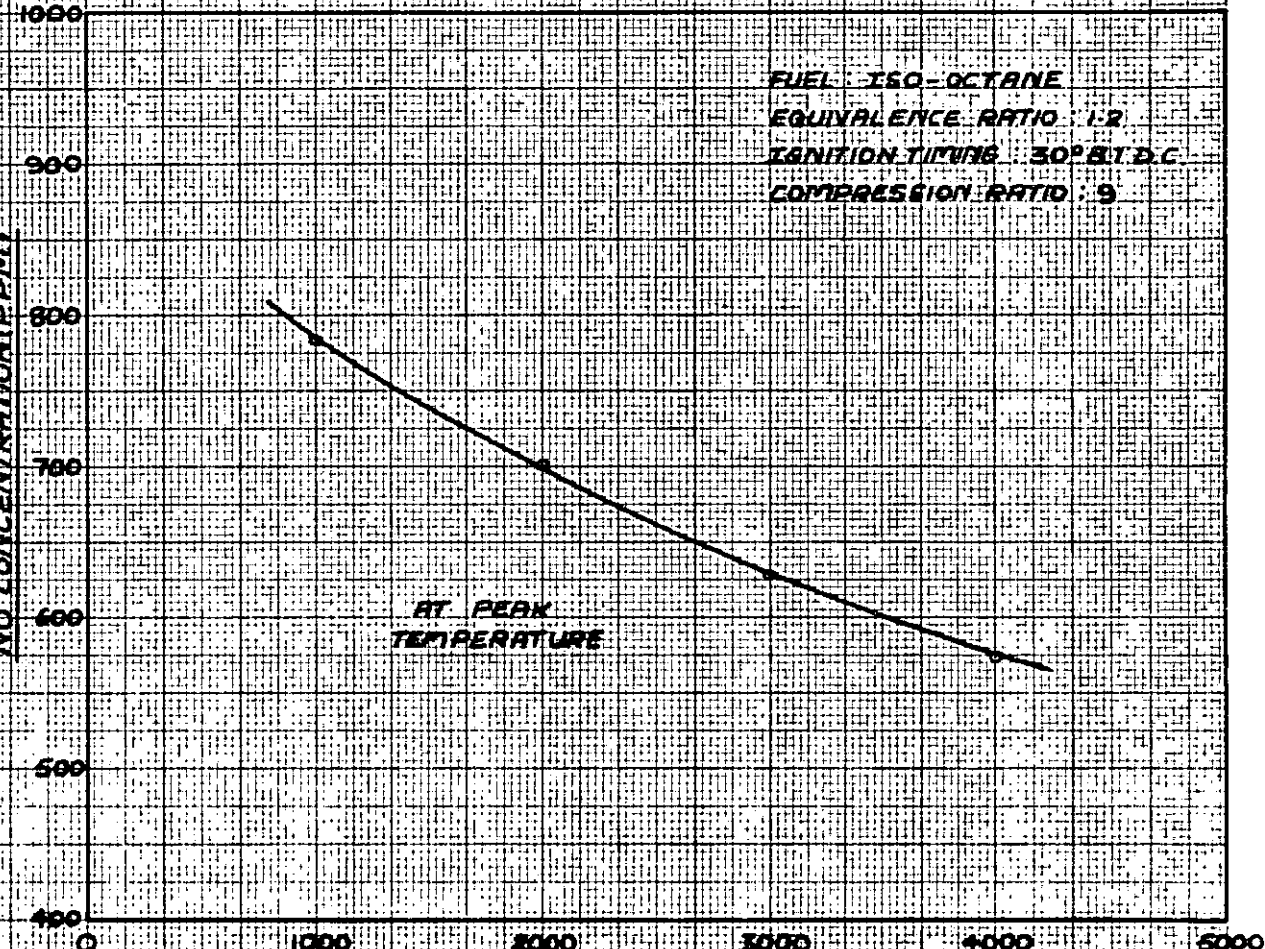

FIG. 8-27 — CALCULATED EFFECT OF ENGINE SPEED ON NITRIC OXIDE CONCENTRATIONS

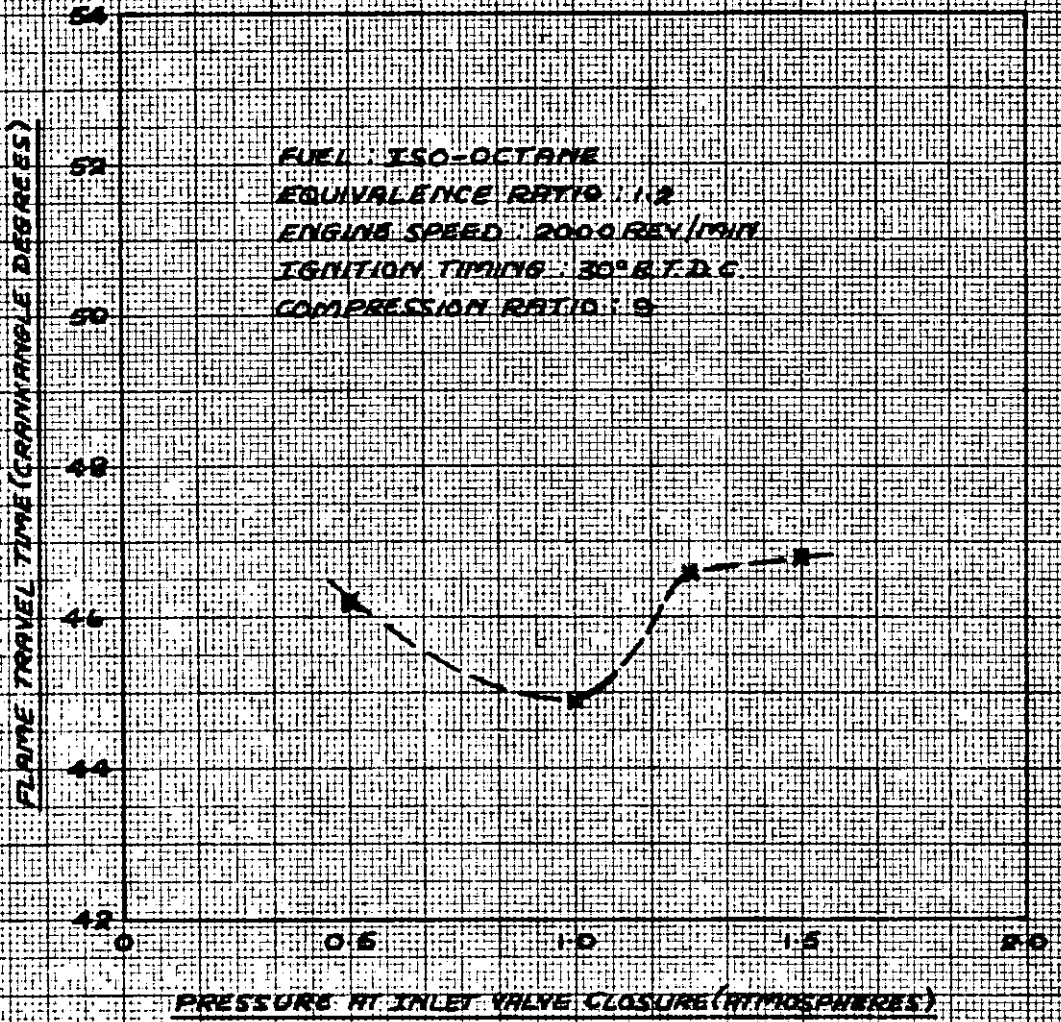

FIG 8-28 — CALCULATED EFFECT OF INITIAL PRESSURE ON FLAME TRAVEL TIME

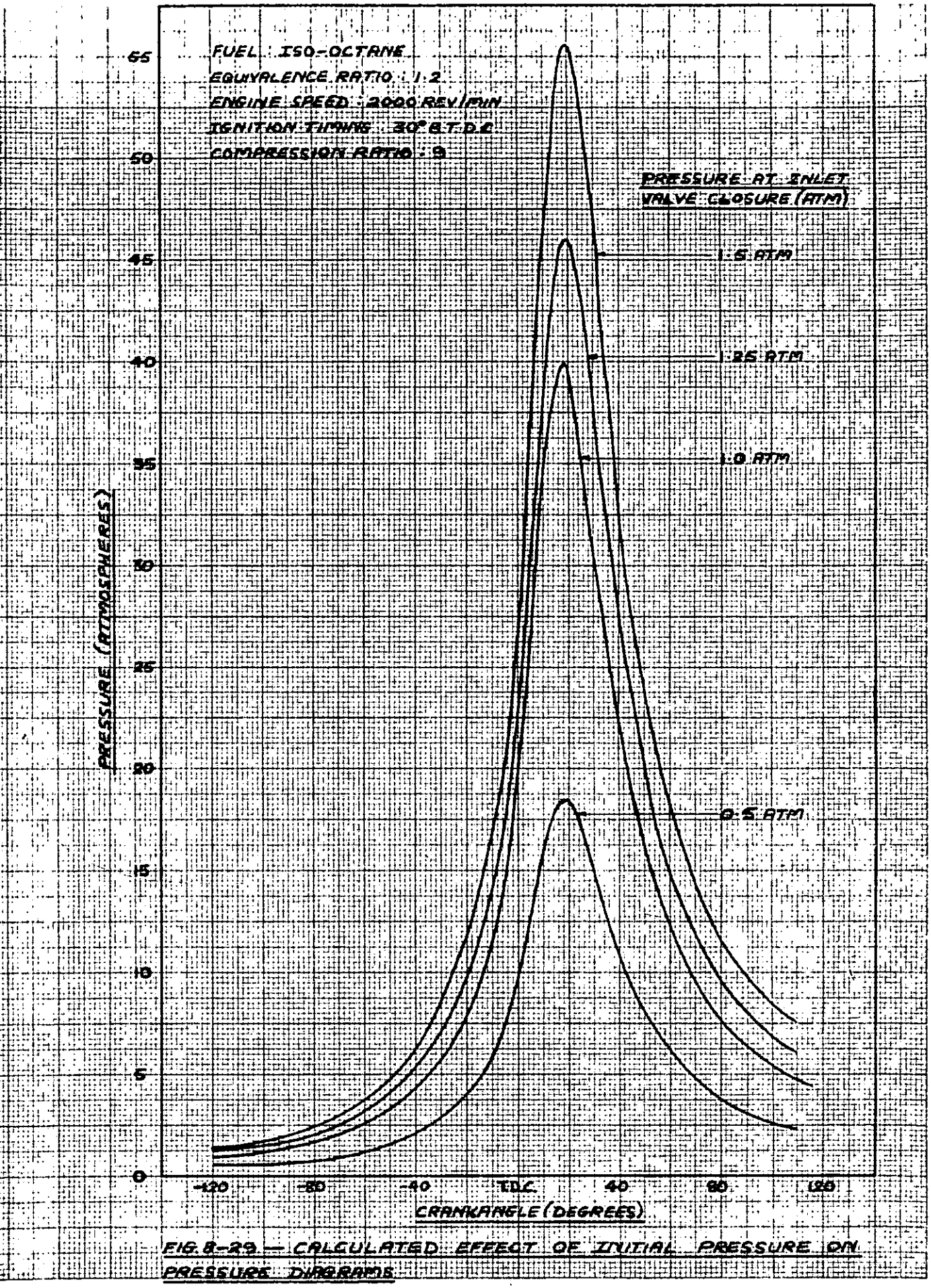

FIG. 8-29.— CALCULATED EFFECT OF INITIAL PRESSURE ON PRESSURE DIAGRAMS.

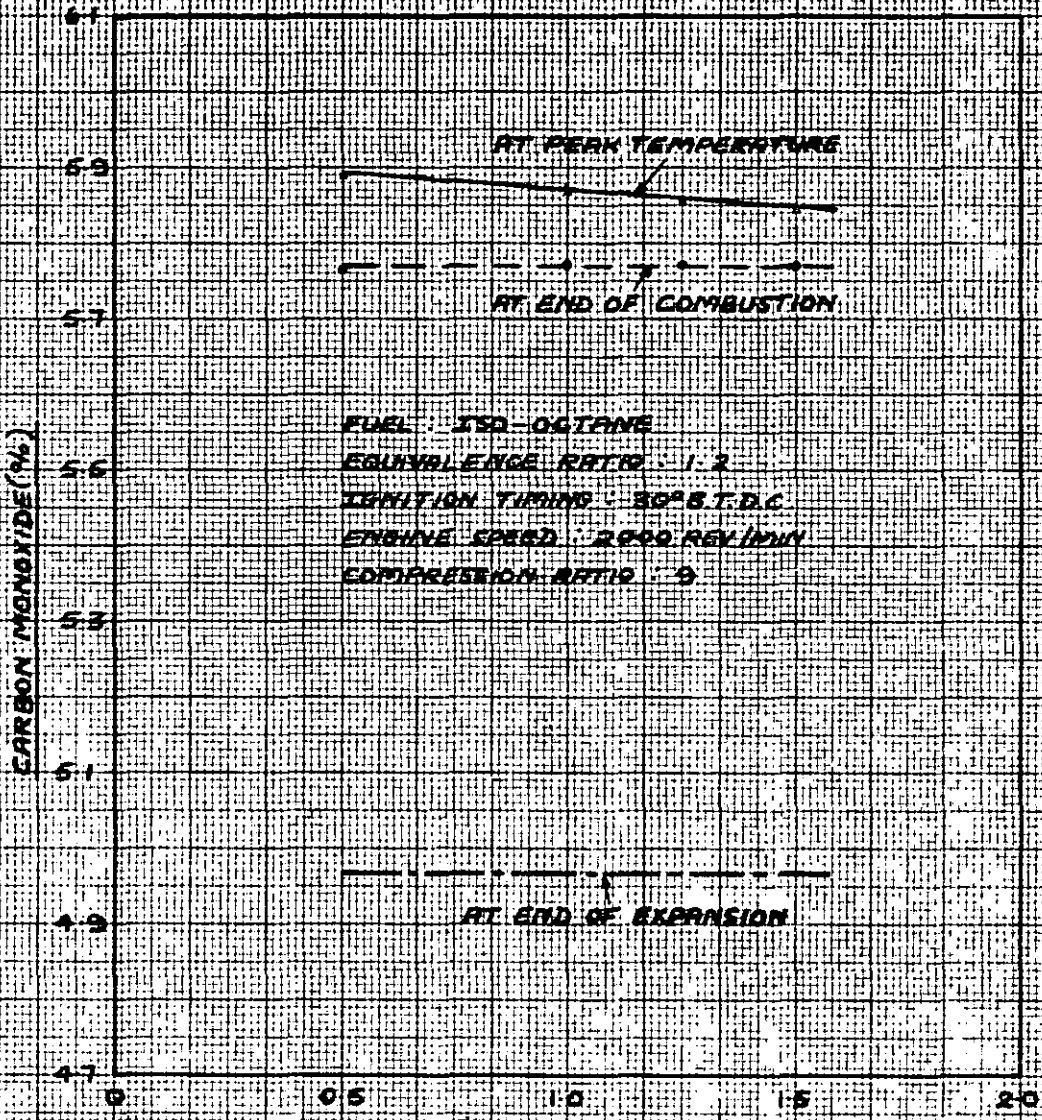

FIG 8-30 — CALCULATED EFFECT OF INITIAL PRESSURE ON CARBON MONOXIDE CONCENTRATIONS

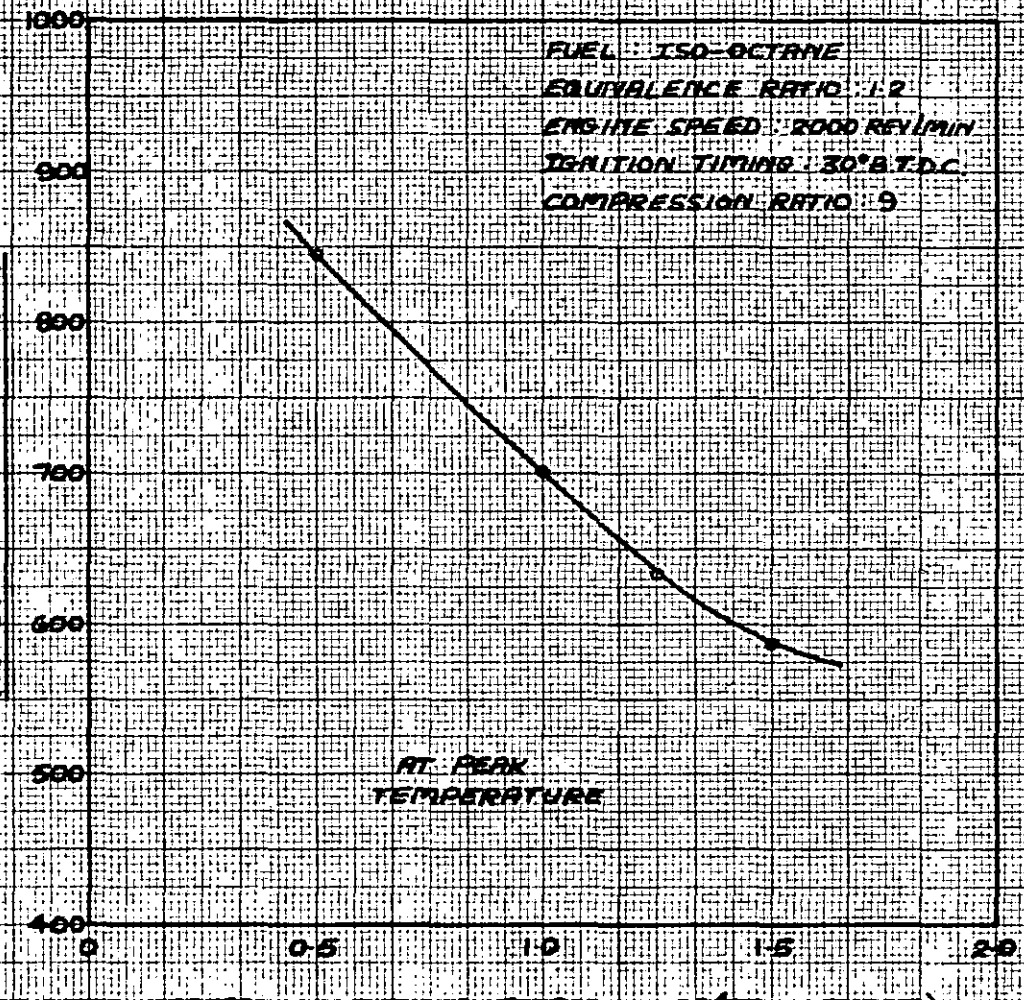

FIG. 8-31 — CALCULATED EFFECT OF INITIAL PRESSURE ON NITRIC OXIDE CONCENTRATIONS.

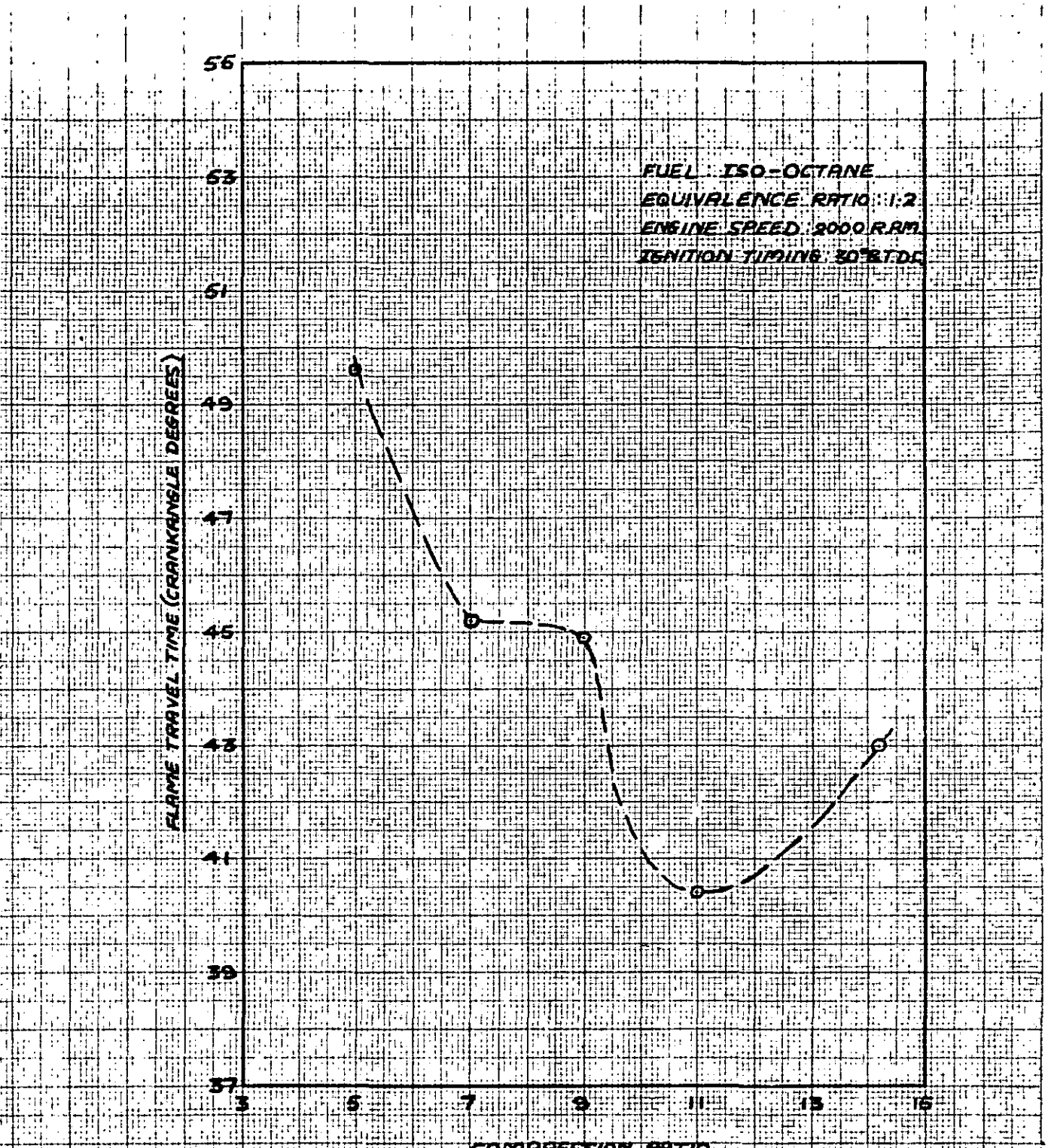

FIG. R-32 — CALCULATED EFFECT OF COMPRESSION RATIO ON FLAME TRAVEL TIME.

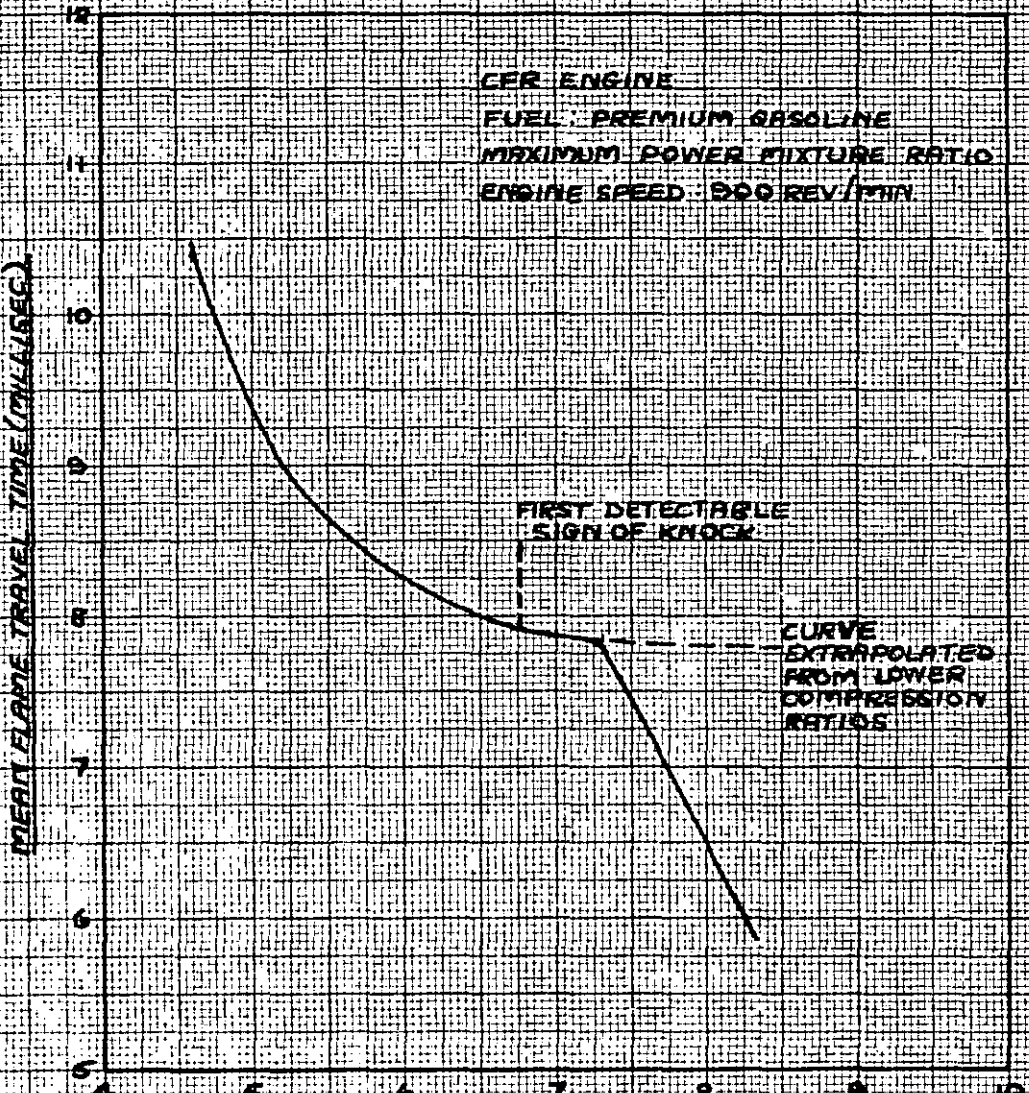

FIG. 8-33 — INFLUENCE OF COMPRESSION RATIO ON MEAN FLAME TRAVEL TIMES (ELLISON, HARROW AND HAYNARD[168])

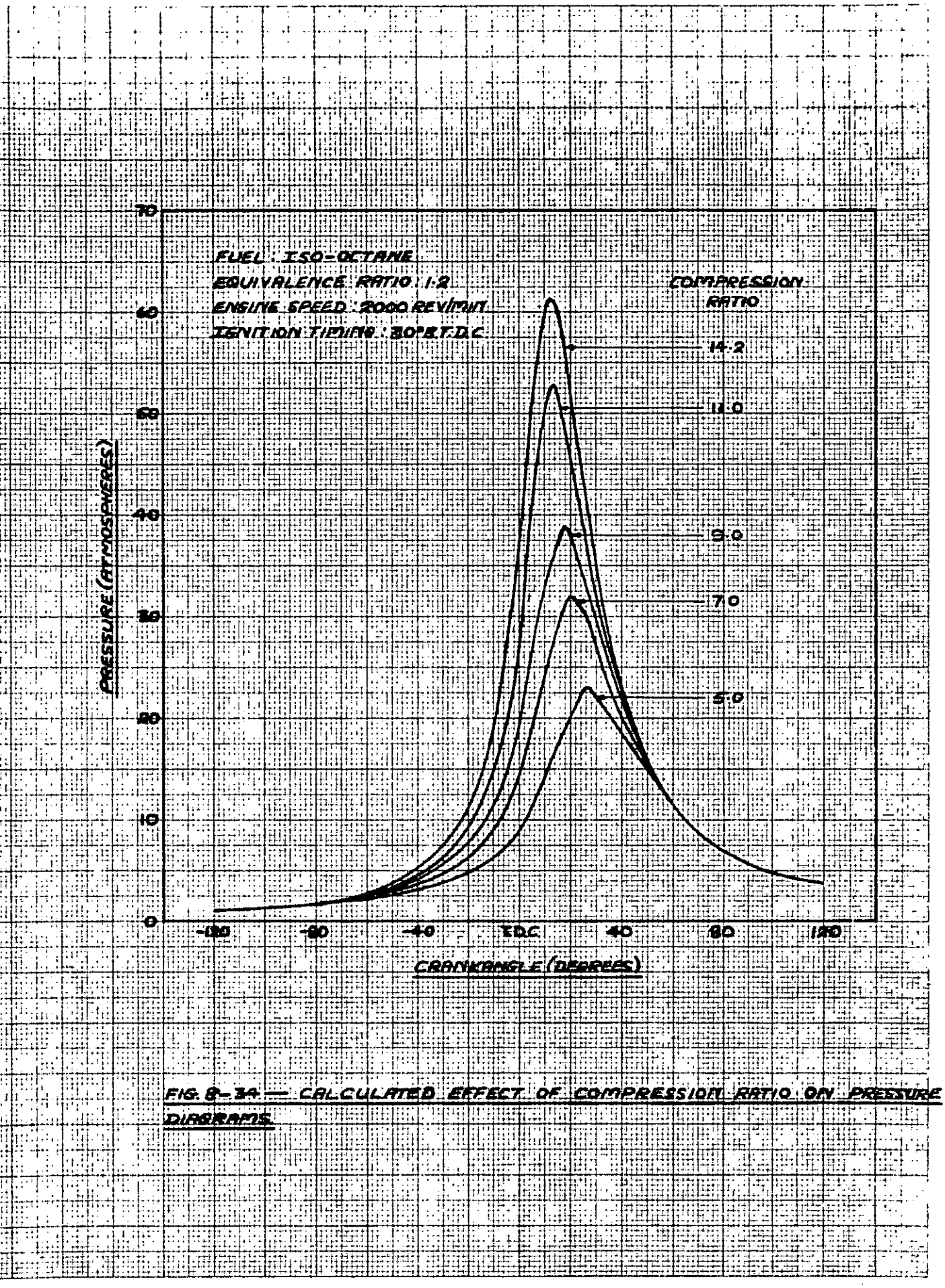

FIG. 8–34 — CALCULATED EFFECT OF COMPRESSION RATIO ON PRESSURE DIAGRAMS.

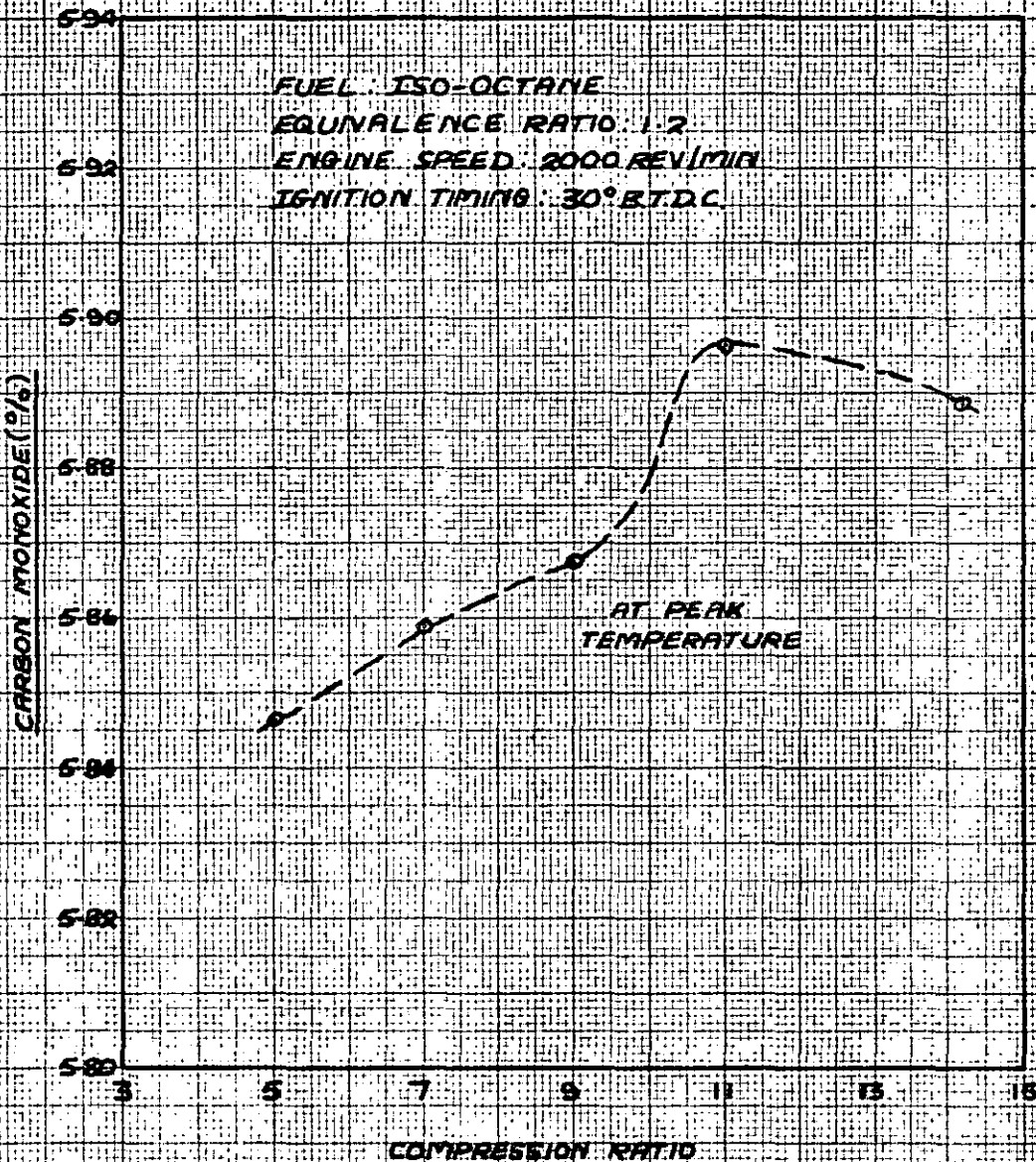

FIG. 8-35 — CALCULATED EFFECT OF COMPRESSION RATIO ON CARBON MONOXIDE CONCENTRATIONS

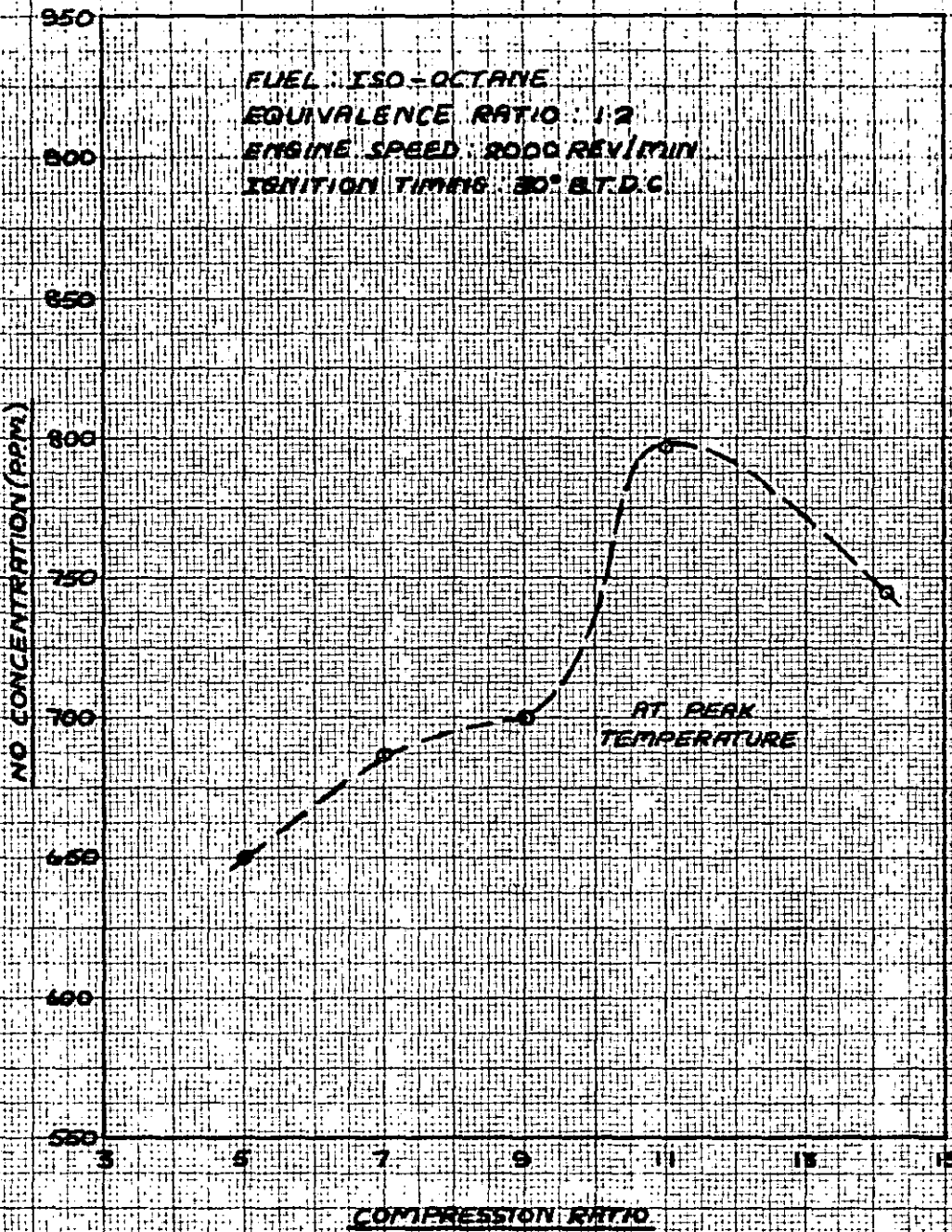

FIG. 2-36 — CALCULATED EFFECT OF COMPRESSION RATIO ON NITRIC OXIDE CONCENTRATIONS

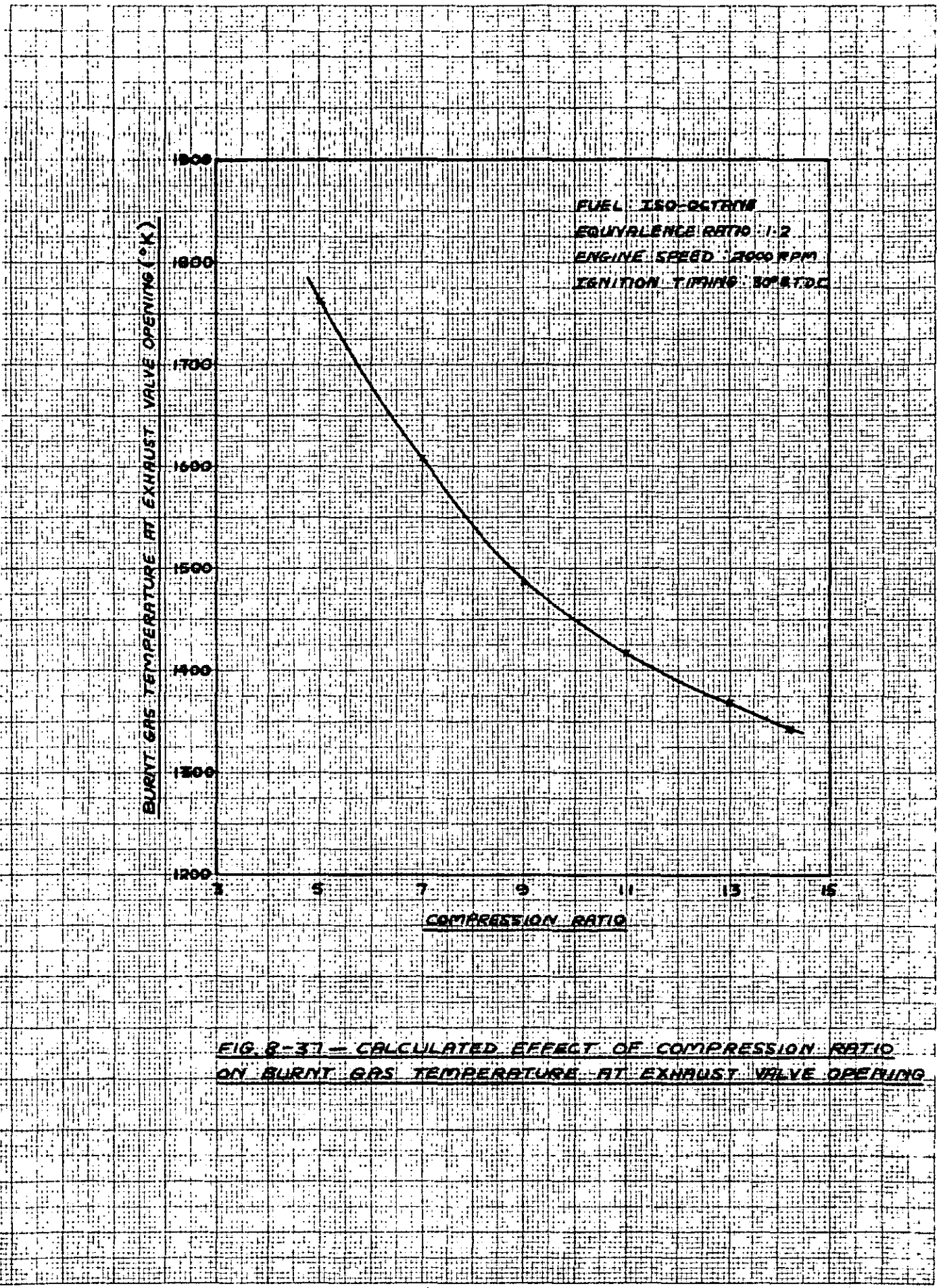

FIG. 8-37 — CALCULATED EFFECT OF COMPRESSION RATIO ON BURNT GAS TEMPERATURE AT EXHAUST VALVE OPENING

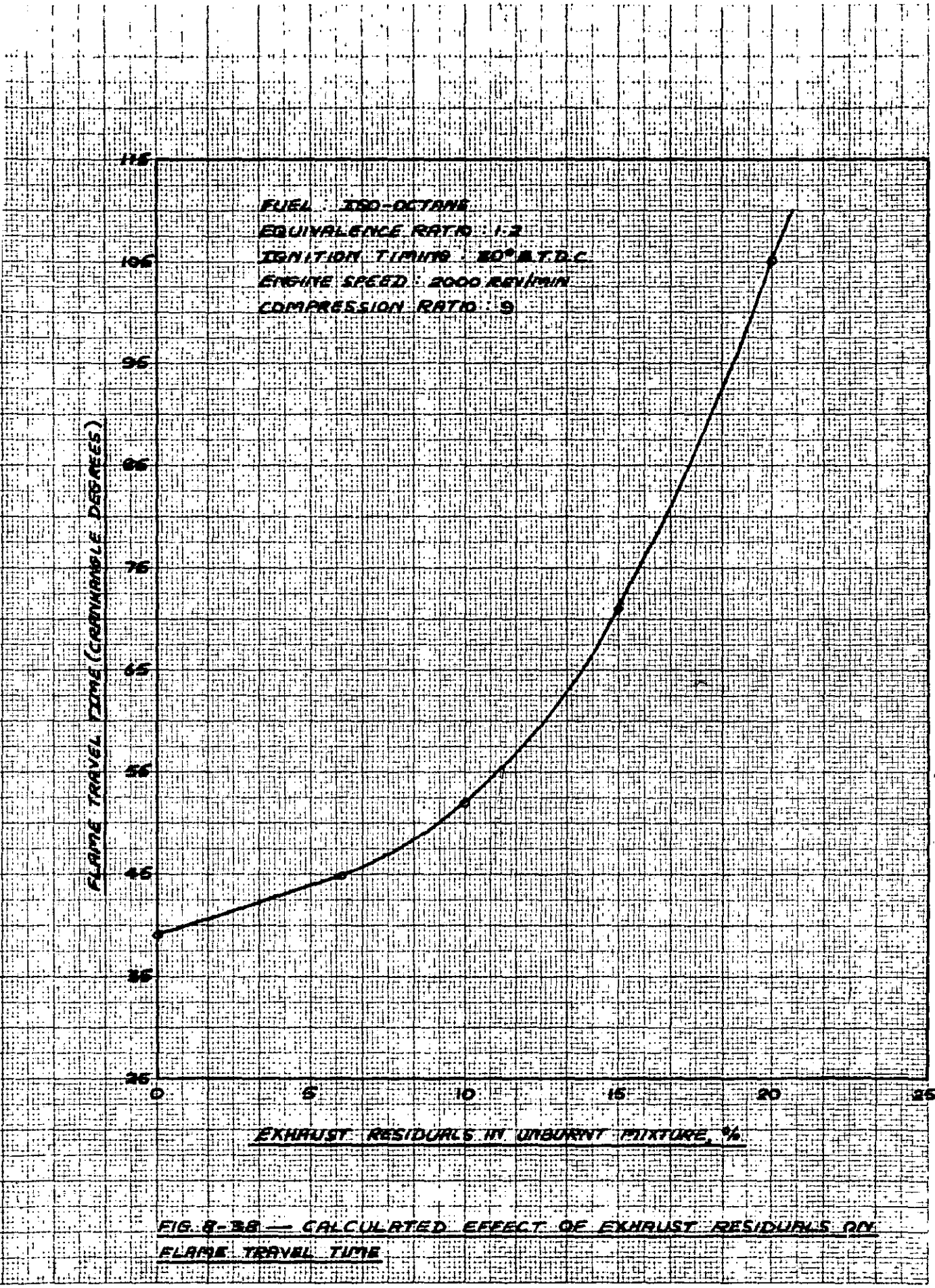

FIG. 8-38 — CALCULATED EFFECT OF EXHAUST RESIDUALS ON FLAME TRAVEL TIME

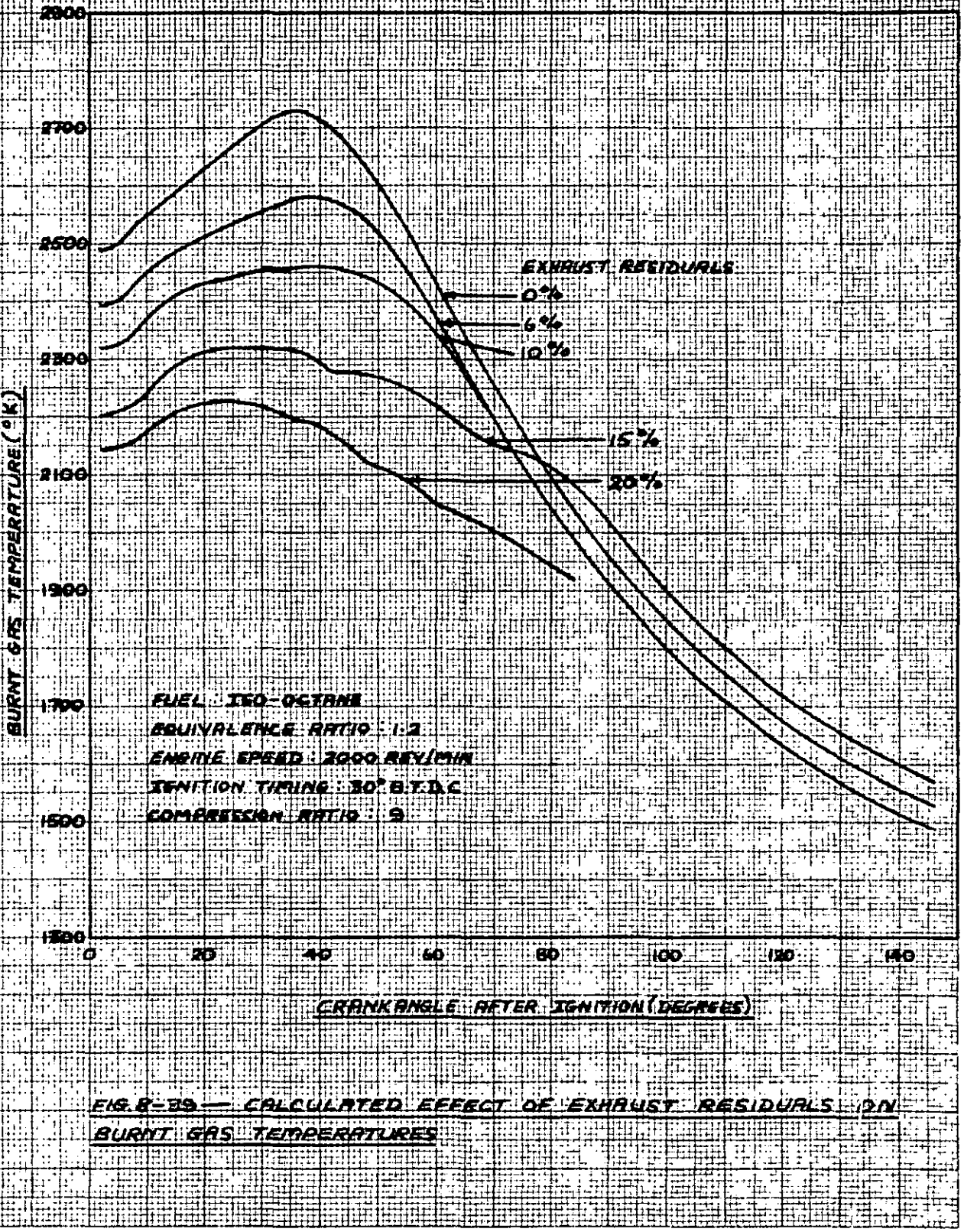

FIG. 8-39 — CALCULATED EFFECT OF EXHAUST RESIDUALS ON BURNT GAS TEMPERATURES

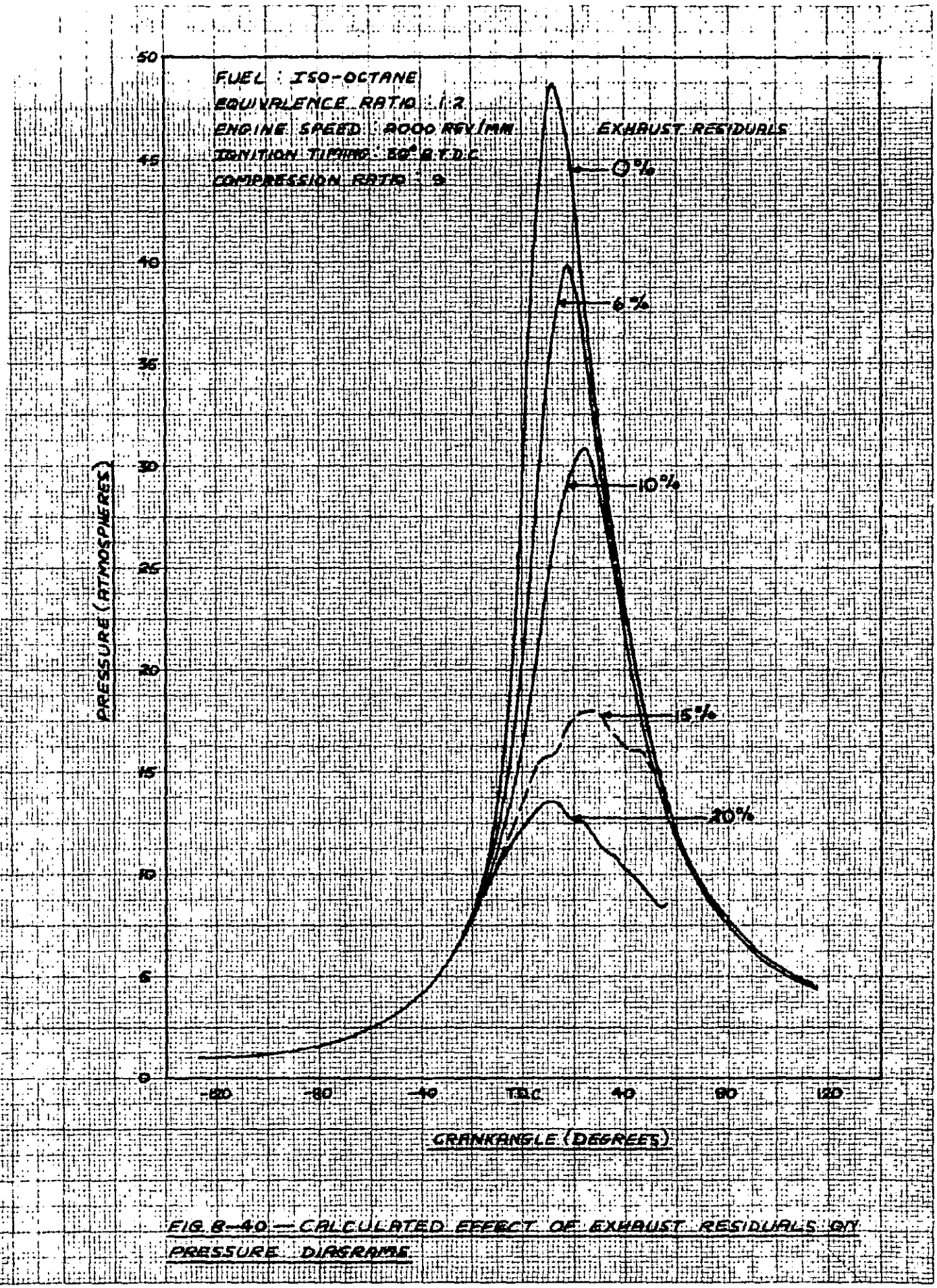

FIG. 8-40 — CALCULATED EFFECT OF EXHAUST RESIDUALS ON PRESSURE DIAGRAMS

paper
mm 10mm
m. 10mm

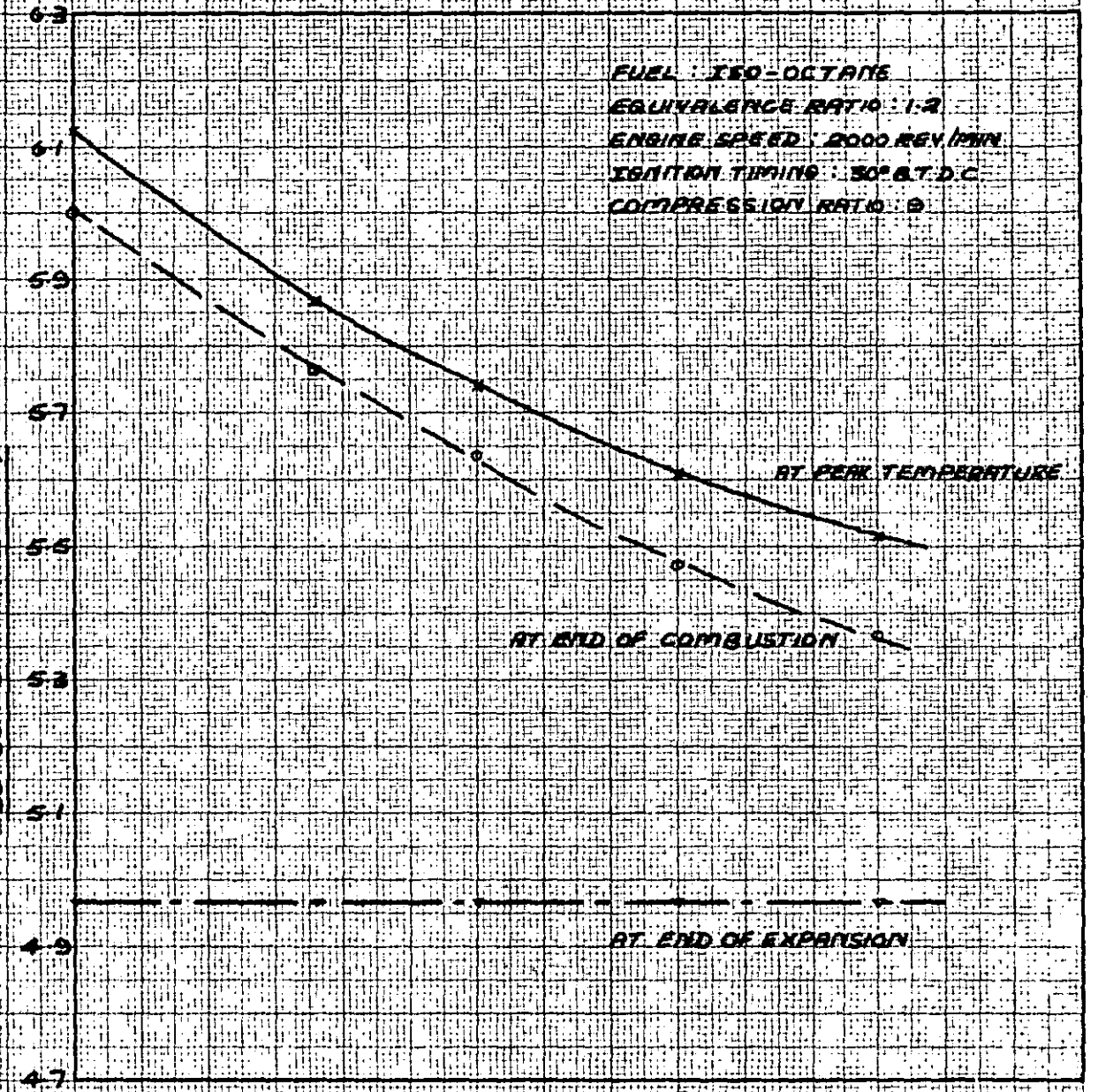

FIG. B-41 — CALCULATED EFFECT OF EXHAUST RESIDUALS ON CARBON MONOXIDE CONCENTRATIONS

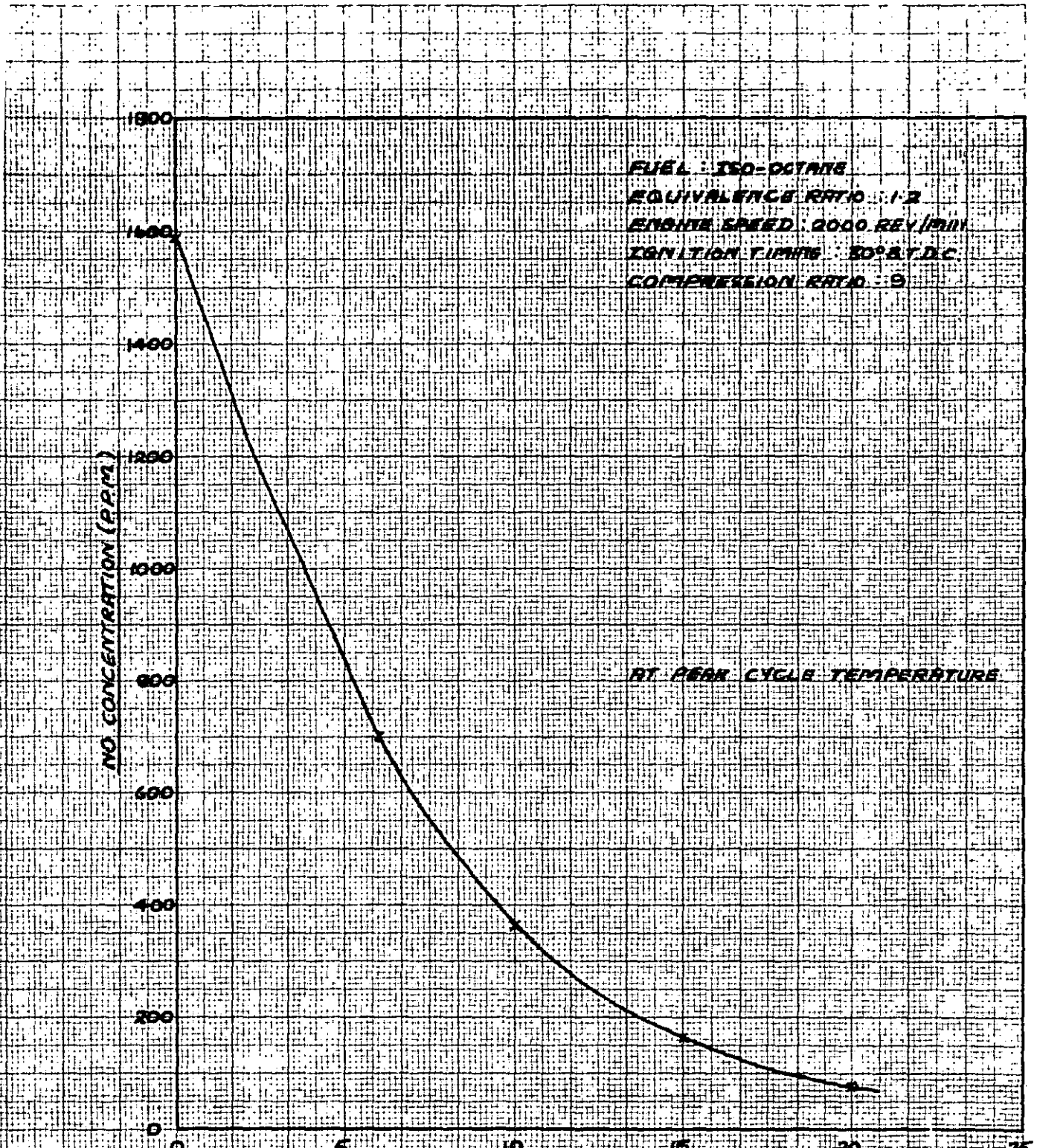

FIG 8-42 — CALCULATED EFFECT OF EXHAUST RESIDUALS ON NITRIC OXIDE CONCENTRATIONS

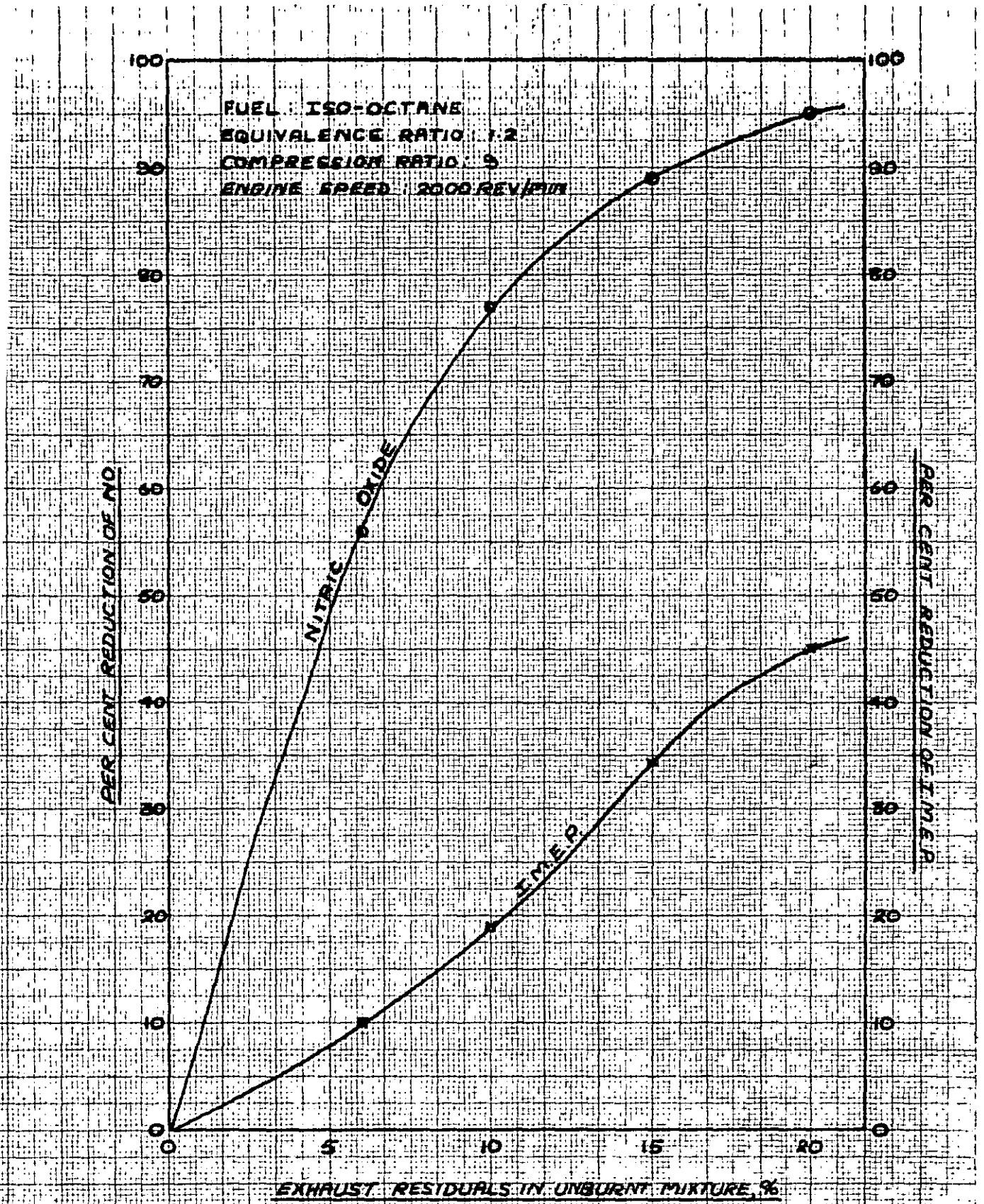

FIG. 8-43 — CALCULATED EFFECT OF EXHAUST RESIDUALS ON PERCENTAGE REDUCTIONS OF NITRIC OXIDE AND I.M.E.P.

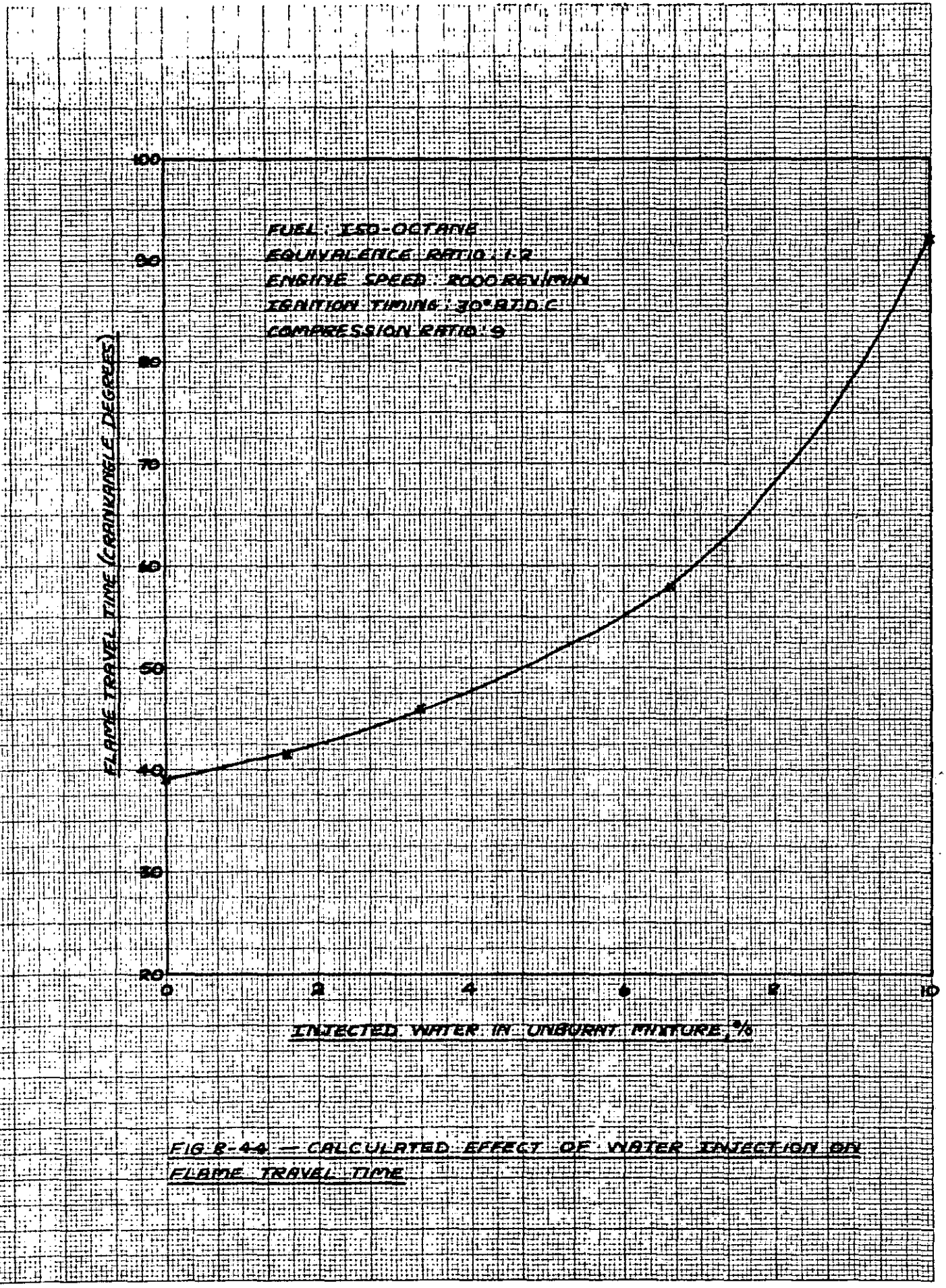

FIG 8-4-4 — CALCULATED EFFECT OF WATER INJECTION ON FLAME TRAVEL TIME

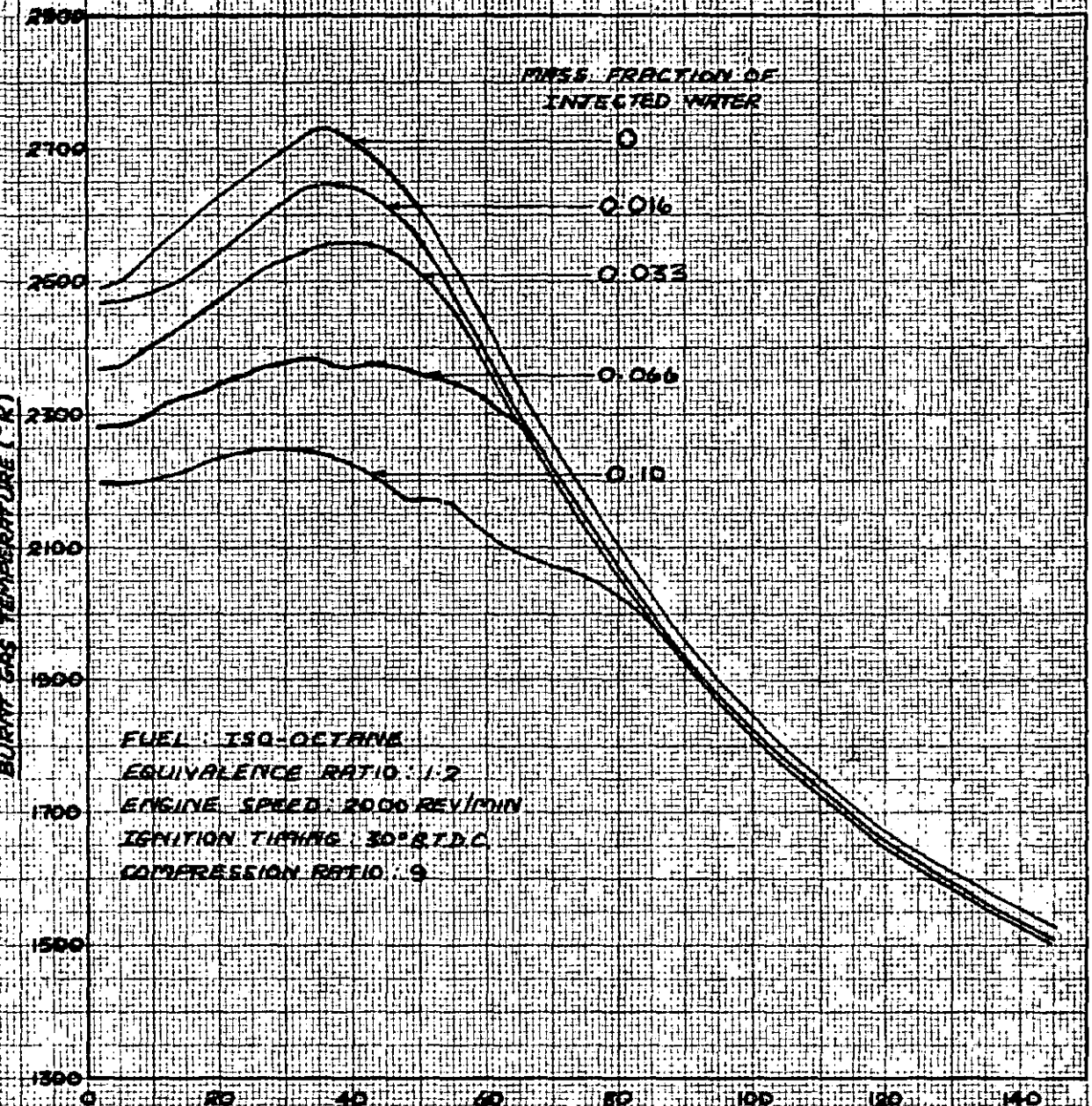

FIG 8-45 — CALCULATED EFFECT OF INJECTED WATER ON BURNT GAS TEMPERATURES

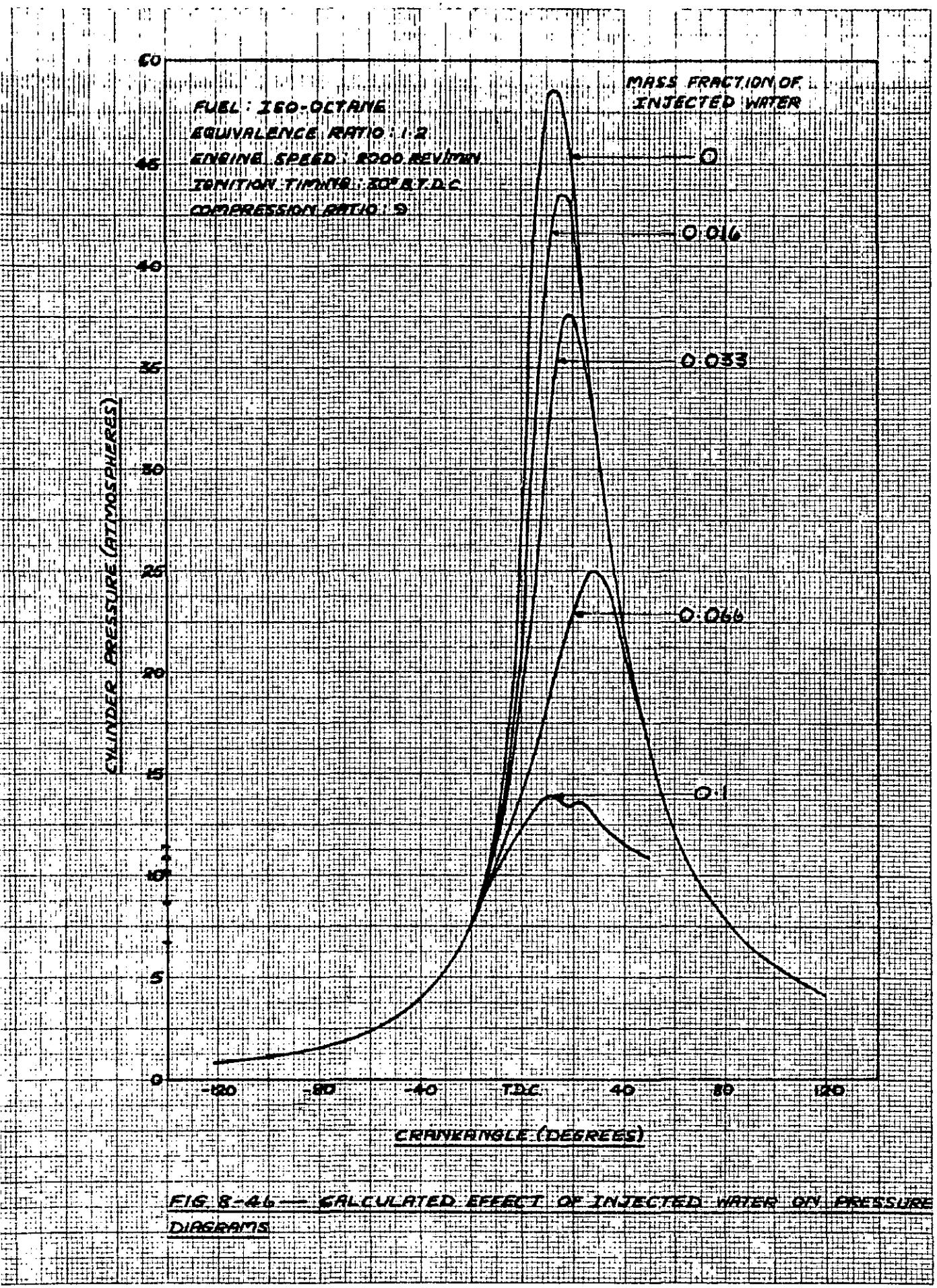

FIG. 8-46 — CALCULATED EFFECT OF INJECTED WATER ON PRESSURE DIAGRAMS

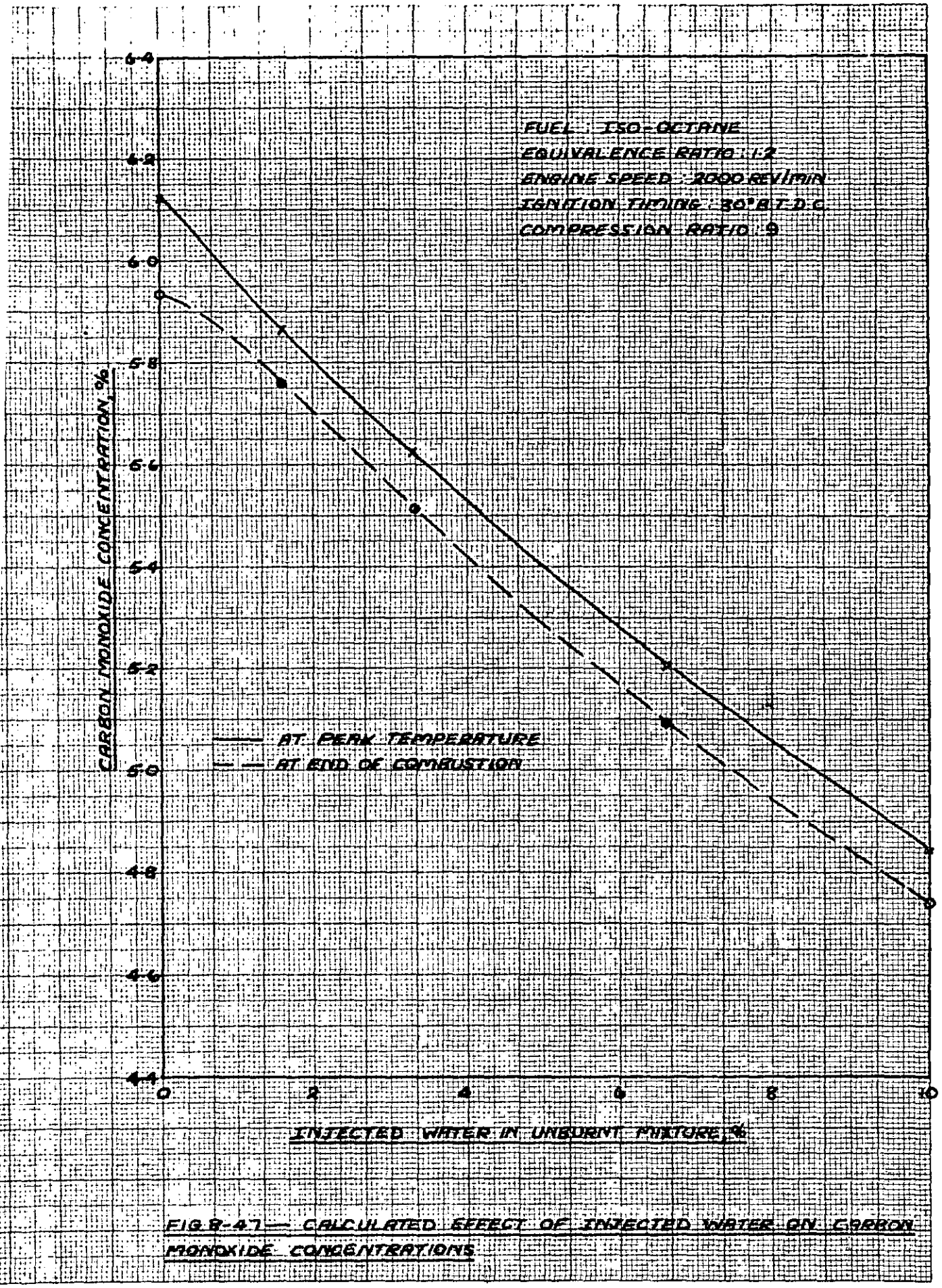

FIG 8-47— CALCULATED EFFECT OF INJECTED WATER ON CARBON MONOXIDE CONCENTRATIONS

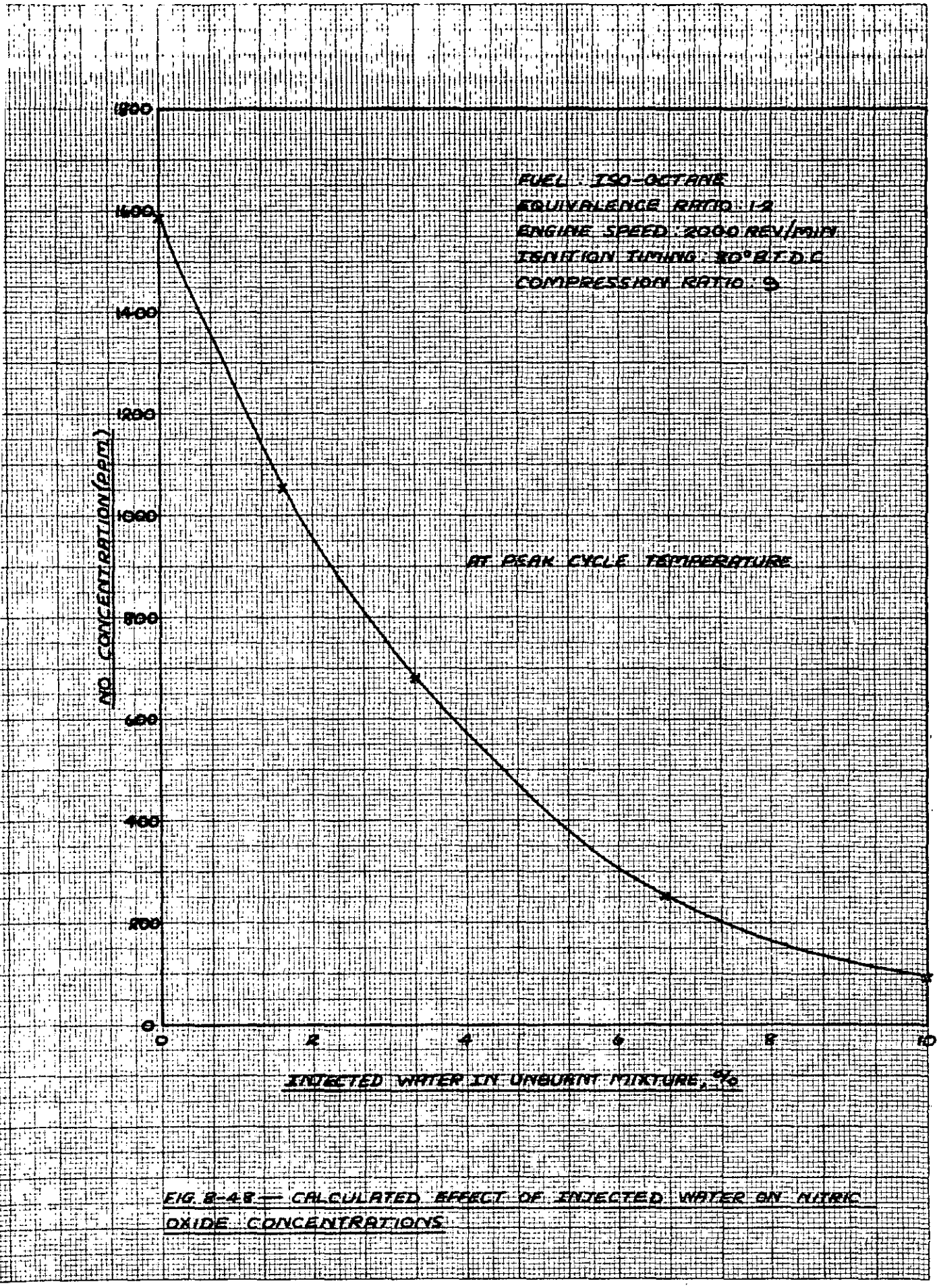

FIG. 8-48 — CALCULATED EFFECT OF INJECTED WATER ON NITRIC OXIDE CONCENTRATIONS

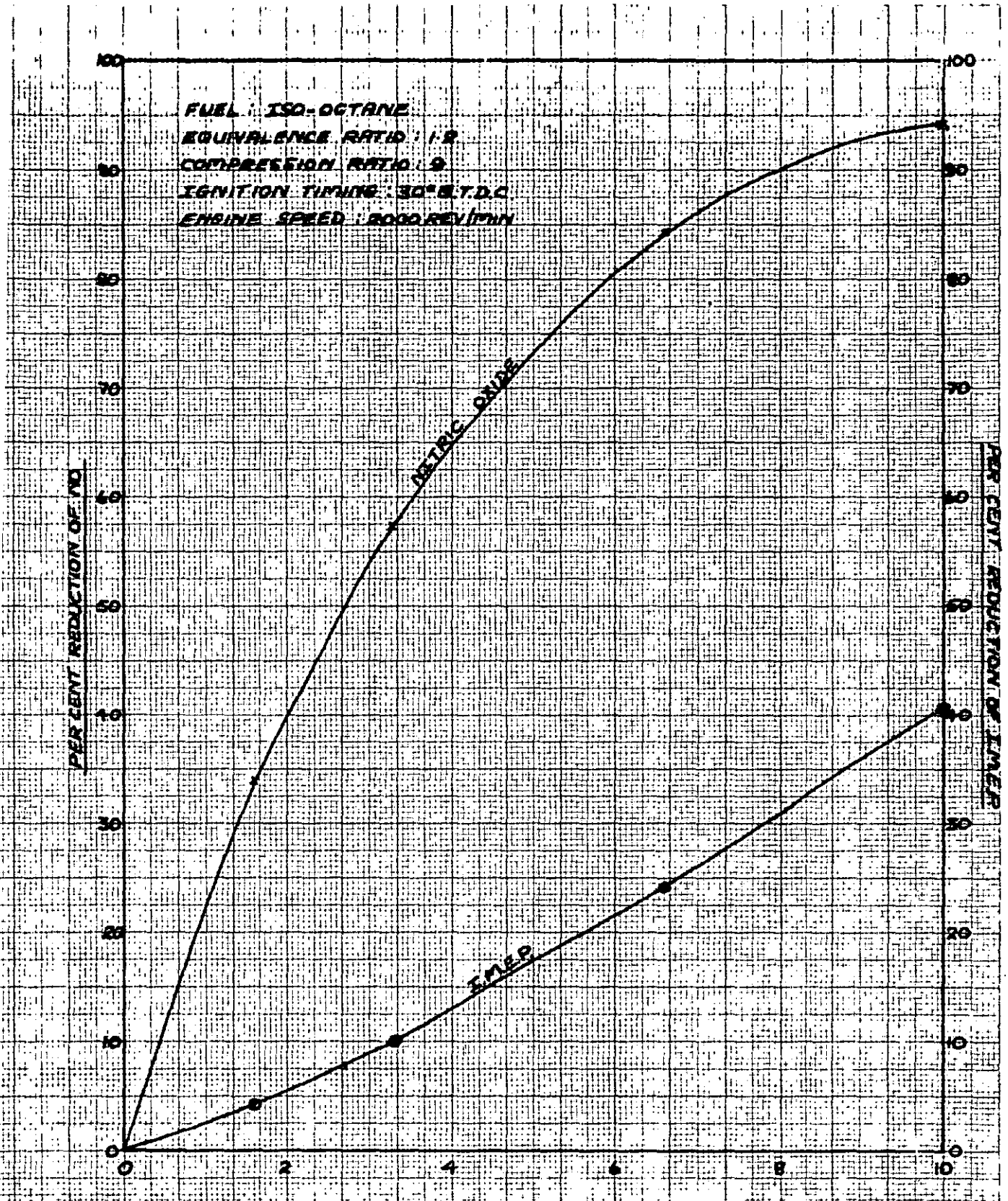

FIG 8-49 — CALCULATED EFFECT OF INJECTED WATER ON PERCENTAGE REDUCTIONS OF NITRIC OXIDE AND I.M.E.P.

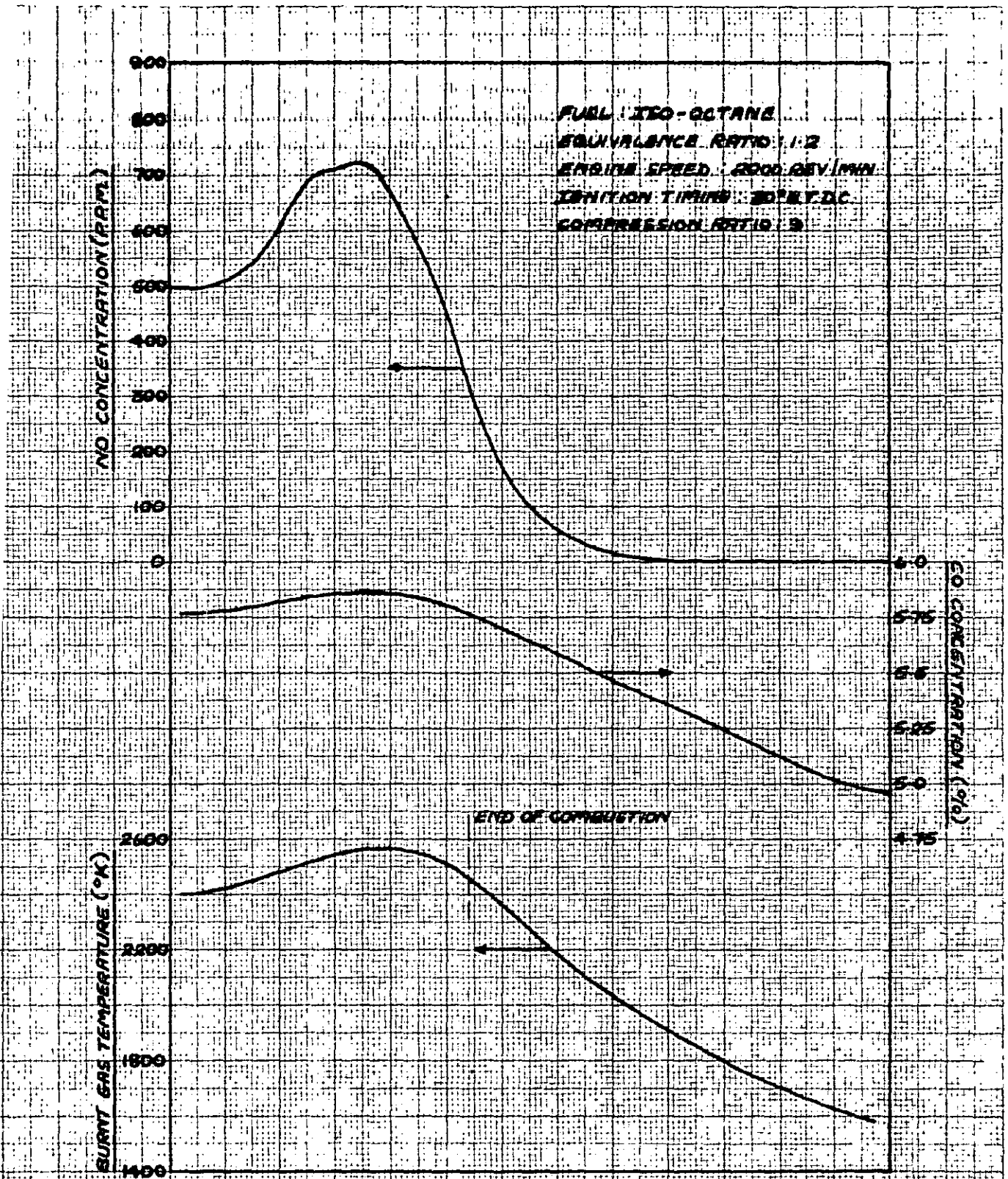

FIG. 8-50 — TYPICAL DEVELOPMENTS OF BURNT GAS TEMPERATURE, NITRIC OXIDE AND CARBON MONOXIDE DURING COMBUSTION AND EXPANSION

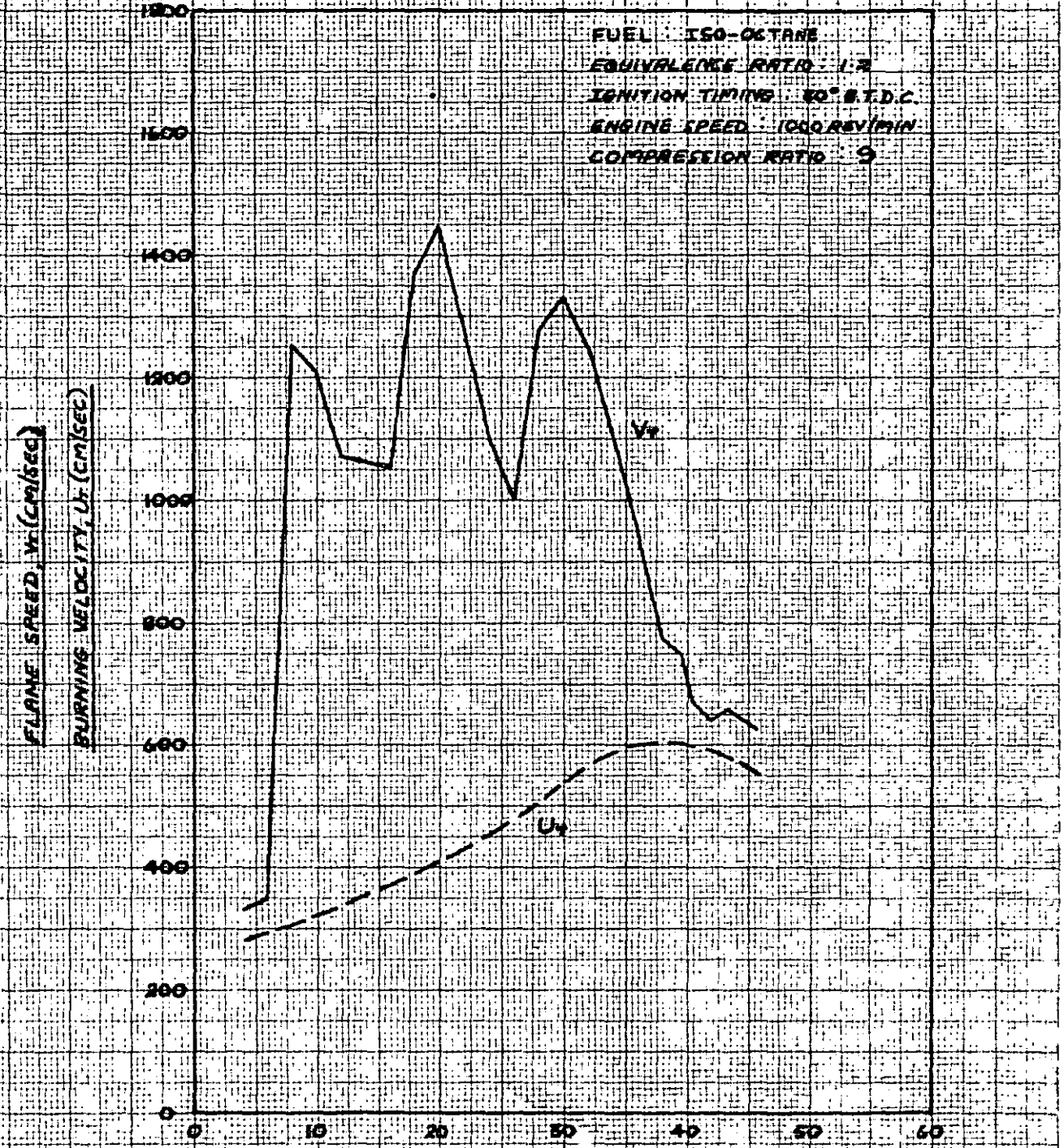

FIG. 8-51 — CALCULATED VARIATION OF BURNING VELOCITY AND FLAME SPEED DURING COMBUSTION PERIOD

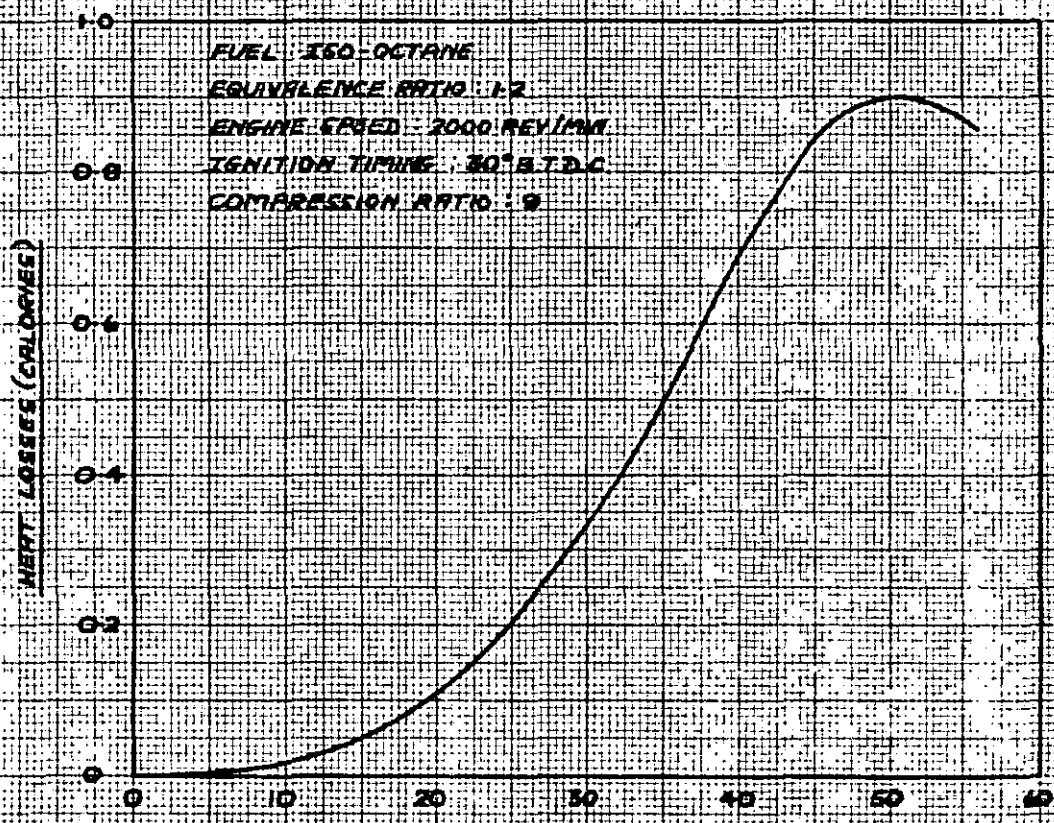

FIG 8-62 — TYPICAL CALCULATED VARIATION IN HEAT LOSSES THROUGH COMBUSTION PERIOD

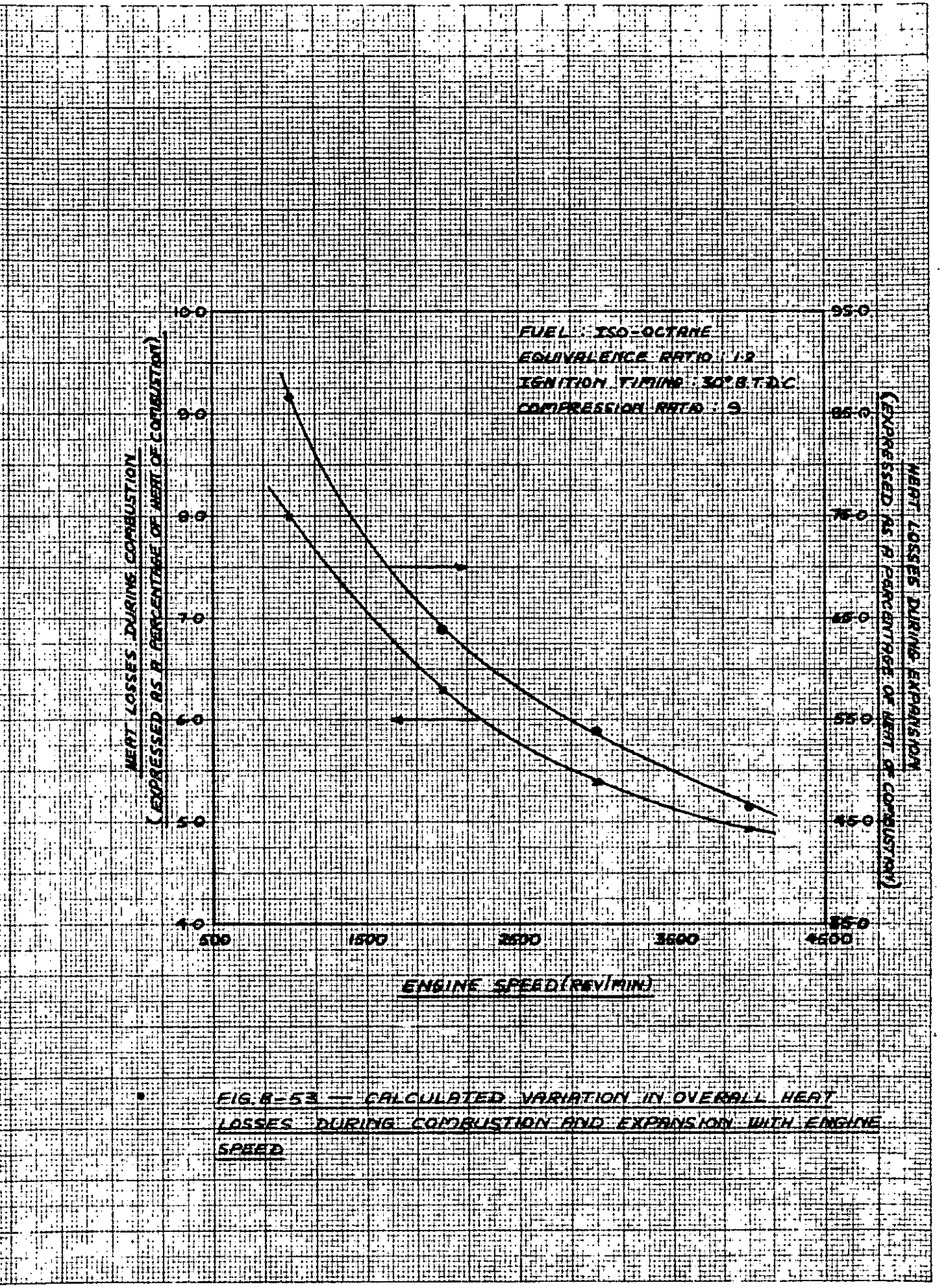

FIG. 8-53 — CALCULATED VARIATION IN OVERALL HEAT LOSSES DURING COMBUSTION AND EXPANSION WITH ENGINE SPEED

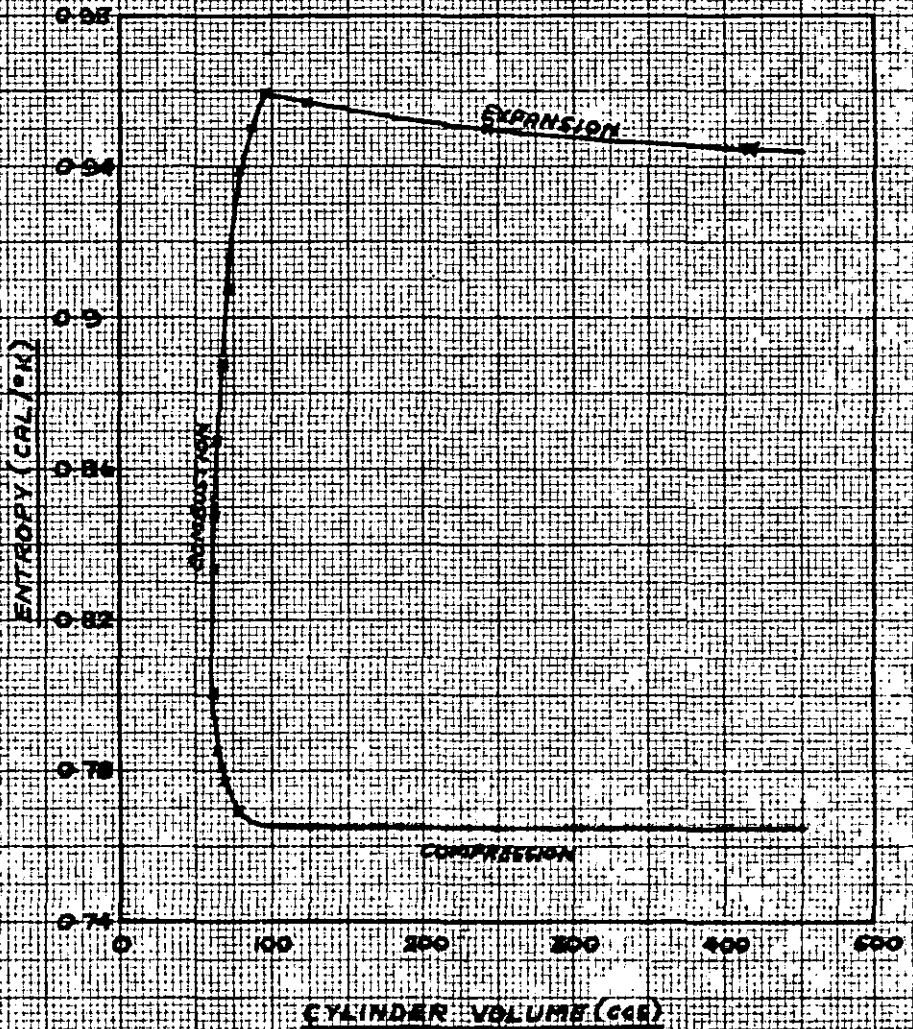

FIG. 8-54 — TYPICAL ENTROPY-VOLUME DIAGRAM DURING COMPRESSION, COMBUSTION AND EXPANSION

CHAPTER 9

FUTURE WORK

CHAPTER 9

FUTURE WORK

It is considered that the main drawbacks to the computer simulated combustion model as presented in this work are the inability to accurately predict

i) the flame travel time variation over the complete equivalence ratio range especially with regard to the equivalence ratio for minimum flame travel time.

ii) the concentrations of carbon monoxide and nitric oxide appearing in the engine exhaust.

As has already been mentioned, the former inaccuracy appears to be the direct result of assuming that turbulent combustion is associated with and similar to laminar combustion. The development of a turbulent flame propagation theory based on a Volume or Three-dimensional conception (see Chapter 4, Section 4.2.4) is proposed. To this end, direct measurements of some turbulence parameters using hot wire anemometry techniques is being conducted. A relationship between the scale and the frequency of the eddies primarily responsible for the propagation of the flame in various types of spark ignition engine combustion chambers is required. Also needed is the variation in the relevant turbulent parameters with engine speed, piston motion, throttling and compression ratio.

The inability to accurately predict CO and NO concentrations in engine exhausts is directly related to the assumptions of chemical equilibrium in the burnt gases.

A more accurate model would consider the effects produced by non-equilibrium conditions. This, however, would involve determinations of specie concentrations from formulae of the kind

$$\frac{d[C_A]}{dt} = k \cdot [C_B] \cdot [C_C]$$

where

C_A is the concentration of specie A(moles/cc)

C_B is the concentration of specie B(moles/cc)

C_C is the concentration of specie C(moles/cc)

and

k is the reaction rate constant (cc/mole sec)

To evaluate these equations, numerical integration techniques would have to be incorporated into the analytical model. Although this is not beyond the realms of possibility, the amount of computer time then required for a single run under specified conditions would be prohibitive. A more convenient, though less accurate, technique could involve the utilization of such a computer program as was devised by Newhall[86] which considers the kinetics of engine generated CO and NO_x during expansion. This would be modified to cover the combustion phase as well with all the required data (e.g. temperatures, pressures, burnt gas volumes, etc.) being fed in from the equilibrium simulation in this work. To facilitate a reasonably fast computer execution time with this method, a much faster numerical integration routine than the Runge-Kutta one (used by Newhall) needs to be available.

A further area in which future work might be brought

to bear is in considerations of the heat release in the unburnt charge ahead of the flame front. In this conneetion, the evaluation of a knock criterion might be possible. The work of Johnson et al[42] and Karim[211] is significant in these considerations.

BIBLIOGRAPHY AND REFERENCES

BIBLIOGRAPHY AND REFERENCES

1. HERSHEY, R.L., EBERHARDT, J.E. and HOTTEL, H.C.

"Thermodynamic properties of the Working Fluid in Internal Combustion Engines".
S.A.E. Journal, Vol. 39 (October 1936), p.409.

2. HOTTEL, H.C., WILLIAMS, G.C., and SATTERFIELD, C.N.

"Thermodynamic Charts for Combustion Processes."
Vols. land 2, New York : John Wiley and Sons (1949).

3. NEWHALL, H.K. and STARKMAN, E.S.

"Thermodynamic Properties of Octane and Air for Engine Performance Calculations."
S.A.E. Progress in Technology, Volume 7, 1964.

4. STARKMAN, E.S., NEWHALL, H.K. and SUTTON, R.D.

"Comparative Performance of Alcohol and Hydrocarbon Fuels."
S.A.E. Special Publication SP-254, 1964.

5. NAGEL, A.

"Versuche uber die Zundgeschwindigkeit Explasiber Gasgemische."
Mitteilungen uber Forschungsarbeiten, Vol. 54, 1908, pp.1-42.

6. FLAMM and MACHE.

Wiens Sitzungsberichte, Vol. 126, 1917, p.9.

7. ROSECRANS, C.Z.

University of Illinois Experimental Station Bulletin 167 (1926)

8. ENDRES, W.

Der Verbrennungsvorgang im Gas and Vergaser Motor,
J. Springer, Berlin, 1928.

9. HOTTEL, H.C. and EBERHARDT, J.F.

Chemical Reviews, 21, (1937), 439

10. RASSWEILER, G.M. and WITHROW, L.

"Motion Pictures of Engine Flames Correlated with Pressure Cards."
S.A.E. Transactions, Vol. 42, No. 5. 1938.

11. RASSWEILER, G.M. and WITHROW, L. and CORNELIUS, W.

"Engine Combustion and Pressure Development."
S.A.E. Transactions, Vol. 46. No. 1, 1940.

12. WITHROW, L. and CORNELIUS, W.

"Effectiveness of the Burning Process."
S.A.E. Transactions, Vol. 47, No. 6, 1940.

13. RABEZZANA, H., KALMAR, S. and CANDELISE, A.

"Combustion : An analysis of burning and expansion in the reaction zone."
Automobile Engineer : October, 1939.

14. EDSON, M.H.

"A Mathematical Model for Combustion in the Otto cycle engine."
Ind. and Eng. Chemistry ; Vol. 52, No. 12, 1960.

15. PATTERSON, D.J.

"A Comprehensive Cycle Analysis and Digital Computer Simulation for Spark-Ignited Engines."
Ph.D. Thesis, University of Michigan, 1962.

16. SEMENOV, N.N.

"Thermal Theory of Combustion and Explosion, III. Theory of Normal Flame Propagation."
N.A.C.A. T.M. No. 1026. 1942.

17. EICHELBERG, G.

"Some New Investigations on old Combustion-Engine Problems."
Engineering, Vol. 148 (1939), pp.463-66, 547-50, 603-5, 682-86.

18. STRANGE, F.M.

"An analysis of the Ideal Otto Cycle, including the Effects of Heat Transfer, Finite Combustion Rates, Chemical Dissociation and Mechanical Losses."
S.A.E. Progress in Technology, Volume 7, 1964.

19. PHILLIPPS, R.A. and ORMAN, P.L.

"Simulation of Combustion in a Gasoline Engine using a Digital Computer."
Advances in Automobile Engineering (Part IV), Pergamon Press - Oxford and New York - 1966.

20. MALLARD, E. and LE CHATELIER, H.

Annales de Mines, 4, p.274, 1883.

21. KRIEGER, R.B., BODY, R.K., MYERS, P.S. and UYEHARA, O.A.

"Simulation of a Crankcase Scavenged, Two-stroke, S.I. Engine and Comparisons with Experimental Data."
S.A.E. paper No. 690135, Jan. 1969.

22. WALKER, G.

"Effect of the Rate of Combustion on Gasoline Engine Performance."
Inl. of the Inst. of Fuel : June, 1964.

23. ANNAND, W.J.D.

"Heat Transfer in the Cylinders of Reciprocating I.C. Engines."
J.Mech.E., Vol. 177, No. 36, 1963.

24. HURTLEY, D.

"Ignition"
Automobile Engineer, March and April, 1969.

25. N.A.C.A. 43rd Annual Report.
Report 1300, 1957.

26. CLARKE, J.S.

"Initiation and some controlling parameters of combustion in the piston engine."
I,Mech.E., No. 5, 1960-61.

27. LEWIS, B and VON ELBE, G.

"Combustion, Flames and Explosions of Gases."
Academic Press Inc., New York and London, 1961.

28. SPALDING, D.B.

"Some Fundamentals of Combustion - Gas Turbine Series."
Butterworths Scientific Publications, London, Vol. 2, p.175, 1955.

29. WEINBERG, F.J. and ODGERS, J.

Private Communication to J.S. Clark (Ref. 26 above).

30. LICHTY, L.

"Combustion Engine Processes"
McGraw-Hill Book Company, 1967.

31. HARROW, G.A. and ORMAN, P.L.

"A study of flame propagation and cyclic dispersion in a spark-ignition engine."
A.S.A.E. Symposium on Combustion in Engines, July, 1965.

32. MARVIN, C.F. and BEST, R.D.

"Flame movement and pressure development in an engine cylinder."
N.A.C.A. Report No. 399 : 1931.

33. SOLTAU, J.P.

"Cylinder Pressure Variations in Petrol Engines."
I.Mech.E. (A.D.), No. 2, 1960-61.

34. CURRY, S.

"A three-dimensional Study of Flame Propogation in a Spark Ignition Engine."
S.A.E. paper 452B, January, 1962.

35. STARKMAN, E.S., STRANGE, F.M. and DAHM, T.J.

"Reaction Front and Pressure Rise Rates measured simultaneously in spark ignition engines."
S.A.E. Journal. Nov. 1959. : S.A.E. Paper 83V, 1959.

36. CURRY, S.

"The Relationship between Flame Propagation and Pressure Development during knocking combustion."
S.A.E. paper 647B.

37. WITHROW, L. and BOYD, T.A.

"Photographic Flame Studies in the Gasoline Engine."
Ind. and Eng. Chemistry, May, 1931.

38. BROEZE, PROF. IR. J.J.

"Combustion in Piston Engines."
De Technische Uitgeveris H. Stam N.V., 1963.

39. WENTWORTH, J.T. and DANIEL, W.A.

"Flame Photographs of Light Load Combustion point the way to Reduction of Hydrocarbons in Exhaust Gas."
S.A.E. Technical Progress Series, Vol. 6

40. HARROW, G.A.

"Some Applications of Basic Combustion Research to Gasoline Engine Development Problems."
Private paper communication.

41. SALOOJA, K.C.

"Studies of Combustion Processes leading to Ignition in Hydrocarbons."
Combustion and Flame, 4, June, 1960, P.117.

42. JOHNSON, J.H., MYERS, P.S. and UYEHARA, O.A.

"End-Gas Temperatures, Pressures, Reaction Rates and Knock."
S.A.E. Paper 650505 : May, 1965.

43. CURRY, S.

"Effect of Antiknocks on flame propagation in a spark ignition engine."
9th Symposium (Inter.) on Combustion, Academic Press.

44. WITHROW, L., LOVELL, W.G. and BOYD, T.A.

"Following Combustion in the Gasoline Engine by Chemical Means."
Ind. and Eng. Chemistry, 22, (1930), p.945.

45. SCHNAUFFER, K.

S.A.E. Journal 34 (1), 1934, 17.

46. KUMAGAI and KUDO

"Flame Studies by means of Ionization Gaps in a high-speed S.I. engine."
9th Symposium (International) on Combustion. Academic Press Inc., New York, 1963.

47. HOPKINSON

"The Gas, Petrol and Oil Engine."
J. Wiley-Sons, New York, 1909, P.191.

48. NEWHALL, H.K.

"Control of Nitrogen Oxides by Exhaust Recirculation - A preliminary theoretical study."
S.A.E. paper 670495, 1967.

49. STARKMAN, E.S., STEWART, H.E. and ZVONOW, V.A.

"An investigation into the formation and modification of Emission Precursors."
S.A.E. paper 690020, 1969.

50. VICHNIEVSKY, R.

"Combustion in Petrol Engines."
Joint Conference on Combustion : I.Mech.E. and A.S.M.E. : 1955.

51. PATTERSON, D.J.

"Cylinder Pressure Variations; A Fundamental Combustion Problem."
S.A.E. Transactions, 1967 : Vol.75, p.621

52. KARIM, G.A.

"An examination of the nature of the random cycle pressure variations in a spark-ignition engine."
Jnl. of Inst. of Petroleum, March 1967. Vol.53, p.112.

53. MAGA, J.A. and KINOSIAN, J.R.

"Motor Vehicle Emission Standards - Present and Future."
S.A.E. paper No. 660104 : January, 1966.

54. STARKMAN, E.S.

"Engine Generated Air Pollution - a study of source and severity."
11th F.I.S.I.T.A. Congress. : June, 1966.

55. HAAGEN-SMIT, A.J.

"Chemistry and Physiology of Los Angeles Smog."
Ind. and Eng. Chemistry, 44, 1952, p.1342.

56. DANIEL, W.A.

"Flame Quenching at the walls of an Internal Combustion Engine."
6th Symposium (International) on Combustion.
Reinhold Publishing Corp. 1957.

57. HULS, T.A., MYERS, P.S. and UYEHARA, O.A.

"Spark Ignition Engine Operation and Design for minimum exhaust emissions."
S.A.E. Transactions, Vol. 75, 1967.

58. STIVENDER, D.L.

"Intake Valve Throttling (IVT) - A Sonic Throttling Valve Engine."
S.A.E. paper No. 680399, May, 1968.

59. TOSEN, J.

"Cleaner yet....."
Motor, May 17th, 1969.

60. WENTWORTH, J.T.

"Piston and Ring Variables affect Exhaust Hydrocarbon Emissions."
S.A.E. paper No. 680109, 1968.

61. SCHEFFLER, C.E.

"Combustion Chamber Surface Area, A key to Exhaust Hydrocarbons."
C.A.E. Progress in Technology Series, Vol. 12, 1967.

62. LAWRENCE, G.

"Mixture pre-treatment for clean exhaust; a Duplex carburation system."
I.Mech.E., Vol. 182, No. 6, 1967-68.

63. BARTHOLOMEW, E.

"Potentialities of Emission Reduction by Design of Induction Systems."
S.A.E. paper No. 660109, 1966.

64. LARBORN, A. and ZACHRISSON, F.

"Dual Manifold as Exhaust Emission Control in Volvo cars."
S.A.E. paper No. 680108, 1968.

65. JACKSON, M.W., WIESE, W.M. and WENTWORTH, J.T.

"The influence of air/fuel ratio, spark timing and combustion chamber deposits on exhaust hydrocarbon emissions."
S.A.E. paper No. 486A, March, 1962.

66. SHINN, J.N. and OLSON, D.R.

"Some factors affecting unburnt hydrocarbons in engine combustion products."
S.A.E. Technical Progress Series, Vol. 6, 1964.

67. BAUDRY, J. and SALE, B.

"Investigations on processes for reducing the emissions of Pollutents by modifying combustion (S.I. engines).
12th F.I.S.I.T.A. Congress : May, 1968, Barcelona.

68. DARTNELL, P.L. and LAMARQUE, P.V.

"The effect of combustion chamber shape and other engine design factors on exhaust emissions."
I.Mech.E. Air Pollution Symposium, November, 1968.

69. LAWRENCE, G.L.

"Emission Control by Carburation."
I.Mech.E. Air Pollution Symposium, November, 1968.

70. DAVIS, H.P., UYEHARA, O.A. and MYERS, P.S.

"The effects of knock on the Hydrocarbon Emissions of a Spark Ignition Engine."
S.A.E. paper No. 690085, January, 1969.

71. SOLTAU, J.P. and CAMPBELL, K.

"The sampling and measurement of exhaust emissions from motor vehicles."
I.Mech.E. Symposium on Air Pollution, November, 1969.

72. JACKSON, M.W.

"Effects of some engine variables and control systems on composition and reactivity of exhaust hydrocarbons."
S.A.E. Transactions, Vol. 75 (1967).

73. OLIVER, W.T.

"Practical emission control systems - air injection into exhaust manifold."
I.Mech.E. Symposium on Air Pollution, November, 1968.

74. ERCKSON, D.A. and STEBAR, R.F.

"Factors influencing the effectiveness of Air Injection in reducing exhaust emissions."
S.A.E. Transactions, Vol. 74, 1966.

75. BECKMAN, E.W., FAGELY, W.S. and SARTO, J.O.

"Exhaust emission control by Chrysler - the Cleaner Air Package."
S.A.E. Transactions, Vol. 75 (1967).

76. SUTTON, D.L.

"Engine tuning to minimize exhaust emissions."
I. Mech.E. Symposium on Air Pollution, November, 1968

77. Report of the Panel on Electrically Powered Vehicles to the Commerce Technical Advisory Board.
S.A.E. Journal : May, June and July, 1968.

78. BOLT, J.A.

"A survey of Alcohal as a Motor Fuel."
S.A.E. Special Publications : SP-254.

79. BAXTER, M.C.

"L.P. Gas - a Superior Motor Fuel"
S.A.E. paper No. 670054, 1967.

80. BAXTER, M.C., LEEK, G.W. and MIZELLE, P.E.

"Total Emission Control possible with LP-Gas Vehicle."
S.A.E. paper No. 680529 : 1968.

81. BAILEY, C.L.

"The influence of motor gasoline characteristics upon carbon monoxide emissions under engine idle conditions."
I.Mech.E. Symposium on Air Pollution. November, 1968.

82. HARRIS, W.L. and HUMMEL, J.W.

"Effects of Inlet-Air Temperature and Humidity on performance of an L.P. Gas Engine."
S.A.E. paper No. 670056 : 1967.

83. NEWHALL, H.K. and STARKMAN, E.S.

"Direct Spectroscopic Determination of Nitric Oxide in reciprocating engine cylinders."
S.A.E. paper No. 670122, January, 1967.

84. CAMPAU, R.M. and NEERMAN, J.C.

"Continuous mass spectrometric determination of Nitric Oxide in automobile exhausts."
S.AE. Transactions, 75, 1967, p.583.

85. STARTMAN, E.S. and NEWHALL, H.K.

"Characteristics of the expansion of reactive gas mixtures as occurring in I.C. engine cycles."
S.A.E. Transactions, 74, 1966, p.826.

86. NEWHALL, H.K.

"Kinetics of Engine Generated Nitrogen Oxides and Carbon Monoxide."
12th Symposium (International) on Combustion.
Poitiers, France, July, 1968.

87. CAPLAN, J.D.

"Smog Chemistry points the way to rational vehicle emission control."
S.A.E. paper No. 650641 : August, 1965.

88. HULS, T.A. and NICKOL, H.A.

"Influence of engine variables on Exhaust Oxides of Nitrogen Concentrations from a multicylinder engine."
S.A.E. paper No. 670462 : 1967.

89. RABEZZANA, H., KALMAR, S. and CANDELISE, A.

"Combustion : An analysis of Burning and Expansion in the reaction zone."
Automobile Engineer : November, 1939.

90. BENSON, J.D.

"Reduction of Nitrogen Oxides in Automobile Exhaust."
S.A.E. paper No. 690019 : January, 1969.

91. DEETER, W.F., DAIGH, H.D. and WALLIN, O.W.

"An approach for controlling Vehicle Emissions."
S.A.E. paper No. 680400 : May, 1968.

92. NICHOLLS, J.E., EL-MESSIRI, A, and NEWHALL, H.K.

"Inlet Manifold Water Injection for control of Nitrogen Oxides - Theory and experiment."
S.A.E. paper No. 690018 : 1969.

93. STARKMAN, E.S.

"Fundamental Processes in Nitric Oxide and Carbon Monoxide production from combustion engines."
12th F.I.S.I.T.A. Congress : Barcelona 1968.

94. KAUFMAN, F. and KELSO, J.K.

"Thermal Decomposition of Nitric Oxide."
J. Chem. Physics, Vol. 23, No. 9, 1955.

95. EYZAT, P. and GUIBET, J.C.

"A new look at Nitrogen Oxides Formation in I.C. engines."
S.A.E. paper No. 680124, January, 1969.

96. KAUFMAN, F and DECKER, L.J.

"Effect of Oxygen on Thermal Decomposition of Nitric Oxide at high temperatures."
7th Symposium (Inter.) on Combustion.
Butterworth's Scientific Publications. 1958.

97. WHITEHOUSE, N.D., STOTTER, A., GOUDIE, G.O. and PRENTICE, B.

"Method of predicting some aspects of performance of a diesel engine using a digital computer."
I.Mech.E., Vol. 176, No. 9. 1962.

98. MCAULAY, K.J., WU, T. and BORMAN, G.L.

"Development and evaluation of the simulation of the compression-ignition engine."
S.A.E. paper No. 650451 : 1965.

99. ANDAND, W.J.D.

"Choice of a computing procedure for digitel computer synthesis of reciprocating engine cycles."
Jnl. of Mech. Eng. Science : Vol. 10, No. 3. 1968.

100. International Critical Tables.
McGraw-Hill, New York, 1, (1928).

101. RICARDO, H.R.

"The High Speed, Internal Combustion Engine."
Blackie and Sons Ltd., London. 1953.

102. WILLIS, D.A., MEYER, W.E. and BIRBIE, C.

"Mapping of Airflow Patterns in engines with Induction Swirl."
S.A.E. paper No. 660093.

103. JOHNSON, J.H.

"Effect of swirl on flame propagation in a Spark Ignition Engine."
S.A.E. paper No. 565C. September, 1962.

104. ROBERTSON, J.M.

"A Turbulence Primer"

University of Illinois Bulletin, Vol. 60, No. 90, May, 1963.

105. OHIGASHI, S., HAMAMOTO, Y. and TANABE, S.

"A new digital method for measuring gas flow velocity by electric discharge."
S.A.E. paper No. 690180 : January, 1969.

106. NAKAJIMA, K., KAJIYA, S. and NAGAO, F.

"An experimental investigation of the Air Swirl Motion and Combustion in the swirl chamber of diesel engines."
12th F.I.S.I.T.A. Congress : Barcelona, May, 1968.

107. HUFFAKER, R.M., FULLER, C.E. and LAWRENCE, E.R.

"Application of Laser Doppler Velocity Instrumentation to the measurement of jet turbulence."
S.A.E. paper No. 690266.

108. SEMENOV, E.S.

"A device for measuring the turbulence in Piston Engines."

Pribory i Tekhnika Eksperimenta, No. 1, 1958.

109. WOLCHANOV, E.K.

"On the problem of Gas Motion and Combustion in a light fuel engine."
Trudy Moskovskogo Automobil'no-dorozhnogo Instituta, Autotransizdat, Moscow. 1955, No. 17.

110. SEMENOV, E.S.

"Studies of Turbulent Gas Flow in piston engines."
Combustion in turbulent flow, Israel Program for Scientific Translations, 1963. Oldebourne Press.

111. ANNAND, W.J.D.

"Engine Breathing."
Automobile Engineer, February, 1969.

112. TANAKA, K.

"Air flow through suction valve of conical seat."
Aero. Research Inst. Report, Tokyo Imperial University, 1929, Part 1, p.260.

113. CLERK, SIR DUGALD.

"The Gas, Petrol and Oil Engine."
J. Wiley and Sons, Inc., New York (1909).

114. BOLT, J.A. and HARRINGTON, D.L.

"The effects of mixture motion upon the lean limit and combustion of spark-ignited mixtures."
S.A.E. paper No. 670467 : May, 1967.

115. SOKOLIK, A.S., KARPOV, V.P. and SEMENOV, E.S.

"The turbulent combustion of gases."
Fizika Goreniya i Vzryva, 1967 (1), p.61-75.

116. SUTTERFIELD, N., REITER, S.H., KEBELY, V. and MASCOLO, R.W.

Jet Propulsion, 1956, 25, 377

117. DE SOETE, G.

"A survey of the effects of turbulence on engine combustion."
A.S.A.E. Symposium on Combustion in Engines, July, 1965.

118. DAMKÖHLER, G.

"The effect of turbulence on the flame velocity in gas mixtures."
N.A.C.A., TM1112, 1947.

119. SHCHELKIN, K.I.

"On combustion in a turbulent flow."
N.A.C.A. TM1110, 1947.

120. KARLOVITZ, B, DENNISTON, D. and WELLS, F.

"Investigation of turbulent flames."
Jour. Chem. Physics, Vol. 19, No. 5, May, 1951.

121. LEASON, D.B.

"Turbulence and flame propagation in premixed gases."
Fuel, Vol. XXX, No. 10., October, 1951.

122. SCURLOCK, A.C. and GROVER, J.H.

"Propagation of turbulent flames."
4th Symposium (Inter.) on Combustion, The Williams and Wilkins Co. (Baltimore), 1953.

123. SOKOLIK, A.S.

"The experimental basis of the theory of turbulent combustion."
Combustion in turbulent flow, Israel Program for Scientific Translations, 1963. Oldebourne Press.

124. SHCHTINKOV.

Combustion in Turbulent flow, Israel Program for Scientific Translations, 1963. Oldebourne Press.

125. WOHL, SHORE, VON ROSENBERG and WEIL.

"The burning velocity of turbulent flames."
4th Symposium (Inter.) on Combustion. 1953.

126. ZELDOVICH and FRANK-KAMENETSKY

Journal of Physical Chemistry (U.S.S.R.), 12, 100, 1938.

127. EVANS, M.W.

"Current theoretical concepts of steady-state flame propagation."
Chemical Reviews, Vol. 51. 1952.

128. DANIELL, P.J.

Proc. Royal Society (London), A126, 1930, p.393

129. JOUGUET, E and CROSSARD, L.

Compt. Rend. 169, (1919), 820.

130 JOUGUET, E.

Compt, rend. 156, (1913), 1058.

131. BARTHOLOMÉ, E.

Naturwissenschaften 36, 171 (1949)

132. BARTHOLOMÉ, E.

Naturwissenschaften 36, 206 (1949)

133. BARTHOLOMÉ, E., DREYER, H.J. and LESEMANN, K.J.

Z. Elektrochem. 54, 246 (1950).

134. JOST. W.

"Explosion and Combustion processes in gases."
Chap. III. : McGraw-Hill Book Co. (1946).

135. DAMKÖHLER, G.

Z. Elektrochem. 46, 601 (1940).

136. BECHERT, K.

Z. Naturforsch. 3A, 584 (1948).

137. EVANS, H.W., HARR, J.A. and STRONG, P.

"Thermal flame propagation."
Computation Laboratory of Harvard University, Dec. 1949.

138. DUGGER, G.L. and HEIMEL, S.

"Flame speeds of methane-air, propane-air and ethylene-air mixtures at low initial temperatures."
N.A.C.A., TN2624, 1952.

139. TANFORD, C.

"Theory of burning velocity I - Temperature and free radical concentrations near the flame front, relative of heat condition and diffusion."
J. Chem. Phys., 15, (7), July, 1947.

140. TANFORD, C. and PEASE, R.N.

"Theory of burning velocity II - the square root law for burning velocity."
J. Chem. Phys., 15, (12), December, 1957.

141. TANFORD, C.

"The role of free atoms and radicals in burner flames."
3rd Symposium on Combustion, Flame and Explosion Phenomena : Williams and Wilkins, 1949.

142. BASLVICH, V., DEVISHEV, M. and KOGARKO, S.

"Influence of active particles of combustion products on the speed of flame propagation in a turbulent flow."
A.R.S. Journal Supplement, January, 1962.

143. MAISON, H.

"Méchanisme de la propagation des déflagrations dans les mélanges gaseux et rôle de la projection des centres actifs." Revue de L'Institut Français du Pétrole et Annales des Combustibles Liquides, Vol. IV, No. 7. July, 1949.

144. VAN TIGGELEN, A.

Bull. soc. chim. Belg., 58, 259 (1949).

145. GAYDON, A.G. and WOLFHARD, H.G.

Fuel, 29, 15, (1950).

146. SACHSSE, H. and BARTHOLOMÉ, E.

Z. Elektrochem. 53, 183 (1949).

147. DUGGER, G and SIMON, D.

"Prediction of flame velocities of hydrocarbon flames." N.A.C.A. report 1158.

148. DUGGER, G and SIMON, D.

"Prediction of flame velocities of hydrocarbon flames." 4th Symposium (Inter.) on Combustion. p.336.

149. HIRSCHFELDER, J. and CURTISS, C.

"Theory of propagation of flames. Pt. 1 - General equations." 3rd Symposium on Combustion, Flame and Explosion Phenomena. Williams and Wilkins Co. 1949.

150. HEIKEL, M., HUTTEL, H. and SPAULDING, W.

3rd Symposium on Combustion, Flame and Explosion Phenomena, p.135. The Williams and Wilkins Co. (1949).

151. BOYS, S.F. and CORNER, J.

Proc. Royal Society, A197, 90 (1949).

152. HIRSCHFELDER, J and CURTISS, C.

J. Chem. Phys., 17, 1076 (1949)

153. GOLDBERG, S. and FELSVIN, V.

"Influence of pressure on rate of flame propagation in turbulent flow."
7th Symposium (Inter.) on Combustion, Butterworth, 1959.

154. EGERTON, A and LEFEBVRE, A.

"Effect of pressure variation on burning velocity."
Proc. Royal Society, A222, 1954.

155. DIEDERICHSEN, J. and WOLFHARD, H.G.

"The burning velocity of methane flames at high pressure."
Trans. Faraday Society. 52, 1956.

156. AGNEW, J. and GRAIFF, L.

"The pressure dependence of laminar burning velocity by the spherical bomb method."
Combustion and Flame, 5, 1961.

157. DUGGER, G. and GRAAB, D.

"Flame velocities of hydrocarbon - oxygen - nitrogen mixtures."
4th Symposium (Inter.) on Combustion. p.302.

158. WALLER, P. and WRIGHT, C.C.

"Hydrocarbon burning velocities predicted by thermal versus diffusional mechanisms."
Jnl. of the American Chemical Society : Vol. 74, August, 1952. p.3769.

159. PATTERSON, D.J. and VAN WYLEN, G.

"A digital computer simulation for spark-ignited engine cycles."
S.A.E. progress in Technology, Vol. 7, 1964.

160. SPALDING, D.B.

Private Communication to Phillippe and Orman[19].

161. BOLLINGER, L.M. and WILLIAMS, D.T.

"Effect of Reynolds Number in turbulent flow range on flame speeds of bunsen burner flames."
N.A.C.A., TN1707, 1949.

162. HIGASHINO, I.

"Flame propagation in spark ignition engines."
J.S.M.E., Vol. 4, No. 15, 1961.

163. HODGETTS, D.

Discussion to Phillipps and Orman paper.[19]

164. ELLISON, R.J., HARROW, G.A. and HAYWARD, B.H.

"The effect of tetraethyl-lead on flame propagation and cylic dispersion in spark-ignition engines."
Jour. of Inst. of Petroleum, Vol. 54, No. 537, Sept. 1968.

165. BOUCHARD, C.L., TAYLOR, C.F. and TAYLOR, E.S.

"Variables affecting flame speed in the Otto-cycle engine."
S.A.E. Jour., Vol. 40-41, 1937.

166. GAYDON, A.G. and WOLFHARD, H.G.

"Flames, their structure, radiation and temperature."
Chapman and Hall, London, 1960.

167. BUGGER, G.L.

"Effect of initial mixture temperature on flame speeds and blow-off limits of propane-air flames."
N.A.C.A., TN2170.

168. SIMON, D.M.

"Flame propagation. III. Theoretical considerations of the burning velocities of hydrocarbons."
Jour. of the American Chemical Society, Vol. 73.
January, 1951.

169. JEANS, J.

"An introduction to the kinetic theory of gases."
Cambridge Univ. Press (London), 1940, p.207.

170. GAYDON, A.G.

"Flames; their structure, radiation and temperature."
Chapman and Hall, London, 1960.

171. LEWIS, B. ET AL.

"High speed aerodynamics and jet propulsion, II, Combustion processes."
Princeton University Press, Princeton, N.J., 1956.

172. GAYDON, A.G.

"Flames; their structure, radiation and temperature."
Chapman and Hall, London, 1960.

173. HOTTEL, H.C., WILLIAMS, G.C., and SATTERFIELD, C.N.

"Thermodynamic charts for combustion processes."
J. Wiley and Sons Inc., New York, 1949.

174. LOVELL, W.G. and BOYD, T.A.

Ind. and Eng. Chem., 17, (1925), 1226.

175. GOODENOUGH, G.A. and FELBECK, G.T.

University of Illinois Experimental Station Bulletin 160, (1927).

176. HUFF, V.N., GORDON, S. and MORRELL, V.E.
N.A.C.A. report 1037, (1951).

177. VICKLAND, C., STRANGE, F., BELL, R. and STARKMAN, E.S.

"A consideration of the high temperature thermodynamics of I.C. Engines."
S.A.E. progress in technology, Vol. 7, 1964.

178. ZELEZNIK, F.J. and GORDON, S.

Nasa TN D-473, 1960.

179. VON STEIN, M.R.

Forschg. Ing. - Wes., 14. (1943), 113.

180. BRINKLEY, S.R.

J. Chem. Phys., 14, No. 9 (1946), 563-564.
J. Chem. Phys., 15, No. 2 (1947), 107-110.

181. KANDINER, H.J. and BRINKLEY, S.R.

"Calculation of complex equilibrium relations."
Ind. and Eng. Chem., 42, (1950), 850.

182. LEWIS, G.N. and RANDALL, M.R.

"Thermodynamics."
2nd Edition, McGraw-Hill, New York, 1961.

183. BENSON, R.S.

"Advanced engineering thermodynamics."
Pergamon Press, 1967.

184. LANCHESTER, F.W.

Inst. Mech. Eng. Proc., 141, (1939), 289

185. JANEWAY, R.N.

"Quantitative analysis of heat transfer in engines."
S.A.E. Journal, 61, (1938), 371.

186. PYE, D.R.

"The Internal Combustion Engine."
Vol. 1, 2nd Ed., Oxford University Press, 1937.

187. DAVID, W.T. and LEAH, A.S.

Journ. and Proc. Inst. Mech. Eng., 143, (1940), 289.

188. SPIERS, H.M.

"Technical data on fuel."
B.N.C. World Power Conference, 6th edition, 1961.

189. BAKER, H.D. and LASERSON, G.L.

Inst. of Mech. Eng. and A.S.M.E., General Discussion on Heat Transfer, 334, (1951).

190. NUSSELT, W.

"Die Wärmeübergang in den Verbrennungs-kraftmaschinen."
Z. Ver. dtsch. Ing., 1923, 67.

191. PINKEL, B.

N.A.C.A. TR 612, (1938)
N.A.C.A. TR 683, (1940)
N.A.C.A. E-131 APR E5J31, (1945)

192. TAYLOR, C.F. and TOONG, T.Y.

"Heat transfer in I.C. engines."
A.S.M.E. paper 57-HT-17, (1957).

193. OVERBYE, V.D., BENNETHUM, J.E., UYEHARA, O.A. and MYERS, P.S.

"Unsteady heat transfer in engines."
S.A.E. Trans., 69, 1961.

194. DAHL, O.G.C.

Trans. A.S.M.E., 46, (1924), 161.

195. JAKOB, M.

"Heat Transfer."
Vol. 1 : J. Wiley and Sons, New York, 1949.

196. OVERBYE, V.D.

"Variation of instantaneous wall temperature, heat transfer and heat transfer coefficients in a S.I. engine."
Ph.D. Thesis, Univ. of Wisconsin, 1960.

197. HOBSON, E.W., WAERMELEITUNG, MATHEMATISCHER.

"Encyklopaedie der mathematischen Wissenschaften."
1903-1921, p.186.

198. OGUNI, T.

"Determination of rate of heat transfer between the gases and the cylinder walls of S.I. engines."
Bulletin of Fac. of Eng., Yokohama Univ., Vol. 9 (1960).
"Theory of heat transfer in the working gases of I.C. engines."
J.S.M.E., 1960, 3,370

199. BRILING.

Quoted in Ref. 202.

200. PFLAUM, W.

Engineers Digest, NY., 1961, 22, 86.

201. ELSER, R.

"Instationare Wärmeübertragung bei periodisch adiabater verdichtung turbulenter gase."
Forsch. Ing. Wes. 1955, 21, 65.

202. CHIRKOV, A. and STEFANOVSKI, B.S.

Trudy Rostovskova Instituta Injyenyerov Zhelyeznodorovnova Transporta, 1958, 21.

203. WOSCHNI, G.

"A universally applicable equation for the instantaneous heat transfer coefficient in the I.C. engine."
S.A.E. paper No. 670931, 1967.

204. HASSAN, H.

"Unsteady heat transfer in a motored I.C. engine."
Ph. D. Thesis, Loughborough University. 1968.

205. LIVENGOOD, J.C., TAYLOR, C.F. and WU, P.C.

"Measurement of gas temperature in an engine by the velocity of sound method."
S.A.E. Trans. Vol. 66 (1958), p.683.

206. "J.A.N.A.F. Thermochemical Data Tables."
Joint Army-Navy-Air Force Thermochemical Panel.
ARPA Program, USAF Contract AF 33 (616) - 6149,
Thermal Lab., Dow Chem. Group, Midland, Michigan,
December, 1960.

207. "The Properties of Liquefied Petroleum Gases."
Shell Inter. Petroleum Co. Ltd. : Report No. 186F :
November, 1966.

208. American Petroleum Institute.
"Selected Values of Physical and Thermodynamic properties of Hydrocarbons and related compounds."
1953.

209, SALÉ, M.B. and VICHNIEVSKY, M.R.

"Étude de la combustion sur le monocylindre I.F.P. Renault C.N.R.S."
Journ. de la Societé des ingenieurs de l'automobile :
No. 9, October, 1958.

210. OBERT, E.

"Internal Combustion Engines."
Inter. Textbook Co., 1968.

211. KARIM, G.A.

"The application of elementary chemical kinetics to engine performance calculations."
A.S.A.E. Symposium on Engines : July, 1965.

212. PROPERTIES OF COMBUSTION GASES/SYSTEM
Vol. II - Chemical Composition of Equilibrium mixtures.
Aircraft Gas Turbine Development Dept. G.E.C. :
McGraw-Hill Book Co.

A P P E N D I X 1.

CALCULATION OF THE COMPOSITION OF THE UNBURNT CHARGE.

APPENDIX 1.

CALCULATION OF THE COMPOSITION OF THE UNBURNT CHARGE.

The unburnt charge is regarded as a homogeneous mixture of air, gaseous fuel and residual exhaust gases. In the following calculations, it is assumed that dry air at sea level has the following composition [100] :

Per 100 moles of dry air:

O_2	20.99
N_2	78.03
A	0.94
CO_2	0.03
H_2	0.01

It appears reasonable to add the concentrations of argon, carbon dioxide and hydrogen to that of nitrogen and assume that these three species have the same thermodynamic properties as nitrogen. Thus, air is assumed to be composed of 79.01 parts of nitrogen and 20.99 parts of oxygen by volume in this work.

A general hydrocarbon fuel of composition $C_m H_n$ is considered and the equivalence ratio is given the symbol ϕ. The stoichiometric equation for the combustion of this fuel is

$$C_m H_n + \left(\frac{4m + n}{2}\right) \cdot O_2 + \frac{79.01}{20.99} \cdot \left(\frac{4m + n}{2}\right) \cdot N_2 = m \cdot CO_2 + \frac{n}{2} \cdot H_2O + \frac{79.01}{20.99} \cdot \left(\frac{4m + n}{2}\right) \cdot N_2 \quad \text{---------- A.1-1}$$

On a weight basis, the stoichiometric air/fuel ratio is obtained from considerations of the molecular weights of the individual constituents on the left hand side of this equation. Thus, the stoichiometric Air/Fuel Ratio =

$$\frac{\left(\frac{4m+n}{2}\right).32 + \frac{79.01}{20.99}.\left(\frac{4m+n}{2}\right).28.016}{(12.011.m + 1.008.n)}$$

which can be simplified into

$$\frac{(66.11\,m + 16.53n)}{(12.011\,m + 1.008n)} \qquad \text{A.1-2}$$

The actual air/fuel ratio can now be evaluated from the equation

$$\frac{\text{Stoichiometric Air/Fuel Ratio}}{\phi} \qquad \text{A.1-3}$$

The mass fraction of the residual exhaust gases is denoted by w_r. In practice, the value of this quantity is most difficult to define accurately since it depends so much on the operating conditions of the engine e.g. the ignition timing, the throttle position, the degree of valve overlap, the compression ratio etc.

Additionally, the mass fraction of injected water in the unburnt mixture (as a means of controlling certain obnoxious emissions) is given the symbol w_w. Values of this quantity can normally be estimated quite accurately.

Thus, having established values for w_r and w_w, the mass fractions of the air, w_a, and the fuel, w_f, can be calculated from:

$$w_a = (1 - w_r - w_w) \,/\, (1 + w_f/w_a) \qquad \text{A.1-4}$$

$$w_f = (1 - w_r - w_w) \,/\, (1 + w_a/w_f) \qquad \text{A.1-5}$$

The composition of the residual exhaust gases must now be determined. It is shown in Chapter 6 that the assumption of chemical equilibrium is quite a good approximation to actuality at high temperatures and pressures. i.e. when the reaction rates are high. However, many authors[85] have shown that a gas mixture which has been rapidly cooled has

a composition corresponding to equilibrium at some higher temperature. This effect has been found to vary with each reaction (see Chapter 6). In this work, however, it is assumed that gas mixtures which have been cooled below 1600° K have a composition corresponding to equilibrium at that temperature. The composition of the residual exhaust gases is governed by this criterion and is determined by the method described in Chapter 6.

APPENDIX 2.

APPENDIX 2.

THE DERIVATION AND APPLICATION TO BURNING VELOCITY CALCULATIONS OF THE MALLARD AND LE CHATELIER THEORY OF LAMINAR FLAME PROPAGATION.

Considering the structure of the burning zone of a flame (see Fig. 4-37), it is convenient for analysis to consider it to be stationary with the unburnt gas flowing with velocity U in the direction of the positive x-axis. The temperatures of the burnt and the unburnt gases are assumed to be T_b and T_u respectively.

Utilising the concept of an "ignition temperature", T_i, it is possible to assume that, at a definite point in the burning zone, this temperature is reached exactly. The fresh gas to the left of it (see Fig. 4-37) is assumed to be heated to T_i by conduction whilst the gas to the right of it is thought to be burnt spontaneously by chemical reaction and gives off heat to the unburnt gases by conduction.

Thus, if ρC_p is the heat capacity of the fresh gas per unit volume, then the quantity of heat which is transferred per unit time by heat conduction in order to raise the unburnt gas temperature, T_u, to the ignition temperature, T_i, is

$$\rho . C_p . U . (T_i - T_u) \quad \text{-------} \quad A.2\text{-}1$$

It is reasonable to suppose that the temperature decrease at T_i is proportional to $(T_b - T_u)$ and, therefore, that the heat flow is

$$k . (T_b - T_i) \quad \text{-------} \quad A.2\text{-}2$$

where k is proportional to the heat conductivity and inversely proportional to the distance in which the temperature rises

from T_i to T_b.

Since Equations A.2-1 and A.2-2 each apply at the ignition point,

$$\rho . C_p . U . (T_i - T_u) = k . (T_b - T_i)$$

and

$$U = \frac{k . (T_b - T_i)}{\rho . C_p . (T_i - T_u)} \quad \text{---------} \quad \text{A.2-3}$$

which can be further modified to

$$U_L = \frac{\lambda . (T_b - T_i)}{\rho . C_p . d . (T_i - T_u)} \quad \text{---------} \quad \text{A.2-4}$$

where

λ is the thermal conductivity

and

d is the distance in which the temperature rises from T_i to T_b.

Equation A.2-4 is the expression for the Mallard and Le Chatelier laminar flame propagation theory.

In calculations using this formula, Phillipps and Orman[19] found it necessary to assume that the following constant values pertain in order to obtain some realistic burning velocities:

i) a constant thermal conductivity value, λ, of 0.0001 cal/cm sec ^{o}K.

ii) a constant reaction zone thickness, d, of 0.02 cm

iii) a constant ignition temperature, T_i, of 950° K.

In addition, the physical and thermodynamic properties of the unburnt mixture were taken to be identical to those of air.

Using these above considerations, it is possible to obtain some burning velocity values. For propane-air mix-

TABLE A.2-A.

UNBURNT GAS TEMPERATURE °K.	BURNT GAS TEMPERATURE °K	BURNING VELOCITY (cm/sec)	
		CALCULATED	EXPERIMENTAL
302.0	2251	35.6	41.5
366.0	2280	48.8	56.5
422.0	2305	63.0	68.5
477.0	2330	80.1	86.5
533.0	2355	102.5	104.0
616.0	2392	149.0	137.0
700.0	2429	229.0	-

tures, assuming an equilibrium flame temperature of 2251°K at an unburnt gas temperature of 302°K [167,168] and also assuming that the following relationship exists [167]

$$\Delta T_b = 0.45 \Delta T_u \qquad \text{----------} \qquad \text{A.2-5}$$

where ΔT_b is the change in T_b resulting from a ΔT_u change in T_u, the results shown in Table A.2-A were obtained. Listed also are some comparative experimental values from Ref. 25. These are plotted in Fig. 4-40.

A P P E N D I X 3.

APPENDIX 3.

A SUMMARY OF THE DERIVATION OF THE TANFORD AND PEASE DIFFUSION THEORY OF LAMINAR FLAME PROPAGATION.

Tanford and Pease[139,140,141] equated the amount of product formed in the combustion zone by a second-order reaction between fuel molecules and hydrogen atoms (or other active particles such as hydroxyl radicals or oxygen atoms) to the amount of product formed at the flame front by conversion of the fresh gas, expressed in terms of initial conditions and flame velocity. Their approximate solution for the flame velocity from this equation is

$$U_L = \left(\frac{C_m \; X^1 \; n_c}{X \cdot \theta_m^2} \sum_i \frac{k_i \; p_i \; D_i}{B_i} \right)^{\frac{1}{2}} \quad \text{---- A.3-1}$$

where

C_m = the total concentration of gas at mean combustion zone temperature (molecules / cm^3).

X^1 = mole fraction of fuel in unburnt gas.

X = mole fraction of potential combustion product in unburnt gas.

θ_m = ratio of mean reaction zone temperature to initial temperature.

n_c = total number of molecules of H_2O and CO_2 in products of combustion per molecule of fuel by stoichiometric equation.

k_i = specific reaction rate constants for reaction between fuel molecules and i'th active particle (cm^3/molecule sec)

p_i = mole fraction of i'th active particle in burnt gas.

D_i = diffusion coefficient of i'th active species into unburnt gas (cm^2/sec).

B_i = term near unity arising from radical recombination.

Dugger and Simon[147,148] suggest three methods of evaluating the predictions of this equation. For all three, the following calculations are the same:

a) the burnt gas temperatures, T_B, and active particle concentrations, p_i, are calculated assuming adiabatic thermal equilibrium.

b) the mean combustion zone temperature is assumed to be $0.7\ T_B$.

c) the diffusion coefficients, D_i, are calculated from $D_i = D_{298}\ (0.7\ T_B/T_{298})^{1.67}$ where D_{298} is the diffusion coefficient at 298°K calculated by the Stefan-Maxwell equation[169].

d) the recombination factor, B_i, is calculated by the method of Tanford[139] for the H atoms and is assumed to be unity for OH and O.

e) the ratio $C_m\ ^{X1}\ n_c/X$ is calculated from a knowledge of the overall oxidation process and the initial concentrations of reactants.

The three methods of evaluation differ in the calculation of k_i. For the first method, only one chain carrier, H, is considered and k_H values are calculated from single point flame velocity determinations by Equation A.3-1.

For the second method, H, O and OH are considered to be the chain carriers and

$$\sum_i \frac{k_i\ p_i\ D_i}{B_i} \simeq k_a \left(\frac{r_H\ D_H}{B_H} + p_{OH}\ D_{OH} + r_O\ D_O\right) \cdot \left(\frac{0.7 T_B}{T_u}\right)^{1.67} \qquad \text{--------- A.3-2}$$

In this expression, k_a is the weighted mean k_i for the three active particles, H, OH and O each reacting with fuel

molecules. Single point k_a values are calculated from experimental flame velocity determinations.

The third method uses an Arrhenius type temperature dependence of the rate constant k_a. Thus,

$$k_a = b_a Z_a \exp(-E_a/R(0.7T_b)) \quad \text{---------- A.3-3}$$

in which

b_a = average value of the steric factor b for the three active particles H, OH and O.

Z_a = average value of the collision number Z for the three active particles, H, OH and O.

E_a = average value of the activation energy E for the three active particles H, OH and O.

The accuracy of prediction is greatest for this method.

APPENDIX 4.

APPENDIX 4.

A SUMMARY OF THE DERIVATION OF THE MANSON THEORY OF LAMINAR FLAME PROPAGATION.

Lewis and Von Elbe[27] obtained the following momentum relationship between the flame velocity and the pressure drop across a plane, steady-state flame front:

$$U_L = \left(\frac{\rho_B}{\rho_u} \cdot \frac{\Delta p}{(\rho_u - \rho_B)} \right)^{\frac{1}{2}} \qquad \text{--------- A.4-1}$$

where Δp is the pressure drop (atmospheres).

Manson[143] suggested that this small pressure drop, Δp, could be caused by the projection of hydrogen atoms into the unburnt gas. Because these tend to recombine to hydrogen molecules at the unburnt gas temperature, Δp was assumed to be one-half of the equilibrium hydrogen atom pressure reduced to this temperature. i.e.

$$\Delta p = \tfrac{1}{2} p_H T_u / T_B \qquad \text{--------- A.4-2}$$

where p_H is the partial pressure of the H atom concentration.

Δp has also been estimated from considerations of the projection of the active particles O and OH into the unburnt gas in addition to the projection of H atoms. i.e.

$$\Delta p = \tfrac{1}{2} \left(p_H + p_{OH} \cdot \frac{D_{OH}}{D_H} + p_O \frac{D_O}{D_H} \right) \frac{T_u}{T_s} \qquad \text{--- A.4-3}$$

A P P E N D I X 5.

APPENDIX 5.

DESCRIPTION OF THE INSTRUMENTATION USED TO FACILITATE THE FLAME SPEED MEASUREMENTS.

In Fig. 4-41, sparking plugs were used for the ionization probes 2, 3 and 4. This was because they are ideally suited for this purpose and because the Renault combustion chamber was equipped with sparking plug holes at these points. For ionization probe 1, however, some degree of difficulty was experienced in inserting a probe close enough to the sparking plug in order to eliminate the varying effects of the 'delay period' from the flame travel time readings. The reason for this was that there was a water jacket and the overhead valve mechanism on top of the combustion chamber. Resort was, thus, eventually made to the piece of equipment shown diagrammatically in Fig. A.5-A.

An 18 mm threaded plug was fabricated to fit into the sparking plug hole in place of the usual 18 mm thread spark plug at this point in the combustion chamber. A 10 mm diameter hole was drilled in this plug to accommodate a 10 mm thread spark plug which served its normal function of providing the spark to ignite the charge. Down the side of this hole was drilled a 3 mm diameter hole, the purpose of which was to take a small ionization probe (see Fig. A.5-A). This was sealed to the fabricated plug by a quantity of 'eutectic' cement. Thus, the ionization probe 1 (see Fig. 4-41) was finally positioned at 5 mm from the sparking plug.

The chain of events which ensues in the processing of a particular signal for viewing on an oscilloscope screen will now be described. A 90 volt d.c. voltage is applied

across the ionization gap so that, when a flame front passes the gap the latter is ionized and a small signal is generated. This is passed through the circuit shown in Fig. A.5-B where it is subjected to:

a) an emitter follower which is, in effect, an impedance changer.

b) a zenner diode, the purpose of which is to transform the signal wave form into a squared waveform.

c) a monostable trigger circuit which has the effect shown in Fig. A.5-B on the signal wave form.

d) a differentiator circuit where a rapid rise and a prolonged fall-off is given to the signal. This is necessary in order to give a clear indication of the ionization on the oscilloscope screen (see Figs. 4-43 and 4-44). The fall-off part of the squared wave form is removed by the diode BX642.

This final differentiated signal was displayed on the screen of a TechtronixStorage Oscilloscope. A reference signal was provided by the sparking plug itself on one channel ofthis. Signals from the remaining probes could be displayed simultaneously. By calibration of these with the time base of the oscilloscope, the delays between the spark firing and the probe gaps being ionized by a flame front could be measured by the distances between the signals on the oscilloscope screen.

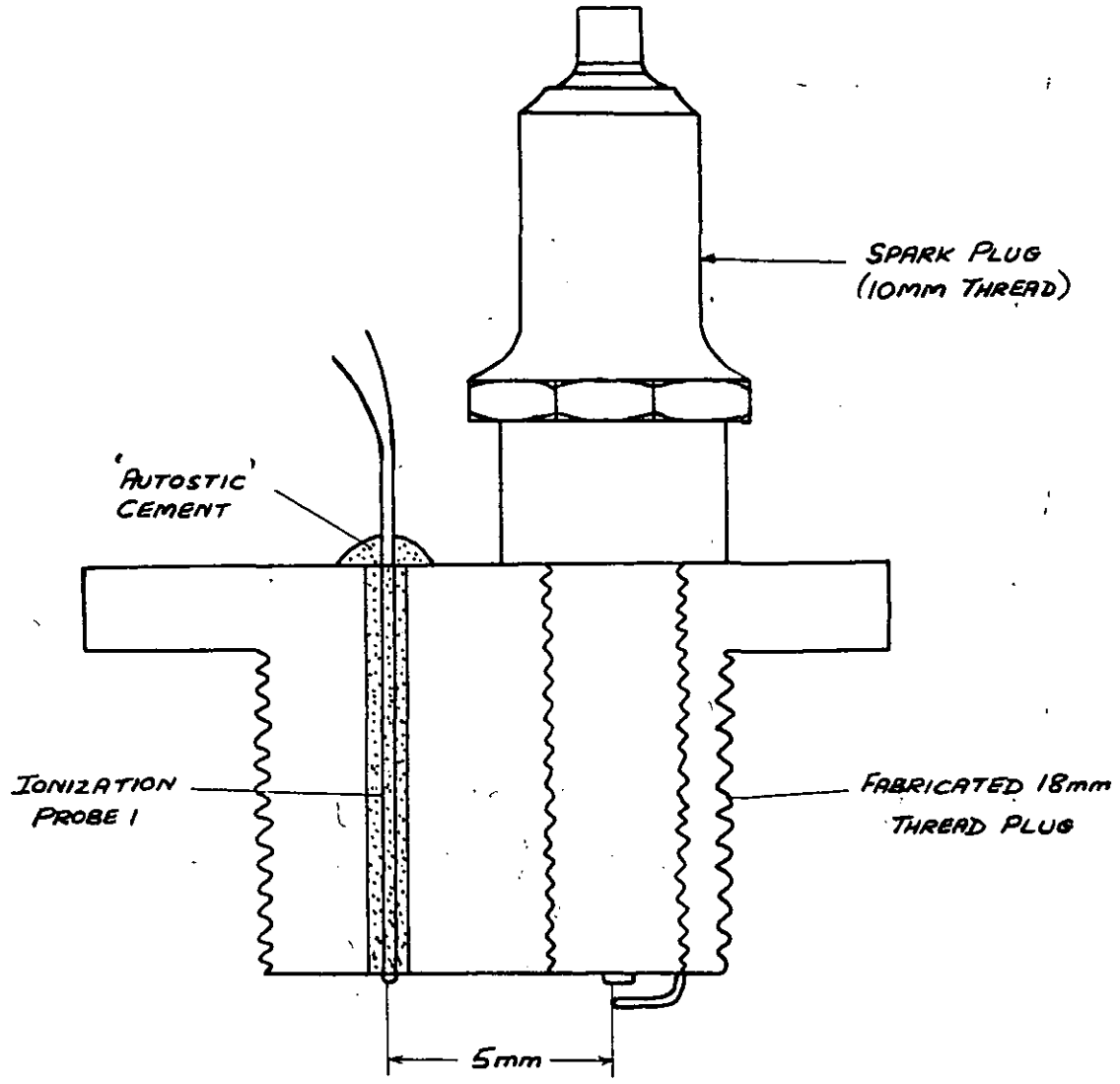

FIG. A.5-A — DIAGRAMMATIC SKETCH OF THE POSITION OF IONIZATION PROBE I RELATIVE TO THE SPARK PLUG

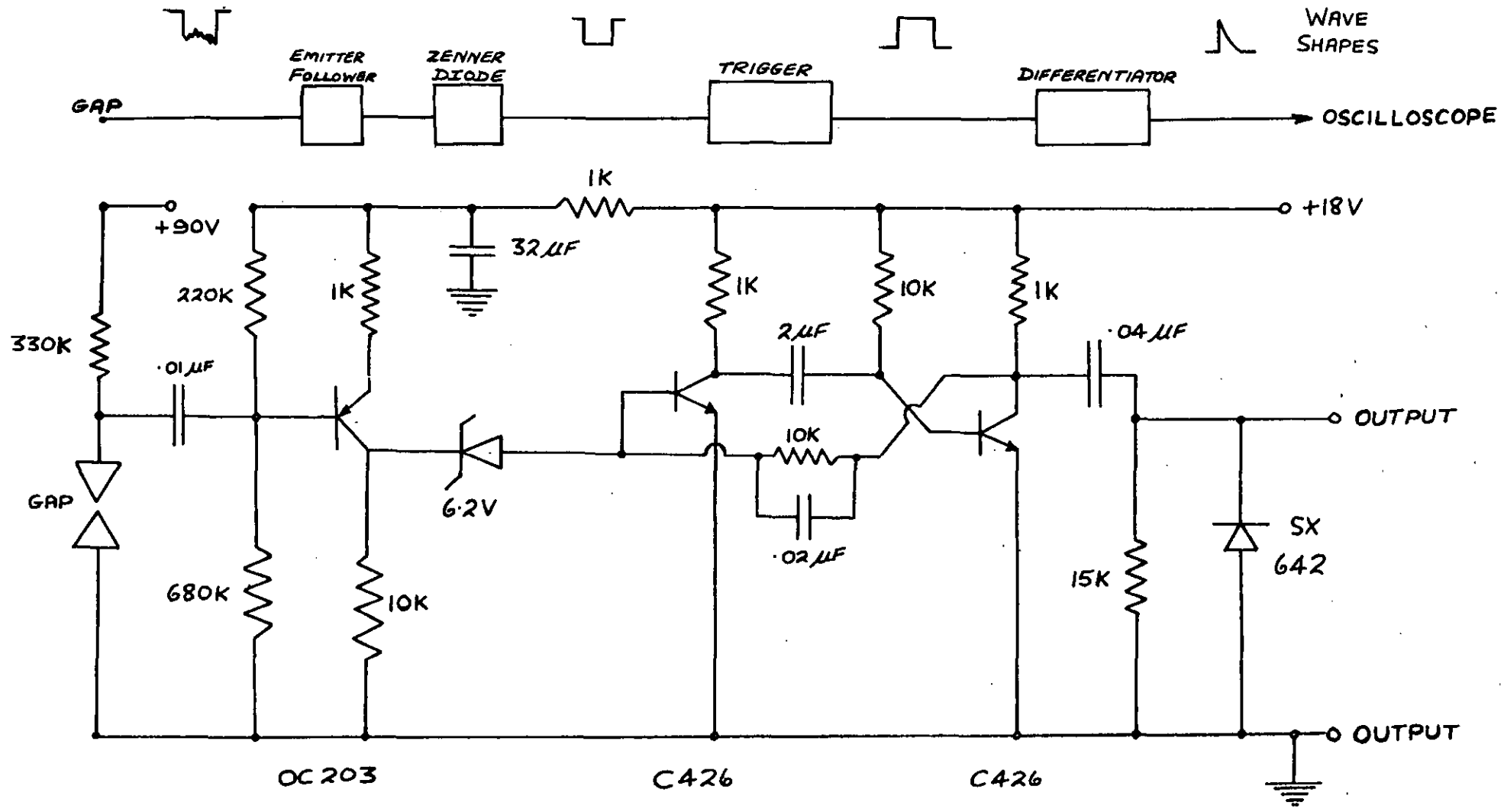

FIG. A.5-B — DIAGRAM OF THE CIRCUIT USED TO PROCESS THE SIGNALS FROM THE IONIZATION GAPS BEFORE BEING FED TO THE OSCILLOSCOPE. ALSO INCLUDED IS A BLOCK DIAGRAM OF THE MAIN COMPONENTS OF THE CIRCUIT.

APPENDIX 6.

APPENDIX 6.

DETERMINATION OF THE EQUILIBRIUM CONSTANTS.

GENERAL.

The reader is referred to a text on chemical engineering thermodynamics (e.g. Lewis and Randall[182]) or on advanced engineering thermodynamics (e.g. Benson[183]) for a more complete treatment of this subject.

If F is the molal free energy of a substance in any given state of temperature and pressure and F_o is the molal free energy in the standard state (i.e. at any given reaction temperature but at unit atmospheric pressure), then

$$F - F_o = RT \log_e \frac{a}{a_o} \quad \text{..... A.6-1}$$

In this equation, 'a' is the fugacity in the given state and 'a_o' is the fugacity in the standard state. The term fugacity is an activity term which is related to the temperature, pressure and composition of the system. It is used to represent deviations from ideal gas law behaviour.

Considering next the chemical reaction

$$n_A.A + n_B.B \rightleftharpoons n_C.C + n_D.D \quad \text{..... A.6-2}$$

where the symbology is the same as in Equation 6-2 in Chapter 6, it is assumed that this is in equilibrium at the reaction temperature, T. The activities of the A, B, C and D components are denoted by a_A, a_B, a_C and a_D respectively.

The change in free energy for this reaction in transforming n_A moles of A and n_B moles of B from the standard state to the equilibrium state is

$$-\left[n_A\left(F_A - F_{AO}\right) + n_B\left(F_B - F_{BO}\right)\right]$$

Correspondingly, the change in transforming n_C moles of C and n_D moles of D from the equilibrium state to the standard state is

$$\left[n_C.\left(F_C - F_{CO}\right) + n_D.\left(F_D - F_{DO}\right)\right]$$

Thus, if n_A moles of A and n_B moles of B in the standard state are transformed into n_C moles of C and n_D moles of D in the standard state, the total change in free energy is:

$$n_C.\left(F_C - F_{CO}\right) + n_D.\left(F_D - F_{DO}\right) - n_A\left(F_A - F_{AO}\right) - n_B\left(F_B - F_{BO}\right) \quad \ldots\ldots\ldots A.6\text{-}3$$

Utilising Equation A.6-1 and defining

$$f = \frac{a}{a_o}$$

where f is the activity in the non-standard state, this total free energy change is also given by:

$$RT \log_e f_C + RT \log_e f_D - RT \log_e f_A - RT \log_e f_B \quad \ldots\ldots\ldots A.6\text{-}4$$

Equating Equations A.6-3 and A.6-4 now, there is obtained the expression

$$\Delta F = \Delta F_o + RT\left[n_C \log_e f_C + n_D . \log_e f_D - n_A \log_e f_A - n_B \log_e f_B\right]$$

$$= \Delta F_o + RT \log_e \left[\frac{f_C^{n_C} . f_D^{n_D}}{f_A^{n_A} . f_B^{n_B}}\right] \quad \ldots\ldots\ldots A.6\text{-}5$$

where

$$\Delta F = F_C + F_D - F_A - F_B$$

and

$$\Delta F_o = F_{C_o} + F_{D_o} - F_{A_o} - F_{B_o}$$

When the reaction has reached a point such that there is no change in the number of moles of any constituent, chemical equilibrium is said to have been attained. The

criterion for this is that, at constant temperature and pressure, there can be no change in the free energy of the system. Consequently, when these limitations are imposed on equation A.6-5, ΔF must be zero for equilibrium and the following familiar expression for equilibrium is obtained:

$$\Delta F_o = - RT \log_e K_f \quad \ldots\ldots\ldots\ldots A.6-6$$

where

$$K_f = \frac{f_c^{n_c} \cdot f_D^{n_D}}{f_A^{n_A} \cdot f_B^{n_B}}$$

For a system in which the behaviour of each gas can be described by the equation of state

$$PV = mRT \quad \ldots\ldots\ldots\ldots A.6-7$$

the fugacity of each component becomes identically equal to its partial pressure in the system at all temperatures and pressures for which equation A.6-7 is valid. When this is the case, equation A.6-6 becomes

$$\Delta F_o = - RT \log_e K_P \quad \ldots\ldots\ldots\ldots A.6-8$$

where the equilibrium constant, K_P, is now denoted by

$$K_P = \frac{P_c^{n_c} \cdot P_D^{n_D}}{P_A^{n_A} \cdot P_B^{n_B}}$$

and P_A, P_B, P_C and P_D are the partial pressures of the components A, B, C and D respectively. K_P is then the equilibrium constant at one atmosphere.

This expression for K_P should be compared with the derived expression in equation 6-5 of Chapter 6 which gives the ratio of the specific rate constants for this same reaction. In this ratio expression, if the concentrations of the components A, B, C and D are replaced by the partial pressures of these components in the system (since one

measure of relative concentrations is partial pressures), the equilibrium constant K_p is obtained.

In Equation A.6-8, the free energy change ΔF_o is termed the standard free energy of the reaction. This quantity depends upon the temperature, the definition of the standard state conditions and the number of moles entering into the stoichiometric equation A.6-2. Once the standard state pressure is fixed, the equilibrium constant becomes independent of the system pressure.

In this work, standard temperature and pressure are taken to be 298.15°K and 1 atmosphere.

Equilibrium Constant Calculations.

From Equation A.6-8, it is possible to obtain the relationship

$$\text{Log}_e K_{P_k} = - \frac{\Delta F_{o_k}}{RT}$$

where the subscript (k(= 5, 15)) refers to the derived constituents present in the burnt mixture. Also,

$$\Delta F_{o_k} = F_{o_{products}} - F_{o_{reactants}}$$

and

$$F_{o_k} = H_{o_k} - T. S_{o_k}$$

In this latter expression,

$$H_{o_k} = HF_k + \overline{C}_{p_k} (T - 298.15) \qquad \text{------- A.6-9}$$

and

$$S_{o_k} = SF_k + \overline{C}_{p_k} \log_e \frac{T}{298.15} - R. \log_e \frac{P}{P_o} \qquad \text{--- A.6-10}$$

where

HF_k = the Heat of Formation of the individual constituent under consideration at 298.15°K (cal/mole)

ΣF_k = the entropy at 298.15° K and one atmosphere pressure (cal/mole °K).

$\overline{C_{pk}}$ = the mean specific heat at constant pressure between T and 298.15°K.

P_o = 1 atmosphere (by definition).

so that

$$\frac{P}{P_o} = 1 \text{ (also by definition).}$$

Equation A.6-10 thus becomes:

$$C_{ok} = \Sigma F_k + \int_{298.15}^{T} \frac{C_{pk}}{T} \cdot dT \qquad \text{------- A.6-11}$$

Appendix 7 contains all the thermodynamic data necessary for these calculations.

Using the derived expressions above, the Free Energy changes, (ΔF_{ok}), at constant temperature and pressure, for the set of equilibrium equations listed in Series 6A of Chapter 6 for the <u>rich and stoichiometric</u> mixtures are (using the same numerical subscripts):

$\Delta F_{05} = F_{05} - 2F_{01} + 2F_{02}$

$\Delta F_{06} = F_{06} - F_{04} - F_{02} + F_{01}$

$\Delta F_{07} = F_{07} - \frac{1}{2} F_{03} - F_{01} + F_{02}$

$\Delta F_{08} = F_{08} - \frac{1}{2} F_{04} - \frac{1}{2} F_{01} + \frac{1}{2} F_{02}$

$\Delta F_{09} = F_{09} - \frac{1}{2} F_{04} - \frac{1}{2} F_{02} + \frac{1}{2} F_{01}$

$\Delta F_{010} = F_{010} - F_{01} + F_{02}$

$\Delta F_{011} = F_{011} - \frac{1}{2} F_{03} - 2 F_{01} + 2 F_{02}$

$\Delta F_{012} = F_{012} - F_{03} - F_{01} + F_{02}$

$\Delta F_{013} = F_{013} - \frac{1}{2} F_{03} - 3/2 F_{04} - 3/2 F_{02} + 3/2 F_{01}$

$\Delta F_{014} = F_{014} - \frac{1}{2} F_{04} - \frac{1}{2} F_{03} - \frac{1}{2} F_{01} + \frac{1}{2} F_{02}$

$$\Delta F_{O15} = F_{O15} - \tfrac{1}{2} F_{O3}$$

Thus, for these mixtures,

$$K_k = \exp.\left(\frac{-\Delta F_{Ok}}{RT}\right)$$

Similarly, for <u>weak mixtures</u>, the Free Energy changes (ΔF_{O_k}), at constant temperature and pressure, for the set of equilibrium equations listed in Series 6D of Chapter 6 are (using the same numerical subscripts):

$$\Delta F_{O5} = F_{O5} - F_{O1} + \tfrac{1}{2} F_{O2}$$

$$\Delta F_{O6} = F_{O6} - F_{O4} + \tfrac{1}{2} F_{O2}$$

$$\Delta F_{O7} = F_{O7} - \tfrac{1}{2} F_{O3} - \tfrac{1}{2} F_{O2}$$

$$\Delta F_{O8} = F_{O8} - \tfrac{1}{2} F_{O4} - \tfrac{1}{4} F_{O2}$$

$$\Delta F_{O9} = F_{O9} - \tfrac{1}{2} F_{O4} + \tfrac{1}{4} F_{O2}$$

$$\Delta F_{O10} = F_{O10} - \tfrac{1}{2} F_{O2}$$

$$\Delta F_{O11} = F_{O11} - \tfrac{1}{2} F_{O3} - F_{O2}$$

$$\Delta F_{O12} = F_{O12} - F_{O3} - \tfrac{1}{2} F_{O2}$$

$$\Delta F_{O13} = F_{O13} - \tfrac{1}{2} F_{O3} - {}^{3}/_{2} F_{O4} + \tfrac{3}{2} F_{O2}$$

$$\Delta F_{O14} = F_{O14} - \tfrac{1}{2} F_{O4} - \tfrac{1}{2} F_{O3} - \tfrac{1}{4} F_{O2}$$

$$\Delta F_{O15} = F_{O15} - \tfrac{1}{2} F_{O3}$$

For these mixtures,

$$G_k = \exp\left(\frac{-\Delta F_{Ok}}{RT}\right)$$

APPENDIX 7

THERMODYNAMIC DATA AND PROPERTIES OF IDEAL GASES

APPENDIX 7

THERMODYNAMIC DATA AND PROPERTIES OF IDEAL GASES

In cycle simulation work, the necessity for accurate thermodynamic data for the many chemical species and substances which comprise the working fluid in the engine needs hardly to be stressed. Since the analytical model for the spark ignition engine presented in this study is designed to be simulated mathematically on a computer, it was considered desirable to calculate as many thermodynamic properties as possible from polynomial equations. Such a system would obviate the use of a large amount of computer storage capacity.

All properties are calculated relative to the standard conditions of 298.15°K and one atmosphere pressure.

Specific Heat Data

In consideration of the 15 species which are present in the combustion products (viz. CO_2, CO, N_2, H_2O, O_2, H_2, NO, OH, H, O, NO_2, N_2O, NH_3, HNO and N), the specific heat at constant pressure, C_p, for each specie is approximated by two sixth-order polynomials over the temperature ranges 273 - 2000°K and 2000 - 6000°K. Thus,

$$C_{p_k} = a_0 + a_1 \cdot x + a_2 \cdot x^2 + a_3 \cdot x^3 + a_4 \cdot x^4 + a_5 \cdot x^5 + a_6 \cdot x^6$$

for the range 273 - 2000°K

and

$$C_{p_k} = b_0 + b_1 \cdot x + b_2 \cdot x^2 + b_3 \cdot x^3 + b_4 \cdot x^4 + b_5 \cdot x^5 + b_6 \cdot x^6$$

for the range 2000 - 6000°K.

In these expressions,

$x = T \times 10^{-3}$

and the subscript k (which has a value from 1 to 15) denotes the individual species. The coefficients are derived from polynomial approximations to tabulated data published in the J.A.N.A.P., tables[206]. They are listed in Tables A.7-A and A.7-B.

In addition, C_p data for dry air and for the three fuels used in this study (viz. propane, iso-octane and benzene) are required. These are also expressed in polynomial form as follows:

$$C_p = c_0 + c_1 \cdot x + c_2 \cdot x^2 + c_3 \cdot x^3 + c_4 \cdot x^4 + c_5 \cdot x^5 + c_6 \cdot x^6$$

where the significance of 'x' is the same as in the previous expressions. The coefficients of these equations are given in Table A.7-C in addition to the source from which they were obtained.

Some calculations in this work require that mean values ($\overline{C_p}$) of C_p be estimated between the standard temperature of 298.15°K and some higher temperature T. These are obtained from the general formula

$$\overline{C_p} = \frac{\int_{298.15}^{T} C_p \cdot dT}{(T - 298.15)} \qquad \text{A.7-1}$$

TABLE A.7-A

IDEAL GAS HEAT CAPACITY (C_p) EQUATION COEFFICIENTS

cal/(gm-mole)- ^{o}K

$$C_p = a_0 + a_1 \cdot x + a_2 \cdot x^2 + a_3 \cdot x^3 + a_4 \cdot x^4 + a_5 \cdot x^5 + a_6 \cdot x^6$$

TEMPERATURE RANGE: 273 - 2000^{o}K

SPECIE	a_0	a_1	a_2	a_3	a_4	a_5	a_6
CO_2	4.324933	20.808952	-22.945905	16.844833	-7.935665	2.121672	-0,240871
CO	7.812249	-6.668293	17.282958	-17.287093	8.860125	-2.314819	0.244778
N_2	7.709929	-5.503897	13.121358	-11.679546	5.233997	-1.173185	0.103883
H_2O	7.988860	-1.506271	6.661376	-4.655970	1.696464	-0.370621	0.039924
O_2	7.361141	-5.369589	20.541786	-25.865263	15.945662	-4.858890	0.586150
H_2	6.183043	4.710657	-10.921355	12.540865	-7.016263	1.923395	-0.208409
NO	8.462334	-10.406686	27.548756	-30.281191	17.185114	-4.957260	0.575528
OH	7.615100	-1.936000	0.877000	-0.615300	-2.690900	0.907890	-0.126950
H	4.968000	0.000000	0.000000	0.000000	0.000000	0.000000	0.000000
O	5.974134	-4.241883	7.931254	-7.944230	4.403357	-1.271341	0.149141
NO_2	6.610077	5.431315	12.725101	-24.939977	17.734952	-5.830404	0.736354
N_2O	4.826714	20.139273	-22.136118	15.855180	-7.265313	1.897833	-0.211745
NH_3	7.040500	1.209100	18.330000	-23.991000	15.183000	-4.949600	0.653370
HNO	7.481815	-1.205998	19.296274	-25.614212	15.652081	-4.715048	0.564725
N	4.966526	0.011505	-0.033335	0.046170	-0.032421	-0.010946	-0.001374

TABLE A.7-B

IDEAL GAS HEAT CAPACITY (C_p) EQUATION COEFFICIENTS

C_p in cal/(gm-mole)-^oK

$$C_p = b_0 + b_1 \cdot x + b_2 \cdot x^2 + b_3 \cdot x^3 + b_4 \cdot x^4 + b_5 \cdot x^5 + b_6 \cdot x^6$$

TEMPERATURE RANGE: 2000 - 6000^oK

SPECIE	b_0	b_1	b_2	b_3	b_4	b_5	b_6
CO_2	8.153021	8.411419	-4.795179	1.543125	-0.283123	0.027656	-0.001113
CO	5.966461	3.288911	-1.660467	0.476445	-0.078536	0.006957	-0.000257
N_2	5.649167	3.579035	-1.794312	0.512130	-0.084187	0.007443	-0.000273
H_2O	3.401967	9.433046	-4.067415	1.049852	-0.162023	0.013774	-0.000494
O_2	8.439106	-0.376523	0.621716	-0.192346	0.028999	-0,002358	0.000086
H_2	4.103273	3.981784	-1.426509	0.269268	-0.018659	-0.000812	0.000124
NO	6.590193	2.604241	-1.291210	0.365114	-0.059370	0.005194	-0.000190
OH	4.946400	3.264500	-1.202600	0.258490	-0.031839	0.002068	-0.000054
H	4.968000	0.000000	0.000000	0.000000	0.000000	0.000000	0.000000
O	4.743426	0.480906	-0.364666	0.127389	-0.021166	0.001705	-0,000054
NO_2	9.949028	4.493565	-2.347261	0.682407	-0.113564	0.010128	-0.000376
N_2O	9.873937	5.610329	-2.906743	0.842392	-0.140197	0.012533	-0.000467
NH_3	20.514999	-14.032000	13.265999	-5.323999	1.105200	-0.115880	0.004861
HNO	7.144250	7.196827	-3.613303	1.025384	-0.168262	0.014899	-0.000551
N	4.845706	0.080796	0.087980	-0.104245	0.036582	-0.004866	0.000226

TABLE A.7-C

IDEAL GAS HEAT CAPACITY (C_p) EQUATION COEFFICIENTS FOR DRY AIR, PROPANE, ISO-OCTANE AND BENZENE

cal/gm-^{o}K

$$C_p = c_o + c_1 \cdot x + c_2 x^2 + c_3 x^3 + c_4 \cdot x^4 + c_5 \cdot x^5 + c_6 \cdot x^6$$

SUBSTANCE	DATA SOURCE	c_0	c_1	c_2	c_3	c_4	c_5	c_6
DRY AIR	Spiers[188]	0.25416	-0.12699	0.34820	-0.31412	0.13867	-0.03021	0.00259
		(valid over the temperature range 273 - 3250^{o}K)						
PROPANE VAPOUR	Shell[207] Publications	0.45597	-3.05099	17.12507	-34.36135	35.46474	-18.61938	3.92578
		(valid over the temperature range 273 - 1273^{o}K)						
ISO-OCTANE VAPOUR	A.P.I.[208]	2.54774	153.63590	-13.33820	-93.77068	70.97913	-16.49594	0.00000
		(units for this equation are cal/(gm-mole)-^{o}K) (valid over the temperature range 298.15 - 1500^{o}K)						
BENZENE VAPOUR	Spiers[188]	0.02893	0.17772	3.49579	-7.10684	6.21113	-2.56909	0.40482
		(valid over the temperature range 273 - 1273^{o}K)						

Specific Heat at constant volume, C_v, data are estimated from

$$C_v = C_p - R \quad \text{A.7-2}$$

where R is the Universal Gas Constant. Mean values ($\bar{C}_v$) of C_v are likewise obtained from

$$\bar{C}_v = \bar{C}_p - R \quad \text{A.7-3}$$

Enthalpy Calculations

Enthalpy values per mole are derived from the formula

$$H = \bar{C}_p \cdot (T - 298.15) \quad \text{A.7-4}$$

However, whenever Heats of Formation are also taken into account, as during equilibrium composition calculations, such values are obtained from expressions of the form

$$H = HF + \bar{C}_p \cdot (T - 298.15) \quad \text{A.7-5}$$

in which HF is the enthalpy of formation of the substance under consideration at 298.15°K. A listing of these HF values for all the constituents which are considered to be present in the working fluid in the spark ignition engine is given in Table A.7-D. The source of such data is also given.

Internal Energy Calculations

The Internal Energy, E, per mole is estimated from the expression:

$$E = \bar{C}_v \cdot (T - 298.15) \quad \text{A.7-6}$$

TABLE A.7-D

HEATS OF FORMATION (HF) AT 298.15°K

SUBSTANCE	DATA SOURCE	HEATS OF FORMATION AT 298.15°K cal/(gm-mole)
CO_2	JANAF[206] TABLES	-94053.999
CO	"	-26416.998
N_2	"	0.000
H_2O	"	-57798.000
O_2	"	0.000
H_2	"	0.000
NO	"	21579.999
OH	"	9431.999
H	"	52100.000
O	"	59559.000
NO_2	"	7909.999
N_2O	"	19610.000
NH_3	"	-10970.000
HNO	"	23800.000
N	"	112965.000
DRY AIR	API PROJECT 44[208]	-28.220
PROPANE	SPIERS[188]	-24820.000
ISO-OCTANE	API PROJECT[208]	-53570.000
BENZENE	"	19820.000

for the dry air and the 15 chemical species in the combustion products. However, in calculations of the gaseous fuel Internal Energies in the unburnt charge, this expression is supplemented by a term which includes the chemical energy in the fuel. Thus,

$$E = \bar{C}_v \cdot (T - 298.15) + Q_v \quad \text{A.7-7}$$

where Q_v is the Lower Calorific Value (also termed the Heat of Combustion) per mole of the fuel under consideration. For the three fuels used in this study, these Heats of Combustion are given in Table A.7-E.

Entropy Calculations

Entropy values are obtained from the standard expression:

$$S - SF = \bar{C}_p \cdot \log_e \frac{T}{298.15} - R \cdot \log_e P \quad \text{A.7-8}$$

in which

S = the entropy at temperature T and pressure P (ATM)

SF = the entropy at 298.15°K and 1 atmosphere pressure.

In equilibrium composition calculations, where the free energies (H - TS) of the individual species which comprise the combustion products are required (see Appendix 6), such evaluations are performed at the equilibrium reaction temperature, T and at a pressure of one atmosphere. Thus, Equation A.7-8 becomes

$$S = SF + \bar{C}_p \cdot \log_e \frac{T}{298.15} \quad \text{A.7-9}$$

TABLE A.7-E

LOWER CALORIFIC VALUES AT CONSTANT VOLUME AND LATENT HEATS OF VAPOURIZATION OF PROPANE, ISO-OCTANE AND BENZENE

FUEL	LOWER CALORIFIC VALUE (FUEL IN VAPOUR PHASE) AT 298.15°K. (cal/(gm-mole)°K)	LATENT HEAT OF VAPOURIZATION AT 298.15°K (cal/(gm-mole)°K)
PROPANE	488,500[207]	3,600[168]
ISO-OCTANE	1,222,000[210]	8,410[210]
BENZENE	752,000[210]	8,080[210]

- - - - -

In Table A.7-F, there is a listing of SF values for all the constituents which are considered to be present in the working fluid.

Viscosity

Values of Absolute Viscosity (μ) for Dry Air were obtained from "THE MOLECULAR THEORY OF GASES AND LIQUIDS" by Hirschfelder et al. In this reference, the μ values are listed in tabular form but, for use in this work, they have been converted into a 6th order polynomial expression which is valid over the temperature range 273 - 3000°K. The expression is:

$$\mu = (0.43868 + 5.13195.x - 1.31065.x^2 - 0.668597.x^3 + 0.922798.x^4 - 0.342237.x^5 + 0.042674.x^6) \times 10^{-4} \text{ gm/cm sec (poises)} \quad \text{A.7-10}$$

where $x = .001 \times T$

Thermal Conductivity

Calculations of thermal conductivity, λ, for Dry Air are made using the formula suggested by Dugger et al[25]. This is

$$\lambda = (C_p + \frac{1.25}{R}). \frac{\mu}{M_a} \quad \text{A.7-11}$$

where M_a is the Molecular Weight of Dry Air. The units of λ are cal/cm sec °K.

TABLE A.7-F

ENTROPY VALUES (SF) AT 298.15°K AND 1 ATMOSPHERE PRESSURE

SUBSTANCE	DATA SOURCE	ENTROPY (SF) AT 298.15°K & 1 ATM (cal/mole °K)
CO_2	JANAF TABLES[206]	51.072
CO	"	47.214
N_2	"	45.770
H_2O	"	45.106
O_2	"	49.004
H_2	"	31.208
NO	"	50.347
OH	"	43.880
H	"	27.392
O	"	38.468
NO_2	"	57.343
N_2O	"	52.546
NH_3	"	46.033
HNO	"	52.729
N	"	36.614
DRY AIR	A.P.I.[208]	47.491
PROPANE	SPIERS[188]	64.510
ISO-OCTANE	A.P.I.[208]	101.150
BENZENE	A.P.I.[208]	64.340

Thermodynamic Properties of Ideal Gas Mixtures

Consider an ideal gas mixture containing n_k moles of the k'th constituent. The total number of moles in the mixture is n_T. On this basis, the following properties of the mixture can be evaluated.

i) Mean Molecular Weight, M

$$M = \frac{\sum n_k \cdot M_k}{n_T} \quad \text{A.7-12}$$

where the summation is over all the constituents of the mixture and M_k is the Molecular Weight of the k'th constituent. These latter values, for all the constituents present in the working fluid, are given in Table A.7-G.

ii) Specific Heat at Constant Pressure, C_p

$$C_p = \frac{\sum n_k \cdot C_{pk}}{n_T} \quad \text{A.7-13}$$

in which C_{p_k} is the molar specific heat at constant pressure of the k'th constituent of the mixture at the temperature of the mixture.

iii) Specific Heat at Constant Volume, C_v

$$C_v = \frac{\sum n_k \cdot C_{v_k}}{M \cdot n_T} \quad \text{A.7-14}$$

where C_{v_k} is the molar specific heat at constant volume of the k'th constituent of the mixture at

TABLE A.7-G

MOLECULAR WEIGHTS OF CONSTITUENTS

SUBSTANCE	MOLECULAR WEIGHT
CO_2	44.011
CO	28.011
N_2	28.016
H_2O	18.016
O_2	32.000
H_2	2.016
NO	30.008
OH	17.008
H	1.008
O	16.000
NO_2	46.008
N_2O	44.016
NH_3	17.032
HNO	31.016
N	14.008
DRY AIR	28.9
PROPANE	44.097
ISO-OCTANE	114.232
BENZENE	78,114

the temperature of the mixture.

iv) Specific Enthalpy, h

$$h = \frac{\sum n_k . H_k}{M . n_T} \quad \text{A.7-15}$$

where H_k is the molar enthalpy of the k^{th} constituent of the mixture at the temperature, T, of the mixture relative to the standard temperature of 298.15°K.

v) Specific Internal Energy, e

$$e = \frac{\sum n_k . E_k}{M . n_T} \quad \text{A.7-16}$$

where E_k is the molar internal energy of the k^{th} constituent of the mixture at the temperature, T, of the mixture relative to the standard temperature (298.15°K). For the gaseous fuel in the unburnt fraction, this term will include the chemical energy of the fuel (see Equation A.7-7).

vi) Specific Entropy, s

$$s = \frac{\sum n_k . SF_k + \sum n_k (\overline{C}_{p_k} . \log_e \frac{T}{298.15} - R . \log_e p_k)}{M . n_T}$$

cal/gm °K

- - - - A.7-17

where

SF_k is the molar entropy of the k'th constituent of the mixture at 298.15^{o}K and one atmosphere pressure.

$\bar{C}_{p_k}$ is the mean molar specific heat at constant pressure of the k'th constituent of the mixture between temperature T and 298.15^{o}K.

and

p_k is the partial pressure of the k'th constituent of the mixture.

If

$$S_k = \Sigma n_k . SF_k + \Sigma n_k . \bar{C}_{p_k} \log_e \frac{T}{298.15}$$

which is the molar enthalby of the k'th constituent of the mixture at the temperature, T, of the mixture and a pressure of one atmosphere, then Equation A.7-17 can be re-written as

$$s = \frac{1}{M . n_T} \left[\Sigma n_k . S_k - \Sigma n_k . R . \log_e p_k \right] \quad \ldots\ldots A7\text{-}18$$

As Daltonis Law of Partial Pressures is obeyed

$$\frac{p_k}{P} = \frac{n_k}{n_T}$$

and substituting this into Equation A.7-18, one obtains

$$s = \frac{1}{M\, n_T} \left[\Sigma n_k S_k - \Sigma n_k . R . \log_e \left(\frac{n_k P}{n_T} \right) \right]$$

which can be finally rearranged into its most useable form:

$$s = \frac{1}{M . n_T} \left[\Sigma n_k . S_k + R \left[n_T \log_e \left(\frac{n_T}{P} \right) - \Sigma n_k . \log_e n_k \right] \right] \quad \ldots\ldots A.7\text{-}19$$

Specific Volume, v

The specific volume, v, of the mixture is given by the equation of state

$$v = \frac{RT}{MP} \qquad \text{A.7-20}$$

In this study, it is also required to estimate the rates of change of

a) the specific internal energy, e

b) the specific entropy, s

c) the specific volume, v

with respect to changes in temperature and pressure (see Chapter 3). Before expressions are derived for these rates of change, however, the following notation is proposed to describe the partial derivatives of n_k and n_T with respect to temperature and pressure since these quantities are themselves functions of these:

$$\left(\frac{\partial n_k}{\partial T}\right)_\rho = n'_{Tk} \quad ; \quad \left(\frac{\partial n_k}{\partial \rho}\right)_T = n'_{\rho k}$$

$$\left(\frac{\partial n}{\partial T}\right)_p = n'_T \quad ; \quad \left(\frac{\partial n}{\partial P}\right)_T = n'_p$$

Using a similar notation, the rates of change of the above mixture properties can now be written as:

$$\left(\frac{\partial e}{\partial T}\right)_p = \frac{1}{M \cdot n_T}\left[\Sigma n_k \cdot C_{vk} + \Sigma E_k \cdot n'_{Tk}\right]$$

$$\left(\frac{\partial e}{\partial P}\right)_T = \frac{1}{M \cdot n_T}\left[\Sigma E_k \cdot n'_{pk}\right]$$

$$\left(\frac{\partial s}{\partial T}\right)_P = \frac{1}{M.n_T}\left[\sum \frac{n_k . C_{pk}}{T} + \sum s_k . n'_{Tk}\right] \quad \text{approx.}$$

$$\left(\frac{\partial s}{\partial P}\right)_T = \frac{1}{M.n_T}\left[\sum s_k . n'_{pk} - \frac{R.n_T}{P}\right] \quad \text{approx.}$$

$$\left(\frac{\partial v}{\partial T}\right)_P = \frac{v}{T}\left[1 + \frac{T.n'_T}{n_T}\right]$$

$$\left(\frac{\partial v}{\partial P}\right)_T = \frac{v}{P}\left[\frac{P.n'_P}{n_T} - 1\right]$$

In this list of equations, C_{vk} and C_{pk} are the molar specific heats at constant volume and constant pressure respectively of the k'th constituent of the mixture at the temperature of the mixture. Values of n'_{Tk}, n'_{pk}, n'_T and n'_P are obtained directly from the equations defining the equilibrium compositions of the burnt fraction of the charge. These techniques are performed in SUBROUTINE DISCN in the listed computer program (see Appendix 8).

APPENDIX 8

APPENDIX 8

FLOW DIAGRAM OF COMPUTER PROGRAM AND PROGRAM LISTING

In the Flow Diagram and the listed computer program in this Appendix, the following symbols have been used to represent certain of the more important quantities and parameters. These are not in agreement with those given at the beginning of this report.

D - equivalence ratio

J FUEL - type of fuel JFUEL = 1 = propane
JFUEL = 2 = iso-octane
JFUEL = 3 = benzene

WR - mass fraction of exhaust residuals in unburnt mixture.

PR - pressure at inlet valve closure (in input data) and cylinder pressure elsewhere (p.s.i.)

T - charge temperature at inlet valve closure (^{o}K)

THETS - crankangle at ignition

THDEG - crankangle at inlet valve closure (in input data) and crankangle elsewhere.

CR - compression ratio

XN - engine speed (rev/min).

THEND - crankangle at exhaust valve closure

TU - unburnt gas temperature (^{o}K)

TB - initial estimate of temperature of burnt portion of charge at ignition (in input data)

and burnt gas temperature elsewhere (^{o}K).

WW - mass fraction of injected water in unburnt mixture.

$C_{p_{DATA}}$ - specific heat data

W - total mass of charge in cylinder (gm)

VB - burnt gas volume (cc)

VU - unburnt gas volume (cc)

WB - mass of burnt gas (gm)

WU - mass of unburnt gas (gm)

<u>During Compression</u>

SUU - entropy at beginning of a step (cal/gm^{o}K)

RHO - density (gm/cc)

TJ - initial or j^{th} estimate of temperature during a particular step (^{o}K)

PJ - initial or j^{th} estimate of pressure during a particular step (p.s.i.)

STUJ - $\frac{\partial s_{uzj}}{\partial T}$ in Chapter 3

SPUJ - $\frac{\partial s_{uzj}}{\partial P}$ in Chapter 3

VTUJ - $\frac{\partial v_{uzj}}{\partial T}$ in Chapter 3

VPUJ - $\frac{\partial v_{uzj}}{\partial P}$ in Chapter 3

SLOSS - entropy loss due to heat transfer (cal/gm^{o}K)

SUJ - s_{uzj} in Chapter 3

VUJ - v_{uzj} in Chapter 3

XP - ΔP_j in Chapter 3

XTU - ΔT_j in Chapter 3

<u>During Combustion</u>

1) <u>Combustion Step</u>

TBJ - initial or j'th estimate of burnt gas temperature (^{o}K)

TUJ - initial or j'th estimate of unburnt gas temperature (^{o}K)

PRJ - initial or j'th estimate of pressure (p.s.i.)

STUJ - $\frac{\partial s_{uj}}{\partial T}$ in Chapter 3

SPUJ - $\frac{\partial s_{uj}}{\partial P}$ in Chapter 3

VTUJ - $\frac{\partial v_{uj}}{\partial T}$ in Chapter 3

VPUJ - $\frac{\partial v_{uj}}{\partial P}$ in Chapter 3

ETUJ - $\frac{\partial e_{uj}}{\partial T}$ in Chapter 3

ETBJ - $\frac{\partial e_{bj}}{\partial T}$ in Chapter 3

EPBJ - $\frac{\partial e_{bj}}{\partial P}$ in Chapter 3

VTBJ - $\frac{\partial v_{bj}}{\partial T}$ in Chapter 3

VPBJ - $\frac{\partial v_{bj}}{\partial P}$ in Chapter 3

EUJ - e_{uj} in Chapter 3

EBJ - e_{bij} in Chapter 3

SUJ - s_{uij} in Chapter 3

VUJ - v_{uij} in Chapter 3

VBJ - v_{bij} in Chapter 3

DP - $(P_i - P_{ij})$ in Chapter 3

DTU - $(T_{ui} - T_{uij})$ in Chapter 3

DTB - $(T_{bi} - T_{bij})$ in Chapter 3

ii) <u>Piston Movement and Heat Transfer Step</u>

TUK - initial or j^{th} estimate of unburnt gas temperature (^{o}K)

TBK - initial or j^{th} estimate of burnt gas temperature (^{o}K)

PRK - initial of j^{th} estimate of pressure (p.s.i.)

STUJ - $\frac{\partial s_{uzj}}{\partial T}$ in Chapter 3

SPUJ - $\frac{\partial s_{uzj}}{\partial P}$ in Chapter 3

STBJ - $\frac{\partial s_{bzj}}{\partial T}$ in Chapter 3

SPBJ - $\frac{\partial s_{bzj}}{\partial P}$ in Chapter 3

VTUJ - $\frac{\partial v_{uzj}}{\partial T}$ in Chapter 3

VTBJ - $\frac{\partial v_{bzj}}{\partial T}$ in Chapter 3

VPUJ - $\frac{\partial v_{uzj}}{\partial P}$ in Chapter 3

VPBJ - $\frac{\partial v_{bzj}}{\partial P}$ in Chapter 3

SUJ - S_{uzj} in Chapter 3

SLOSSU - entropy loss due to heat transfer from unburnt charge (cal/gm°K)

SLOSSB - entropy loss due to heat transfer from burnt charge (cal/gm°K)

SBJ - S_{bzj} in Chapter 3

VUJ - v_{uzj} in Chapter 3

VBJ - v_{bzj} in Chapter 3

SP - $(P_z - P_{zj})$ in Chapter 3

STU - $(T_{uz} - T_{uzj})$ in Chapter 3

STB - $(T_{bz} - T_{bzj})$ in Chapter 3

<u>During Expansion</u>

TBI - initial or j'th estimate of burnt gas temperature (°K)

PRI - initial or j'th estimate of pressure (p.s.i.)

STBJJ - $\frac{\partial s_{bzj}}{\partial T}$ in Chapter 3

SPBJJ - $\frac{\partial s_{bzj}}{\partial P}$ in Chapter 3

VTBJJ - $\frac{\partial v_{bzj}}{\partial T}$ in Chapter 3

VPBJJ - $\frac{\partial v_{bzj}}{\partial P}$ in Chapter 3

SBJJ - s_{bzj} in Chapter 3

SLSSB - entropy loss due to heat transfer (cal/gm°K)

VBBJ - v_{bzj} in Chapter 3

DPJ - $(P_z - P_{zj})$ in Chapter 3

DTBJ - $(T_{bz} - T_{bzj})$ in Chapter 3

FLOW DIAGRAM

(ONLY THE MORE IMPORTANT STEPS ARE SHOWN)

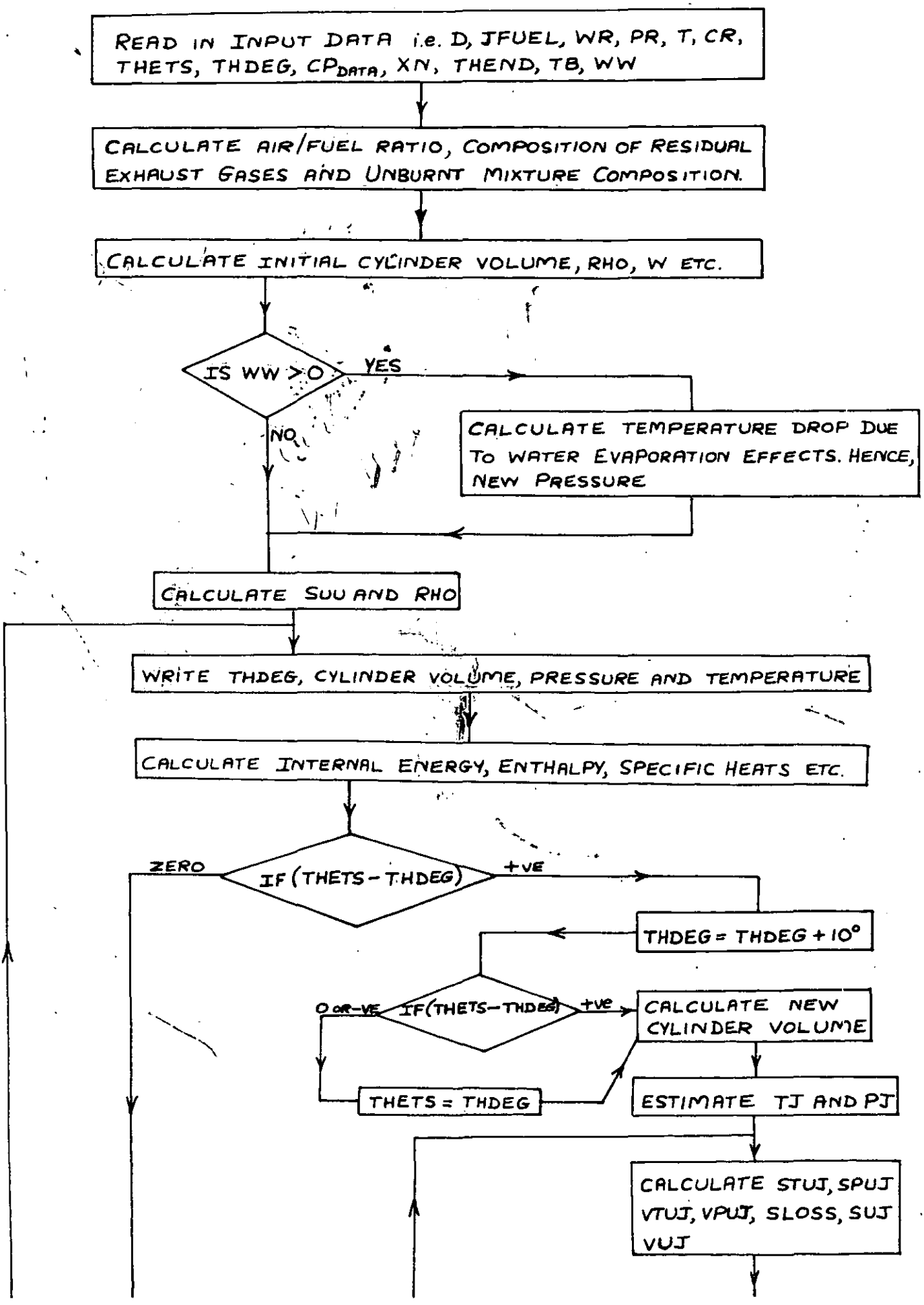

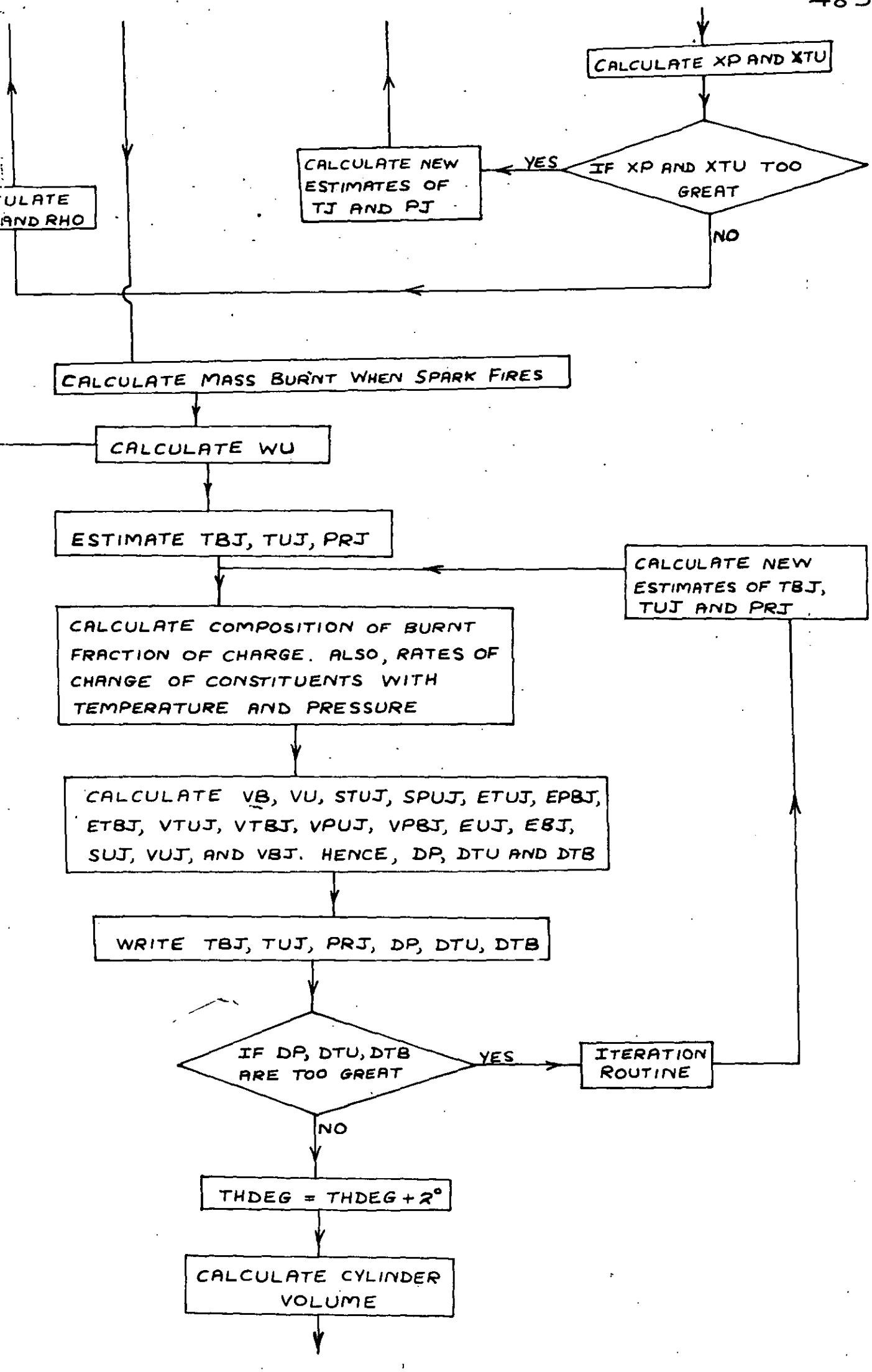
CALCULATE XP AND XTU
IF XP AND XTU TOO GREAT
YES
CALCULATE NEW ESTIMATES OF TJ AND PJ
NO
ULATE AND RHO
CALCULATE MASS BURNT WHEN SPARK FIRES
CALCULATE WU
ESTIMATE TBJ, TUJ, PRJ
CALCULATE NEW ESTIMATES OF TBJ, TUJ AND PRJ
CALCULATE COMPOSITION OF BURNT FRACTION OF CHARGE. ALSO, RATES OF CHANGE OF CONSTITUENTS WITH TEMPERATURE AND PRESSURE
CALCULATE VB, VU, STUJ, SPUJ, ETUJ, EPBJ, ETBJ, VTUJ, VTBJ, VPUJ, VPBJ, EUJ, EBJ, SUJ, VUJ, AND VBJ. HENCE, DP, DTU AND DTB
WRITE TBJ, TUJ, PRJ, DP, DTU, DTB
IF DP, DTU, DTB ARE TOO GREAT
YES
ITERATION ROUTINE
NO
THDEG = THDEG + 2°
CALCULATE CYLINDER VOLUME

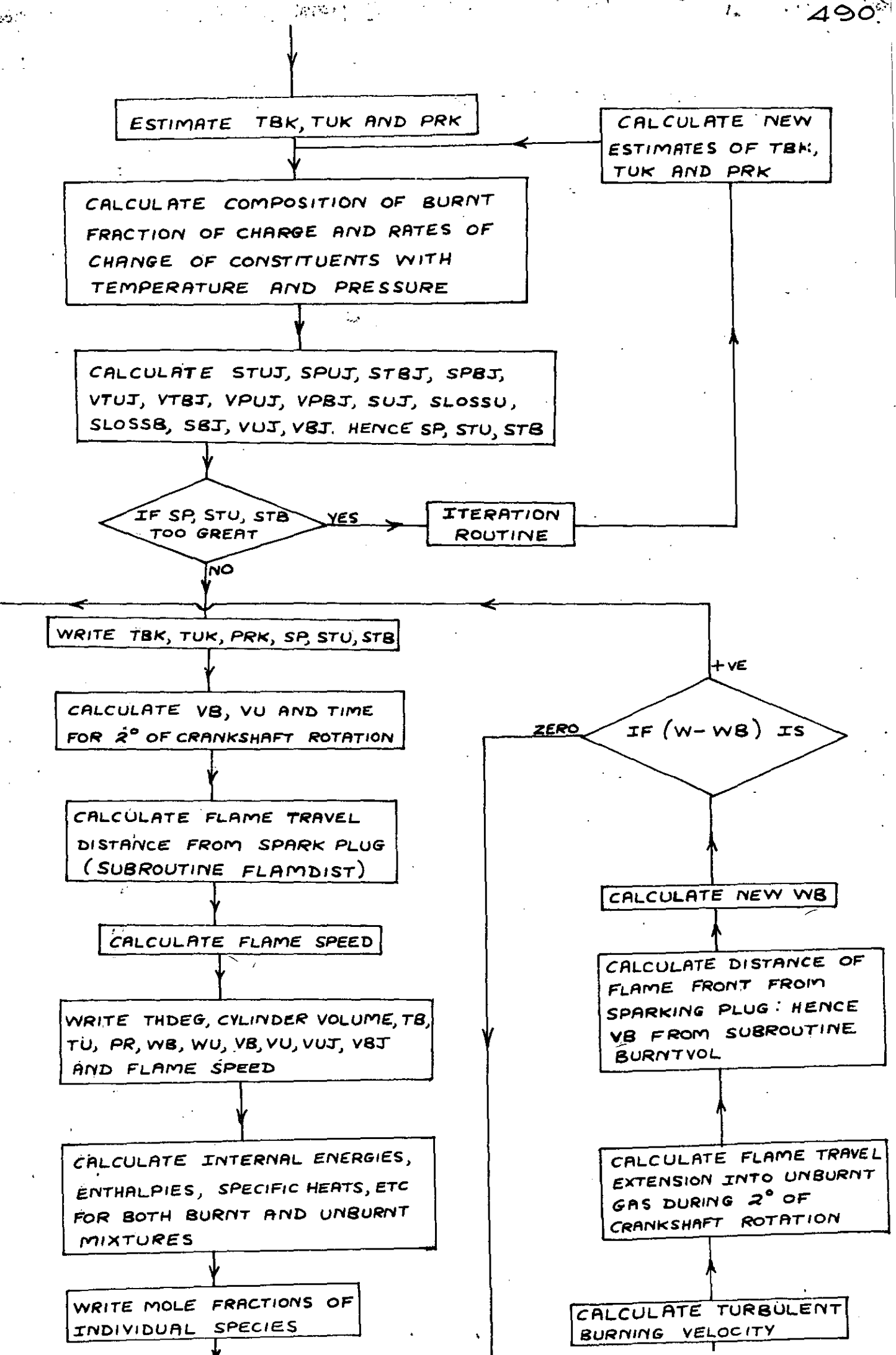
ESTIMATE TBK, TUK AND PRK
CALCULATE NEW ESTIMATES OF TBK, TUK AND PRK
CALCULATE COMPOSITION OF BURNT FRACTION OF CHARGE AND RATES OF CHANGE OF CONSTITUENTS WITH TEMPERATURE AND PRESSURE
CALCULATE STUJ, SPUJ, STBJ, SPBJ, VTUJ, VTBJ, VPUJ, VPBJ, SUJ, SLOSSU, SLOSSB, SBJ, VUJ, VBJ. HENCE SP, STU, STB
IF SP, STU, STB TOO GREAT
YES
ITERATION ROUTINE
NO
WRITE TBK, TUK, PRK, SP, STU, STB
CALCULATE VB, VU AND TIME FOR 2° OF CRANKSHAFT ROTATION
CALCULATE FLAME TRAVEL DISTANCE FROM SPARK PLUG (SUBROUTINE FLAMDIST)
CALCULATE FLAME SPEED
WRITE THDEG, CYLINDER VOLUME, TB, TU, PR, WB, WU, VB, VU, VUJ, VBJ AND FLAME SPEED
CALCULATE INTERNAL ENERGIES, ENTHALPIES, SPECIFIC HEATS, ETC FOR BOTH BURNT AND UNBURNT MIXTURES
WRITE MOLE FRACTIONS OF INDIVIDUAL SPECIES
+VE
IF (W-WB) IS
ZERO
CALCULATE NEW WB
CALCULATE DISTANCE OF FLAME FRONT FROM SPARKING PLUG: HENCE VB FROM SUBROUTINE BURNTVOL
CALCULATE FLAME TRAVEL EXTENSION INTO UNBURNT GAS DURING 2° OF CRANKSHAFT ROTATION
CALCULATE TURBULENT BURNING VELOCITY

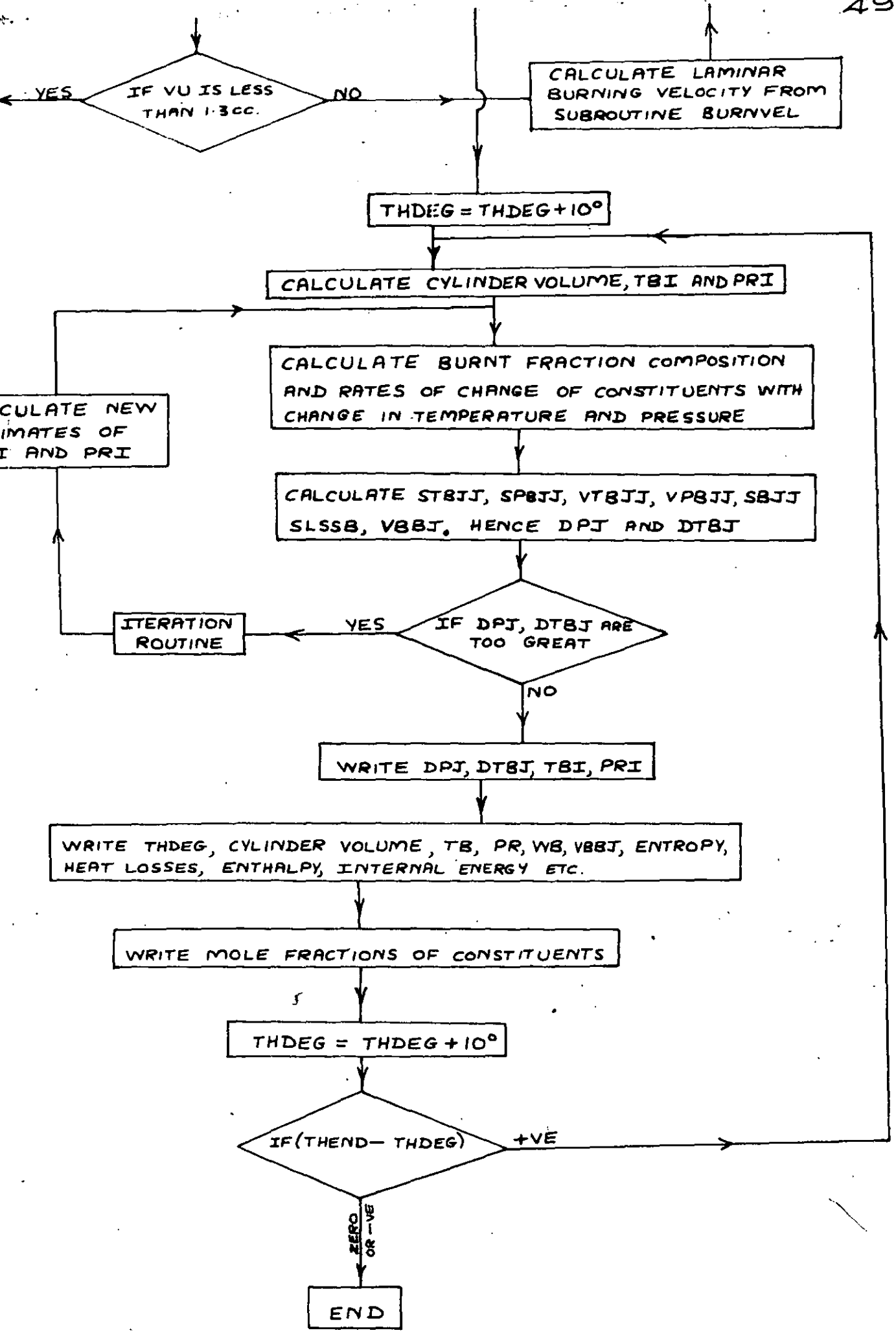
IF VU IS LESS THAN 1·3cc.
YES
NO
CALCULATE LAMINAR BURNING VELOCITY FROM SUBROUTINE BURNVEL
THDEG = THDEG + 10°
CALCULATE CYLINDER VOLUME, TBI AND PRI
CALCULATE BURNT FRACTION COMPOSITION AND RATES OF CHANGE OF CONSTITUENTS WITH CHANGE IN TEMPERATURE AND PRESSURE
CULATE NEW IMATES OF I AND PRI
CALCULATE STBJJ, SPBJJ, VTBJJ, VPBJJ, SBJJ SLSSB, VBBJ. HENCE DPJ AND DTBJ
IF DPJ, DTBJ ARE TOO GREAT
YES
ITERATION ROUTINE
NO
WRITE DPJ, DTBJ, TBI, PRI
WRITE THDEG, CYLINDER VOLUME, TB, PR, WB, VBBJ, ENTROPY, HEAT LOSSES, ENTHALPY, INTERNAL ENERGY ETC.
WRITE MOLE FRACTIONS OF CONSTITUENTS
THDEG = THDEG + 10°
IF(THEND − THDEG)
+VE
ZERO OR −VE
END

```
      MASTERB100
      DIMENSION C(15),XC(15),RC(15),CVU(15),XNT(15),XNP(15),YC(15),BC(15
     1),CVBB(15)
      COMMON /CPDATA/ CPD(14,15),S0(15),HF(15)
      DO 17 J=1,15
   17 READ(1,18)(CPD(I,J),I=1,14)
      DO 373 KLKL=1,3
      READ(1,2)D,JFUEL,WR,PR,T,THETS,THDEG,CR,XN,THEND,TB,WW
      CALL ITIME(I1)
      B=8.0
      XL=10.0
      XXL=18.0
      WRITE(2,9001)(I1)
      WRITE(2,9000)
      WRITE(2,9005)XN
      WRITE(2,9006)
      WRITE(2,9007)
      WRITE(2,9008)CR
      WRITE(2,9009)THETS
      WRITE(2,9010)D
      WRITE(2,9011)WR
      WRITE(2,1758)WW
      WRITE(2,9012)THDEG
      WRITE(2,9013)THEND
      WRITE(2,9014)T
      WRITE(2,9015)PR
      GO TO(3,4,5),JFUEL
    3 AFA=688./(44.097*D)
      STAF=688./44.097
      WMSA=688.*AFA/STAF
      WRITE(2,9002)
      CA=3.
      HY=8.
      GO TO 6
    4 AFA=1718./(114.232*D)
      STAF=1718./114.232
      WMSA=1718.*AFA/STAF
      WRITE(2,9003)
      CA=8.
      HY=18.
      GO TO 6
    5 AFA=1030./(78.114*D)
      STAF=1030./78.114
      WMSA=1030.*AFA/STAF
      WRITE(2,9004)
      CA=6.
      HY=6.
    6 WA=(1.-WR-WW)/(1./AFA)
```

```
      WF=(1.-WR-WW)/(1.+AFA)
      AM=.233*WMSA/32.+.767*WMSA/28.016
      FM=1.
      P=PR/14.7
      TM=1600.
      KJ=0
      DO 555 J=1,15
555   XC(J)=0.0
      CALL DISCN (TM,P,CA,HY,AM,FM,D,C,RWMOL,RHOR,CVMR,GAMR,PR,CTT,XNT,X
     1NP,XNA,XNB,CPMRR,XC,KJ)
      RM=WR*WMSA/(WA*RWMOL)
      WM=WW*WMSA/(WA*18.)
      TMOLES=AM+FM+RM+WM
      DO 11 I=1,15
11    XC(I)=RM*C(I)/CTT
      XC(4)=XC(4)+WM
      WMOLR=(XC(1)*44.011+XC(2)*28.011+XC(3)*28.016+XC(4)*18.016+XC(5)*3
     12.+XC(6)*2.016+XC(7)*30.008+XC(8)*17.008+XC(9)*1.008+XC(10)*16.+XC
     2(11)*46.008+XC(12)*44.016+XC(13)*17.032+XC(14)*31.016+XC(15)*14.00
     38)/TMOLES
      GO TO (12,13,14),JFUEL
12    WMOL=(FM*44.097+AM*28.9)/TMOLES+WMOLR
      GO TO 15
13    WMOL=(FM*114.232+AM*28.9)/TMOLES+WMOLR
      GO TO 15
14    WMOL=(FM*78.114+AM*28.9)/TMOLES+WMOLR
15    F=1.986/WMOL
      VV=1.
      CALL CALCS(T,XC,JFUEL,CPM,CVM,GAM,E,H,FM,AM,VV)
      R=XL/2.
      THETA=THDEG*3.1416/180.
      V1=((3.1416*B**2)/4.)*((2.*R/(CR-1.))+R+XXL-R*COS(THETA)-SQRT(XXL*
     1*2-R**2*SIN(THETA)**2))
      RHO=PR*144.*.01602/(F*1400.*T)
      W=RHO*V1
      WT=W/WMOL
      DO 16 I=1,15
16    RC(I)=XC(I)*WT/TMOLES
      RCF=FM*WT/TMOLES
      RCA=AM*WT/TMOLES
      WRITE (2,7001)RC(3),RC(5),RCA
      IF (WW)9264,9264,0
      T=T-539.3*18.*RC(4)/CPM
      PR=RHO*F*1400.*T/(144.*.01602)
      P=PR/14.7
9264  CONTINUE
      CALL SPECENT(P,RC,T,WT,S,JFUEL,RCF,RCA)
      SUU=S/WMOL
```

```
      WRITE (2,9016)
   42 RHO=PR*144.*.01602/(F*1400.*T)
      S=SUU*WMOL
      WRITE(2,38)THDEG,V1,PR,T
      VV=1.
      CALL CALCS(T,RC,JFUEL,CPM,CVM,GAM,E,H,RCF,RCA,VV)
      IF (THETS-THDEG)19,19,0
      THDEG=THDEG+10.
      IF (THETS-THDEG)140,140,0
      GO TO 141
  140 THDEG=THETS
  141 THETA=THDEG*3.1416/180.
      V2=((3.1416*B**2)/4.)*((2.*R/(CR-1.))+R+XXL-R*COS(THETA)-SQRT(XXL*
     1*2-R**2*SIN(THETA)**2))
      TJ=T*(V1/V2)**(GAM-1.)
      PJ=PR*((V1/V2)**GAM)
C     CALCULATE STUJ,SPUJ,SVU,VTUJ,VPUJ,SLOSS,SUJ,VUJ
  125 CRR=0.0
      DO 120 I=1,15
  120 CRR=CRR+RC(I)*SHCP(I,TJ)
      GO TO (121,122,123),JFUEL
  121 CRM=(RCF*PROPCP(TJ)*44.097+RCA*AIRCP(TJ)*28.9)+CRR
      GO TO 124
  122 CRM=(RCF*CPISO(TJ)*114.232+RCA*AIRCP(TJ)*28.9)+CRR
      GO TO 124
  123 CRM=(RCF*BENCP(TJ)*78.114+RCA*AIRCP(TJ)*28.9)+CRR
  124 STUJ=CRM/(WMOL*WT*TJ)
      P=PJ/14.7
      SPUJ=-(1.986*WT/P)/(WT*WMOL)
      VUJ=F*1400.*TJ/(PJ*144.*.01602)
      VTUJ=VUJ/TJ
      VPUJ=-VUJ/P
      RHO=1./VUJ
      JJJ=-1
      YT=0.
      CALL HTRAN(TJ,RHO,B,XN,R,QLS,QLSB,V2,YT,JJJ)
      SLOSS=(2.*QLS)/(W*(T+TJ))
      CALL SPECENT(P,RC,TJ,WT,SUI,JFUEL,RCF,RCA)
      SUJ=SUI/WMOL
      Z1=STUJ
      Z2=SPUJ
      Z3=RUU+SLOSS-SUJ
      Z4=W*VTUJ
      Z5=W*VPUJ
      Z6=V2-W*VUJ
      XP=(Z6*Z1-Z4*Z3)/(Z5*Z1-Z4*Z2)
      XTU=(Z3-Z2*XP)/Z1
      IF ((ABS(XP).LT.0.0001).AND.(ABS(XTU).LT.0.001)) GO TO 126
```

```
      TJ=TJ+XTU/2.
      PJ=PJ+XP*14.7/2.
      GO TO 125
126   T=TJ
      PR=PJ
      V1=V2
      SUU=SUU+SLOSS
      GO TO 42
C     HEAT SUPPLIED BY SPARK IS ABOUT 20 MILLIJOULES (0.0047769 CALORIES)
C     ASSUMED IGNITION TEMPERATURE IS 950 DEGK
 19   WMOLU=WMOL
      CSP=CPM/WMOLU
      WB=.0047769/(CSP*(950.-T))
      E0=E
      SU0=SUU
      V0=V1
      TU=T
      P=PR/14.7
      WBUW=-1.
      YXZ=0.
      PRJ=PR
      KLM=0
853   WU=W-WB
      UNMOL=WU/WMOLU
      DO 59 J=1,15
59    BC(J)=RC(J)*UNMOL/WT
      BCF=RCF*UNMOL/WT
      BCA=RCA*UNMOL/WT
      PD=0.
      UTD=0.
      BTD=0.
      JT=1
      TBJ=TB
      YYY=0.
      IM=-15
 84   P=PRJ/14.7
      KJ=1
      IF (KLM-4)0,9665,9665
      CALL DISCN(TBJ,P,CA,HY,AM,FM,D,C,WMOLB,RHOB,CVMB,GAMB,PB,CTT,XNT,X
     1NP,XNA,XNB,CPMB,XC,KJ)
      GO TO 9666
665   RHOB=P*WMOLB/(82.0575*TBJ)
666   CONTINUE
      KLM=KLM+1
      BMOL=WB/WMOLB
      VB=WB/RHOB
      VU=V0-VB
      IF (YYY)0,0,95
```

```
      TUJ=TU
   95 DO 58 I=1,15
   58 YC(I)=C(I)*BMOL/CTT
      TO CALCULATE STUJ
      CPR=0.0
      DO 60 I=1,15
   60 CPR=CPR+BC(I)*SHCP(I,TUJ)
      GO TO (61,62,63),JFUEL
   61 CZM=(BCF*PROPCP(TUJ)*44.097+BCA*AIRCP(TUJ)*28.9)+CPR
      GO TO 64
   62 CZM=(BCF*CPISO(TUJ)*114.232+BCA*AIRCP(TUJ)*28.9)+CPR
      GO TO 64
   63 CZM=(BCF*BENCP(TUJ)*78.114+BCA*AIRCP(TUJ)*28.9)+CPR
   64 STUJ=CZM/(WMOLU*UNMOL*TUJ)
      TO CALCULATE SPUJ
      SPUJ=-(1.986*UNMOL/P)/(UNMOL*WMOLU)
      TO CALCULATE ETUJ
      DO 65 J=1,15
   65 CVU(J)=SHCP(J,TUJ)-1.986
      CVA=AIRCP(TUJ)*28.9-1.986
      SHCV=0.0
      DO 66 I=1,15
   66 SHCV=SHCV+BC(I)*CVU(I)
      GO TO (67,68,69),JFUEL
   67 SCV=SHCV+BCF*(PROPCP(TUJ)*44.097-1.986)+BCA*CVA
      GO TO 70
   68 SCV=SHCV+BCF*(CPISO(TUJ)*114.232-1.986)+BCA*CVA
      GO TO 70
   69 SCV=SHCV+BCF*(BENCP(TUJ)*78.114-1.986)+BCA*CVA
   70 ETUJ=SCV/(WMOLU*UNMOL)
      TO CALCULATE ETBJ
      DO 71 J=1,15
   71 CVBB(J)=SHCP(J,TBJ)-1.986
      HCV=0.0
      DO 72 J=1,15
   72 HCV=HCV+YC(J)*CVBB(J)
      ECV=0.0
      DO 73 I=1,15
   73 ECV=ECV+XNT(I)*YC(I)*(TBJ-298.16)*ENERINT(I,TBJ)
      EOV=ECV+XNT(2)*YC(2)*67636.1+XNT(6)*YC(6)*68317.4
      ETBJ=(HCV+EOV)/(BMOL*WMOLB)
      TO CALCULATE EPBJ
      PCV=0.0
      DO 74 J=1,15
   74 PCV=PCV+XNP(J)*YC(J)*ENERINT(J,TBJ)*(TBJ-298.16)
      POV=PCV+XNP(2)*YC(2)*67636.1+XNP(6)*YC(6)*68317.4
      EPBJ=POV/(BMOL*WMOLB)
      TO CALCULATE VTUJ
```

```
      VUJ=P*TUJ*1400./(PRJ*144.*.01602)
      VTUJ=VUJ/TUJ
C     TO CALCULATE VTBJ
      VBJ=PB*TBJ*1400./(PRJ*144.*.01602)
      VTBJ=(1+TBJ*XNA/BMOL)*VBJ/TBJ
C     TO CALCULATE VPUJ AND VPBJ
      VPUJ=-VUJ/P
      VPBJ=(VBJ/P)*(P*XNB/BMOL-1.)
      CALL SPECENT(P,BC,TUJ,UNMOL,SUJ,JFUEL,BCF,BCA)
      SUJ=SUJ/WMOLU
C     TO CALCULATE EUJ
      EJ=0.0
      DO 76 J=1,15
   76 EJ=EJ+BC(J)*ENERINT(J,TUJ)*(TUJ-298.16)
      EJT=EJ+BC(2)*67636.1+BC(6)*68317.4
      GO TO (77,78,79),JFUEL
   77 ET=(BCF*CVFIN(TUJ)*(TUJ-298.16)+BCF*488500.)+(BCA*CVAIN(TUJ)*(TUJ-
     1298.16))+EJT
      GO TO 80
   78 ET=(BCF*CVFIN(TUJ)*(TUJ-298.16)+BCF*1.2220*10.0**6.0)+(BCA*CVAIN(T
     1UJ)*(TUJ-298.16))+EJT
      GO TO 80
   79 ET=(BCF*CVBIN(TUJ)*(TUJ-298.16)+BCF*752000.0)+(BCA*CVAIN(TUJ)*(TUJ
     1-298.16))+EJT
   80 EUJ=ET/(WMOLU*UNMOL)
C     TO CALCULATE EBJ
      EJJ=0.0
      DO 82 J=1,15
   82 EJJ=EJJ+YC(J)*ENERINT(J,TBJ)*(TBJ-298.16)
      ETJ=EJJ+YC(2)*67636.1+YC(6)*68317.4
      EBJ=ETJ/(WMOLB*BMOL)
      X1=STUJ
      X3=SPUJ
      X4=SUO-SUJ
      X5=WU*ETUJ
      X6=WB*ETBJ
      X7=WB*EPBJ
      X8=EO-WU*EUJ-WB*EBJ
      X9=WU*VTUJ
      X10=WB*VTBJ
      X11=WU*VPUJ+WB*VPBJ
      X12=VO-WU*VUJ-WB*VBJ
      DP=(X6*X9*X4-X10*X5*X4+X1*X8*X10-X1*X6*X12)/(X1*X10*X7-X11*X1*X6-X
     15*X3*X10+X6*X9*X3)
      DTU=(X4-X3*DP)/X1
      DTB=(X12-X11*DP-X9*DTU)/X10
      TUJ=TUJ+DTU/2.
      TBJ=TBJ+DTB/2.
```

```
      PRJ=PRJ+DP*44.7/2.
      WRITE (2,997)DP,DTU,DTB,TUJ,TBJ,PRJ
      IF ((ABS(DP).LT.0.0015).AND.(ABS(DTU).LT.0.003).AND.(ABS(DTB).LT.0
     1.006)) GO TO 83
      XPDX=PD-DP
      XUTDX=UTD-DTU
      XBTDX=BTD-DTB
      PD=DP
      UTD=DTU
      BTD=DTB
      YYY=YYY+1
      IF ((ABS(XPDX).LT.0.001).AND.(ABS(XUTDX).LT.0.001).AND.(ABS(XBTDX)
     1.LT.0.001)) GO TO 3636
      IF (IM-255)0,83,83
      IF (IM-240)0,4883,0
      IF (IM-225)0,2514,0
      IF (IM-210)0,2514,0
      IF (IM-195)0,2514,0
      IF (IM-180)0,2514,0
      IF (IM-165)0,2514,0
      IF (IM-150)0,2514,0
      IF (IM-135)0,2514,0
      IF (IM-120)0,2514,0
      IF (IM-105)0,2514,0
      IF (IM-90)0,4195,0
      IF (IM-75)0,8686,0
      IF (IM-60)0,8640,0
      IF (IM-45)0,8430,0
      IF (IM-30)0,5050,0
      IF (IM-15)0,145,0
      GO TO 3638
3636  GO TO (145,5050,8430,8640,8686,4195,2514,4883,83),JT
3638  IM=IM+1
      GO TO 84
145   CONTINUE
      IF (WB-.04)2951,0,0
      PRJ=PRJ+5.*DP*14.7
      TUJ=TUJ+20.*DTU
      TBJ=TBJ+50.*DTB
      GO TO 2952
2951  TBJ=TBJ+75.*DTB
2952  CONTINUE
      IM=16
      JT=2
      KLM=0
      GO TO 84
5050  CONTINUE
      IF (WB-.04)2953,0,0
```

```
      TUJ=TUJ+20.*DTU
      TBJ=TBJ+45.*DTB
      PRJ=PRJ+5.*DP**14.7
      GO TO 2954
953   TBJ=TBJ+60.*DTB
954   CONTINUE
      JT=3
      IM=31
      KLM=0
      GO TO 84
430   CONTINUE
      IF (WB=.04)2111,0,0
      PRJ=PRJ+5.*DP**14.7
      TUJ=TUJ+20.*DTU
      TBJ=TBJ+40.*DTB
      GO TO 2112
111   TBJ=TBJ+50.*DTB
112   CONTINUE
      JT=4
      IM=46
      KLM=0
      GO TO 84
640   CONTINUE
      IF (WB=.04)2113,0,0
      TUJ=TUJ+20.*DTU
      TBJ=TBJ+20.*DTB
      PRJ=PRJ+5.*DP**14.7
      GO TO 2114
113   TBJ=TBJ+30.*DTB
114   CONTINUE
      JT=5
      IM=61
      KLM=0
      GO TO 84
686   CONTINUE
      IF (WB=.04)2116,0,0
      TUJ=TUJ+20.*DTU
      TBJ=TBJ+20.*DTB
      PRJ=PRJ+5.*DP**14.7
      GO TO 2117
116   TBJ=TBJ+20.*DTB
117   CONTINUE
      JT=6
      IM=76
      KLM=0
      GO TO 84
195   CONTINUE
      IF (WB=.04)2118,0,0
```

```
      TUJ=TUJ+20.*DTU
      TBJ=TBJ+20.*DTB
      PRJ=PRJ+5.*DP*14.7
      GO TO 2119
118   TBJ=TBJ+20.*DTB
119   CONTINUE
      JT=7
      IM=91
      MI=91
      KLM=0
      GO TO 84
514   CONTINUE
      TUJ=TUJ+20.*DTU
      TBJ=TBJ+20.*DTB
      PRJ=PRJ+5.*DP*14.7
      JT=7
      MI=MI+15
      IM=MI
      IF (IM-226)967,0,0
      JT=8
967   KLM=0
      GO TO 84
883   CONTINUE
      TBJ=TBJ+5.*DTB
      TUJ=TUJ+5.*DTU
      PRJ=PRJ+2.*DP*14.7
      JT=9
      IM=241
      KLM=0
      GO TO 84
 83   WRITE (2,997)DP,DTU,DTB,X4,X8,X12
      IF (WB-.08)0,0,429
      IF (YXZ)0,0,3621
      IF (ABS(X12).LT.0.003) GO TO 429
      IF (X12-.003)428,429,3622
3621  IF (ABS(X12).LT.0.035) GO TO 429
      IF (X12-0.035)428,429,3622
3622  IF (YXZ)0,0,3623
      TBJ=TBJ+5.
      GO TO 3624
3623  TBJ=TBJ+0.6
3624  CONTINUE
      KLM=0
      PD=0.
      UTD=0.
      BTD=0.
      JT=1
      IM=-15
```

```
      GO TO 84
428   IF (YX2)0,0,3625
      TBJ=TBJ-5.
      GO TO 3626
625   TBJ=TBJ-0.4
626   CONTINUE
      KLM=0
      PD=0.
      UTD=0.
      BTD=0.
      JT=1
      IM=-15
      GO TO 84
429   CONTINUE
      CALL SPECENT(P,YC,TBJ,BMOL,SBT,JFUEL,0.,0.)
      SB1=SBT/WMOLB
      THDEG=THDEG+2.
      THETA=THDEG*3.1416/180.
      V2=((3.1416*B**2)/4.)*((2.*R/(CR-1.))+R+XXL-R*COS(THETA)-SQRT(XXL*
     1*2-R**2*SIN(THETA)**2))
      VBV=WB*VBJ
      CALL FLAMDIST(THDEG,V2,VBV,SXD)
      TB1=TBJ
      SU1=SU0
      TU1=TUJ
      TUK=TU1*((V0/V2)**(GAMU-1.))
      IF (WB-.015)0,0,7631
      TBK=TB1
      GO TO 7632
7631  TBK=TB1*((V0/V2)**(GAMB-1.))+(QLSB*WMOLB)/(WB*CPMB)
7632  CONTINUE
      PRK=PRJ*V0*TBK/(TB1*V2)
      RHOB=PRK*144.*.01602/(FB*TBK*1400.)
      JJJ=0
      CALL HTRAN(TBK,RHOB,B,XN,R,QLS,QLSB,V2,SXD,JJJ)
      IF (WB-.015)7633,0,0
      TBK=TB1*((V0/V2)**(GAMB-1.))+(QLSB*WMOLB)/(WB*CPMB)
7633  CONTINUE
      PRK=PRJ*V0*TBK/(TB1*V2)
      III=0
      KLL=0
      KTV=0
      PS=0.
      UTS=0.
      BTS=0.
995   P=PRK/14.7
      KJ=1
      IF (KLL-2)0,8192,8192
```

```
      CALL DISCN(TBK,P,CA,HY,AM,FM,D,C,WMOLB,RHOB,CVMB,GAMB,PB,CTT,XNT,X
     1NP,XNA,XNB,CPMB,XC,KJ)
      GO TO 8193
192   RHOB=P*WMOLB/(82.0575*TBK)
193   CONTINUE
      KLL=KLL+1
      BMOL=WB/WMOLB
      DO 85 I=1,15
 85   YC(I)=C(I)*BMOL/CTT
C     TO CALCULATE STUJ
      CPS=0.0
      DO 86 I=1,15
 86   CPS=CPS+BC(I)*SHCP(I,TUK)
      GO TO (87,88,89),JFUEL
 87   CPQ=(BCF*PROPCP(TUK)*44.097+BCA*AIRCP(TUK)*28.9)+CPS
      GO TO 90
 88   CPQ=(BCF*CPISO(TUK)*114.232+BCA*AIRCP(TUK)*28.9)+CPS
      GO TO 90
 89   CPQ=(BCF*BENCP(TUK)*78.114+BCA*AIRCP(TUK)*28.9)+CPS
 90   STUJ=CPQ/(WMOLU*UNMOL*TUK)
C     TO CALCULATE SPUJ
      SPUJ=-(1.986*UNMOL/P)/(UNMOL*WMOLU)
C     TO CALCULATE STBJ
      CPL=0.0
      DO 91 I=1,15
 91   CPL=CPL+YC(I)*SHCP(I,TBK)
      SKNTK=0.0
      DO 92 J=1,15
 92   SKNTK=SKNTK+XNT(J)*ENTRPY(J,TBK)
      STBJ=(CPL/TBK+SKNTK)/(WMOLB*BMOL)
C     TO CALCULATE SPBJ
      SKNPK=0.0
      DO 93 I=1,15
 93   SKNPK=SKNPK+XNP(I)*ENTRPY(I,TBK)
      SPBJ=(SKNPK-1.986*BMOL/P)/(WMOLB*BMOL)
C     TO CALCULATE VTUJ,VTBJ,VPUJ,VPBJ
      VUJ=F*TUK*1400./(PRK*144.*.01602)
      VTUJ=VUJ/TUK
      VBJ=FB*TBK*1400./(PRK*144.*.01602)
      VTBJ=(1+TBK*XNA/BMOL)*VBJ/TBK
      VPUJ=-VUJ/P
      VPBJ=(VBJ/P)*(P*XNB/BMOL-1.)
C     TO CALCULATE SUJ
      CALL SPECENT(P,BC,TUK,UNMOL,SOK,JFUEL,BCF,BCA)
      SUJ=SOK/WMOLU
C     TO CALCULATE SLOSSU
      RHOU=1./VUJ
      SLOSSU=0.
```

```
TO CALCULATE SLOSSB
   CALL HTRAN(TBK,RHOB,R,XN,R,QLS,QLSB,V2,SXD,JJJ)
   SLOSSB=(2.*QLSB)/(WB*(TB1+TBK))
TO CALCULATE SBJ
   CALL SPECENT(P,YC,TBK,BMOL,SOL,JFUEL,0.,0.)
   SBJ=SOL/WMOLB
   Y1=STUJ
   Y2=SPUJ
   Y3=SU1+SLOSSU-SUJ
   Y4=STBJ
   Y5=SPBJ
   Y6=SB1+SLOSSB-SBJ
   Y7=WU*VTUJ
   Y8=WB*VTBJ
   Y9=WU*VPUJ+WB*VPBJ
   Y10=V2-WU*VUJ-WB*VBJ
   SP=(Y4*Y1*Y10-Y1*Y8*Y6-Y4*Y7*Y3)/(Y9*Y4*Y1-Y8*Y5*Y1-Y7*Y2*Y4)
   STU=(Y3-Y2*SP)/Y1
   STB=(Y6-Y5*SP)/Y4
   XPS=PS-SP
   XUTS=UTS-STU
   XBTS=BTS-STB
   PS=SP
   UTS=STU
   BTS=STB
   TUK=TUK+STU/2.
   TBK=TBK+STB
   PRK=PRK+SP*14.7
   IF ((ABS(SP).LT.0.001).AND.(ABS(STU).LT.0.003).AND.(ABS(STB).LT.0.
  1003)) GO TO 94
   IF ((ABS(XPS).LT.0.001).AND.(ABS(XUTS).LT.0.001).AND.(ABS(XBTS).LT
  1.0.001)) GO TO 529
   IF (IIII-15)0,146,0
   IIII=IIII+1
   GO TO 995
146 CONTINUE
   IF (KTV-15)0,0,94
   PRK=PRK+5.*SP*14.7
   TUK=TUK+10.*STU
   TBK=TBK+20.*STB
   IIII=0
   KLL=0
   KTV=KTV+1
   GO TO 995
529 IF (KTV-15)0,0,94
   KTV=KTV+1
   IIII=0
   KLL=0
```

```
      PRK=PRK+5.*SP*14.7
      TUK=TUK+5.*STU
      TBK=TBK+80.*STB
      GO TO 995
   94 WRITE (2,997)SP,STU,STB,V3,Y6,Y10
      WRITE (2,997)SP,STU,STB,TUK,TBK,PRK
      TU=TUK
      TB=TBK
      PR=PRK
      V0=V2
      VB=VBJ*WB
      VU=V0-VB
      VU1=VU
      VUD=VUJ*WU
      TIME=1./(3.*XN)
      CALL FLAMDIST(THDEG,V0,VB,DDS)
      IF (YXZ)0,0,681
      FS=DDS/TIME
      GO TO 682
  681 FS=(DDS-AB)/TIME
  682 KLM=0
      SU2=SU1+SLOSSU
      SU0=SU2
      AB=DDS
      IF (YXZ)375,375,0
      PRV=2.*PRJ-PRY
      GO TO 376
  375 PRV=PRJ+1.
  376 CONTINUE
      YXZ=1.
      WRITE(2,100)
      WRITE (2,99)THDEG,V2,TU,TB,PR,WB,WU,VU,VB,VUJ,VBJ,VUD
      VV=1.
      CALL CALCS(TU,BC,JFUEL,CPMU,CVMU,GAMU,EU,HU,BCP,BCA,VV)
      CALL CALCS(TB,YC,JFUEL,CPMB,CVMB,GAMB,EB,HB,0.,0.,0.)
      E0=EU+EB
      H=HU+HB
      WRITE (2,9021)
      WRITE (2,9020)SU2,SB1,QLSB,HU,HB,H,EU,EB,E0,GAMU,GAMB
      DO 936 I=1,15
      C(I)=C(I)/CTT
  936 WRITE (2,9036)I,C(I)
      WRITE (2,7001)YC(7),BMOL,UNMOL
      IF (WBWW)0,0,829
      IF (VUD-1.3)0,0,683
      WB=W-.0001
      WBWW=1.
      GO TO 853
```

```
 683 CALL BURNVEL(TU,TB,PR,D,JFUEL,UF)
     UT=UF*(1.+.00197*XN)
     IF (DDS-0.35)7070,0,0
     VS=UT/(3.*XN)
     GO TO 7071
7070 VS=UF/(3.*XN)
7071 DS=DDS+VS
     WRITE (2,9023)
     WRITE (2,9024)UF,UT,FS,VS
     CALL BURNTVOL(V0,DS,VOL,THDEG)
     DVOL=VOL-VB
     WB1=WB+DVOL*RHOU
     PRV=PRJ
     PRJ=PRV
     IF (W-WB1)829,829,0
     IF (WB1-.025)721,0,0
     TB=((TB-TJ+TU)*DVOL*RHOU+WB*TB)/WB1
 721 CONTINUE
     WB=WB1
     GO TO 853
 829 TU=0.
     WU=0.
     VU=0.
     VUJ=0.
     VUD=0.
     GAMU=0.
     EU=0.
     SU2=0.
     HU=0.
     IIX=0
     PRV=0.
     P=PR/14.7
     THDEG=THDEG+10.
C    TO CALCULATE SB1
 726 CALL SPECENT(P,YC,TB,BMOL,SVV,JFUEL,0.,0.)
     SB1=SVV/WMOLB
     IX=0
     THETA=THDEG*3.1416/180.
     V2=((3.1416*B**2)/4.)*((2.*R/(CR-1.))+R*XXL-R*COS(THETA)-SQRT(XXL*
    1*2-R**2*SIN(THETA)**2))
     TBI=((V0/V2)**(GAMB-1.))*TB+(QLSB*WMOLB)/(WB*CPMB)
     PRI=PR*V0*TBI/(TB*V2)
 731 P=PRI/14.7
     KJ=1
     IF (IX-2)0,0,6183
     CALL DISCN(TBI,P,CA,HV,AM,FM,D,C,WMOLB,RHOB,CVMB,GAMB,FB,CTT,XNT,X
    1NP,XNA,XNB,CPMB,XC,KJ)
6183 CONTINUE
```

```
      BMOL=WB/WMOLB
      DO 740 I=1,15
740   YC(I)=C(I)*BMOL/CTT
C     TO CALCULATE STBJJ
      CYL=0.0
      DO 741 I=1,15
741   CYL=CYL+YC(I)*SHCP(I,TBI)
      SNTK=0.0
      DO 742 J=1,15
742   SNTK=SNTK+XNT(J)*ENTRPY(J,TBI)
      STBJJ=(CYL/TBI-SNTK)/(WMOLB*BMOL)
C     TO CALCULATE SPBJJ
      SNPK=0.0
      DO 743 I=1,15
743   SNPK=SNPK+XNP(I)*ENTRPY(I,TBI)
      SPBJJ=(SNPK-1.986*BMOL/P)/(WMOLB*BMOL)
C     TO CALCULATE VTBJJ,VPBJJ
      VBBJ=FB*TBI*1400./(PRI*144.*.01602)
      VTBJJ=(1.+TBI*XNA/BMOL)*VBBJ/TBI
      VPBJJ=(VBBJ/P)*(P*XNB/BMOL-1.)
C     TO CALCULATE SBJJ
      CALL SPECENT(P,YC,TBI,BMOL,SVY,JFUEL,0.,0.)
      SBJJ=SVY/WMOLB
C     TO CALCULATE SLSSB
      RHOB=1./VBBJ
      JJJ=1
      YW=0.
      CALL HTRAN(TBI,RHOB,B,XN,R,QLS,QLSB,V2,YW,JJJ)
      SLSSB=(2.*QLSB)/(WB*(TB+TBI))
      G1=STBJJ
      G2=SPBJJ
      G3=SB1+SLSSB-SBJJ
      G4=WB*VTBJJ
      G5=WB*VPBJJ
      G6=V2-WB*VBBJ
      DPJ=(G6*G1-G4*G3)/(G5*G1-G4*G2)
      DTBJ=(G3-G2*DPJ)/G1
      TBI=TBI+DTBJ
      PRI=PRI+DPJ*14.7
      IF ((ABS(DPJ).LT.0.001).AND.(ABS(DTBJ).LT.0.003)) GO TO 730
      IF (IX-10)0,0,535
      IX=IX+1
      GO TO 731
535   CONTINUE
      IF (IIX-20)0,0,730
      PRI=PRI+5.*DPJ*14.7
      TBI=TBI+50.*DTBJ
      IX=0
```

```
      IIX=IIX+1
      GO TO 731
730   CONTINUE
      WRITE (2,997)DPJ,DTBJ,TBI,PRI,G3,G6
      PR=PRI
      TB=TBI
      IIX=0
      CALL CALCS(TB,YC,JFUEL,CPMB,CVMB,GAMB,EB,HB,0.,0.,0.)
      WRITE (2,100)
      WRITE (2,99)THDEG,V2,TU,TB,PR,WB,WU,VU,V2,VUJ,VBBJ,VUD
      WRITE (2,9021)
      WRITE (2,9020)SU2,SBJJ,QLSB,HU,HB,HB,EU,EB,EB,GAMU,GAMB
      THDEG=THDEG+10.
      DO 9035 I=1,15
      C(I)=C(I)/CTT
9035  WRITE (2,9036)I,C(I)
      IF (THEND-THDEG)725,0,0
      P=PR/14.7
      V0=V2
      GO TO 726
725   CALL ITIME(I2)
      WRITE (2,9001)(I2)
373   CONTINUE
100   FORMAT(117H CRANK  CYL.VOL UNBURNT GAS  BURNT GAS      PRESS    MASS
     1 BURNT  MASS UNBURNT  UNBURNT  BURNT VOL  VUJ        VBJ     VUD/118
     2H ANGLE   (CCS)   TEMP(DEGK)   TEMP(DEGK)   (PSI)      (GMS)
     3 (GMS)      VOL(CC)     (CCS)    (CC/GM)  (CC/GM)   (CC))
99    FORMAT(F6.1,F8.2,F11.2,F11.1,F12.1,2F11.5,F14.2,F10.2,2F9.2,F7.1/)
9021  FORMAT(109H UNB.SPEC.  BURNT.SPEC.   HEAT    UNBURNT  BURNT    TO
     1TAL    UNBURNT    BURNT    TOTAL    UNBURNT     BURNT/113H ENTROP
     2Y     ENTROPY    TRANSFER  ENTHALPY  ENTHALPY ENTHALPY INT.ENER.
     3INT.ENER. INT.ENER. GAS CONST  GAS CONST/110H (CAL/DEGK)  (CAL/DEG
     4K)   (CALS)     (CALS)    (CALS)    (CALS)     (CALS)     (C
     5ALS)     (CAL/MOLE DEGK))
9020  FORMAT(F7.2,F13.2,3F11.3,2F9.3,2F10.3,2F10.5/)
9023  FORMAT(56H LAM.BURNING  TURB.BURN.        FLAME          FLAME TRAVEL
     1/57H VEL(CM/SEC)  VEL(CM/SEC)    SPEED(CM/SEC)     INCREASE(CM))
9024  FORMAT(F9.2,F13.2,F14.2,F16.4/)
9036  FORMAT(12H CONSTITUENTI4,17H   MOLE FRACTION=F18.12//)
 18   FORMAT(11X,E13.8,7X,E13.8,7X,E13.8)
  2   FORMAT(F0.0,I0,10F0.0)
9000  FORMAT(30X50H COMPUTER SIMULATION OF COMBUSTION IN A S.I.ENGINE//)
9001  FORMAT(I8)
9002  FORMAT(16H FUEL IS PROPANE//)
9003  FORMAT(19H FUEL IS ISO-OCTANE//)
9004  FORMAT(16H FUEL IS BENZENE//)
9005  FORMAT(24H ENGINE SPEED(REV/MIN) =F7.1/)
9006  FORMAT(14H BORE = 8.0CMS/)
```

```
9007 FORMAT(17H STROKE = 10.0CMS/)
9008 FORMAT(20H COMPRESSION RATIO =F6.2/)
9009 FORMAT(18H IGNITION TIMING =F6.1/)
9010 FORMAT(20H EQUIVALENCE RATIO =F5.2/)
9011 FORMAT(55H MASS FRACTION OF EXHAUST RESIDUAL IN UNBURNT MIXTURE =F
   15.2/)
9012 FORMAT(28H INLET VALUE CLOSING ANGLE =F6.1/)
9013 FORMAT(30H EXHAUST VALVE OPENING ANGLE =F6.1/)
9014 FORMAT(46H TEMP OF CHARGE AT INLET VALVE CLOSURE(DEGK) =F6.1/)
9015 FORMAT(36H PRESS. AT INLET VALVE CLOSURE(PSI)=F5.1/)
9016 FORMAT(30H CRANK CYL.VOL PRESS TEMP/32H ANGLE (CCS) (PSI
   1) (DEG K))
 38 FORMAT(4F8.2)
 997 FORMAT(6F12.3)
7001 FORMAT(3F25.20)
1758 FORMAT(53H MASS FRACTION OF INJECTED WATER IN UNBURNT MIXTURE =F5.
   12/)
     END

ENGTH 4075, NAME B100
```

```
      SUBROUTINE SPECENT(P,RC,T,WT,S,JFUEL,RCF,RCA)
      DIMENSION RC(15)
      SR=0.0
      DO 37 J=1,15
   37 SR=SR+(RC(J)*(ENTRPY(J,T)-1.986*ALOG(RC(J))))
      ST=SR+1.986*WT*ALOG(WT/P)
      U=.29815
      CA0=6.12689+U*(1.29054-0.33474*U+0.05419*U**2-0.004889*U**3+0.0001
     1877*U**4)
      U=.001*T
      CA1=6.12689+U*(1.29054-0.33474*U+0.05419*U**2-0.004889*U**3+0.0001
     1877*U**4)
      GO TO (38,39,40),JFUEL
   38 U=.29815
      CP0=(0.45596-U*(1.52545-5.7083*U+8.5878*U**2-7.0929*U**3+3.1032*U*
     1*4-0.56083*U**5))*44.097
      U=.001*T
      CP1=(0.45596-U*(1.52545-5.7083*U+8.5878*U**2-7.0929*U**3+3.1032*U*
     1*4-0.56083*U**5))*44.097
      IF (RCF)0,12,0
      SS=ST+(RCF*(CP1*ALOG(T)-CP0*ALOG(298.15)+64.51-1.986*ALOG(RCF)))+(
     1RCA*(CA1*ALOG(T)-CA0*ALOG(298.15)+47.4906-1.986*ALOG(RCA)))
      GO TO 13
   12 SS=ST
   13 S=SS/WT
      GO TO 41
   39 U=.29815
      CP0=2.547736+U*(76.81795-4.44605*U-23.44267*U**2+14.19583*U**3-2.7
     1149323*U**4)
      U=.001*T
      CP1=2.547736+U*(76.81795-4.44605*U-23.44267*U**2+14.19583*U**3-2.7
     1149323*U**4)
      IF (RCF)0,15,0
      SS=ST+(RCF*(CP1*ALOG(T)-CP0*ALOG(298.15)+101.15-1.986*ALOG(RCF)))+
     1(RCA*(CA1*ALOG(T)-CA0*ALOG(298.15)+47.4906-1.986*ALOG(RCA)))
      GO TO 16
   15 SS=ST
   16 S=SS/WT
      GO TO 41
   40 U=.29815
      CP0=-10.6247+U*(62.9086-29.90944*U+5.00834*U**2+1.70782*U**3-0.645
     112*U**4)
      U=.001*T
      CP1=-10.6247+U*(62.9086-29.90944*U+5.00834*U**2+1.70782*U**3-0.645
     112*U**4)
      IF (RCF)0,18,0
      SS=ST+(RCF*(CP1*ALOG(T)-CP0*ALOG(298.15)+64.34-1.986*ALOG(RCF)))+(
     1RCA*(CA1*ALOG(T)-CA0*ALOG(298.15)+47.4906-1.986*ALOG(RCA)))
```

```
      GO TO 19
   18 SS=ST
   19 S=SS/WT
   41 RETURN
      END

ENGTH   517, NAME -- SPECENT
```

```
      SUBROUTINE CALCS(T,RC,JFUEL,CPM,CVM,GAM,E,H,RCP,RCA,VV)
      DIMENSION RC(15)
      COMMON /CPDATA/ CPD(14,15),SO(15),HF(15)
      CPR=0.0
      DO 21 I=1,15
   21 CPR=CPR+RC(I)*SHCP(I,T)
      GO TO (22,23,24),JFUEL
   22 CPM=(RCF*PROPCP(T)*44.097+RCA*AIRCP(T)*28.9)+CPR
      GO TO 25
   23 CPM=(RCF*CPISO(T)*114.232+RCA*AIRCP(T)*28.9)+CPR
      GO TO 25
   24 CPM=(RCF*BENCP(T)*78.114+RCA*AIRCP(T)*28.9)+CPR
   25 CONTINUE
      WT=RCF+RCA+RC(1)+RC(2)+RC(3)+RC(4)+RC(5)+RC(6)+RC(7)+RC(8)+RC(9)+R
     1C(10)+RC(11)+RC(12)+RC(13)+RC(14)+RC(15)
      CPM=CPM/WT
      CVM=CPM-1.986
      GAM=CPM/CVM
      YX=(T-298.16)
      ER=0.0
      DO 27 I=1,15
   27 ER=ER+RC(I)*ENERINT(I,T)*YX
      ERR=ER+RC(2)*67636.1+RC(6)*68317.4
      GO TO (28,29,30),JFUEL
   28 E=(RCF*CVPIN(T)*YX+RCF*488500.)+(RCA*CVAIN(T)*YX)+ERR
      GO TO 31
   29 E=(RCF*CVIIN(T)*YX+RCF*1.2220*10.0**6.0)+(RCA*CVAIN(T)*YX)+ERR
      GO TO 31
   30 E=(RCF*CVBIN(T)*YX+RCF*752000.0)+(RCA*CVAIN(T)*YX)+ERR
   31 HR=0.
      DO 32 I=1,15
      IF (VV)60,60,0
      HR=HR+(RC(I)*ENTHAL(I,T))
      GO TO 32
   60 HR=HR+(RC(I)*(HF(I)+ENTHAL(I,T)))
   32 CONTINUE
      GO TO (33,34,35),JFUEL
   33 H=(RCF*CPPIN(T)*YX+RCA*CPAIN(T)*YX)+HR
      GO TO 36
   34 H=(RCF*CPIIN(T)*YX+RCA*CPAIN(T)*YX)+HR
      GO TO 36
   35 H=(RCF*CPBIN(T)*YX+RCA*CPAIN(T)*YX)+HR
   36 RETURN
      END

ENGTH   435, NAME - CALCS
```

```
      SUBROUTINE DISCN(T,P,CA,HY,AM,PM,D,CZZ,WMOL,DENS,CV,GAM,R,CZV,XNT,
     1XNP,XNA,XNB,CP,XC,KJ)
      DIMENSION EF(15),P(11),EC(11),Q(4),C(15),CLP(4),CM(15),XC(15),XNT(
     115),XNP(15),CB(15),CD(15),CZZ(15),CY(4),CW(4)
      COMMON /CPDATA/ CPD(14,15),SO(15),HF(15)
C     1    2    3    4    5    6    7    8    9   10   11   12   13   14   15
C   CO2   GO   N2  H2O   O2   H2   NO   OH    H    O  NO2  N2O  NH3  HNO    N
C                       1    2    3    4    5    6    7    8    9   10   11
      IJ=0
      II=0
      JJ=-500
      TTT=T
      IF (T-1600.)0,940,940
      T=1600.
  940 DO 36 J=1,15
      EF(J)=(HF(J)+ENTHAL(J,T)-T*ENTRPY(J,T))
   36 CONTINUE
      IF (D-1.)941,941,0
      P(1)=2.*(EF(1))-2.*(EF(2))-(EF(5))
      P(2)=(EF(4)+EF(2)-EF(1)-EF(6))
      P(3)=0.5*(EF(3))+EF(1)-EF(2)-EF(7)
      P(4)=0.5*EF(4)+0.5*EF(1)-0.5*EF(2)-EF(8)
      P(5)=0.5*EF(4)+0.5*EF(2)-0.5*EF(1)-EF(9)
      P(6)=EF(1)-EF(2)-EF(10)
      P(7)=0.5*EF(3)+2.0*EF(1)-2.0*EF(2)-EF(11)
      P(8)=EF(3)+EF(1)-EF(2)-EF(12)
      P(9)=0.5*EF(3)+1.5*EF(4)+1.5*EF(2)-1.5*EF(1)-EF(13)
      P(10)=0.5*EF(4)+0.5*EF(3)+0.5*EF(1)-0.5*EF(2)-EF(14)
      P(11)=0.5*EF(3)-EF(15)
      GO TO 555
  941 P(1)=EF(1)-0.5*EF(5)-EF(2)
      P(2)=EF(4)-0.5*EF(5)-EF(6)
      P(3)=0.5*EF(3)+0.5*EF(5)-EF(7)
      P(4)=0.5*EF(4)+0.25*EF(5)-EF(8)
      P(5)=0.5*EF(4)-0.25*EF(5)-EF(9)
      P(6)=0.5*EF(5)-EF(10)
      P(7)=0.5*EF(3)+EF(5)-EF(11)
      P(8)=EF(3)+0.5*EF(5)-EF(12)
      P(9)=0.5*EF(3)+1.5*EF(4)-0.75*EF(5)-EF(13)
      P(10)=0.5*EF(4)+0.5*EF(3)+0.25*EF(5)-EF(14)
      P(11)=0.5*EF(3)-EF(15)
  555 DO 34 I=1,11
   34 EC(I)=EXP(P(I)/(1.986*T))
      IF (IJ)32,0,32
      IF (D-1.)0,0,28
      Q(2)=.21*AM-CA-HY/4.
      Q(1)=CA
      Q(3)=.79*AM
```

```
      Q(4)=HV/2.
      C(2)=Q(2)
      C(1)=Q(1)
      GO TO 1060
   28 Q(1)=(0.42*AM-HV/2.-CA)
      Q(2)=CA-Q(1)
      Q(3)=0.79*AM
      Q(4)=HV/2.
      R2=(0.43*T/(10.0**4)-.0835)
      R3=(0.252*T/(10.0**4)-.0041)
      IF (T-2780.)0,0,624
      R5=(0.457*T/(10.0**4)-.088)
      GO TO 625
  624 R5=(0.73*T/(10.0**4)-.164)
  625 R6=(0.415*T/(10.0**4)-.0382)
      R9=R2+(R3-R2)*(D-1.)/0.2
      R10=R5+(R6-R5)*(D-1.)/0.2
      IF (P-10.)0,0,628
      C(2)=R10
      GO TO 635
  628 C(2)=R9+(R10-R9)*(100.-P)/90.
  635 C(2)=C(2)*(AM+FM)
      IF (C(2)-0.3)0,0,502
      C(2)=0.6
  502 C(1)=CA-C(2)
      GO TO 1788
 1060 IF (C(2)-0.1)0,0,1788
      C(2)=0.2
 1788 DO 484 J=5,15
  484 C(J)=0.
      C(3)=0.79*AM
      C(4)=HV/2.
   32 CT=C(1)+C(2)+C(3)+C(4)+C(5)+C(6)+C(7)+C(8)+C(9)+C(10)+C(11)+C(12)+
     1C(13)+C(14)+C(15)
      DO 3 I=1,4
      CW(I)=C(I)/CT
    3 CLP(I)=C(I)
      IF (D-1.)1070,1070,0
      C(5)=EC(1)*CT/P*(C(1)**2)/(C(2)*C(2))
      C(6)=EC(2)*C(2)*C(4)/C(1)
      C(7)=EC(3)*SQRT((CT/P)*C(3))*C(1)/C(2)
      C(8)=EC(4)*SQRT((CT/P)*C(1)*C(4)/C(2))
      C(9)=EC(5)*SQRT((CT/P)*C(2)*C(4)/C(1))
      C(10)=EC(6)*(CT/P)*C(1)/C(2)
      C(11)=EC(7)*SQRT((CT/P)*C(3))*C(1)*C(1)/(C(2)*C(2))
      C(12)=EC(8)*C(1)*C(3)/C(2)
      C(13)=EC(9)*(P/CT)*(C(2)**1.5)*(C(4)**1.5)*SQRT(C(3))/(C(1)**1.5)
      C(14)=EC(10)*SQRT(C(1)*C(3)*C(4)/C(2))
```

```
      C(15)=EC(11)*SQRT((CT/P)*C(3))
      C 1)=Q(1)-2.*C(5)+C(6)-C(7)-0.5*C(8)+0.5*C(9)-C(10)-2.*C(1
     1+1.5*C(13)-0.5*C(14)
      C(2)=Q(2)+2.*C(5)-C(6)+C(7)+0.5*C(8)-0.5*C(9)+C(10)+2.*C(1
     1-1.5*C(13)+0.5*C(14)
      IF (500+I)0,0,500
      IF (C(2))0,0,500
      C(2)=0.9*CLP(2)
      GO TO
  500 CONTINUE
      C(3)=Q(3)-0.5*C(7)-0.5*C(11)-C(12)-0.5*C(13)-0.5*C(14)-0.5*C(15)
      C(4)=Q(4)-C(6)-0.5*C(8)-0.5*C(9)-1.5*C(13)-0.5*C(14)
      GO TO 1080
 1070 C(5)=EC(1)*C(1)*SQRT(CT/(P*C(2)))
      C(6)=EC(2)*C(4)*SQRT(CT/(P*C(2)))
      C(7)=EC(3)*SQRT(C(2)*C(3))
      C(8)=EC(4)*SQRT(C(4))*(CT*C(2)/P)**0.25
      C(9)=EC(5)*SQRT(C(4))*(1./C(2))**0.25*(CT/P)**0.75
      C(10)=EC(6)*SQRT(C(2)*CT/P)
      C(11)=EC(7)*C(2)*SQRT(C(3)*P/CT)
      C(12)=EC(8)*C(3)*SQRT(P*C(2)/CT)
      C(13)=EC(9)*SQRT(C(3))*(C(4))**1.5*(P/CT)**0.25*(1./C(2))**0.75
      C(14)=EC(10)*SQRT(C(3)*C(4))*(C(2)*P/CT)**0.25
      C(15)=EC(11)*SQRT(C(3)*CT/P)
      C(1)=Q(1)-C(5)
      C(2)=Q(2)+0.5*C(5)+0.5*C(6)-0.5*C(7)-0.25*C(8)+0.25*C(9)-0.5*C(10)
     1-C(11)-0.5*C(12)+0.75*C(13)-0.25*C(14)
      C(3)=Q(3)-0.5*C(7)-0.5*C(11)-C(12)-0.5*C(13)-0.5*C(14)-0.5*C(15)
      C(4)=Q(4)-C(6)-0.5*C(8)-0.5*C(9)-1.5*C(13)-0.5*C(14)
 1080 CONTINUE
      CXT=C(1)+C(2)+C(3)+C(4)+C(5)+C(6)+C(7)+C(8)+C(9)+C(10)+C(11)+C(12)
     1+C(13)+C(14)+C(15)
      DO 372 I=1,4
  372 CY(I)=C(I)/CXT
      J=0
      DO 4 I=1,4
      IF (ABS(CW(I)-CY(I))-.0001)5,6,6
    6 J=1
    5 CONTINUE
    4 CONTINUE
      IF(J)8,9,8
    8 CONTINUE
      DO 364 I=1,4
  364 C(I)=0.6*CLP(I)+0.4*C(I)
      JJ=JJ+1
      GO TO 32
    9 CTT=CXT
      IF (-IJ)884,61,886
```

```
884 DO 330 I=1,15
330 CB(I)=C(I)
    CEE=CTT
    IF (II)0,0,449
    DO 831 I=1,15
831 XNT(I)=(CB(I)-CD(I))/30.
    XYY=XNT(2)
    IF (D-1.)0,0,1150
    XNT(2)=XNT(5)
    XNT(5)=XYY
1150 CONTINUE
    XNA=(CLL-CEE)/30.
    GO TO 972
886 DO 840 I=1,15
840 CB(I)=C(I)
    CLL=CTT
    IF (II)0,0,450
    T=T-30.
    IJ=-1
    GO TO 940
61  DO 600 I=1,15
600 CZZ(I)=C(I)
    ZXZ=CZZ(2)
    CZY=CTT
    IF (KJ)0,0,900
    GO TO 978
900 T=T+15.
    IJ=1
    GO TO 940
972 IJ=1
    II=1
    P=P+0.8
    T=T+15.
    GO TO 940
450 P=P-1.6
    IJ=-1
    II=1
    GO TO 940
449 DO 448 J=1,15
448 XNP(J)=(CB(J)-CD(J))/1.6
    YYX=XNP(2)
    IF (D-1.)0,0,1160
    XNP(2)=XNP(5)
    XNP(5)=YYX
1160 CONTINUE
    XNB=(CLL-CEE)/1.6
    P=P+0.8
978 IF (D-1.)0,0,1300
```

```
      CZZ(2)=CZZ(5)
      CZZ(
   77 DO 80 I=1,15
   80 CM(I)=CZZ(I)/CZY
      DO 950 I=1,15
  950 CZZ(I)=CZZ(I)+XC(I)
      CZY=CZZ(1)+CZZ(2)+CZZ(3)+CZZ(4)+CZZ(5)+CZZ(6)+CZZ(7)+CZZ(8)+CZZ(9)
     1+CZZ(10)+CZZ(11)+CZZ(12)+CZZ(13)+CZZ(14)+CZZ(15)
      WMOL=(44.01*CZZ(1)+28.011*CZZ(2)+28.016*CZZ(3)+18.016*CZZ(4)+32.0
     1CZZ(5)+2.016*CZZ(6)+33.008*CZZ(7)+17.008*CZZ(8)+1.008*CZZ(9)+16.0*C
     2ZZ(10)+46.008*CZZ(11)+44.016*CZZ(12)+17.032*CZZ(13)+31.016*CZZ(14)
     3+14.006*CZZ(15))/CZY
      H=0.
      CP=0.
      DO 30 I=1,15
      CP=CP+CZZ(I)*SHCP(I,TTT)/CZY
      H=H+CZZ(I)*(ENTHAL(I,TTT)+HF(I))/CZY
   30 CONTINUE
      DENS=P*WMOL/(82.0575*TTT)
      CV=CP-1.986
      GAM=CP/CV
      R=1.986/WMOL
      T=TTT
      RETURN
      END

ENGTH  2033, NAME  DISCN
```

```
      SUBROUTINE BURNTVOL(V0,S,VOL,THDEG)
      PP=(V0-37.7)/(16.*3.1416)
      IF (S-0.55)0,0,1
    0 VS0=(2.*3.1416*S**3)/3.
      IF (S-0.33)0,0,2
    1 VS1=(4.*3.1416*S**3)/3.
      GO TO 100
    2 VS1=-0.000998+0.11248*S-2.4388*S**2+23.792996*S**3-69.5752*S**4+11
     113.30974*S**5-73.93575*S**6
  100 VS2=(4.*3.1416*S**3)/3.
      IF((PP.GT.0.0).AND.(PP.LT.0.3)) GO TO 3
      IF ((PP.GT.0.3).AND.(PP.LT.0.6)) GO TO 4
      IF (PP.GT.0.6) GO TO 5
    3 VOL=VS0+(VS1-VS0)*PP/0.3
      GO TO 40
    4 VOL=VS1+(VS2-VS1)*(PP-0.3)/0.3
      GO TO 40
    5 VOL=VS2
      GO TO 40
    1 IF (S-4.2)0,0,6
      VM1=0.442423-3.31084*S+8.73565*S**2-6.744733*S**3+2.64581*S**4-0.4
     18081*S**5+0.03314*S**6
      VM2=-1.82471+6.825502*S-6.52272*S**2+4.14741*S**3-1.119412*S**4+0.
     1150371*S**5-0.007909*S**6
      VM3=-1.29148+6.090813*S-7.41785*S**2+6.626472*S**3-2.53625*S**4+0.
     148635*S**5-0.036745*S**6
      VM4=2.706252+10.159603*S-10.849974*S**2+7.67821*S**3-2.33474*S**4
     1+0.3558*S**5-0.02191*S**6
      VM5=-4.37204+19.01944*S-27.93397*S**2+22.53945*S**3-8.36542*S**4+1
     1.51323*S**5-0.106731*S**6
      VM6=-7.620762+33.61079*S-52.11141*S**2+41.09278*S**3-15.256374*S**
     14+2.747*S**5-0.191942*S**6
      VM7=-6.127099+26.76913*S-40.11872*S**2+30.85586*S**3-10.83528*S**4
     1+1.8512*S**5-0.123921*S**6
      VM8=-9.754346+41.90956*S-63.41182*S**2+47.63857*S**3-16.837733*S**
     14+2.90505*S**5-0.195971*S**6
      VM9=-22.17359+93.69136*S-143.43225*S**2+106.18132*S**3-38.36856*S*
     1*4+6.77541*S**5-0.46613*S**6
      VM10=-20.48114+86.60723*S-132.32871*S**2+97.81252*S**3-35.14812*S*
     1*4+6.16852*S**5-0.421382*S**6
      VM11=-18.67093+79.284202*S-121.44792*S**2+90.26278*S**3-32.586793*
     1S**4+5.7674*S**5-0.398065*S**6
      GO TO 20
    6 VM1=571.99054-484.23473*S+152.61666*S**2-19.83437*S**3+0.4857162*S
     1**4+0.111960673*S**5-0.0073825455*S**6
      VM2=393.079611-306.073592*S+79.790617*S**2-4.147829*S**3-1.333842*
     1S**4+0.217594516*S**5-0.00970275845*S**6
      VM3=54.49181-99.00816*S+50.862001*S**2-10.4200121*S**3+1.01767758*
```

```
     1S**4-0.0391808996*S**5
      VM4=194.11939-155.21103*S+38.38681*S**2+0.401294*S**3-1.268754*S**
     14+0.16861353 9*S**5-0.00709839563*S**6
      VM5=1279.17977-1164.34827*S+416.78103*S**2-72.15407*S**3+6.17186S*
     1S**4-0.209937*S**5
      VM6=750.5077-735.7465*S+280.389*S**2-50.6299*S**3+4.49993*S**4-0.1
     1158898*S**5
      VM7=669.18746-521.0284*S+133.3936*S**2-5.59529*S**3-2.48510032*S**
     14+0.37990146*S**5-0.016464617*S**6
      VM8=235.922-246.52821*S+97.64835*S**2-16.83912*S**3+1.445848*S**4-
     10.050986*S**5
      VM9=-467.75621+303.13454*S-69.761607*S**2+8.177523*S**3-0.371675*S
     1**4
      VM10=-202.24122+67.80228*S+10.66266*S**2-5.132906*S**3+0.717022*S*
     1*4-0.035551*S**5
      VM11=-1100.82485+786.802716*S-217.587245*S**2+31.075494*S**3-2.147
     1374*S**4+0.055059*S**5
   20 IF ((PP.GT.0.0).AND.(PP.LT.0.3)) GO TO 21
      IF ((PP.GT.0.3).AND.(PP.LT.0.6)) GO TO 22
      IF ((PP.GT.0.6).AND.(PP.LT.0.9)) GO TO 23
      IF ((PP.GT.0.9).AND.(PP.LT.1.2)) GO TO 24
      IF ((PP.GT.1.2).AND.(PP.LT.1.5)) GO TO 25
      IF ((PP.GT.1.5).AND.(PP.LT.1.8)) GO TO 26
      IF ((PP.GT.1.8).AND.(PP.LT.2.1)) GO TO 27
      IF ((PP.GT.2.1).AND.(PP.LT.2.4)) GO TO 28
      IF ((PP.GT.2.4).AND.(PP.LT.2.65)) GO TO 29
      IF ((PP.GT.2.65).AND.(PP.LT.3.0)) GO TO 30
   21 VOL=VM1+(VM2-VM1)*PP/0.3
      GO TO 40
   22 VOL=VM2+(VM3-VM2)*(PP-0.3)/0.3
      GO TO 40
   23 VOL=VM3+(VM4-VM3)*(PP-0.6)/0.3
      GO TO 40
   24 VOL=VM4+(VM5-VM4)*(PP-0.9)/0.3
      GO TO 40
   25 VOL=VM5+(VM6-VM5)*(PP-1.2)/0.3
      GO TO 40
   26 VOL=VM6+(VM7-VM6)*(PP-1.5)/0.3
      GO TO 40
   27 VOL=VM7+(VM8-VM7)*(PP-1.8)/0.3
      GO TO 40
   28 IF (S-1.6)0,0,70
      VOL=VM8
      GO TO 40
   70 VOL=VM8+(VM9-VM8)*(PP-2.1)/0.3
      GO TO 40
   29 IF (S-1.6)0,0,71
      VOL=VM8
```

```
      GO TO 40
   71 VOL=VM9+(VM10-VM9)*(PP-2.4)/0.25
      GO TO 40
   30 IF (S-1.6)0,0,72
      VOL=VM8
      GO TO 40
   72 VOL=VM10+(VM11-VM10)*(PP-2.65)/0.35
   40 RETURN
      END

ENGTH  1146,  NAME  BURNTVOL
```

```
      SUBROUTINE BURNVEL(TO,TF,PA,PHI,JFUEL,UF)
      D=PHI
      YY=.001*TF
      R=1.986
      CPF=AIRCP(TF)
      CPM=CPF*28.9
      XMUF=(0.43868+5.13195*YY-1.31065*YY**2-0.668597*YY**3+0.922798*YY*
     1*4-0.342237*YY**5+0.042674*YY**6)/10.0**4
      RHOF=PA*144.*.01602/(96.*TF)
      RHO0=PA*144.*.01602/(96.*TO)
      DF=1.336*XMUF/RHOF
      TKF=(CPM+1.25/R)*XMUF/28.9
      A=6.0*10.0**23
      CPAV=CPMEAN(TF,TO)
      GO TO (10,11,12),JFUEL
C THIS STATEMENT ALLOWS FOR THE VARIOUS FUELS BEING USED.  1 IS PROPANE,  2
C ISO-OCTANE,  3 IS BENZENE.
   10 BETAP=R*TF*TF/40000./(TF-TO)
      AFAP=688./(44.097*PHI)
      XMF0P=1./(AFAP+1.)
      CF0P=XMF0P*RHO0*A/44.097
      IF (PHI-0.9)8,8,9
    8 UF=(0.961*BETAP/CPF/DF)*SQRT((2.*(TKF**3)*CF0P*(1.-PHI*(1.-BETAP))
     1*4.62)/(RHO0**3*CPAV*PHI*0.2*EXP(40000./(R*TF))*10.0**8))
      GO TO 69
    9 IF (PHI-1.1)0,200,200
      PHI=0.9
      UW=(0.961*BETAP/CPF/DF)*SQRT((2.*(TKF**3)*CF0P*(1.-PHI*(1.-BETAP))
     1*4.62)/(RHO0**3*CPAV*PHI*0.2*EXP(40000./(R*TF))*10.0**8))
      PHI=1.1
      UR=(0.961*BETAP/CPF/DF)*SQRT((2.*(TKF**3)*CF0P*(1.-(1.-BETAP)/PHI)
     1*4.62)/(RHO0**3*CPAV*PHI*0.2*EXP(40000./(R*TF))*10.0**8))
      PHI=D
      UF=(UR-UW)*(PHI-0.9)/0.2+UW
      GO TO 69
  200 UF=(0.961*BETAP/CPF/DF)*SQRT((2.*(TKF**3)*CF0P*(1.-(1.-BETAP)/PHI)
     1*4.62)/(RHO0**3*CPAV*PHI*0.2*EXP(40000./(R*TF))*10.0**8))
      GO TO 69
   11 BETAI=R*TF*TF/40000./(TF-TO)
      AFAI=1718./(114.232*PHI)
      XMF0I=1./(AFAI+1.)
      CF0I=XMF0I*RHO0*A/114.232
      IF (PHI-0.9)20,20,90
   20 UF=(0.948*BETAI/CPF/DF)*SQRT((2.*(TKF**3)*CF0I*(1.-PHI*(1.-BETAI))
     1*4.04)/(RHO0**3*CPAV*PHI*0.08*EXP(40000./(R*TF))*10.0**8))
      GO TO 69
   90 IF (PHI-1.1)0,21,21
      PHI=0.9
```

```
      UW=(0.948*BETAI/CPF/DF)*SQRT((2.*(TKF**3)*CFOI*(1.-PHI*(1.-BETAI))
     1*4.04)/(RHO0**3*CPAV*PHI*0.08*EXP(40000./(R*TF))*10.0**8))
      PHI=1.1
      UR=(0.948*BETAI/CPF/DF)*SQRT((2.*(TKF**3)*CFOI*(1.-(1.-BETAI)/PHI)
     1*4.04)/(RHO0**3*CPAV*PHI*0.08*EXP(40000./(R*TF))*10.0**8))
      PHI=D
      UF=(UR-UW)*(PHI-0.9)/0.2+UW
      GO TO 69
   21 UF=(0.948*BETAI/CPF/DF)*SQRT((2.*(TKF**3)*CFOI*(1.-(1.-BETAI)/PHI)
     1*4.04)/(RHO0**3*CPAV*PHI*0.08*EXP(40000./(R*TF))*10.0**8))
      GO TO 69
   12 BETAB=R*TF*TF/40000./(TF-T0)
      AFAB=1030./(78.114*PHI)
      XMFOB=1./(AFAB+1.)
      CFOB=XMFOB*RHO0*A/78.114
      IF (PHI-0.9)40,40,41
   40 UF=(0.988*BETAB/CPF/DF)*SQRT((2.*(TKF**3)*CFOB*(1.-PHI*(1.-BETAB))
     1*4.63)/(RHO0**3*CPAV*PHI*0.1335*EXP(40000./(R*TF))*10.0**8))
      GO TO 69
   41 IF (PHI-1.1)0,300,300
      PHI=0.9
      UW=(0.988*BETAB/CPF/DF)*SQRT((2.*(TKF**3)*CFOB*(1.-PHI*(1.-BETAB))
     1*4.63)/(RHO0**3*CPAV*PHI*0.1335*EXP(40000./(R*TF))*10.0**8))
      PHI=1.1
      UR=(0.988*BETAB/CPF/DF)*SQRT((2.*(TKF**3)*CFOB*(1.-(1.-BETAB)/PHI)
     1*4.63)/(RHO0**3*CPAV*PHI*0.1335*EXP(40000./(R*TF))*10.0**8))
      PHI=D
      UF=(UR-UW)*(PHI-0.9)/0.2+UW
      GO TO 69
  300 UF=(0.988*BETAB/CPF/DF)*SQRT((2.*(TKF**3)*CFOB*(1.-(1.-BETAB)/PHI)
     1*4.63)/(RHO0**3*CPAV*PHI*0.1335*EXP(40000./(R*TF))*10.0**8))
   69 RETURN
      END

ENGTH  953,  NAME  BURNVEL
```

```
      SUBROUTINE FLAMDIST(THDEG,V0,V,S)
      P=(V0-37.7)/(16.*3.1416)
      IF (V-0.35)0,0,1
      S0=(3.*V/6.2832)**0.333
      S1=0.137504+1.697968*V-2.848866*V**2-2.50892*V**3+21.710038*V**4-3
     -15.31142*V**5+19.47104*V**6
      S2=(3.*V/(4.*3.1416))**0.333
      IF ((P.GT.0.0).AND.(P.LT.0.3)) GO TO 2
      IF ((P.GT.0.3).AND.(P.LT.0.6)) GO TO 3
      IF (P.GT.0.6) GO TO 4
    2 IF (V-0.17)0,0,430
      S=S2+(S0-S2)*(0.3-P)/0.3
      GO TO 100
  430 S=S1+(S0-S1)*(0.3-P)/0.3
      GO TO 100
    3 IF (V-0.17)0,0,431
      S=S2
      GO TO 100
  431 S=S2+(S1-S2)*(0.6-P)/0.3
      GO TO 100
    4 S=S2
      GO TO 100
    1 IF (V-1.8)0,0,30
      IF (P-0.6)0,0,120
      D0=0.551448-0.878889*P+4.489277*P**2-16.74066*P**3+37.77968*P**4-4
     -14.604095*P**5+21.112674*P**6
      GO TO 150
  120 D0=0.436
  150 IF (P-0.6)0,0,121
      D1=0.580058-0.902286*P+4.37882*P**2-15.41922*P**3+32.44843*P**4-35
     -1.185463*P**5+14.98899*P**6
      GO TO 151
  121 D1=0.453
  151 IF (P-0.6)0,0,122
      D2=0.629606-0.76216*P+2.71659*P**2-8.471752*P**3+17.76463*P**4-20.
     -1354972*P**5+9.586852*P**6
      GO TO 152
  122 D2=0.487
  152 IF (P-0.6)0,0,123
      D3=0.670407-0.614142*P+1.596678*P**2-4.09598*P**3+6.18758*P**4-3.1
     -10367*P**5-0.703387*P**6
      GO TO 153
  123 D3=0.52
  153 IF (P-0.6)0,0,124
      D4=0.713214-0.488121*P+0.684471*P**2-2.82294*P**3+10.57395*P**4-17
     -1.290141*P**5+10.07037*P**6
      GO TO 154
  124 D4=0.5525
```

```
      IF (P-0.8)0,0,125
        D5=0.762328-0.402374*P-0.58838*P**2+4.704884*P**3-11.10711*P**4+12
     1.0657*P**5-4.949674*P**6
        GO TO 155
  125 D5=0.58
  155 IF (P-0.9)0,0,126
        D6=0.811045-0.381406*P-0.525007*P**2+2.820133*P**3-4.722765*P**4+3
     1.817039*P**5-1.21479*P**6
        GO TO 156
  126 D6=0.608
  156 IF (P-0.92)0,0,127
        D7=0.859708-0.488838*P+0.473116*P**2-1.221672*P**3+2.889225*P**4-3
     1.01037*P**5+1.14356*P**6
        GO TO 157
  127 D7=0.638
  157 IF (P-0.92)0,0,128
        D8=0.94601-0.496541*P+0.34094*P**2-0.26192*P**3+0.227691*P**4-0.02
     10005*P**5-0.047289*P**6
        GO TO 158
  128 D8=0.695
  158 IF (P-0.92)0,0,129
        D9=1.042639-0.391906*P-1.068193*P**2+5.32964*P**3-9.96492*P**4+8.4
     196231*P**5-2.697846*P**6
        GO TO 159
  129 D9=0.753
  159 IF (P-0.92)0,0,130
        D10=1.135798-0.765678*P+1.424637*P**2-2.817115*P**3+3.704313*P**4-
     12.830825*P**5+0.955979*P**6
        GO TO 160
  130 D10=0.8111
  160 IF (P-0.92)0,0,131
        D11=1.217053-0.815508*P+1.907718*P**2-5.398768*P**3+9.940817*P**4-
     19.659053*P**5+3.680592*P**6
        GO TO 161
  131 D11=0.865
  161 IF (V-0.4)0,0,40
        S=D0+(D1-D0)*(V-0.35)/0.05
        GO TO 100
   40 IF (V-0.5)0,0,41
        S=D1+(D2-D1)*(V-0.4)/0.1
        GO TO 100
   41 IF (V-0.6)0,0,42
        S=D2+(D3-D2)*(V-0.5)/0.1
        GO TO 100
   42 IF (V-0.7)0,0,43
        S=D3+(D4-D3)*(V-0.6)/0.1
        GO TO 100
   43 IF (V-0.8)0,0,44
```

```
      S=D4+(D5-D4)*(V-0.7)/0.1
      GO TO 100
   44 IF (V-0.9)0,0,45
      S=D5+(D6-D5)*(V-0.8)/0.1
      GO TO 100
   45 IF (V-1.0)0,0,46
      S=D6+(D7-D6)*(V-0.9)/0.1
      GO TO 100
   46 IF (V-1.2)0,0,47
      S=D7+(D8-D7)*(V-1.0)/0.2
      GO TO 100
   47 IF (V-1.4)0,0,48
      S=D8+(D9-D8)*(V-1.2)/0.2
      GO TO 100
   48 IF (V-1.6)0,0,49
      S=D9+(D10-D9)*(V-1.4)/0.2
      GO TO 100
   49 S=D10+(D11-D10)*(V-1.6)/0.2
      GO TO 100
   30 IF (V-20.0)0,0,33
      IF (P-0.92)0,0,220
      D11=1.217053-0.815508*P+1.907718*P**2-5.398768*P**3+9.940817*P**4-
     19.639053*P**5+3.680592*P**6
      GO TO 260
  220 D11=0.865
  260 IF (P-0.95)0,0,221
      D12=1.300295-0.898996*P+2.781073*P**2-9.39628*P**3+17.723696*P**4-
     116.48304*P**5+5.907791*P**6
      GO TO 261
  221 D12=0.925
  261 IF (P-0.95)0,0,222
      D13=1.3831A-0.919757*P+1.787505*P**2-3.839631*P**3+5.431597*P**4-4
     1.30282*P**5+1.42705*P**6
      GO TO 262
  222 D13=0.975
  262 IF (P-0.95)0,0,223
      D14=1.46712-0.970594*P+1.641174*P**2-2.983216*P**3+3.839598*P**4-3
     1.05846*P**5+1.080765*P**6
      GO TO 263
  223 D14=1.025
  263 IF (P-1.1)0,0,224
      D15=1.540613-0.894902*P+0.51317*P**2+1.341475*P**3-4.027788*P**4+3
     1.683515*P**5-1.087338*P**6
      GO TO 264
  224 D15=1.07
  264 IF (P-1.0)0,0,225
      D16=1.61615-1.03458*P+1.563231*P**2-3.201058*P**3+5.319885*P**4-5.
     118206*P**5+2.022986*P**6
```

```
      GO TO 265
  225 D16=1.105
  265 IF (P-1.5)0,0,226
      D17=1.68394-1.237875*P+2.731306*P**2-5.28924*P**3+5.217345*P**4-2.
     1343167*P**5+0.38436*P**6
      GO TO 266
  226 D17=1.12
  266 IF (P-1.15)0,0,227
      D18=2.050094-1.55087*P+3.71893*P**2-9.77705*P**3+13.28448*P**4-8.3
     195732*P**5+2.01478*P**6
      GO TO 267
  227 D18=1.325
  267 IF (P-1.45)0,0,228
      D19=2.30022-1.194295*P-0.876*P**2+4.56191*P**3-6.123342*P**4+3.663
     1322*P**5-0.82021*P**6
      GO TO 268
  228 D19=1.425
  268 IF (P-2.3)0,0,229
      D20=3.206189-1.80432*P+1.29269*P**2-1.1766*P**3+0.841235*P**4-0.29
     14947*P**5+0.03827*P**6
      GO TO 269
  229 D20=1.8
  269 IF (P-2.4)0,0,230
      D21=3.87505-2.45601*P+3.59489*P**2-5.029494*P**3+3.70406*P**4-1.26
     1543*P**5+0.16095*P**6
      GO TO 270
  230 D21=2.05
  270 IF (P-2.4)0,0,231
      D22=4.44708-2.83322*P+3.87203*P**2-4.83376*P**3+3.27889*P**4-1.053
     143*P**5+0.12692*P**6
      GO TO 271
  231 D22=2.3
  271 IF (V-2.0)0,0,60
      S=D11+(D12-D11)*(V-1.8)/0.2
      GO TO 100
   60 IF (V-2.2)0,0,61
      S=D12+(D13-D12)*(V-2.0)/0.2
      GO TO 100
   61 IF (V-2.4)0,0,62
      S=D13+(D14-D13)*(V-2.2)/0.2
      GO TO 100
   62 IF (V-2.6)0,0,63
      S=D14+(D15-D14)*(V-2.4)/0.2
      GO TO 100
   63 IF (V-2.8)0,0,64
      S=D15+(D16-D15)*(V-2.6)/0.2
      GO TO 100
   64 IF (V-3.0)0,0,65
```

```
      S=D16+(D17-D16)*(V-2.8)/0.2
      GO TO 100
   65 IF (V-4.0)0,0,66
      S=D17+(D18-D17)*(V-3.0)
      GO TO 100
   66 IF (V-5.0)0,0,67
      S=D18+(D19-D18)*(V-4.0)
      GO TO 100
   67 IF (V-10.0)0,0,68
      S=D19+(D20-D19)*(V-5.0)/5.0
      GO TO 100
   68 IF (V-15.0)0,0,69
      S=D20+(D21-D20)*(V-10.0)/5.0
      GO TO 100
   69 S=D21+(D22-D21)*(V-15.0)/5.0
      GO TO 100
   33 IF (P-2.4)0,0,320
      D22=4.44708-2.83322*P+3.87203*P**2-4.83376*P**3+3.27889*P**4-1.053
     143*P**5+0.12692*P**6
      GO TO 360
  320 D22=2.3
  360 IF (P-2.5)0,0,321
      D23=5.0055-3.03634*P+3.00788*P**2-2.85113*P**3+1.71819*P**4-0.5336
     19*P**5+0.06506*P**6
      GO TO 361
  321 D23=2.55
  361 IF (P-2.8)0,0,322
      D24=5.66456-4.71969*P+6.573843*P**2-6.4742*P**3+3.54449*P**4-0.974
     126*P**5+0.105334*P**6
      GO TO 362
  322 D24=2.8
  362 IF (P-0.3)0,0,550
      D25=6.548511-10.75898*P+125.83127*P**2-1874.7619*P**3+14828.9285*P
     1**4-56027.0748*P**5+80959.0024*P**6
      GO TO 551
  550 D25=6.15575-4.7176*P+5.69325*P**2-5.01643*P**3+2.50697*P**4-0.6333
     17*P**5+0.06322*P**6
  551 IF (P-0.35)0,0,552
      D26=7.720798-8.70428*P-45.74396*P**2+419.52177*P**3-1213.12472*P**
     14+1393.36353*P**5-392.1096*P**6
      GO TO 553
  552 D26=7.17862-7.40751*P+9.29873*P**2-7.244303*P**3+3.12372*P**4-0.68
     1615*P**5+0.060192*P**6
  553 IF (P-0.5)0,0,554
      D27=10.86096-36.07918*P+219.7114*P**2-1002.23116*P**3+2670.7505*P*
     1*4-3690.2477*P**5+2039.7432*P**6
      GO TO 555
  554 D27=8.805363-8.6684*P+7.01227*P**2-2.57412*P**3+0.10311*P**4+0.159
```

```
     1192*P**5-0.02726*P**6
555  IF (P-0.6)0,0,556
     D28=17.12398+20.2738*P-460.2935*P**2+1556.0863*P**3-2123.011*P**4+
    11053.48362*P**5
     GO TO 557
556  D28=10.60703-10.3463*P+6.66596*P**2-1.27667*P**3-0.58942*P**4+0.30
    18314*P**5-0.03897*P**6
557  IF (P-0.8)0,0,558
     D29=-16.31119+408.26303*P-1514.5899*P**2+1749.8867*P**3+662.8086*P
    1**4-2588.6824*P**5+1321.7165*P**6
     GO TO 559
558  D29=6.12908+11.44842*P-27.74478*P**2+25.296213*P**3-11.52462*P**4+
    12.61416*P**5-0.23507*P**6
559  IF (P-0.9)0,0,560
     D30=79.91303-144.52108*P-1.43652*P**2-83.96773*P**3+645.55198*P**4
    1-747.55963*P**5+258.83419*P**6
     GO TO 561
560  D30=3.05155+29.16958*P-56.15808*P**2+46.79129*P**3-20.04823*P**4+4
    1.32851*P**5-0.373163*P**6
561  IF (P-1.1)0,0,562
     D31=893.3886-2334.9653*P+1556.6091*P**2-39.62892*P**3+893.06174*P*
    1*4-1528.3937*P**5+567.57714*P**6
     GO TO 563
562  D31=5.437612+32.17036*P-68.3289*P**2+59.09721*P**3-25.80489*P**4+5
    1.63161*P**5-0.48878*P**6
563  IF (P-1.3)0,0,564
     D32=336.13506-415.59947*P-623.7129*P**2+1422.5397*P**3-898.0738*P*
    1*4+189.90884*P**5
     GO TO 565
564  D32=34.539494-50.5186*P+33.29233*P**2-7.76243*P**3-1.25269*P**4+0.
    188453*P**5-0.11207*P**6
565  IF (P-1.4)0,0,566
     D33=215.03674-101.83804*P-228.32415*P**2+67.77096*P**3+133.53742*P
    1**4-58.7891*P**5
     GO TO 567
566  D33=50.96236-63.07771*P+15.19691*P**2+20.94372*P**3-16.36751*P**4+
    14.452142*P**5-0.43215*P**6
567  IF (P-1.65)0,0,568
     D34=1743.7282-3569.2266*P+2404.3628*P**2-380.06392*P**3-180.1482*P
    1**4+53.12321*P**5
     GO TO 569
568  D34=118.6255-224.5556*P+183.49535*P**2-75.81684*P**3+15.6872*P**4-
    11.295192*P**5
569  D35=601.73039-1276.0538*P+1096.7124*P**2-469.61262*P**3+99.86103*P
    1**4-8.42534*P**5
     IF (P-2.2)0,0,570
     D36=971.72125-520.55123*P-108.40274*P**2-29.660793*P**3+63.5071*P*
    1*4+0.48738*P**5-4.32394*P**6
```

```
      GO TO 571
570   D36=66.97904-69.73935*P+16.25923*P**2+16.70046*P**3-12.5588*P**4+3
     1.21301*P**5-0.290798*P**6
571   IF (P-2.6)0,0,572
      D37=-2381.3328+1674.405*P-309.32205*P**2+169.72667*P**3-38.55949*P
     1**4-37.87224*P**5+11.02623*P**6
      GO TO 573
572   D37=140.30014-194.91024*P+75.49191*P**2+7.2647*P**3-9.1519*P**4+1.
     1.130613*P**5
573   D38=25.49037-22.5901*P+16.55936*P**2-8.25527*P**3+2.365663*P**4-0.
     1.122717*P**5-0.01726*P**6
      IF (V-25.0)0,0,80
      S=D22+(D23-D22)*(V-20.0)/5.0
      GO TO 100
   80 IF (V-30.0)0,0,81
      S=D23+(D24-D23)*(V-25.0)/5.0
      GO TO 100
   81 IF (V-35.0)0,0,82
      S=D24+(D25-D24)*(V-30.0)/5.0
      GO TO 100
   82 IF (V-40.0)0,0,83
      S=D25+(D26-D25)*(V-35.0)/5.0
      GO TO 100
   83 IF (V-50.0)0,0,84
      S=D26+(D27-D26)*(V-40.0)/10.0
      GO TO 100
   84 IF (V-60.0)0,0,85
      S=D27+(D28-D27)*(V-50.0)/10.
      GO TO 100
   85 IF (V-70.0)0,0,86
      S=D28+(D29-D28)*(V-60.0)/10.
      GO TO 100
   86 IF (V-80.0)0,0,87
      S=D29+(D30-D29)*(V-70.0)/10.
      GO TO 100
   87 IF (V-90.0)0,0,88
      S=D30+(D31-D30)*(V-80.0)/10.
      GO TO 100
   88 IF (V-100.0)0,0,89
      S=D31+(D32-D31)*(V-90.0)/10.
      GO TO 100
   89 IF (V-110.0)0,0,90
      S=D32+(D33-D32)*(V-100.0)/10
      GO TO 100
   90 IF (V-120.0)0,0,91
      S=D33+(D34-D33)*(V-110.0)/10.
      GO TO 100
   91 IF (V-140.0)0,0,92
```

```
      S=D34+(D35-D34)*(V-120.0)/20.
      GO TO 100
   92 IF (V-160.0)0,0,93
      S=D35+(D36-D35)*(V-140.0)/20.
      GO TO 100
   93 IF (V-180.0)0,0,94
      S=D36+(D37-D36)*(V-160.0)/20.
      GO TO 100
   94 S=D37+(D38-D37)*(V-180.0)/5.
  100 WRITE (2,200)
  200 FORMAT(37H CRANK  CYL.VOL  BURNT  PISTON  FLAME/40H ANGLE   (CC8)
     1 VOL(CC) POINT   POSITION)
      WRITE (2,201)THDEG,V0,V,P,S
  201 FORMAT(F6.1,F9.2,F8.2,F7.3,F11.6/)
      RETURN
      END

ENGTH 2903, NAME PLAMDIST
```

```
      SUBROUTINE HTRAN(T,RHO,B,XN,R,QLS,QLSB,V,DS,JJJ)
C     JJJ=1 IS COMPRESSION, 0 IS BURNT FRACTION, 1 IS EXPANSION
      A=0.4
      C=1.03/(10.0**13)
      G=.001*T
      CPM=AIRCP(T)*28.9
      XMU=(0.4387+5.13195*G-1.31065*G**2-0.6686*G**3+0.9228*G**4-0.36224
     1*G**5+0.042674*G**6)/10.0**4
      VP=XN*R/15.
      RE=RHO*VP*B/XMU
      TK=(CPM+1.25/1.986)*XMU/28.9
      PVOL=V-37.7
      PP=PVOL/(16.*3.1416)
      AC=3.1416*B*PP
      AH=65.0
      AP=3.1416*B**2/4.
      AT=AC+AP+AH
      IF (JJJ)1,2,3
    1 TC=390.
      TP=515.
      TH=415.
      TIME=1.667/XN
      TW=(AC*TC+AP*TP+AH*TH)/AT
      QLS=-(AT*A*TK*(RE**0.7)*(T-TW)/B)*TIME
      QLSB=0.
      RETURN
    2 IF (DS-1.0)0,0,20
      AHS=1.4*DS
      GO TO 21
   20 AHS=0.1332-1.0194*DS+2.6205*DS**2-0.1722*DS**3
   21 C0=0.0
      IF (DS-0.8)0,0,48
      P0=0.0
      GO TO 49
   48 P0=0.608-2.3076*DS+3.0082*DS**2-0.4994*DS**3+0.07023*DS**4-0.00479
     16*DS**5
   49 IF (DS-1.0)0,0,50
      C1=0.27*DS
      GO TO 51
   50 C1=0.031796-0.842021*DS+1.77556*DS**2-0.99203*DS**3+0.26679*DS**4-
     10.03401*DS**5+0.001659*DS**6
   51 IF (DS-1.0)0,0,52
      P1=DS
      GO TO 53
   52 P1=-0.003-1.4244*DS+2.604*DS**2-0.30731*DS**3+0.01403*DS**4
   53 IF (DS-1.0)0,0,54
      C2=0.5*DS
      GO TO 55
```

```
54 C2=-0.158+0.8463*DS-0.6215*DS**2+0.41618*DS**3-0.08596*DS**4+0.005
   1876*DS**5
55 P2=P1
   IF (DS-0.7)0,0,58
   C3=0.0
   GO TO 59
58 C3=0.02713-1.3377*DS+3.57442*DS**2-1.85728*DS**3+0.489035*DS**4-0.
   1062676*DS**5+0.003111*DS**6
59 IF (DS-1.1)0,0,60
   P3=0.0
   GO TO 61
60 P3=P1
61 IF (DS-0.9)0,0,62
   C4=0.0
   GO TO 63
62 C4=0.159423-3.38594*DS+6.249943*DS**2-3.08562*DS**3+0.77597*DS**4-
   0.09579*DS**5+0.004611*DS**6
63 IF (DS-1.5)0,0,64
   P4=0.0
   GO TO 65
64 P4=-35.56898+46.62064*DS-21.16275*DS**2+4.84602*DS**3-0.48243*DS**
   4+0.01719*DS**5
65 IF (DS-0.9)0,0,66
   C5=0.0
   GO TO 67
66 C5=0.24867-4.7969*DS+8.53769*DS**2-4.30413*DS**3+1.092575*DS**4-0.
   113418*DS**5+0.0063565*DS**6
67 IF (DS-1.5)0,0,68
   P5=0.0
   GO TO 69
68 P5=P4
69 IF (DS-0.9)0,0,70
   C6=0.0
   GO TO 71
70 C6=0.14696-3.38826*DS+6.23105*DS**2-2.93752*DS**3+0.72648*DS**4-0.
   1088341*DS**5+0.004218*DS**6
71 IF (DS-1.6)0,0,72
   P6=0.0
   GO TO 73
72 P6=-8.547+7.492*DS-2.0719*DS**2+0.6138*DS**3-0.04446*DS**4
73 IF (DS-0.9)0,0,74
   C7=0.0
   GO TO 75
74 C7=0.09412-2.72668*DS+5.07613*DS**2-2.0942*DS**3+0.47447*DS**4-0.0
   153847*DS**5+0.002475*DS**6
75 IF (DS-2.2)0,0,76
   P7=0.0
   GO TO 77
```

```
   P7=-14.099+3.879*DS+1.5314*DS**2-0.1236*DS**3
   IF (DS-0.8)0,0,78
      C8=0.0
      GO TO 79
78 C8=0.128-2.113*DS+3.3228*DS**2-0.6151*DS**3+0.04441*DS**4
79 IF (DS-2.5)0,0,80
      P8=0.0
      GO TO 81
80 P8=-62.92452+46.5997*DS-12.4965*DS**2+1.81102*DS**3-0.09445*DS**4
81 IF (DS-0.8)0,0,82
      C9=0.0
      GO TO 83
82 C9=0.12281-2.548784*DS+4.69361*DS**2-1.76524*DS**3+0.40994*DS**4-0
   1.049271*DS**5+0.0023856*DS**6
83 IF (DS-2.8)0,0,84
      P9=0.0
      GO TO 85
84 P9=-20.229+3.601*DS+1.8077*DS**2-0.1446*DS**3
85 IF (DS-0.8)0,0,86
      C10=0.0
      GO TO 87
86 C10=.33-2.881*DS+3.994*DS**2-0.7511*DS**3+0.05468*DS**4
87 IF (DS-2.9)0,0,88
      P10=0.0
      GO TO 89
88 P10=-14.72-1.279*DS+2.7948*DS**2-0.20294*DS**3
89 CONTINUE
      IF ((PP.GT.0.0).AND.(PP.LT.0.3)) GO TO 30
      IF ((PP.GT.0.3).AND.(PP.LT.0.6)) GO TO 31
      IF ((PP.GT.0.6).AND.(PP.LT.0.9)) GO TO 32
      IF ((PP.GT.0.9).AND.(PP.LT.1.2)) GO TO 33
      IF ((PP.GT.1.2).AND.(PP.LT.1.5)) GO TO 34
      IF ((PP.GT.1.5).AND.(PP.LT.1.8)) GO TO 35
      IF ((PP.GT.1.8).AND.(PP.LT.2.1)) GO TO 36
      IF ((PP.GT.2.1).AND.(PP.LT.2.4)) GO TO 37
      IF ((PP.GT.2.4).AND.(PP.LT.2.65)) GO TO 38
      IF ((PP.GT.2.65).AND.(PP.LT.3.0)) GO TO 39
30 ACB=C0+(C1-C0)*PP/0.3
      APB=P1+(P0-P1)*(0.3-PP)/0.3
      GO TO 90
31 ACB=C1+(C2-C1)*(PP-0.3)/0.3
      APB=P2
      GO TO 90
32 ACB=C2+(C3-C2)*(PP-0.6)/0.3
      APB=P3
      GO TO 90
33 ACB=C3+(C4-C3)*(PP-0.9)/0.3
      APB=P4
```

```
      GO TO 90
   34 ACB=C4+(C5-C4)*(PP-1.2)/0.3
      APB=P5
      GO TO 90
   35 ACB=C5+(C6-C5)*(PP-1.5)/0.3
      APB=P6
      GO TO 90
   36 ACB=C6+(C7-C6)*(PP-1.8)/0.3
      APB=P7
      GO TO 90
   37 ACB=C7+(C8-C7)*(PP-2.1)/0.3
      APB=P8
      GO TO 90
   38 ACB=C8
      APB=P9
      GO TO 90
   39 ACB=C9+(C10-C9)*(PP-2.65)/0.35
      APB=P10
   90 AREA=ACB+APB+AHB
      TCB=395.
      TPB=520.
      THB=420.
      TWB=(ACB*TCB+APB*TPB+AHB*THB)/AREA
      TIME=1./(3.*XN)
      QLSB=-((AREA*A*TK*(RE**0.7)*(T-TWB)/B)+(C*AREA*(T**4-TWB**4)))*TIM
     1E
      QLS=0.
      RETURN
    3 TC=400.
      TP=525.
      TH=425.
      TW=(AC*TC+AP*TP+AH*TH)/AT
      TIME=1.6667/XN
      QLSH=-((AT*A*TK*(RE**0.7)*(T-TW)/B)+(C*AT*(T**4-TW**4)))*TIMR
      QLS=0.
      RETURN
      END

LENGTH  1250, NAME  HTRAN
```

```
      FUNCTION SHCP (N,T)
      COMMON /CPDATA/ CP(14,15),S0(15),HF(15)
      U=T*0.001
      IF (T.GT.2000.0) GO TO 1
      SHCP=CP(1,N)+U*(CP(2,N)+U*(CP(3,N)+U*(CP(4,N)+U*(CP(5,N)+U*(CP(6,N
     1)+U*CP(7,N))))))
      RETURN
    1 SHCP=CP(8,N)+U*(CP(9,N)+U*(CP(10,N)+U*(CP(11,N)+U*(CP(12,N)+U*(CP(
     113,N)+U*CP(14,N))))))
      RETURN
      END



      FUNCTION ENTHAL (N,T)
      COMMON /CPDATA/ CP(14,15),S0(15),HF(15)
      U=0.29815
      E0=U*(CP(1,N)+U*(CP(2,N)*0.5+U*(CP(3,N)/3.0+U*(CP(4,N)*0.25
     7    +U*(CP(5,N)*0.2+U*(CP(6,N)/6.0+U*CP(7,N)/7.0))))))
      U=AMIN1(2000.0,T)*0.001
      E1=U*(CP(1,N)+U*(CP(2,N)*0.5+U*(CP(3,N)/3.0+U*(CP(4,N)*0.25
     7    +U*(CP(5,N)*0.2+U*(CP(6,N)/6.0+U*CP(7,N)/7.0))))))
      IF (T.GT.2000.0) GO TO 1
      ENTHAL=(E1-E0)*1000.0
      RETURN
    1 E2=U*(CP(8,N)+U*(CP(9,N)*0.5+U*(CP(10,N)/3.0+U*(CP(11,N)*0.25
     7    +U*(CP(12,N)*0.2+U*(CP(13,N)/6.0+U*CP(14,N)/7.0))))))
      U=0.001*T
      E3=U*(CP(8,N)+U*(CP(9,N)*0.5+U*(CP(10,N)/3.0+U*(CP(11,N)*0.25
     7    +U*(CP(12,N)*0.2+U*(CP(13,N)/6.0+U*CP(14,N)/7.0))))))
      ENTHAL=(E3-E2+E1-E0)*1000.0
      RETURN
      END



      FUNCTION ENTRPY (N,T)
      COMMON /CPDATA/ CP(14,15),S0(15),HF(15)
      U=0.29815
      E0=CP(1,N)*ALOG(U)+U*(CP(2,N)+U*(CP(3,N)*0.5+U*(CP(4,N)/3.0
     7    +U*(CP(5,N)*0.25+U*(CP(6,N)*0.2+U*CP(7,N)/6.0)))))
      U=AMIN1(2000.0,T)*0.001
      E1=CP(1,N)*ALOG(U)+U*(CP(2,N)+U*(CP(3,N)*0.5+U*(CP(4,N)/3.0
     7    +U*(CP(5,N)*0.25+U*(CP(6,N)*0.2+U*CP(7,N)/6.0)))))
      IF (T.GT.2000.0) GO TO 1
      ENTRPY=E1-E0+S0(N)
      RETURN
    1 E2=CP(8,N)*ALOG(U)+U*(CP(9,N)+U*(CP(10,N)*0.5+U*(CP(11,N)/3.0
     7    +U*(CP(12,N)*0.25+U*(CP(13,N)*0.2+U*CP(14,N)/6.0)))))
      U=0.001*T
      E3=CP(8,N)*ALOG(U)+U*(CP(9,N)+U*(CP(10,N)*0.5+U*(CP(11,N)/3.0
     7    +U*(CP(12,N)*0.25+U*(CP(13,N)*0.2+U*CP(14,N)/6.0)))))
      ENTRPY=E3-E2+E1-E0+S0(N)
      RETURN
      END
```

```
      FUNCTION CVBIN(T)
      U=0.29315
      CV0=0.02893*U+0.08886*U**2+1.16526*U**3-1.77671*U**4+1.2422*U**5-0
     1.42318*U**6+0.05783*U**7
      U=.001*T
      CV1=0.02893*U+0.08886*U**2+1.16526*U**3-1.77671*U**4+1.2422*U**5-0
     1.62818*U**6+0.05783*U**7
      CVBIN=(CV1-CV0)/(U-0.29815)*78.114-1.986
      RETURN
      END
```

```
      FUNCTION CVAIN(T)
      U=0.29815
      CV0=0.25416*U-0.063495*U**2+0.116066*U**3-0.07853*U**4+0.027734*U*
     1*5-0.005034*U**6+0.0003706*U**7
      U=.001*T
      CV1=0.25416*U-0.063495*U**2+0.116066*U**3-0.07853*U**4+0.027734*U*
     1*5-0.005034*U**6+0.0003706*U**7
      CVAIN=(CV1-CV0)/(U-0.29815)*28.9-1.986
      RETURN
      END
```

```
      FUNCTION CVPIN(T)
      U=0.29815
      CV0=0.45596*U-1.52545*U**2+5.70833*U**3-8.58783*U**4+7.09294*U**5-
     13.10322*U**6+0.560826*U**7
      U=.001*T
      CV1=0.45596*U-1.52545*U**2+5.70833*U**3-8.58783*U**4+7.09294*U**5-
     13.10322*U**6+0.560826*U**7
      CVPIN=(CV1-CV0)/(U-0.29815)*44.097-1.986
      RETURN
      END
```

```
      FUNCTION CVIIN(T)
      U=0.29815
      CV0=2.54774*U+76.81795*U**2-4.44607*U**3-23.44267*U**4+14.195826*U
     1**5-2.749323*U**6
      U=.001*T
      CV1=2.54774*U+76.81795*U**2-4.44607*U**3-23.44267*U**4+14.195826*U
     1**5-2.749323*U**6
      CVIIN=(CV1-CV0)/(U-0.29815)-1.986
      RETURN
      END
```

```
      FUNCTION ENERINT (N,T)
      ENERINT=((ENTHAL(N,T))/(T-298.15))-1.986
      RETURN
      END
```

```
      FUNCTION CPPIN(T)
      U=.29815
      CV0=0.45596*U-1.52545*U**2+5.70833*U**3-8.58783*U**4+7.09294*U**5-
     13.10322*U**6+0.560826*U**7
      U=.001*T
      CV1=0.45596*U-1.52545*U**2+5.70833*U**3-8.58783*U**4+7.09294*U**5-
     13.10322*U**6+0.560826*U**7
      CPPIN=(CV1-CV0)/(U-0.29815)*44.097
      RETURN
      END
```

```
      FUNCTION CPIIN(T)
      U=.29815
      CV0=2.54774*U+76.81795*U**2-4.44607*U**3-23.44267*U**4+14.198826*U
     1**5-2.749323*U**6
      U=.001*T
      CV1=2.54774*U+76.81795*U**2-4.44607*U**3-23.44267*U**4+14.198826*U
     1**5-2.749323*U**6
      CPIIN=(CV1-CV0)/(U-0.29815)
      RETURN
      END
```

```
      FUNCTION CPBIN(T)
      U=0.29815
      CV0=0.02893*U+0.08886*U**2+1.16526*U**3-1.77671*U**4+1.2422*U**5-0
     1.42818*U**6+0.05783*U**7
      U=.001*T
      CV1=0.02893*U+0.08886*U**2+1.16526*U**3-1.77671*U**4+1.2422*U**5-0
     1.42818*U**6+0.05783*U**7
      CPBIN=(CV1-CV0)/(U-0.29815)*78.114
      RETURN
      END
```

```
      FUNCTION CPAIN(T)
      U=0.29815
      CV0=0.25416*U-0.063495*U**2+0.116066*U**3-0.07853*U**4+0.027734*U*
     1*5-0.005034*U**6+0.0003706*U**7
      U=.001*T
      CV1=0.25416*U-0.063495*U**2+0.116066*U**3-0.07853*U**4+0.027734*U*
     1*5-0.005034*U**6+0.0003706*U**7
      CPAIN=(CV1-CV0)/(U-0.29815)*28.9
      RETURN
      END
```

```
      FUNCTION PROPCP (T)
      U=.001*T
      PROPCP=0.45596-3.0509*U+17.125*U**2-34.3513*U**3+35.4647*U**4-18.6
     1193*U**5+3.92578*U**6
      RETURN
      END
```

```
      FUNCTION CPISO (T)
      U=.001*T
      CPISO=(2.54774+153.6359*U-13.3382*U**2-93.77068*U**3+70.97913*U**4
     1-16.49594*U**5)/114.232
      RETURN
      END
```

```
      FUNCTION BENCP (T)
      U=.001*T
      BENCP=0.02893+0.17772*U+3.49579*U**2-7.10684*U**3+6.21113*U**4-2.5
     16909*U**5+0.40482*U**6
      RETURN
      END
```

```
      FUNCTION CPMEAN(T,UU)
      X=UU*.001
      CV0=0.25416*X-0.063495*X**2+0.116066*X**3-0.07853*X**4+0.027736*X*
     1*5-0.005034*X**6+0.0003706*X**7
      U=.001*T
      CV1=0.25416*U-0.063495*U**2+0.116066*U**3-0.07853*U**4+0.027736*U*
     1*5-0.005034*U**6+0.0003706*U**7
      CPMEAN=(CV1-CV0)/(U-X)
      RETURN
      END
```

```
      FUNCTION AIRCP (T)
      U=.001*T
      AIRCP=0.25416-0.12699*U+0.348198*U**2-0.31412*U**3+0.13867*U**4-0.
     1030206*U**5+0.0025942*U**6
      RETURN
      END
```

```
      BLOCK DATA
      COMMON /CPDATA/ CP(14,15),S0(15),HF(15)
      DATA S0/
     -      .51071998E 2,      .47213998E 2,      .45770000E 2,
     -      .45106000E 2,      .49004000E 2,      .31208000E 2,
     -      .50347000E 2,      .43879998E 2,      .27302000E 2,
     -      .38468000E 2,      .57342999E 2,      .52545999E 2,
     -      .46032999E 2,      .52728999E 2,      .36613999E 2/
      DATA HF/
     -     -.94053999E 5,     -.26416998E 5,      .00000000E-0,
     -     -.57798000E 5,      .00000000E-0,      .00000000E-0,
     -      .21579999E 5,      .94319998E 4,      .52100000E 5,
     -      .59559000E 5,      .79099999E 4,      .19610000E 5,
     -     -.10970000E 5,      .23800000E 5,      .11296500E 6/
      END
```

APPENDIX 9

APPENDIX 9

DETAILS OF THE RENAULT VARIABLE COMPRESSION RATIO, RESEARCH ENGINE

TYPE	-	RENAULT 664 SPARK IGNITION
FUEL INTRODUCTION	-	CARBURETION
NUMBER OF CYLINDERS	-	1
BORE	-	80mm
STROKE	-	100mm
CONNECTING ROD LENGTH	-	189mm
SWEPT VOLUME	-	502.6cc
COMPRESSION RATIO	-	4.5 - 13:1
MAXIMUM SPEED	-	4500rev/min.
INDICATOR TAPPINGS	-	2 x 14mm. AND 2 x 18mm

VALVE TIMING

INLET OPENS - 12°B.T.D.C. : INLET CLOSES - 64°A.B.D.C.

EXHAUST OPENS - 64°B.B.D.C. : EXHAUST CLOSES - 12°A.T.D.C.